UiT
THE ARCTIC UNIVERSITY OF NORWAY

Faculty of science and technology

Department of geology

A comparative seismic study of gas chimney structures from active and dormant seepage sites offshore mid-Norway and west-Svalbard

Roberts Vīrs

GEO-3900 Master thesis in geology
May 2015

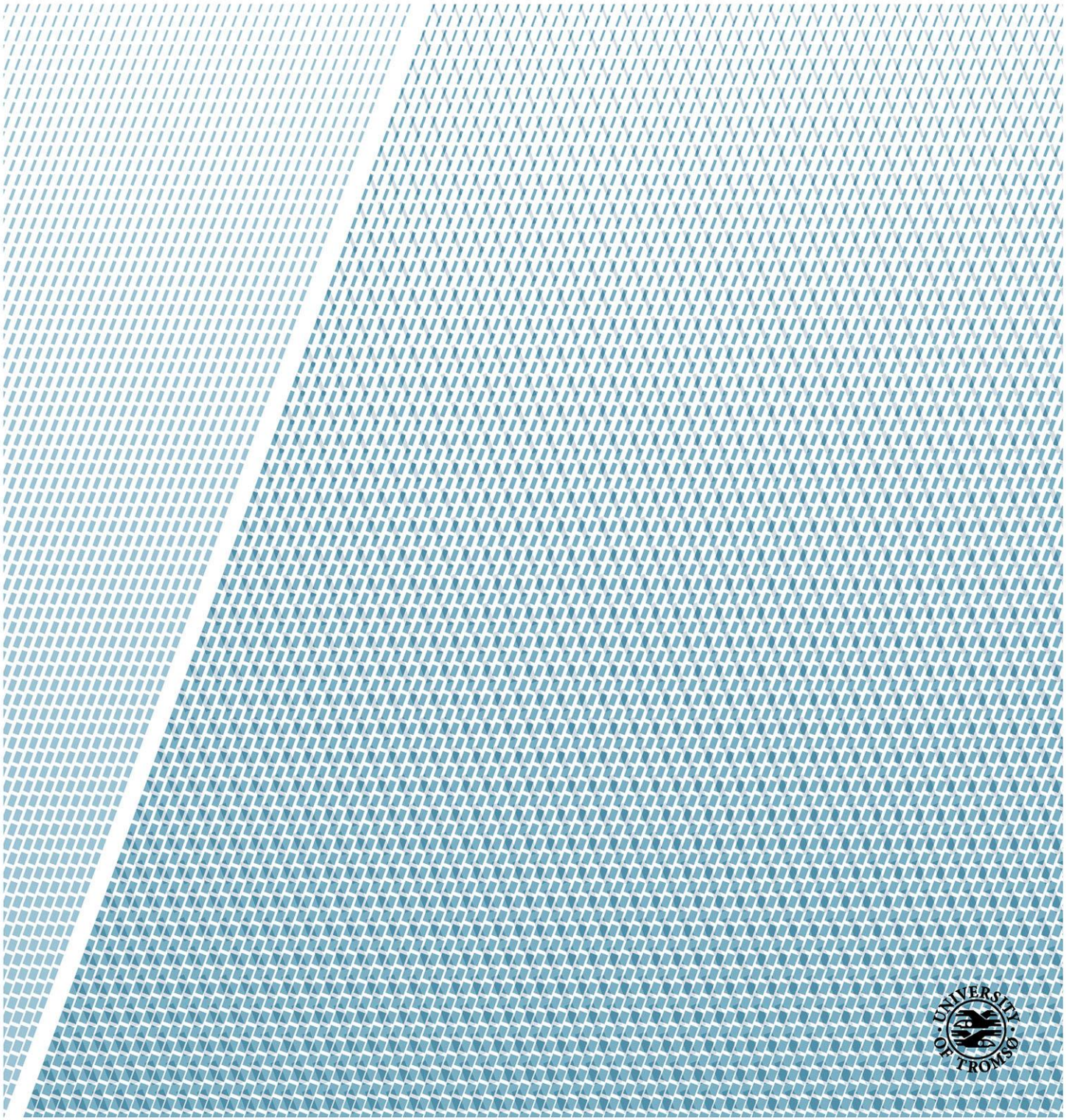

Abstract

Understanding the fluid flow and the related fluid expulsion from gas chimneys and pipe structures is very important to our environment, since seeping methane has a great influence on our Earth's climate. Chimneys are found in many places in the world, for instance at the Vestnesa ridge offshore western Svalbard and at the Nyegga region on the mid Norwegian margin. Plumbing systems and chimney structures are different in their characteristics and in their sediments. Since early times activity and dormant periods in these regions were responsible for driving fluids out to the seabed and to the water column. Key structures that act as a gateway for gas and gaseous fluids are called pockmarks which are highly abundant in these areas. Faults, fractures, sedimentation rate, permeability, compaction, overpressure generation, gas hydrates, free gas and source are features that are relevant to the plumbing system and the functioning mode of a chimney.

Comparing these two areas is important in order to understand how they differ from each other and to determine their driving force. In the future this might help to predict the occurrence of a new seepage of methane or hazards such as submarine slides. High tectonic activity and heat define the Vestnesa ridge and make it different from Nyegga which shows less of such activities. Sub-seabed features in Vestnesa include more chaotic and wider chimney structures compared to Nyegga.

Faults are known as good pathways for fluids helping them migrate vertically and laterally. Truncations of the flanks of continuous layers where chimney and pipe structures pierce through could mark the timing of an active period in all three areas.

In this study, chimney models and essential characteristics of chimneys were investigated, and a comparison of seeping systems was conducted.

Preface

My journey to Tromsø started when my older sister asked me: “Do you want to continue your studies abroad?” My first thought was – definitely, and it will be in Norway. I wasn’t afraid to take this chance and followed my feelings into this challenge. These years in Tromsø have been the best of my life. After the first semester my beautiful girlfriend gave birth to our baby princess Emily. First of all I want to thank her for the patience, because she took care of our baby, while I was at the work and spent late hours at University.

I would like to thank my supervisor Andreia Plaza-Faverola for her good ideas and sharing her knowledge with me. Without her it would have been almost impossible to pursue my way. Thanks to Kai Mortensen who always answered my questions related with studies. Thanks to all my friends, who supported me during these years especially Alexey, Boris, Charlie, Yohannes, Isac, and of course to my job in Posten Norge, which gave me the opportunity to work and support my family here in Tromsø. Last but not least my love goes to my mother in Latvia and sister in France who supported me, gave endurance and strength of will.

Norway, Tromsø, 15 May, 2015

Roberts Vīrs

Table of contents

1. Introduction

Seabed fluid escape is found in many parts of the world, both in active and passive continental margins. Pockmarks, craters, seeps and mounds are not the only features that are associated with fluid expulsion. Gas hydrates, mud volcanoes and gas chimneys are also commonly documented at seafloor fluid escape sites. The pipe structures, chimneys and polygonal faults are features that allow fluids to migrate upwards. Besides, the complex system called 'plumbing system' covers the area from the source to the seabed in the water column, where fluid expulsion, venting and seeping are present (Talukder, 2012). There are several processes that can cause fluid expulsion, e.g., faulting because of sediment compaction and volcanism controlled processes (Berndt, 2005). On the other hand these pathways can block, preventing further gas flow.

One of the possible explanations of fluid expulsion is that icebergs have affected sediments during the last deglaciation and afterwards they allowed fluids to migrate easily through the seabed sediments (Judd and Hovland, 2007). Focused fluid flow may be responsible for causing tsunamis and submarine landslides (Bugge et al., 1987). It is important to understand that fluid flow transports a huge amount of carbon into the atmosphere. Methane escape to the seabed largely affects underwater life and may also have an effect on climate (Berndt, 2005).

Petroleum seepage from the seafloor is just one of the forms of fluid expulsion that has been known for hundreds of years. Even ancient reports describe submarine groundwater discharge occurring like a spring offshore (Judd and Hovland, 2007).

1.1. Main objectives

In my Master thesis I will compare gas chimney systems offshore West Svalbard with chimneys in the Norwegian margin. The main goal is to analyze the differences in the structure of currently active and inactive gas chimneys for a better understanding of the dynamics of seafloor fluid escape systems. In this study I will conduct a detailed 3D seismic mapping of the Nyegga region and the Vestnesa ridge (Figure 2.1.1, 2.1.3 and 2.2.1) in order to see differences between their chimneys and gain new information about the seismic expression of relict and active seepage systems. While there are a large number of papers documenting fluid flow and hydrate systems in these two regions, a comparison of these two areas in terms of chimney structures has not previously been done. The questions I would like to answer are: Are they different? From what kind of sediments are the gas chimneys made of

in Nyegga and in the Vestnesa ridge? Fluxes of fluid flow are released from the chimneys to the seabed, but why did they stop the gas release, why was the flow reactivated and how wide can gas chimney spread? Why do gas chimneys terminate in different depths? Does the gas hydrate stability zone depth (GHSZ) differ and are there differences in the overall plumbing system?

The following sub-sections provide a description of a range of concepts that are relevant for this study:

1.2. Features of a fluid flow system in gas hydrate provinces

Gas hydrates

There are 3 aspects why gas hydrates are important. First, they are submarine hazards because if unstable, they can cause submarine slides. Second, gas hydrates resemble a potential future energy resource due to the large amount of methane inside them, and finally they can affect climate, because of their release of methane (greenhouse gas) (Kvenvolden, 1993).

Gas beneath the sediments always tries to migrate upwards and laterally. Gas will migrate by buoyancy with other fluids as for example, brines and formation water, from places with higher pressure to places with lower pressure. On the other hand, gas accumulation in sediments depends on the sediment type and its porosity. Gas hydrates form if the right conditions of temperature, pressure and gas source are given (Kvenvolden, 1993). Temperature increases with depth, and when it is too deep underneath several hundred meters of sediments, temperature is too high for gas hydrate stability (Figure 1.1) (Talukder, 2012).

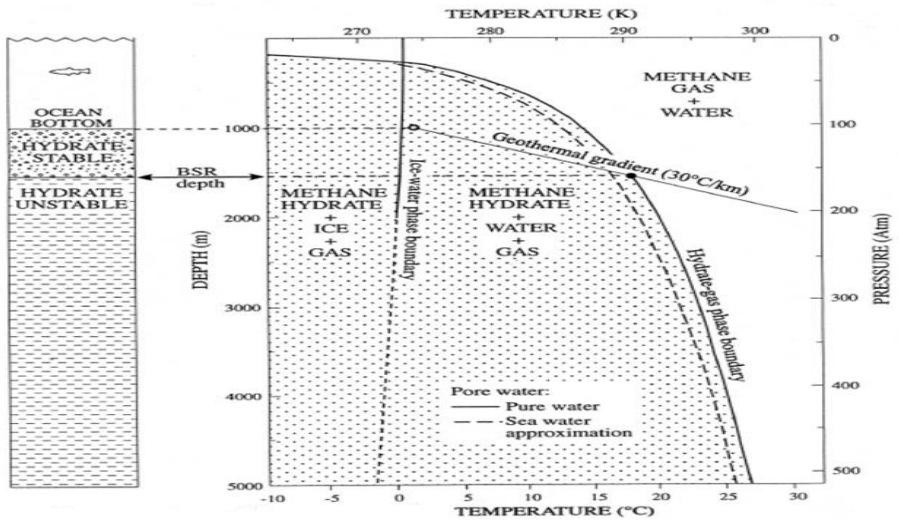

Figure 1.1: *To the left hydrate stability diagram. To the right, the diagram shows where within the sediments methane hydrates will be stable. Diagram adapted from (Andreassen, 2009).*

Gas hydrates often form in areas where the absorption of hydrocarbon gases in the pore fluids beats saturation in relation to the solid hydrate (Talukder, 2012).

The typical characteristics of gas hydrates (Figure 1.2) are a massive ice-like mix which consists mainly of methane gas where molecules are knotted in water and made boundaries (Judd and Hovland, 2007). Gas hydrates form in marine sediments within the gas hydrate stability zone (Plaza-Faverola et al., 2011). They are restricted to two regions: the polar and the deep oceanic regions, because of pressure, temperature and gas volume requirements (Kvenvolden, 1993). Gas hydrates can be stable and unstable. They are stable in very particular conditions only, with high pressure and low temperatures. Often these conditions are found in Polar Regions: where they are associated with permafrost onshore and offshore, and in deep oceanic regions- at the outer continental margins all around the world, in a cold marine environment, where ocean floor sediments are deeper than 300 m with low temperatures and high pressure (Kvenvolden, 1993). Beneath the hydrate stability zone additional gas, so called ‘free’ gas accumulates.

Figure 1.2: *Gas hydrate recovered from piston corer at 2550 m water depth. Photo by Helen Gibbons, ECS Project, 2010).*

There is an example from Blake Ridge, offshore North Carolina, where huge amounts of free gas accumulated beneath a gas hydrate stability zone (Talukder, 2012). The concentration of the gas hydrate is much higher at the base of the gas hydrate stability zone (GHSZ), than anywhere else at a given area (Talukder, 2012). They can be hazardous, because when gas moves through a gas pipe it can compress the snow and the line can get blocked and lead to explosion (Hammerschmidt, 1934). As gas hydrates form in the pore space as cement, several formation types that can be distinguished. It can form as lamina, hydrate veins or as nodules of pure hydrate (Andreassen, 2009). Most scientists believe that the presence of gas hydrates is related to the so called bottom simulating reflection (BSR) (Andreassen, 2009).

The source of seepages on the seabed can also be caused by a dissociation of gas hydrate, when during a dissociation process overpressure is generated which results in hydro fracturing above the dissociation area. It is one of the trigger mechanisms for upward gas migration (Talukder, 2012).

Bottom simulating reflection - BSR

The BSR is found at depths where the stability zone for methane hydrate occurs (Andreassen, 2009). The BSR is usually the first strong reflection which has reversed polarity reflection (compared with seabed) and that follows the seafloor reflection. The BSR results from a high impedance contrast, either because of high velocity of gas hydrates in the gas hydrate stability zone (GHSZ) which is above the BSR; or due to low velocity of free gas trapped at the base of the GHSZ (Judd and Hovland, 2007).

Yet the question remains of what actually produces the BSR, because the BSR normally indicates the presence of gas hydrates or free gas trapped beneath hydrate bearing sediments. It is commonly assumed that if there is no BSR, there will be no gas hydrates, but this is not necessarily true. One example is the drilling near the Ormen Lange petroleum field. Researchers drilled the BSR near Storegga Slide, but no gas hydrates were found. Yet, at the same time gas hydrates may occur in places without the BSR (Judd and Hovland, 2007). Cragg et al. (1996) suggested that the BSR has a biogeochemical origin, because when they stimulated the zone above the BSR, the methane oxidation rate was much higher than normal and micro bacterial presence significantly higher.

Normally, the BSR causes seismic reflection that is parallel to the seafloor, because the base of gas hydrate bearing sediments follows iso-temperature lines (Andreassen, 2009).

Pockmarks

55 years back, in the 1960's, seabed features called 'pockmarks' were found and people saw expulsions of the gaseous fluids from the seabed reaching the ocean surface. These seeps are a very important geologic discovery and an indicator of fluid flow processes. Interestingly, pockmarks have similar shapes like meteorite craters. In earlier days, in the beginning of the 1960's, in the Baltic Sea pockmarks were interpreted as artifacts from torpedo testing (Edgerton et al., 1966). However, after many years of research scientists have developed a more realistic idea, that they are craters in the seabed caused by fluids migrating through sediments (Figure 1.5) and they play a role in the carbon cycle between the water column and the sediments. It should be noted, that pockmarks can not only be formed by gas, but also by groundwater flowing through sediments (Judd and Hovland, 2007).

Plaza-Faverola et al. (2010) agree with Edgerton et al. (1966) that pockmark occurrence on the seabed is one of the main indicators of fluid flow. It is not a secret that the diameter of pockmarks can reach up to 700 m and depressions up to 10 m deep as it is typically found on the Norwegian margin (Hustoft et al., 2009). King and MacLean (1970) believed that "*the crater-like nature of the pockmarks strongly suggests that they are erosional features, and the main agent responsible for the formation of pockmarks is either ascending gas or water*", because during formation sediments were removed from the seabed. Pockmarks are exit pathways for fluids, but not all of them are actively seeping gas. Some of them are inactive and after a while reactivated whereas others never become active again. Pockmarks have different morphologies, size (height, width), orientation and shapes. For example, in the North Sea in general, they reach depths between one to three meters with diameters ranging from 50 - 100 m (Judd and Hovland, 2007). As Hovland (1981) suggested and measured, most pockmarks (42%) in the Norwegian Trench are orientated parallel to ocean bottom currents - pointing from northwest to southeast. In general, pockmark shapes and sizes can vary. They can be standard circular, elliptical, asymmetric, string-like, composite, elongated pockmarks and troughs, unit and giant pockmarks. These last ones are formed by fast migration of pore fluids which are gas-charged and flowing from deeper reservoirs (Heggland, 1998). Nevertheless, there are so called buried ('fossil') pockmarks which got their name because they are buried, plus occur at various horizons (Judd and Hovland, 2007). Long (1992) described them as "*pockmarks that have ceased venting and have subsequently been covered by sediments*". Sometimes they can be confused with linear features, such as plough marks (Judd and Hovland, 2007), because they can look similar not

only on the seabed, but also in the subsurface in a seismic section. Buried pockmarks are relevant since they represent the time when gas seepage was active and the time when there was a new deposition of sediments over pockmark and when this process stopped (Long, 1992). These buried pockmarks can form when gas escapes and the sediments then collapse, filling the free space. Buried pockmarks can also be reactivated when a pockmark overlies a deep succession which is connected with vertical columns of disturbed sediments (Judd and Hovland, 2007).

The most common pockmarks probably are standard circular and elliptical. For example, on the slope of the Norwegian Trench the axes are arranged parallel to the slope, signifying that there is a relationship between pockmark shape and slope. In the areas where there is flat seabed, their orientation is based on the dominant tidal current (Judd and Hovland, 2007). Asymmetric pockmarks on side-scan sonar records look as if they have a diverse and very long 'tail' and on one side they show strong back wall reflection. These back wall reflections often occur where slope and seabed are very gentle. One of the sides is gentle, the other steep (Judd and Hovland, 2007).

Composite pockmarks occur in places where normal pockmarks fuse in one another, later some of them can form into complex shapes. Pockmark strings include individual pockmarks that are arranged in chains or strings and follow each other. They often group together in lines and spread in different directions from larger pockmark. Sometimes these strings can develop in one long single pockmark (Judd and Hovland, 2007).

Elongated pockmarks (Figure 1.3) remind of gullies or troughs (Judd and Hovland, 2007). In these troughs older sediments are frequently exposed as the topmost sediment layer (Hovland, 1983).

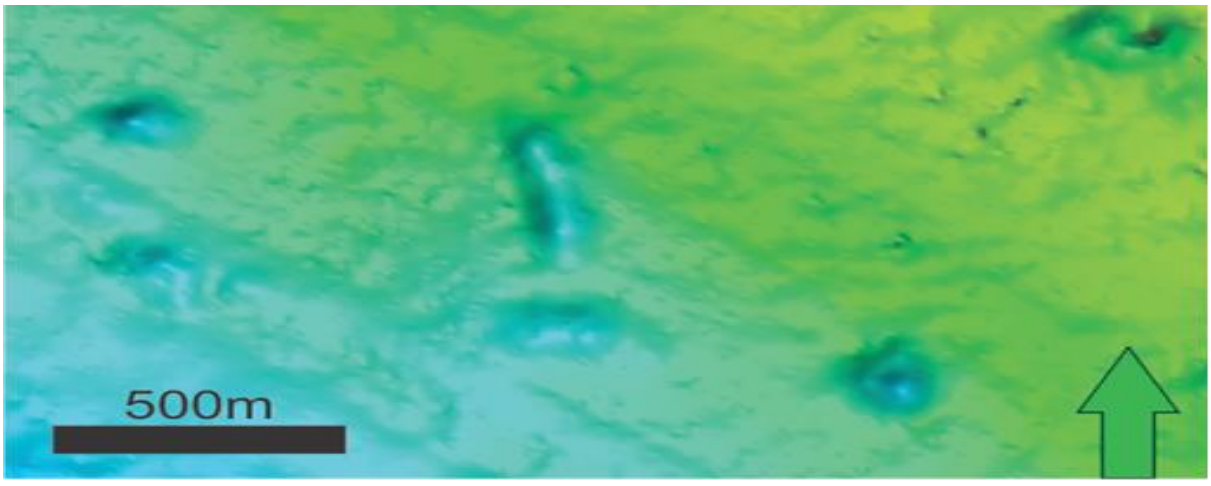

Figure 1.3: *Elongated like depression from Nyegga.*

Formations of pockmarks are usually found in fine grained sediments and caused by gas and other fluids (Judd and Hovland, 2007). Pockmarks are generally located above high amplitude anomalies (Figure 1.4), which mean that they may have been associated with shallow gas reservoirs (Løseth et al., 2009).

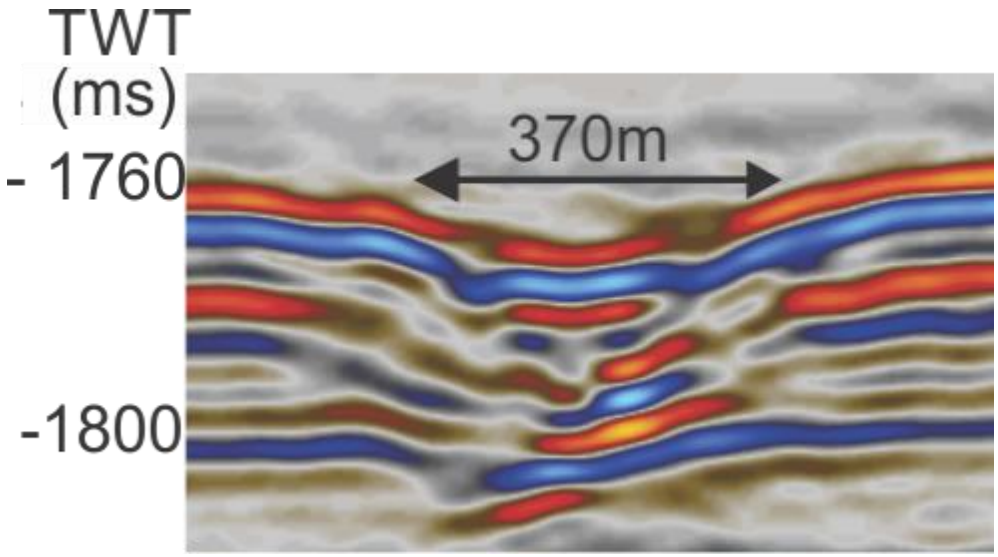

Figure 1.4: *Pockmark cross section from Vestnesa less active (A1) area inline 219 in seismic data. High amplitude underneath can be interpreted as shallow gas, hydrates or carbonates.TWT: Two-way travel time.*

The factors that define the distribution of pockmarks are: formation mechanism and sediment suitability for pockmark formation (Figure 1.5). Pockmark size can be related to sediment grain size. If sediments have an increased grain size, (e.g. Gullfaks field), it is possible that in this area smaller pockmarks/depressions will form, compared to sediments that hold smaller grain sizes (e.g. Vestnesa ridge (A2)). Silty clays are the ideal sediment for pockmarks to form (can be found in Nyegga and Vestnesa ridge); though there can be exceptions (Judd and Hovland, 2007).

From history it is known, that in the North Sea gas was trapped beneath sub seabed permafrost and gas hydrates. When gas hydrates dissociated, giant pockmarks were formed. This process happened when Arctic waters were flushed by Atlantic waters and the melting of the sub seabed occurred. During this particular time a lot of pockmarks were formed, shown by a great density of buried pockmarks (e.g. Long, 1992; Judd and Hovland, 2007).

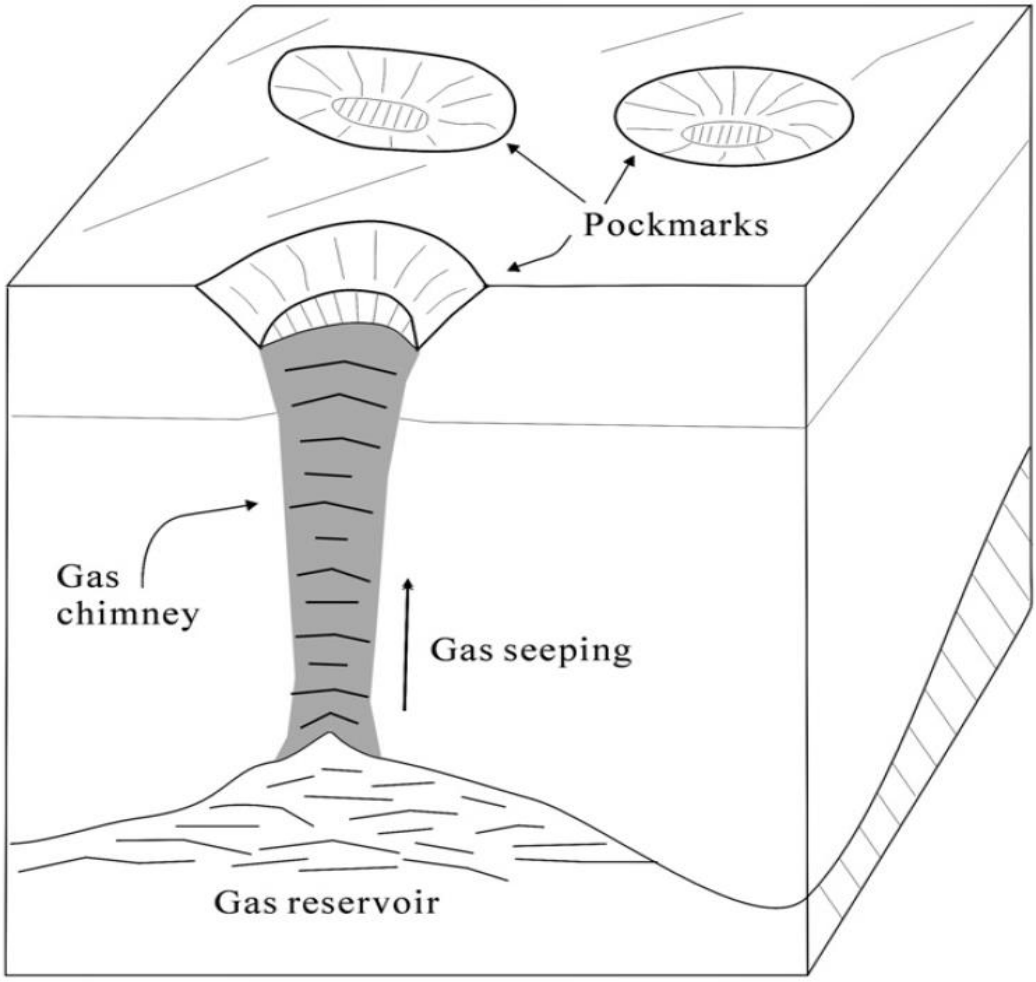

Figure 1.5: *Model for pockmark formation. Pockmarks are mostly located above gas chimneys. Slow gas leakage through the chimney supports vent communities which produce carbonate mounds in the pockmark. Image adapted from Cathles* et al.*, 2010.*

Gas chimneys

Looking through a seismic section, gas chimneys are easy to detect. Gas chimneys appear as vertical zones where sediments are disturbed compared to the adjacent areas (Judd and Hovland, 2007). The gas chimney shape can be a foggy type, which is either an almost vertical pipe with chaotically distributed reflections inside (Figure 1.6), or a cigar shape (Løseth et al., 2009). Gas chimneys may form under pockmarks and can represent gas and fluid migration upwards to the seafloor (Petersen et al., 2010). In fact, bacteria mats can be related to active seeping of methane (Linke et al., 1994), as well as the shallow accumulations of gas hydrate, which can also present evidence for recent fluid migration activity (Plaza-Faverola et al., 2011). Commonly, when looking at the seismic section at gas chimney outer borders the viewer can observe up-bending reflections or down-bending reflections. Up-bending (pull-up) reflections are the result of mechanical strata deformations due to upward seeping fluids, or they can be a velocity artifact, caused by the fact that sediments in the

chimney consist of higher velocity material (Westbrook et al., 2008; Plaza-Faverola et al., 2010). Down-bending (push-down) is often seen underneath the chimney because of low velocity. Incidentally, low amplitude and variance of dips characterizes gas chimneys as well (Westbrook et al., 2008). At the top of gas chimney a frequently high amplitude anomaly is observed (Løseth et al., 2009). Sediments in gas chimneys are disturbed because of previous gas migration through sediments or by ongoing migration. Some believe that small wraps of trapped gas might play a role (Judd and Hovland, 2007).

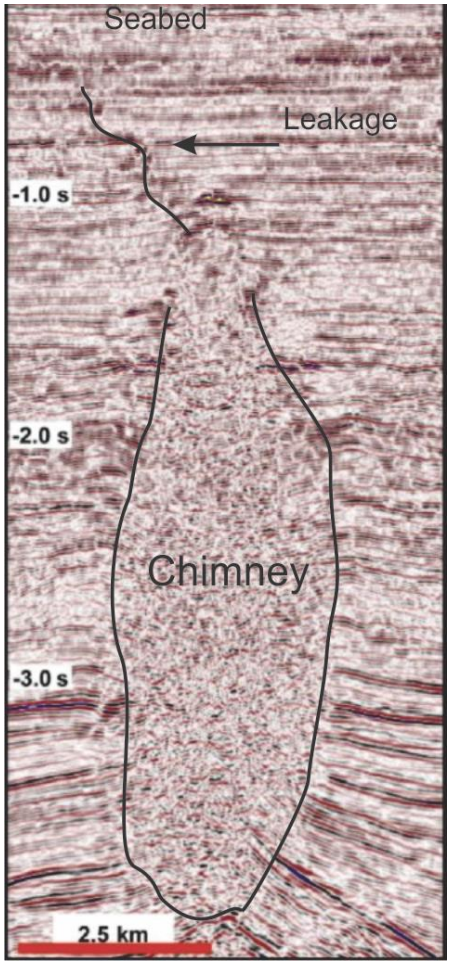

Figure 1.6: *Seismic section showing gas chimney. Modified from (Andreassen, 2009).*

The internal structure of gas chimneys includes the presence of gas hydrate inside. Main elements of the internal structure of a fluid escape chimney are described by velocity that increases laterally towards the center of the chimney. Beneath the GHSZ (gas hydrate stability zone) velocity remains constant. The presence of gas hydrate inside the chimney is the main cause for high velocity. Plaza-Faverola et al. (2010) suggest that because of hydrates inside the veins and fractures within the GHSZ, up-doming has formed, whereas up-doming is not as significant below the GHSZ. High velocity material that causes pull-up reflections can not only be gas hydrates, but also small carbonate accumulations emplaced in the conduit (Plaza-Faverola et al., 2010; Plaza-Faverola et al., 2011). Chimneys occur in fine grained marine sediments and glacial marine clays (Berg et al., 2005; Plaza-Faverola et al., 2012) and thereby a fracture-filling model is suitable for the formation of hydrate. Fundamentally, gas chimneys are formed with the help of violent gas venting, resulting in a fracture/fault structure, inside which hydrate develops (Cathles et al., 2010). With the flow of the gaseous methane, fluids through the chimney fractured network developed up to the seafloor, as well as the formation of authigenic carbonate precipitation could be formed (Mazzini et al., 2006). In the early stages of a gas chimney formation, hydrate reduces the amount of gas reaching the seabed, but hydrate dissolution preserves methane supply up to the surface when the supply of methane has been reduced. This means that gas chimneys have an important role in disabling and

enabling methane escape from places beneath the GHSZ (Plaza-Faverola et al; 2010). Where gas chimneys breach the seafloor, pockmarks lying above often have the same diameter as the chimney. As seen in seismic, chimneys frequently originate on top of shallow gas pockets (Cathles et al., 2010).

Mud volcanoes

Guliev (1992) defined mud volcanos as "*periodic expulsion from deep parts of the sediment cover of mixtures of water, various gases and solid material*". Mud volcanoes vary in size and height; from less than 1 m up to 3 - 4 km in diameter and 1 - 400 m in height (Løseth et al., 2009). According to Løseth et al. (2009) mud volcanoes can even exceed 25 km in diameter. Among mud volcanoes the most popular shape is circular.

Apart from the famous Azerbaijan volcanoes, another famous mud volcano is found in Barents Sea on the Bear Island Fan Slide complex. Researchers discovered the interesting fact that the temperature in the center of the mud volcano was only around 16^{o} C (Judd and Hovland, 2007). While Egorov et al. (1999) pointed out that methane concentration out of the volcano was 7 times higher than in the surrounding area.

Mud volcanoes, similarly to gas chimneys, occur in environments with pressurized fluids beneath the surface (Blinova et al., 2003). Their driving forces are overpreassured pore-fluids (gas and water) which help transport the mud-mix up to the surface (Dimitrov, 2002). Because of gases that contain methane, mud volcanoes are closely related to petroleum systems (Blinova et al., 2003)

Mud volcanoes can be the result of tectonic movement, like for instance in Azerbaijan where the Arabian Plate and the Eurasia Plate are colliding. There is also a close relationship between tidal cycles and mud volcanoes. Sometimes earthquake activity results in the formation of mud-volcanoes and vice versa (Judd and Hovland, 2007).

Craters

Craters are large depressions and are interpreted as gas blowout structures (Løseth et al., 2001). Some say, because of its wider zone of ruined seismic data, it can be interpreted as a gas chimney (Heggland, 1998). Many scientists have different views on how craters may originate. For example, Judd and Hovland, (2007) suggest that they can be formed because of karst - the dissolution of soluble rocks. However, other scientists have a theory that they are made by sub-glacial melt-water. The most frequently used theory, however, is that they are formed by leaking hydrocarbons (Løseth et al., 2009). Disturbed reflections beneath craters

suggest that acoustic masking and push down effects occur because of the presence of free gas in the sediments (Heggland, 1998).

Mud remobilization features

Mud mobilization occurs when primary structures of muddy sediments are altered or affected by post-depositional mobilization. Hydrocarbon leakages usually are connected with any kind of mud mobilization (Graue, 2000). Although mud mobilization often occurs at more than 3 km depth, it can also take place in a relatively shallow subsurface in less than 1000 m (Løseth et al., 2003). In the seismic data mobilized sediments are seen as chaotic seismic reflection under mounds or depressions (Judd and Hovland, 2007; Løseth et al., 2003). Below mobilized sediments gas chimneys are frequently found (Løseth et al., 2009).

Seabed ecosystems

Gas and fluid flow from the subsurface do not only form pockmarks and craters but also other features. Hydrocarbons seepings, migrating up to the seafloor, act as nutrients and increase biological activity around the affected area. Where the seeps are active for a long time, several types of biological masses can appear. This is commonly referred to as bioherm- an accumulation of shells and mounds on the seabed by corals, mollusks, and authigenic carbonate concretions (Hovland and Judd, 1998). The precipitation of authigenic carbonates is often related to the seepage of methane and is a result of anaerobic methane oxidation. Methane-derived authigenic carbonates (MDAC) form at cold seeps and depending on the particular conditions, diverse authigenic carbonates precipitate (Magalhaes et al., 2012). According to Traynor and Sladen (1997) hydrocarbon leakage can cause the formation of carbonate buildups. When seeps are long lasting they are indicated by stacked bioherms and can thus be easily seen, for instance, on RMS amplitude maps (Heggland, 1998).

Polygonal faults

Polygonal fault systems are non-tectonic class faults (Cartwright, 1996). These fault systems are mostly found in the sediment basins which contain fine grained sediments (Cartwright and Dewhurst, 1998) or in places where gas hydrates and glacial debris flow occur in the overburden (Berndt et al., 2003). They formed as de-watering pathways, permitting pore fluid escape when sediments shrink and fluids expel (Judd and Hovland, 2007). One of the processes during their development is explained by syneresis of colloidal sediments (Dewhurst et al. 1999). These faults are thought to be formed during early burial as the sediments were compacted (Judd and Hovland, 2007) or they start to evolve after burial

(Cartwright, 1996). Polygonal faults control fluid flow and they are often associated with pockmarks and shallow gas (Judd and Hovland, 2007). Understanding the polygonal fault system is vital, because they cooperate with reservoirs nearby (Berndt et al., 2003). There is a large number of polygonal faults in the central North Sea. The faults are found in Eocene, Oligocene and Early Miocene (Judd and Hovland, 2007). The Vøring basin in the mid-Norwegian sea is a great example of a long term fluid flow from a polygonal fault system (Berndt et al., 2003). Nevertheless, in this region polygonal faults terminate into a layer, where high amplitudes are found (Berndt et al., 2003).

Lithified and soft sediments undergo brittle deformations. In the first case it is in response to stress, second because of high strain rates. There are different ways how sedimentary rocks will respond to the stress: faulting, folding and fracturing. Fracturing increases permeability, and fracture propagation can cause fluids to flow/leak. Fracture propagation and associated fluid leakage is a mechanism that occurs above salt domes, fault zones, hydro-fractures and micro-fractures (Løseth et al., 2009).

Fault zones can contain many smaller fractures which resemble good pathways for fluids to flow and can also be vertical conduits (smaller than pipes). Those fractures containing ductile clay may be sealing, but can begin to leak under overpressure (Løseth et al., 2009).

Hydraulic fracturing occurs when pore pressure exceeds the sum of minimums horizontal stress. Pore fluid pressure; for example, can be up to 1450.3 PSI (pound per square inch) which is equal to almost 100 bar (Wensaas et al., 2000).

2. Study areas and their geological framework

2.1 The Vestnesa Ridge

2.1.1 Geological framework

The Vestnesa ridge is located offshore the west-Svalbard margin in the Fram Strait (Figure 2.1.1). The crest of the ridge is located at approximately 1200 - 1300 m below sea level (Bünz et al., 2012). From the history, this part of the region is least explored. This area was opened for drilling in 1980, since then exploration has skyrocketed (Gabrielsen et al., 1990).

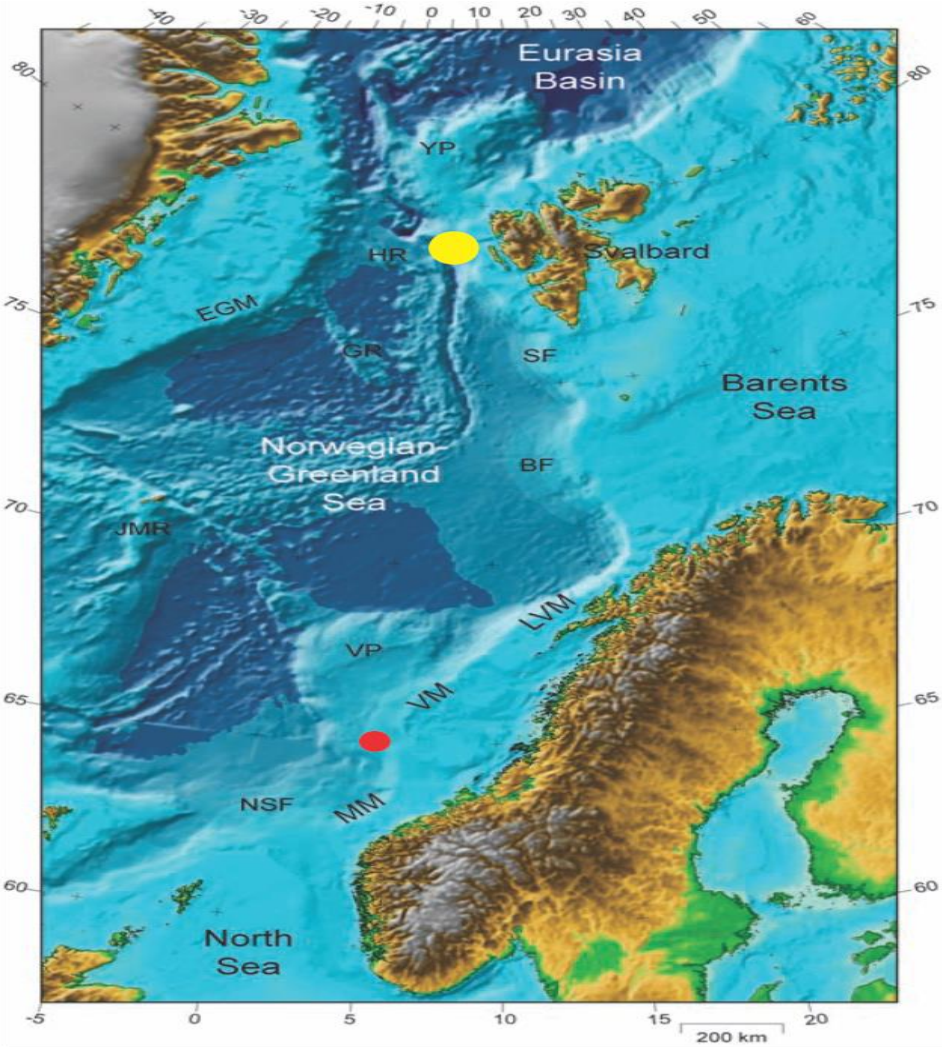

Figure 2.1.1: *Regional location of study areas. Regional setting of the Norwegian continental margin, which formed in response to the Cenozoic opening of the Norwegian-Greenland Sea. Bathymetry/ topography from the 1x1 elevation grid of Jakobsson* et al. *(2007). BF – Bjørnøya Fan, EGM- East Greenland Margin, GR- Greenland Ridge, HR- Hovgård Ridge, JMR- Jan Mayen Ridge, LVM- Lofoten-Vesterålen Margin, MM- Møre Margin, NSF- North Sea Fan, SF- Storfjorden Fan, VM-Vøring Margin, VP- Vøring Plateau, YP- Yermak Plateau. Red circle shows Nyegga region and Yellow circle – Vestnesa ridge. Modified from (Faleide* et al.*, 2008).*

The Fram Strait is a narrow deep-water gate way that connects the North Atlantic and the Arctic Ocean (Figure 2.1.2). Through this channel fairly warm, saline waters exchange with cold and less saline waters (Gebhardt et al., 2014; Eiken and Hinz, 1993).

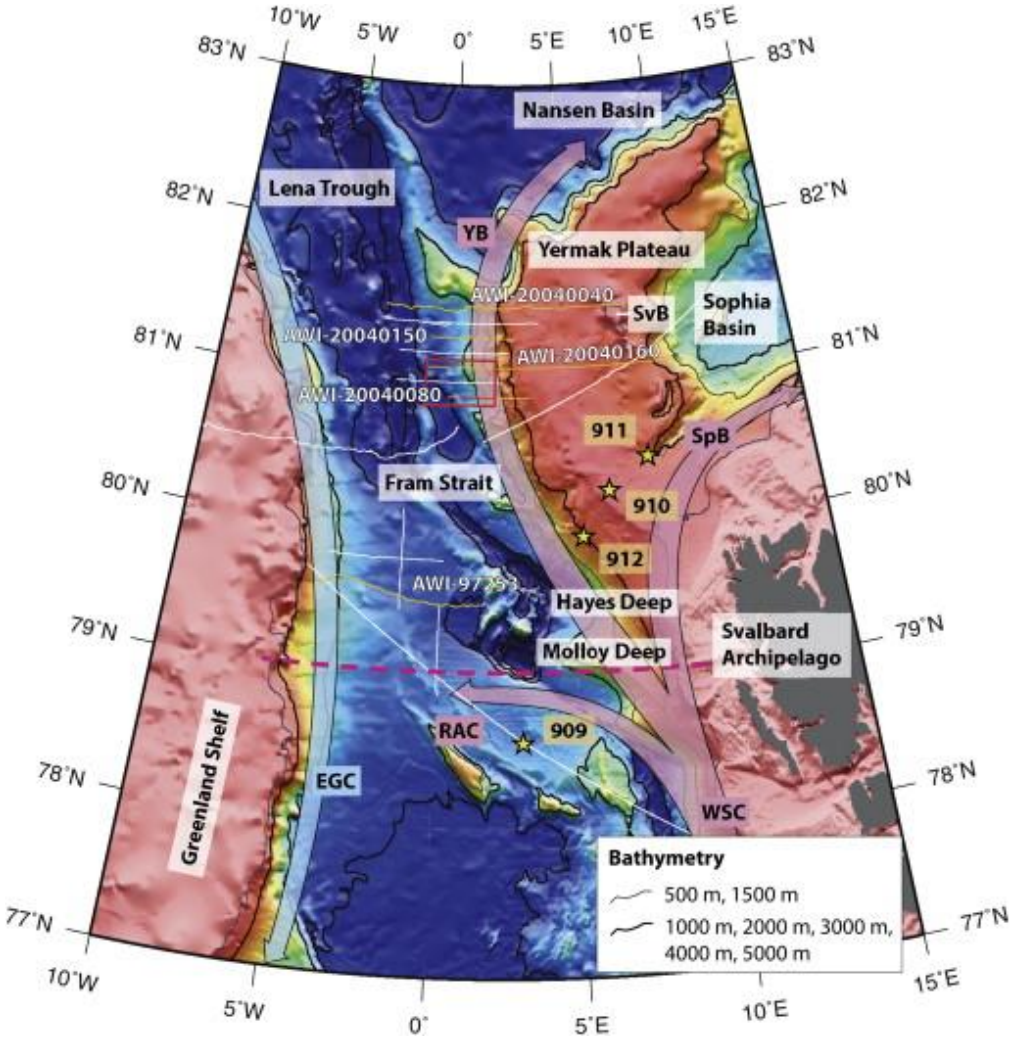

Figure 2.1.2: *Geographical overview of the Fram Strait and its surroundings. Blue and red arrows mark the present-day predominant surface water flows. Picture adapted from (Gebhardt* et al.*, 2014).*

The Fram Strait is 1 - 2 km thick sediment drift that lies between Greenland and Svalbard (Vogt et al, 1994). Two study sub areas, active (A2) and less active (A1) are located at the eastern spreading segments of the Molloy Ridge in the Fram Strait west of Svalbard and lie within the Vestnesa ridge (Hustoft et al., 2009). The distance between the two areas A1 and A2 is approximately 20 km (Figure 2.1.3).

In the Late Cretaceous seafloor spreading in the central Atlantic propagated northwards, but the Arctic Ocean remained remote from the Atlantic Ocean when 35 Myr (million years) ago the separations started (Morgan et al., 2006; Jokat et al., 2008). Deep

water exchange and ventilation in the Arctic Ocean started 18.2 Myr ago (Figure 2.1.4) (Jakobsson et al., 2007).

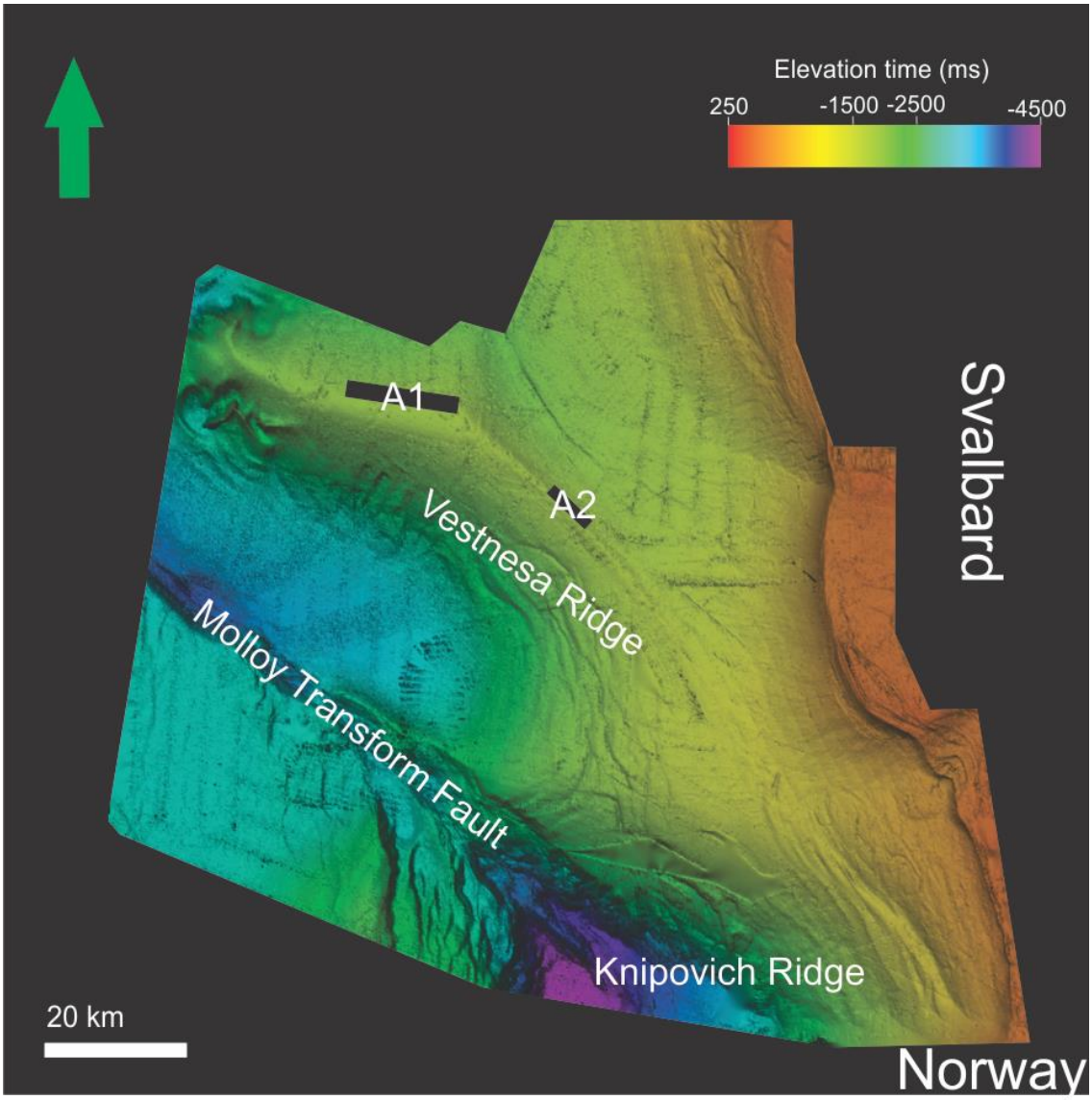

Figure 2.1.3: *Bathimetry map showing 2 study locations in the Vestnesa ridge, offshore Barents Sea. Black rectangular A1 - less active region, black rectangular A2 - active region.*

Vestnesa ridge is one of the northernmost gas hydrate provinces inside the Arctic continental margins (Eiken and Hinz, 1993). Geologically not so long ago Svalbard was tectonically uplifted which is why it's true to say that the Vestnesa ridge is a sediment drift located on 'hot and young' (20 Ma) oceanic crust (Engen et al., 2008; Hustoft et al.,2009).

On the flanks of Vestnesa ridge and northeast of Molloy ridge plate-boundary earthquakes have triggered sediment slip offs (Vogt et al, 1994).

The history of the circulation regime in the Arctic Ocean was unclear because of the absence of data from Cenozoic sediments. In the Early Miocene occurred a conversion from

poorly oxygenated to fully oxygenated conditions in the Arctic Ocean (Jakobsson et al., 2007).

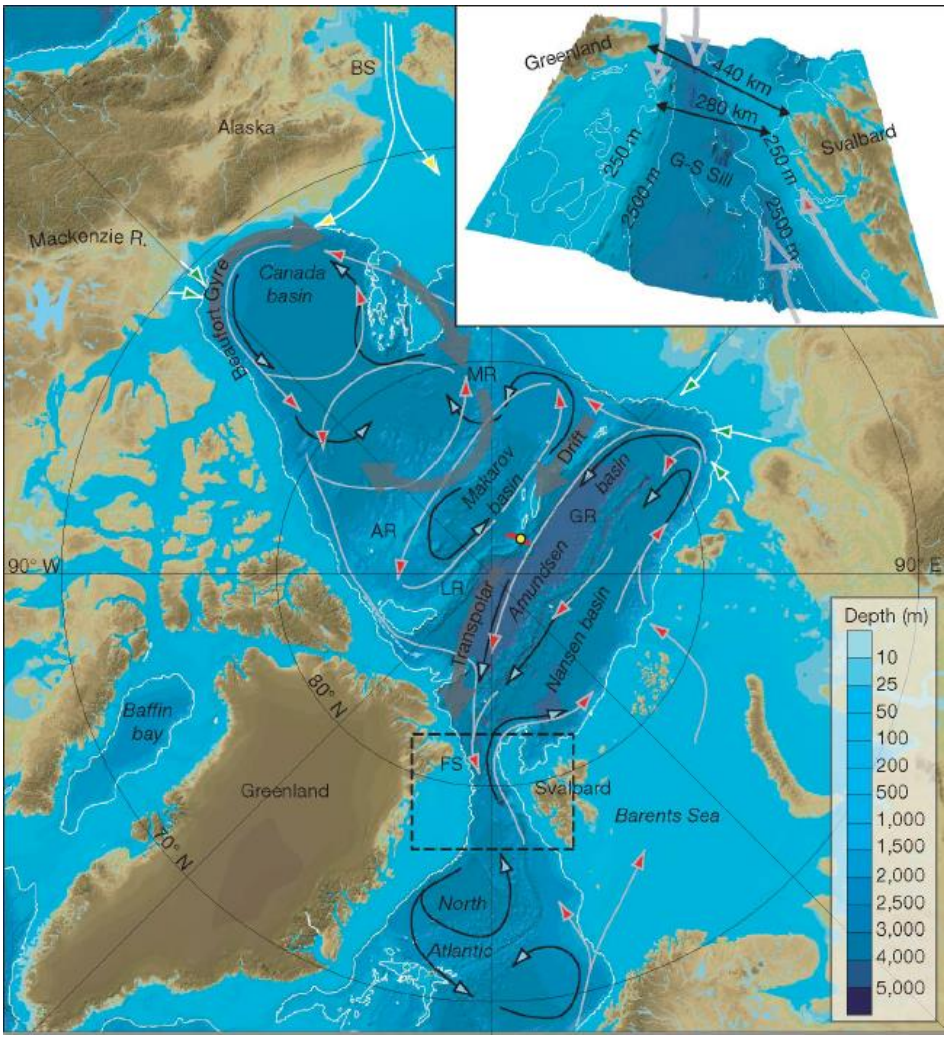

Figure 2.1.4: *Schematic map that shows present ocean circulation in the Arctic Ocean. Present circulation of intermediate waters of Atlantic origin shown with grey arrows, red arrowheads. Deep waters are marked with black arrows, light blue arrowheads. Major freshwater inputs by rivers marked with white arrows, green arrowheads. With white arrows, yellow arrowheads are shown Pacific water influx through the Bering Strait. Physiographic features: AR, Alpha ridge; BS, Bering Strait; FS, Fram Strait; GR, Gakkel ridge; LR, Lomonosov ridge; MR, Mendeleev ridge. Picture from (Jakobsson* et al.*, 2007).*

Reconstruction and physical analysis of the developing Fram Strait show that the Arctic Ocean changed from an oxygen poor ‘lake stage’ to a transitional ‘estuarine Sea’ phase 17.5 Myr ago. The ‘Estuarine Sea’ phase was described as with adjustable ventilation that during development evolved as fully ventilated phase, which allowed inflow and outflow of the waters to interchange (Jakobsson et al., 2007).

Changes in sediment properties show a transition from a poorly ventilated to a well ventilated saline Ocean. Evidence for that is the appearance of benthic firmly glued together foraminifers and other plankton that appear in oxygen rich conditions. The timing is

established relying on several organisms that lived in this specific time interval (Jakobsson et al., 2007).

Jakobsson et al. (2007) claim that in the late Early Miocene the Fram Strait was the only gateway which connected and allowed the inflow of fresh water from the Arctic Ocean to the North Atlantic (Figure 2.1.4). In general, straits are strongly affecting the circulation of the waters by localizing wide and ample current flows in the narrow gateways. The Fram Strait opened and deepened during the Miocene (13.7 Myr ago) in great depths < 2000 m. Through continuous sea floor spreading, water exchange between Arctic and North Atlantic seasoned many changes that influenced the ventilation conditions at the Arctic Ocean (Jakobsson et al., 2007).

During the late early Miocene sea level changes were significant, up to 30 m. These changes were important, because they influence ocean circulation. For example, during low sea level (lake stage) there will be only one direction - one layer outflow, but during high sea level (estuarine) - two directions and two layer flows (Jakobsson et al., 2007).

When the Strait became wider final transition occurred. The outflow in the upper layer was controlled rotationally. This means that the outflow of low salinity surface water was concentrated at the western (Greenland) continental slope. As a fact, inflow through the Fram Strait in the present is up to 10 times larger than the outflow of low-salinity surface water (Jakobsson et al., 2007).

Seafloor spreading at the Molloy Ridge might have already started at 19.6 Ma (Engen et al., 2008). Last but not the least, the Vestnesa Ridge is covered by more than 2 km thick sediments deposited as contourites (Eiken and Hinz, 1993).

Contourites or contourite systems are deposited sediments which are affected by bottom currents energy. The term ‘contourite’ was first defined as sediments that are deposited in the ocean by contour-parallel bottom currents. Depth and current type influence contourites and are significantly important for them. Thermohaline bottom currents influence sedimentation in oceans, thus they flow parallel to the bathimetric contours. There are a variety of bottom currents that operate in deep water e.g thermohaline, wind driven circulation patterns. Contourites are important in terms of hydrocarbon exploration, slope stability and paleoclimatology. Paleoclimatology - because it gives information about current velocity, oceanographic history and basin interconnectivity. In the oil industry it mainly affects oil and gas reservoir development, because weak flows may influence the accumulation of source

rocks and violent flows may create feasible mechanism of forming clean sands in the deep sea. In slope stability contourites have an important role (loading/unloading), because when over pressured glide planes move (loaded with rapid water content, collapsing by diagenesis) they can cause hazardous submarine landslides. It is not easy to determinate contourites, since they accumulate slowly and continuously. By knowing current strength and grain size it is easier to distinguish them from other ocean floor facies, like fine grained turbidites and hemipelagites. Contourites are mostly made from fine-grained mud and they are low-permeable. The top of the Vestnesa Ridge contains silty turbidites and muddy-silty contourites of the Holocene and the mid-Weichselian (last glacial period) (Howe et al., 2008). Last but not least, contourites are covering large parts of the ocean floor and the continental margins (Rebesco, 2005).

Finally, there is a lot of evidence suggesting that sediment drift formed by bottom currents largely during the late Miocene and Pliocene, for instance, through internal seismic-reflection structure, the topographic shape and obvious sediment thicknesses (from 1 km in the west to >2 km in the east) (Eiken and Hinz, 1993). Vogt (1986) considers that deposition was led by an irregular underlying oceanic basement that reduced the speed of the northward directed West Spitsbergen Current.

2.1.2 Evolution of the Barents Sea

Many authors and researchers agree that the Barents Sea is underlain by thick sedimentary sequences - more than 10 km thick. The age of the sediments varies from the Paleozoic to Mesozoic and the wedge along the western margin consists of Cenozoic age. The Barents Sea consists of a system of basins, diapiric provinces, ridges and major fault zones (Eldholm et al., 1984). Through the geologic history not all Barents Sea basins were affected by the same tectono-sedimentary events, where some of them experienced uplifts and subsidence (Eldholm et al., 1984).

2.1.3 Tectonic setting of East Greenland and the Barents Sea margin

The Greenland margin has a slim continental shelf that propagates in wideness towards the north. There is a crustal difference of the East Greenland margin that accords with the West Jan Mayen Fracture Zone. Voss and Jokat (2007) emphasized that the lower crust body is wider and thicker than anyone thought. Therefore, the lower crust body is larger on the Greenland side than the one in the mid-Norwegian margin. Comparing these two neighboring margins shows that biggest difference is the asymmetrical shape. In Greenland

offshore several basins and highs are seen on seismic data while broad sill intrusions inhabit deep basins that coincide with Mesozoic basins on the mid-Norwegian margin, as well as in the SW Barents Sea (Faleide et al., 2008).

The SW Barents Sea margin has been passive since early Oligocene time along the Senja Fracture Zone. The margin developed during the Eocene when the Norwegian-Greenland Sea opened. It was a complex process because of two shear settings, first continent - continent shear and later continent - ocean shear (Grogan et al., 1999).

In the Eocene - Oligocene transition, significant events happened in adjacent areas. For example, Sørvestsnaget basin became shallower (Ryseth et al., 2003). During the Early Eocene rifting, faults reactivated in the Vestbakken Volcanic Province due to plate motions resulting in volcanism (Jebsen and Faleide, 1998). In the early Oligocene grabens developed along the Svalbard margin as a result of transpressional movements that were replaced by oblique rifting and spreading (Faleide et al., 2008).

2.1.4 Norwegian Greenland Sea continental margin evolution

The passive rifted margin between the Norwegian and Greenland Sea was a result of the process when the mid-Norwegian margin was subjected to subsidence and sedimentation from the Middle Eocene (Hjelstuen et al., 2007).

The Miocene sediments clearly show contourite sediment drifts that prove that there was deep- water sedimentation (Eiken and Hinz, 1993) which is further explained in chapter 2.1.1 and showed in figure 2.1.4. It is still under debate when exactly the Fram Strait opened. A broader point of view is presented by Engen et al. (2008) who suggest that this huge impact on ocean circulation and deep water exchange was 20 - 10 Ma.

The pre-glacial tectonic uplift theory of the Barents shelf is viewed by Jebsen and Faleide, (1998) who think it is related to the Late Miocene uplift because of increased amplitudes in this region.

Over the Barents shelf, unconformity marks the transition of glacial sediment deposition in Pliocene, which is characterized by ice-rafted debris and glaciers where fans were scoured by ice streams and thereby eroding the shelf (Faleide et al., 1996). In Plio-Pleistocene, a regional tilt along the margin was a result of uplift and glacial erosion of the Barents shelf, where glacial deposits were placed. These huge deposition rates in the fans created sediment instability and high excess pore pressure, which led to a submarine landslide (Hjelstuen et al., 2007).

2.1.5 Evolution of Western Barents Sea

It is thought, that the Caledonites are creating the metamorphic basement of the western Barents shelf. During the late Silurian to Early Devonian the Caledonites were consolidated and the result was the collision between the North America-Greenland and the Fennoscandian-Russian plates. In the Early Devonian arid continental conditions existed in the western Barents Sea, then after a robust uplift the Caledonites were eroded and molasse sediments were deposited in the Svalbard and East Greenland area (Faleide et al., 1984). According to Harland, (1965) and Ziegler, (1978) the late Devonian Caledonian compressional system changed and strike-slip movements prevailed in the Arctic-North Atlantic region. In Svalbard a significant graben and folding formation started (Faleide et al., 1984).

Extensional faults, which occurred from the Late Devonian to Early Carboniferous, are considered following pre-existing Caledonian structures, because they are mostly directed towards the north-east (Rønnevik et al., 1982; Faleide et al., 1984). The compressional features are thought to be associated with wrench faulting (Faleide et al., 1984). This fault model is explained by Ziegler (1978), who believed in the theory, that a major sinistral shear fault was vigorous at the west side of the Barents Sea. Thick layers of sediments were deposited in the grabens covering large basin zones (Faleide et al., 1984). According to Nalivkin (1973) The Upper Devonian basin is occupied with same age deposits as in the Pechora Basin respective - a mixture of carbonates and evaporates. However, the Upper Devonian rocks are absent in Svalbard (Faleide et al., 1984).

The carbonate shelf from the Sverdrup Basin to the Pechora Basin was formed in the Middle Carboniferous. Carbonate sediments contain an assortment of different facies, including evaporates and clastics. The thickness of the Middle Carboniferous- Lower Permian classification shows that there was a quiet and inactive tectonic period in almost the whole area, except between Bjørnøya and the coast of Norway, where faulting occurred (Faleide et al., 1984).

At the end of the Early Permian giant changes happened from a regional point of view. Terrigenous marine clastics prevailed. After uplift the Late Permian sediments were extensively deposited while carbonate-evaporate deposition stopped in Svalbard, Pechora (south from Novaya Zemlja) and the Wandel (East Greenland) sea basins (Faleide et al., 1984). Zielger (1978) believes that these changes are responsible for developing the sea

passage between the Arctic and the North West European Permian basins (Faleide et al., 1984).

Faulting activity during the Late Permian to the Early Triassic stopped except for the neighboring tilted block, which was later buried inside Loppa High. Regional subsidence between the Svalbard Platform and the region to the south attached high sedimentation rates and led to development of thick Triassic strata (Faleide et al., 1984). Thick Triassic layers are also found in the Sverdrup basin (Balkwill, 1978) and in East Greenland (Birkelund and Perch-Nielsen, 1976). Sea level fluctuations occurred irregularly and were related to unconformity and erosion (Faleide et al., 1984).

In the Early and Middle Triassic thick shales, siltstones and sandstones were deposited in Svalbard. While in the Late Triassic water became shallower and low energy sediments deposits formed (Faleide et al., 1984).

Many Mesozoic basins in northwest Europe, show simultaneous tectonic events, which can be related to rifting in the Arctic-North Atlantic region (e.g Zielger, 1978; 1981). The Arctic-North Atlantic rift system slowly opened in the Mesozoic resulting in a crustal separation between the two plates (North American-Greenland and European) (Talwani and Eldholm, 1977). The area was exposed to tensional stresses, which was followed by crustal separation and drifting in Northwestern Europe (Zielger, 1978).

The Mid Kimmerian phase affected the rift system in the Middle to Late Jurassic followed by subsidence in the Middle Jurassic and afterwards in Late Jurassic respectively. A deposition of a reedy layer of clay sediments in the rift basins followed (Faleide et al., 1984). This could be the reason why basin circulation became motionless. It is known that Upper Jurassic clays are a good source of rocks for petroleum because of their high content of organic material (Gloppen and Westre, 1982; Faleide et al., 1984). Mid Kimmerian tectonic movements stopped around the Upper Jurassic and further the Late Kimmerian regime began at the Jurassic-Cretaceous transition (Faleide et al., 1984).

In the Late Kimmerian between Norway and Greenland subsidence increased and large faults were created and later subsidence created new structural elements (Faleide et al., 1984).

2.1.6 Stratigraphy

Post-rift sedimentary succession of the eastern Vestnesa Ridge (Ritzmann et al.,2004) is subdivided into three units as established by Eiken and Hinz (1993), from bottom to top - YP1, YP2 and YP3 (Figure 2.1.6). The bottom YP1 sequence consists of syn and post rift deposits. YP2 which is located between YP1 and YP3 is characterized by contourites. The base of the glacial deposits represents a boundary, an unconformity between YP2 and YP3 that is believed to be 2.7 Ma old and it is the onset of the Plio-Pleistocene glaciations (Hustoft et al., 2009). The YP3 sediments at Vestnesa Ridge consist of late Miocene silty turbidites, hemipelagites (Bünz et al., 2012) and muddy-silty contourites of Weichselian and Holocene age, and it is believed that the rate of deposition was 9.6 cm/ka (thousand years) (Howe et al., 2008). However, sediment core analysis by Howe et al. (2008) showed that the last glacial maximum (LGM) was dominated by silty turbidites and resulted in high sediment deposition. Moreover, calculations showed that during the Mid to Late Weichselian the sedimentation rate was 105 cm/ka and decreased to +/- 10 cm/ka during the time between the LGM and the Early Holocene (Bünz et al., 2012).

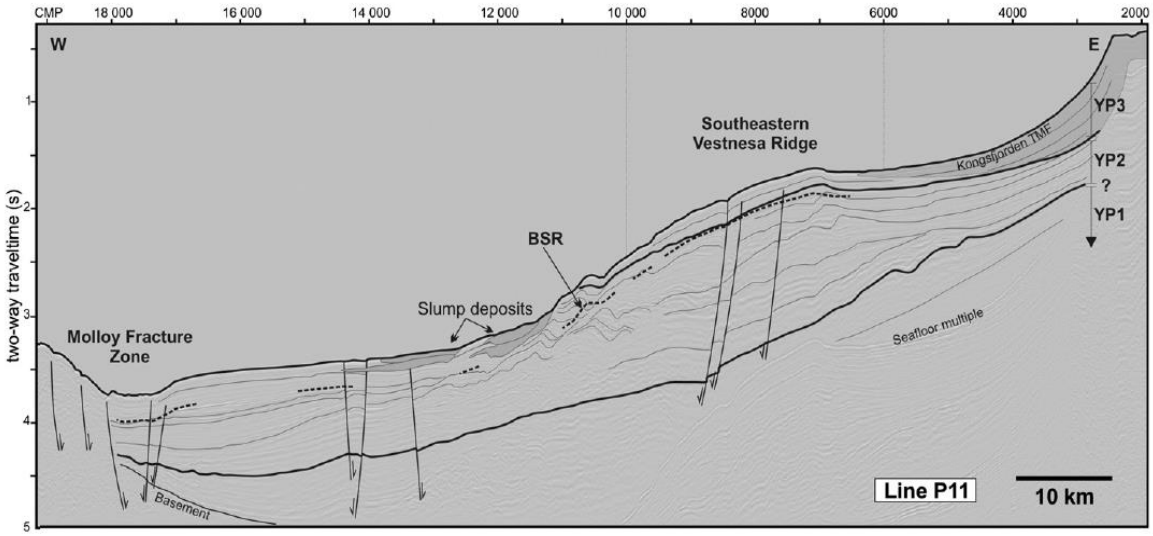

Figure 2.1.6: *Seismic stratigraphy of eastern Vestnesa Ridge. Subdivisions YP1, YP2 and YP3 are shown. The BSR is marked by a dashed line. Picture adapted from (Hustoft* et al.*, 2009).*

2.2 The Nyegga region

2.2.1 Geological framework

The Nyegga region lies in a water depth of around - 700 to - 800 m in the mid continental margin (Figure 2.2.1). The area is located at the northern side of the Storegga slide (Plaza-Faverola et al., 2011) with over 400 pockmarks lying on the seabed (Weibull et al., 2010; Hustoft et al., 2009). The area includes sediments within the gas hydrate stability zone

of the Naust formation (Plaza-Faverola et al., 2011). The glacial-interglacial sediment deposits are abundant in the Naust formation (Berg et al., 2005; Hjelstuen et al., 1999; Nygård et al., 2005). Sediments in this area contain several 100 m of debris flow deposits interbedded with thinner hemipelagic and contouric sediment deposits (Bryn et al., 2005). In the Storegga region, hemipelagic sediments and contouritic sediments which were deposited along the slope, dominated before the shelf edge glaciations. The ice sheet reached the shelf-edge throughout peak glaciations, and the slope was dominated by glacigenic debris flow deposition. The age of the Naust formation is definite to approximately 2.8-0 Ma (Rise et al., 2006). During the Eocene-Pliocene periods sedimentation rate was steady. During the Naust time with increasing sedimentation rate in water depths of 500 to 1000 m, sedimentation occurred from the inner shelf on the way to the continental slope (Eidvin et al., 2000; Rise et al., 2005).

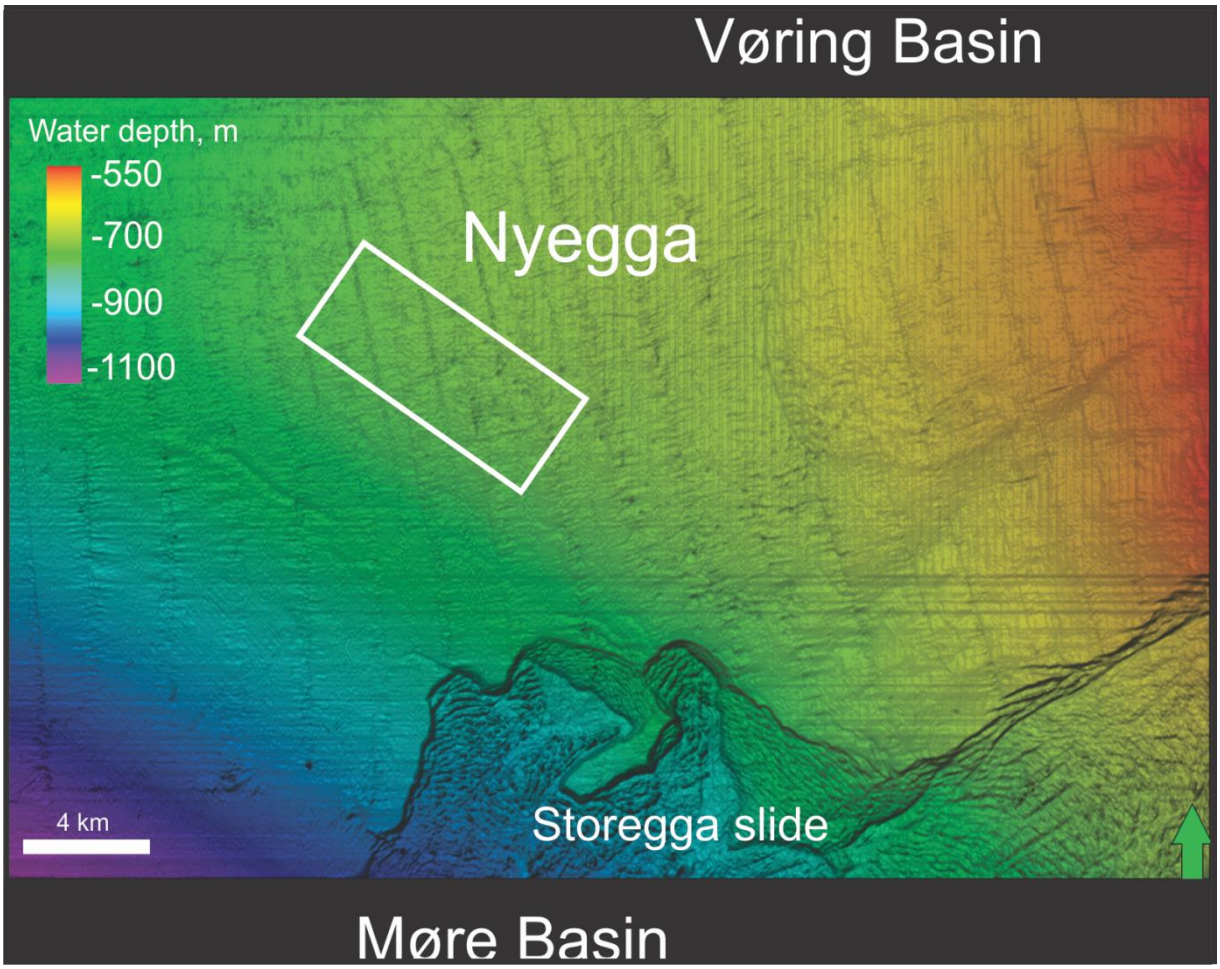

Figure 2.2.1: *Bathimetry map of Nyegga, offshore in the Norwegian Sea. White rectangular marks: location of dataset. Vertical exaggeration is set to 20.*

The Norwegian continental margin offshore mid-Norway from 62 - 70^{o} N contains a rifted volcanic margin which changes further up from 70 - 82^{o} to a sheared margin and continues along the western Barents Sea (Faleide et al., 2008).

The Norwegian margin consists of a shelf and slope which have significant differences in steepness and width. Earlier, before the formation of the NE Atlantic Ocean in the early Cenozoic, North and Barents Seas were part of a large Epicontinental Sea. The margins around this sea were connected and had a long history of post-Caledonian extension, which started in Devonian times, through Mesozoic, when finally in the early Cenozoic it experienced a breakup. Intrusive and extrusive magmatism on the rifted margins was left by igneous activity during the breakup (Faleide et al., 2008).

The transition between oceanic and continental crust is different when comparing rifted and sheared margins. The crustal thicknesses vary from 4 - 10 km in the ocean to 32 km near the coast (Faleide et al., 2008).

On the Norwegian margin three areas (Vøring, Møre and Lofoten-Vesterålen) are located which are separated by the East Jan Mayen Fracture Zone and the Bivrost Lineament/transfer zone. In the Møre and Vøring margins the lower crustal body builds the lower part of crust underneath the marginal highs and continues to the west with a thick crust. To the east it endures below the crust which was extended and thinned before the breakup (Faleide et al., 2008).

When the mid-Norwegian margin formed, several tectono-magmatic processes took place: 1) Lithospheric extension during Cretaceous-Paleocene that resulted in plate breakup and separation. 2) During late rifting, significant igneous activity and central rift uplift occurred resulting in flux of lavas in the Early Eocene. 3) From the Middle Eocene to present - continental margin subsidence and further maturation occurred (Faleide et al., 2008).

A slim shelf and a wide and prone slope describe the Møre Margin which is underlain by the deep and widespread Møre basin. It consists of several sub-basins separated by highs which were built during rifting. The Møre basins are in filled with sediments from Cretaceous times. The thickest sedimentary succession is located along the western part of the basin and is approximately 16 km thick shrinking landwards to 12 km thickness. In western and central parts of the Møre basin in Cretaceous succession, sill intrusions are frequently found because the western part is occupied by lava flows (Faleide et al., 2008).

The Vøring margin consists of several elements: the Trøndelag Platform, the Halten and Dønna terraces, the Vøring basin and the Vøring Marginal High. The Trøndelag Platform basin is filled with Triassic and Upper Paleozoic sediments. The Vøring basin as well as the Møre, can be divided in sub-basins and highs showing diverse vertical movements from the Late Jurassic to the Early Cretaceous. The Moho boundary is irregular and lying 25 km deep below basin. The thickness of the lower crustal body changes significantly, looking laterally through the area - from 0 to 9 km. Faleide et al. (2008) suggest that this is either because of variations in magma distribution processes or variations in pre-breakup structure (Faleide et al., 2008).

The Vøring plateau includes the Vøring Escarpment and the Vøring Marginal High. Last consists of rarely thick oceanic crust in the outer part and stretched continental crust roofed by thick Early Eocene basalts and mafic intrusions in the landward part (Faleide et al., 2008).

The Bivrost Lineament splits the Vøring and Lofoten-Vesterålen margins and denotes the end of the Vøring segments. This transfer zone is important in terms of margin structure, breakup and lithosphere stretching (Faleide et al., 2008).

The Lofoten-Vesterålen margin is distinguished by a narrow shelf and a steep slope. This margin differs from the Vøring and Møre margins, since sedimentary basins under the shelf are thinner and slimmer in width. The sedimentary basin has characteristic half graben structures with several basement highs (Faleide et al., 2008).

2.2.2 Breakup-related tectonism and magmatism

During the Mesozoic, after the Late Cretaceous - Paleocene, rifting breakup occurred in the NE Atlantic. Nowadays, NW Europe and Greenland lie within the area which once was the epicontinental Sea. The Campanian time which was famous for its brittle faulting resulted in rifting where many structures up domed Cretaceous sediments. Late Cretaceous - Paleocene deformations along Møre and Lofoten-Vesterålen margins are masked with lavas. The Late Cretaceous – Paleocene extension between Norway and Greenland was dominated by strike-slip movements (transform boundary, where two plates slide past each other) (Svensen et al., 2004).

The last breakup at the Norwegian margin occurred somewhere between the Paleocene and Eocene. During transition, sills disturbed the thick Cretaceous successions in Møre and Vøring basins. Greenhouse gasses started to evaporate into the atmosphere from

hydrothermal vents along the Norwegian margin, because of magma invading organic-rich sediments. Finally, after 5 myr of enormous magmatic activity during the breakup, the transition ended (Svensen et al., 2004).

2.2.3 Tectonic settings

Rifted margins, sometimes also called Atlantic-type or passive margins, may contain enormous stocks with hydrocarbons which is why they receive a lot of attention in terms of exploration efforts (Beaumont et al., 1982a).

The Mid-Norway basin covers the continental margin containing sediments raging in age from the Late Paleozoic (Devonian 419 - 359 Ma) to the Late Cenozoic (66 - 0 Ma). The tectonic evolution of the Mid-Norway and East Greenland continental margins consists of three main rifting events: Permian-Triassic (Paleozoic/Mesozoic), Late Jurassic - Early Cretaceous and Late Cretaceous - Early Tertiary (Mesozoic/Cenozoic) (Bukovics and Ziegler, 1984; Brekke, 2000). The mid-Norway continental margin consists of several sedimentary basins, which were laid over on the Caledonian seam between two cratons - Fennoscandian and Greenland. Subsidence in some basins started in the Devonian and was followed by a crustal extension during the early Late Carboniferous. The wrench movements caused fracturing and weakening of the crust in wide areas during the Devonian to the Early Carboniferous. The rifting processes were active for 270 Ma and persisted until the early Eocene. In the early Eocene crustal separation developed between Greenland and Fennoscandia - 56 - 48 Ma back. The long rifting stage and tectonic activity, which also continued after the crustal separation, is the biggest difference that separates the Mid-Norway continental margin from other passive margins in the world (Bukovics and Ziegler; 1984).

2.2.4 Paleozoic

The Paleozoic basin evolution started with two plate collisions which gave rise to the Ordovican - Early Devonian Caledonian orogeny. The Greenland - Laurentan and Fennoscandian - Russian plates collided. Moreover, the Norwegian - Greenland Sea was affected several times by sinistral movements from the Middle Devonian to the Late Carboniferous. Sinistral movement or left handed happens when the block which is located on the other side of the fault starts to move to the left. These movements provoked quick subsidence of the Old Red Sandstone basins. When these basins dropped, there was volcanic activity and movement of magma underground in the rocks (intrusive activity) (Haller, 1971; Steel, 1976; Bukovics and Ziegler, 1984).

Regional crustal extension occurred in the Norwegian - Greenland Sea, as well as in the Svalbard - Barents Sea at the early Late Carboniferous (Bukovics and Ziegler, 1984). Carboniferous and Permian clastics and carbonates, accumulated in half grabens during the extensive rift system in eastern Greenland (Haller, 1971). However, Bukovics and Zielger (1984) suggested that similar structures sank into the Norwegian Shelf, because of rare seismic evidence in Vega High. During the Late Palaeozoic, the Trøndlag platform sank rapidly and horsts were formed. As the crustal extension was active during the Late Permian, that led the Arctic Permian Seas to the transgression, meaning, the sea level started to rise (Bukovics and Ziegler; 1984).

2.2.5 Mesozoic

The Mesozoic can be characterized as complicated and long rifting stage, which can be divided in early and late phases. When the crustal extension accelerated in the Early Triassic (Early Mesozoic), rifting spread southward into the North Sea (Ziegler, 1982). Meanwhile, in Trøndelag Platform and Halten Terrace, syndepositional tensional faulting and listric faulting resulted in an accumulation of Triassic sediments (Figure 2.2.2) (Bukovics and Ziegler; 1984).

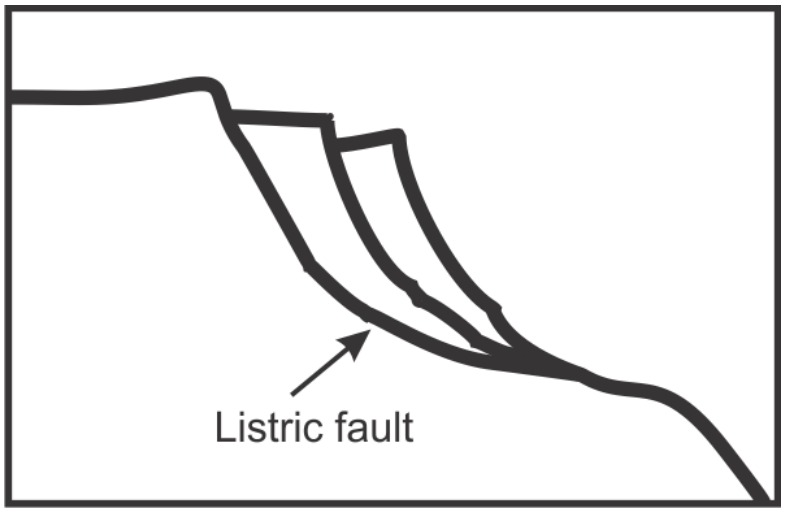

Figure 2.2.2: *Listric fault model. Modified from (Universidade Fernando Pessoa, Basic principles in tectonics).*

However, there was no evidence of Triassic or Mid-Jurassic volcanic activity (Bukovics and Ziegler; 1984) and more intense faulting during the Jurassic took place in the western part of the Trøndelag basin than in the eastern part (McKenzie, 1978). From the Late Paleozoic to the early Mesozoic relief in the Norwegian continental margin was smoothened by sedimentation (Eldholm et al 1989). A huge system with basins and ridges was formed in middle to late Jurassic time (Figure 2.2.3).

From the Late Paleozoic to the Mid-Mesozoic subsidence in the Norwegian-Greenland Sea during rifting was defined with intense thinning of the crust and mechanical stretching (McKenzie, 1978).

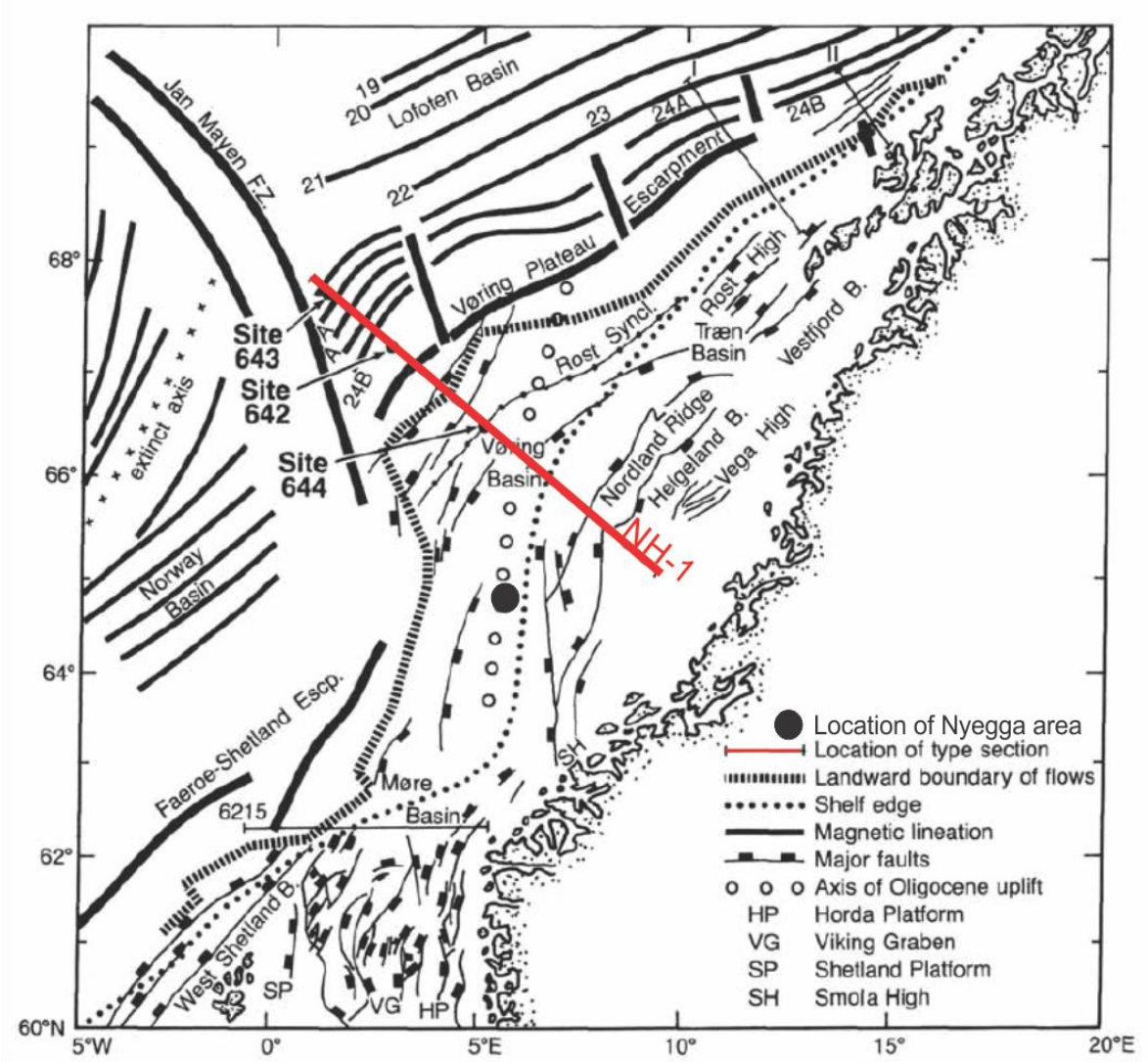

Figure 2.2.3: *Main regional features of the Norwegian continental margin. Modified from (Eldholm* et al.*, 1984).*

During the second stage of rifting the Trøndelag Platform was little affected by faulting during the Late Jurassic and Early Cretaceous. The whole area offshore mid-Norway was strongly affected during the Jurassic to the Cretaceous, when major rift systems in Møre and Vøring basins started to subside rapidly, while eastern parts of the Møre and Vøring rift system uplifted (Bukovics and Ziegler, 1984).

Several different authors suggest numerous mechanisms for rifting that could promote uplift of the main rift flanks (Hellinger and Sclater, 1983; Bukovics and Ziegler, 1984):

- A) Geometric reasons: There is a geological statement that doming leads to rifting, because there is a genetic relationship between them (Bott, 1981).

- B) Non-uniform extension: also referred to as the depth-dependent extension model. Separation of lithosphere in two different depth zones, where each of them undergoes dissimilar volumes of extension. By using this model one can find out subsidence, temperature change, crustal and lithospheric thinning, when the size of the extension has been specified (Beaumont et al., 1982a).
- C) Failure of the continental lithosphere by tensional stresses (Bukovics and Ziegler, 1984). Rifts are often associated with crustal doming (Neugebauer et al., 1983) and from model calculations it is shown that flanks on both sides of a rift can be uplifted while the middle rapidly subsided (Bukovics and Ziegler, 1984; Neugebauer, 1978).
- D) Cause of mantle plumes (Morgan, 1972). "*The heat flux from the lower mantle heats the subducted oceanic crust until it becomes buoyantly unstable and forms an upper mantle plume*" (Turcotte, 1981; Morgan, 1972).
- E) Regional isostatic adjustment: "*The thermal and rheological consequences of lithospheric extension at rift margins make flexural subsidence relatively less important than in foreland basins*" (Beaumont et al., 1982b). Flexure can be responsible for uplift during rifting (Bukovics and Ziegler, 1984; Beaumont et al., 1982b).

All these mentioned types can explain uplift of the flanks of subsiding grabens as the origin of rifting are changes in lithospheric emplacement due to extension (Bukovics and Ziegler, 1984; Bott, 1979).

There are few different opinions why Cretaceous subsidence was rapid (Bukovics and Ziegler, 1984). Ziegler (1982, 1983) mentions possible mechanism, which led the Møre-Vøring area to rapidly subside during the Cretaceous. In his opinion, this was because of crustal thinning by sub crustal erosion. On the contrary, Hanisch (1984) assumed that subsidence in the Møre and Vøring basins was due to mid and Late Cretaceous sea floor spreading (Hanisch, 1984).

The Vøring margin, which is also called Nordland margin, is cut by the Kristiansund - Bodø Fault complex transition zone. This area consists of the Nordland Ridge, Vega high and the Helgeland Basin. The Vøring basin in the west was formed by block faulting and subsidence and holds thick Upper Cretaceous sequences (Figure 2.2.4) (Eldholm et al., 1989).

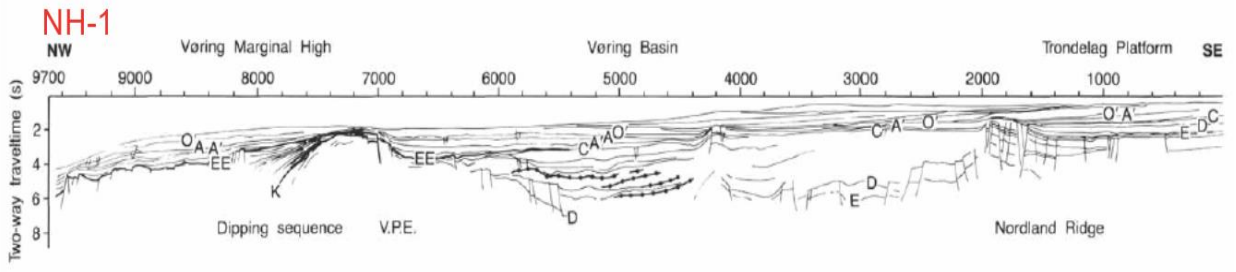

Figure 2.2.4: *Interpreted seismic section across the Vøring margin, showing main geological provinces and structural elements modified from (Skogseid, 1983). Location of seismic section is shown in figure 2.2.3 - red line.*

When in the Early Cretaceous Møre and Vøring basins subsided, their sides remained high (Bukovics and Ziegler, 1984). In the mid-Cretaceous major faulting terminated and rifting activity became less active. After approximately 30 million years in the Late Cretaceous an already wider area, including the Trøndelag platform and the Halten Terrace subsided (Bukovics and Ziegler, 1984).

The Cretaceous evolution lasted for around 79 million years. During this time the area experienced subsidence where major rift events induced graben subsidence by crustal stretching. In the Late Cretaceous rifting decreased but did not yet stop. In this time the subsidence in the Mid-Norway shelf was probably indolent and related to lithospheric cooling (Bukovics and Ziegler, 1984).

2.2.6 Cenozoic

The Paleogene crustal separation occurred in the end of the Cretaceous and Paleocene when rifting increased again (Bukovics and Ziegler, 1984). After a quiet period during the Early Paleogene, a rifting termination phase developed, when only Western Møre and Vøring basins were affected by intrusive and extrusive igneous activity (Bukovics and Ziegler, 1984). Nowadays the total Cenozoic sediment sequence at the Vøring Margin is 2 - 2.5 s (seconds) two-way travel time (TWT) thick, but 3.5 s (TWT) in Møre (Bøen et al., 1984). Furthermore the marginal highs are covered with less sediment sequences than the areas in the landward basins (Eldholm et al., 1989).

The phase of crustal extension is reactivated in the Paleocene - Early Eocene. In the Early Eocene crustal separation and seabed spreading occurred between the Norwegian-Greenland Sea. Vøring sediments subsided slower than Møre sediments (Bukovics and Ziegler, 1984). The continental break-up phase in Møre shelf was educed by volcanic extrusions (Bugge et al., 1978). In this late rifting phase dyke (cuts stratification vertical) intrusion into the crust probably played a major role (Hinz et al., 1982). To the west of the Møre and Vøring basin axis, there was obvious igneous activity, where dykes and sills (cuts stratification horizontal) were located in Jurassic to Eocene sediments and they continued

westwards, where younger stratigraphical levels occurred (Bukovics and Ziegler, 1984). During the crustal separation in the Late Paleogene, subsidence of the Norwegian margin was influenced not only by the cooling of lithosphere and loading of sediments, but also by compressional deformations, for example, in the Jan Mayen fracture zone, as transform movements (Bukovics and Ziegler, 1984).

During the Pleistocene, the erosion of the coastal basin margin is thought to be affected by the ice melting, unloading in mainland areas (Bukovics and Ziegler, 1984).

In the Cenozoic Møre and Vøring basins were tectonically affected, but not in the same way (Bukovics and Ziegler, 1984). Vøring basin was affected significantly by Oligo-Miocene transpressional deformations. However, Møre basin, in which the famous Storrega slide is located, was activated by Holocene tectonic activity (Bugge et al., 1979).

2.2.7 Stratigraphy

The closest wells that are located near the Nyegga region provide information about sediments, age and deposition environment, as well as insight on lithology and stratigraphy of the surrounding area (Figure 2.2.5).

Nordland Group (Nordland gruppen): Contains two formations - Naust and Kai. They consist of variable claystone, siltstone and sandstone. Age varies from Miocene to recent. Depositional environment: marine, where the upper part is of glacial to glacio-marine origin.

Naust Formation (Naustformasjoen): The name of this formation comes from a Norwegian word meaning '*boathouse*'. This formation belongs to the Nordland group. The thickness of the Naust formation is not precisely known, but generally the Naust Formation is several hundred meters thick in the Haltenbanken - Trænabanken area. Lithology is described with interbedded claystone, siltstone and sand, where in the upper part it is made of very coarse clastics. The Naust Formation is continuous across the mid-Norwegian Shelf. The Naust Formation is of Late Pliocene age and could be 2.8 - 0 Ma (Rise et al., 2006). Depositional environment: marine environment, where transition to glaciomarine environment occurs in the upper part.

Kai Formation (Kaiformasjonen): This formation belongs to the Nordland group. Lithology is described with clay stone, siltstone and sandstone with stringers. Glauconitic, pyrite and shell fragments are found as admixture. The formation is of Early Miocene to Late Pliocene.

Hordaland Group (Hordalandgruppen): In the Hordaland Group only one formation is found and called 'Brygge formation'. The Hordaland Group occurs throughout Haltenbanken. It thins eastwards and is eroded on the Nordland Ridge. In the Haltenbanken area the group consists of clay stones and some sandstone. The age of this group is interpreted between Eocene to Early Miocene. Deposition environment is described as a deep marine environment.

Brygge Formation (Bryggeformasjonen): This Formation belongs to the Hordaland group. Lithology consists mainly of clay stone with stringers of sandstone, siltstone, limestone and marl. As well as in the Kai Formation, glauconitic, pyrite and shell fragments are seen in sandstones. From Early Eocene to Early Miocene time, sediments were deposited in deep marine environment which is describing this Formation.

Rogaland Group (Rogalandgruppen): The Rogaland Group consists of two Formations: Tang and Tare. This Group on Haltenbanken consists of clay stone with some siltstone. Tuff is found in the upper part. The group represents ages from Danian to Late Paleocene. Depositional environment is characterized as deep marine.

Tare Formation (Tareformasjonen): One of two formations, which belong to Rogaland Group. Lithology is made from dark grey to brown clay stone, with selected sandstone stingers and some tuff. Formation is of Late Paleocene age and deposited in deep marine environment.

Tang Formation (Tangformasjoen): Lithology is described with dark grey to brown claystone with some sandstone and limestone. Deposited in a deep marine during Danian to late Paleocene (Dalland et al., 1988).

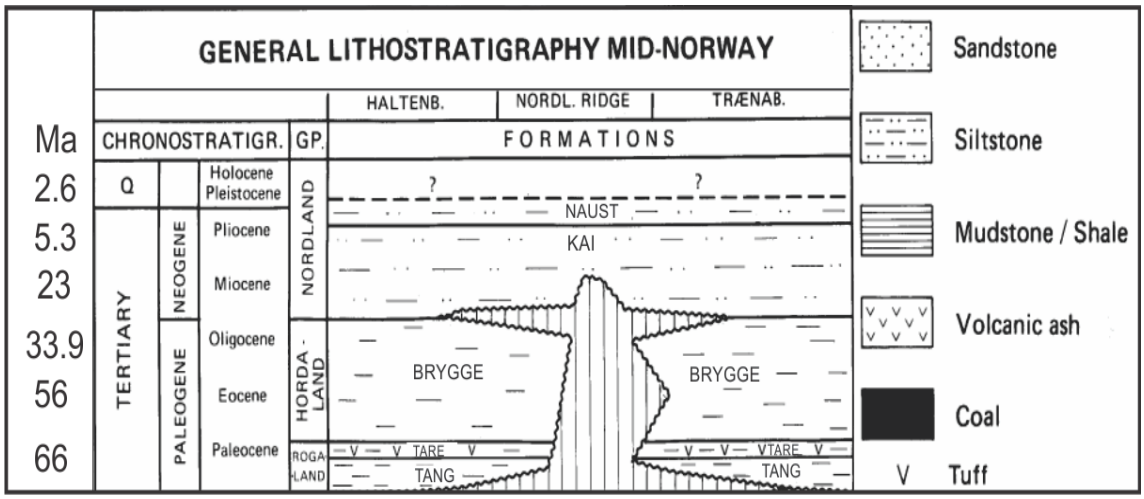

Figure 2.2.5: *Time and lithostratigraphic section from the Halten Terrace. Modified from (Dalland* et al.*, 1988).*

There are 5 seismic units that represent glacial and thinner interglacial sediment layers inserted in between. These interglacial sediments consist of contour current-controlled deposits (Bryn et al., 2005; Plaza-Faverola et al., 2010).

- **Naust N** contains of glaciofluvial and marine processes (1.5 - 2.8 Ma) (Rise et al., 2006).
- **Naust A** (1.5 - 1.6 s (TWT)) (Figure 2.2.6) consists of hemiplegic marine sediments and remains from land based glaciers. Seismic facies characterized by enhanced reflections. Top of the Naust U is a regional unconformity (Plaza-Faverola et al., 2010).
- **Naust U** (1.3 - 1.5 s (TWT)) shows periods of glaciations and consists of glacial marine sediments and interglacial sediments (clays with sands and gravels). Characterized by strong amplitudes (Plaza-faverola et al., 2010).
- **Naust S** (1.2 - 1.3 s (TWT)) consists of glacial marine sediments, indicate local contourite deposits.
- **Naust T** (1 - 1.2 s (TWT)) is separated by lower and upper part by intra Naust T (INT) and it consists of marine sediments that were partly removed by Storegga slide events (Berg et al., 2005).

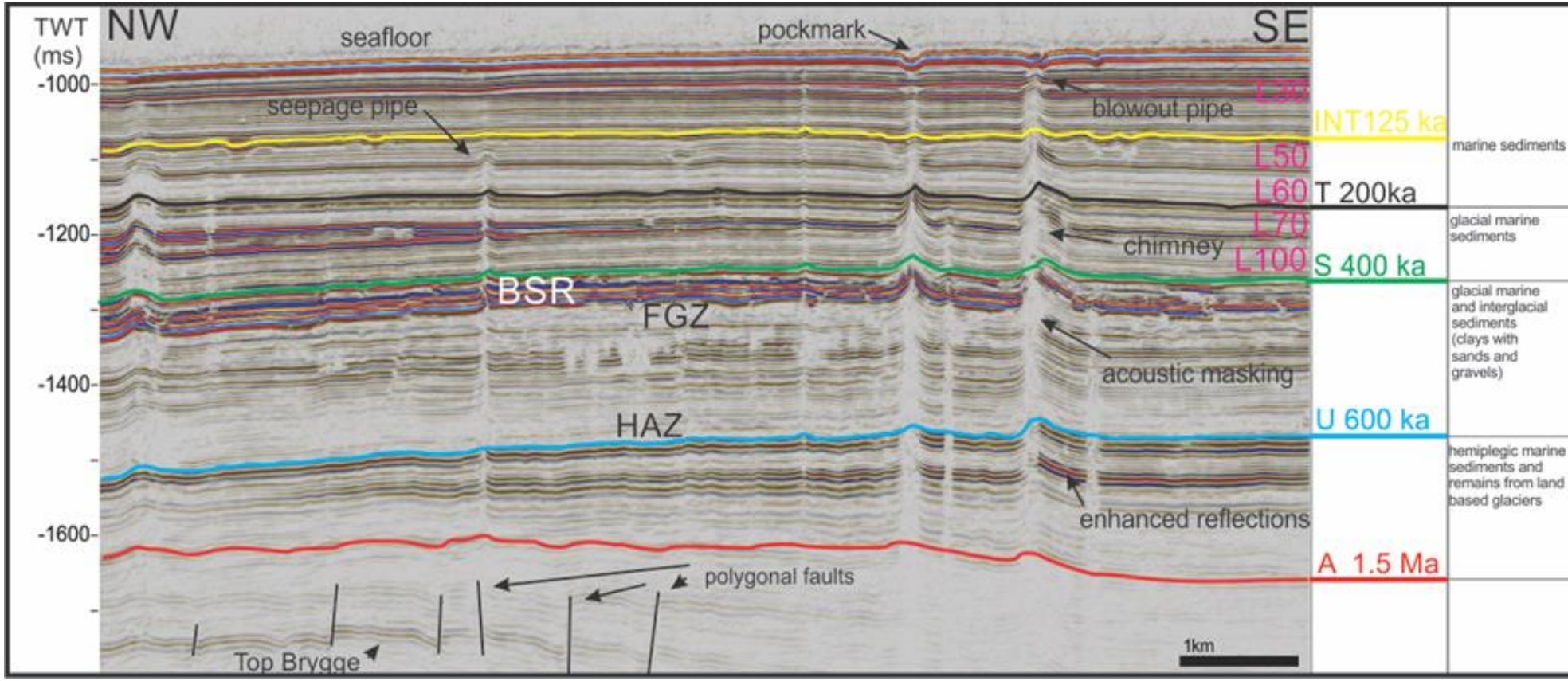

Figure 2.2.6: *Stratigraphy for Nyegga region. Ages from (Rise* et al.*, 2006). Used X line 194 to show stratigraphy for region. In pink color seismic layers from (Plaza-Faverola* et al.*, 2010b).*

3 Fluid flow systems

3.1 Focused fluid flow systems on passive continental margins

Berndt (2005) has developed 4 types of systems that control fluid flow: compaction controlled, volcanism controlled, freshwater and petroleum systems.

Lithology, sedimentation rate and stratigraphy are processes that are responsible for fluid enhancing that were expelled during compaction (Berndt, 2005). Sandy sediments have high permeability and hydraulic conductivity, which allows pore fluids to scatter fast (Bredehoeft and Hanshaw, 1968). In General, sediment consolidation is a very slow process, which keeps constant hydrostatic pressure, on the other hand, some water-expelling rocks are under high excess pore pressure, since high sedimentation rates impedes pore fluids to be scattered at the same rate as the load rises through sediment compaction (Dugan and Flemings, 2000). Sometimes overpressure can change fluid flow from homogenous scattering to focused flow (Berndt, 2005). Dalland et al. (1988) mention that in the Norwegian margin polygonal faults are placed in very fine-grained hemipelagic sediments that belong to stratigraphic layer - Kai Formation (Dalland et al., 1988) and they terminate in pipe structures (Figure 2.2.6) (Berndt et al., 2003). Mostly pipes are rising from the polygonal faults, but sometimes it is believed that their source is gas reservoirs in Tertiary times sediments. However, it is vague if pipes originate from episodic blow-outs or from continuous flow (Berndt, 2005). Gay et al. (2004) question, if polygonal faults that are connected to pipes help fluids to continue their flow, because faults can hold less permeable sediments, than adjacent areas. Cartwright et al. (2003) believe there are three processes that form polygonal fault systems: gravitational collapse, synaeresis of clay minerals and density inversions (Berndt, 2005).

Svensen et al. (2004) discovered during their research that on the mid-Norwegian margin around 3000 pipe structures are found and are linked to previous mentioned processes (Berndt, 2005).

3.1.1 Pipe bypass systems

In general, pipes are vertical zones of fluid expressions, which can be found in my data beneath the pockmarks (Figure 3). They can be defined as seismically columnar zones with disturbed reflections, so called gas chimneys. Sometimes they can be confused with artifacts, for instance, velocity anomalies or migration anomalies (Løseth et al., 2001, 2003).

To determine artifacts from true features, it is important to consider stratigraphic and structural background (Cartwright et al., 2007). Among many authors, the structure of the pipes and chimneys is not well understood. There are varieties of pipe structures that prove that they are not identical. They can consist of stacked pockmark craters, up bended, down bended reflections or high amplitudes, that are small gas accumulation pockets. Inside the pipes deformed reflections are formed due to faulting and folding (Figure 5.3.4) (Løseth et al., 2001, 2003). One reason to describe pipes can be from Cartwright et al. (2007) who suggested dividing pipe bypass systems into 4 categories: dissolution pipes, blowout pipes, seepage pipes and hydrothermal pipes.

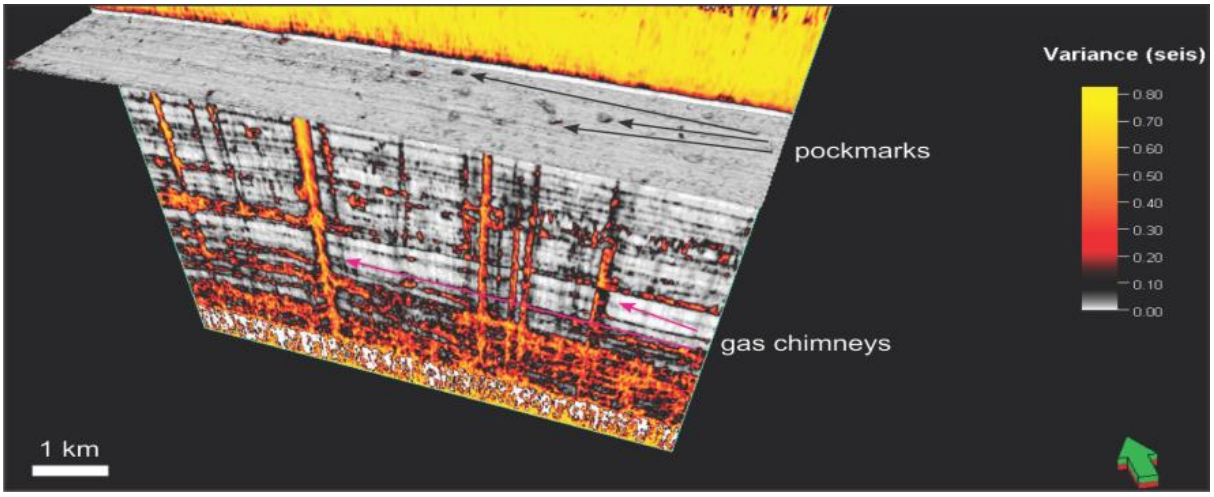

Figure 3: *3D variance of surface attributes 15ms (TWT) below seafloor in Nyegga. Seismic section of X line 238 is shown and vertical exaggeration is 10.Orange vertical lines are chimneys shown by pink arrows. Some of them are connected to pockmark marked with black arrows.*

Dissolution pipes can be found in regions of evaporites or carbonates. They are formed by dissolution of rocks (karst). Their size is related to dissolution size and the strength of overburden (Branney, 1995). These types of pipes are formed by the rate of solution (Stanton, 1966).

Hydrothermal pipes are formed when there is a high pressure of hydrothermal fluids, which are associated with igneous intrusions. They can affect sealing sequences of cap rock. Hydrothermal pipes are documented on seismic data, because they have a direct connection with sills, even more, pipes are fed by igneous sill. They can be recognized with their high amplitude reflections (Cartwright et al 2007). By the fact that pipes are associated with mafic sills, they are common sites of mineralization and referred to as breccia pipe bodies (Barrington and Kerr, 1961; Bryner, 1961). Breccia pipe bodies are formed by huge amounts of high velocity fluid flow (Rove, 1947; Sohnge, 1963). From their formation, in seismic data

it is seen even after millions of years that hydrothermal pipes can act as a fluid conduit despite huge time gaps in between (Svensen et al., 2004; Hansen et al., 2005).

Blowout pipes (5.2.12 and 2.2.6) are seen on seismic data as a columnar zone of disturbed reflections or vertically stacked amplitude anomalies. They are notable with paleo pockmarks (Løseth et al., 2001). Mostly pipes are circular even though sometimes they emanate from fault planes. They can be found in places where there is over pressured fluid flow, for example, at the crests of structures or above gas reservoirs (Figure 3.1.1). High pressure gradient drives fluids and they are resulting in columnar pipes (Cartwright et al., 2007). They are complicated to understand. One of the main arguments can be that they represent rapid blowout (Løseth et al., 2001). Cartwright et al. (2007) suggest that blowout pipes are formed in highly dynamic processes and therefore maximum fluid flow occurred at the time of formation. While vertical stacking of pockmark craters shows evidence of episodic fluid flow (Cartwright et al., 2007).

In their seismic characteristics **seepage pipes** (5.2.12 and 2.2.6) are similar to blowout pipes because they form above gas reservoirs. One of the characteristics that seepage pipes lack of blowout pipes is the chaotic fluid eruption below upper pipe termination, and no link to the pockmark (Figure 2.2.6). The main difference between these pipes is that seepage pipes occur in sand or silt sediments, but blowout pipes in fine-grained sealing sequences respectively (Cartwright et al., 2007).

In all three areas: Nyegga, Vestnesa active (A2), Vestnesa less active (A1) respectively, seepage and blowout pipes are the most abundant. However, chimneys/pipe structures vary in diameter, height and whether or not they reach the seafloor.

3.2 Plumbing system

A plumbing system is a highly complex system which includes fluid expulsion, seepage and venting in both passive and active continental margins (Talukder, 2012).

Cold seeps only concern seepage and venting from seabed structures as pockmarks, mud volcanoes, where the main agents are gas, water and sediments. Furthermore, the main elements of the plumbing system (such as venting and seeping features) transport fluids through the subsurface into the water column. A plumbing system covers the whole area from the source up to the seabed, where fluids expel (Talukder, 2012). However, since pathways for fluids are long, branched, cranky and complex, the seepage on the seabed is not always located directly above their accumulation (Figure 2.2.6) (Abrams, 2005).

Talukder (2012) divides fluid expulsions in 2 types, where fast flow of the fluids is described as venting and slow fluid leak as seeping. While Mazzini et al. (2009) compare chimney related structures with mud volcanoes, as seeping of the gas is continuing during quiescent period while in active, episodic period fluidized sediments are expelled. Generally rock/sediment structure, tectonics and interaction between them, play a very important role in making plumbing system (Talukder, 2012).

A plumbing system mostly depends on, how sediments will act during different mechanical deformations. The moment of overpressure generation is very important in terms of defining the permeability of sediments, because different over pressured sediments can act differently (Talukder, 2012). Certain sediments become ductile after being exposed to overpressure. If the sediments are over-pressured in the later stages, they become over-consolidated and can act brittle (Brown, 1994). Moreover, developments of fractures and faults are acting as pathways for fluids. Cold seeps are mostly present when there is an over pressured layer somewhere in the sediment column. The cause of the overpressure is a steady decline of the disequilibrium triggered by fast sediment/tectonic loading or if the permeability of the sediments is too low. During slow burial or if there are highly permeable sediments, equilibrium between overburden and reducing pore fluids preserves and accordingly compaction occurs. For compaction to occur pore water must be expelled during burial and in normal conditions pore pressure will increase with depth (normal hydrostatic gradient) (Talukder, 2012).

In the case of fast burial or if there are low permeable sediments, a disequilibrium will occur and pore pressure will increase up to supra-hydrostatic level, because dewatering is hindered (Osborne and Swarbrick, 1997).

Overpressure delays compaction, but increases as burial develops (Osborne and Swarbrick, 1997). Disequilibrium compaction is the main cause for overpressure in passive margins and is frequent in clay, mud, and shale, because they have a low permeability. During the process when sediments are enhanced with organic matter it can lead to overpressure, because hydrocarbon fluids implicate volume increase (Dimitrov, 2002). Overpressure in active margins if compared with passive can be greater (Saffer and Tobin, 2011), because development of vertical and lateral compression leads to heavy tectonic loading of sediments (Taylor and Leonard, 1990), nevertheless, also accumulation of sediments is different (Talukder, 2012). Based on these assumptions, fluid production, as well as the whole hydrological system in active margins is more complicated than in passive margins (Saffer

and Tobin, 2011). Overpressure development and accordingly high fluid pressure is mostly found in areas of lateral compression (Behrmann, 1991) and places where sediments are low permeable causing short blockage of flow (Neuzil, 1986). Chemical process where smectite forms to illite can be responsible for overpressure, which further leads to seeping fluids (Mascle and Moore, 1990).

3.2.1 Faults

Permeability of the faults could be one of the main controlling factors in a plumbing system. For instance, layers that are next to each other but with different permeability can affect fluid flow. When gas is migrating out of the reservoir to reduce pore pressure, a fault can seal again. Nevertheless, seepage can be also stopped because the development of carbonate may seal the plumbing system (Talduker, 2012). First the seepage gets slower, then stops, since carbonate crust blocked the pipe (Hovland, 2002).

When fault dilates, fluid pressure can overcome lithostatic pressure so evoking sediment failure and fluids can easily migrate upwards through the fractures or pass faults. After escape of the fluids, pore pressure drops and fluid pathways can close until the next overpressure develops. When fluid migrates upwards through the faults (e.g. Figures 5.1.6A, 5.1.8, 5.2.7A and 5.2.7B) it reaches shallow depths where fault sometimes is not permeable, but because of buoyancy and decreased lithostatic pressure, fluids can move through the overburden and reach the surface. Thereby seeps are sometimes not aligned with the fault, but can be laterally aside (Talukder, 2012). In a few places in the mid-Norwegian Margin polygonal faults are connected with the seafloor (Berndt et al., 2003). The varying fluid pressure in subsurface will define if the fault will let fluids through, or block them (Talukder, 2012).

3.2.2 Background on fluid flow

Not only in active continental margins has fluid flow played an important role, but also in passive continental margins, because their sediments are the same dynamic environments. Fluid escape from compacted sediments through the seafloor and changes in water temperature forces gas hydrate systems to move their location as well as magmatic intrusions that boil the pore water and push fluids up to the surface. This process includes fluid migration into the sedimentary basins and out of them. Focused fluid flow covers chimneys, pipes and hydrothermal vents. Results, that are making these features are visible on the seafloor as pockmarks (Figures 5.1.1, 5.2.1, 5.3.1) mud mounds, craters (Figure 5.3.1)

(Berndt, 2005). In addition, Bugge et al. (1987) has mentioned that focused fluid flow can be reason for submarine slides (e.g. Storegga slide) and Tsunamis.

In general, fluid migration couldn't exist without fluid supply, besides all fluid types have the ability to migrate upwards to the seafloor. Fluid migration can occur at any depth, furthermore different types (coarse grained, fine grained, muddy, soft, compacted) of sediments will affect migration differently, but the same characteristic inherent to every fluid escape through the seabed remain – eroding of the sediments. There are two main driving forces responsible for fluid movement that work solitarily and together: Buoyancy and excess pore fluid pressure (overpressure) (Figure 3A) (Judd and Hovland, 2007).

The buoyancy is a function of bulk-density contrast (Judd and Hovland, 2007). It will drive gas bubbles and other fluids up to the surface (Clayton and Hay, 1994), while overpressure occurs if during burial, pore fluids cannot drain from fine grained sediments, because the speed of burial is faster than compaction. During burial, contact between mineral grains reduces and sediments with high fluid content will not be compacted but remain unconsolidated (Judd and Hovland, 2007). Sediments are compacted when they are buried deeper thus the load of the overburden increases. Also density increases, but porosity and permeability decrease. The sediment compaction depends of lithology and diagenetic processes. Pore fluid pressure is rising due to overburden. The pore pressure increases with depth and it is equal to hydrostatic pressure. If the rate of fluid pressure generation results from either loading, biogenic or thermogenic processes, gas production is lower than the rate of dispersion (Berndt, 2005).

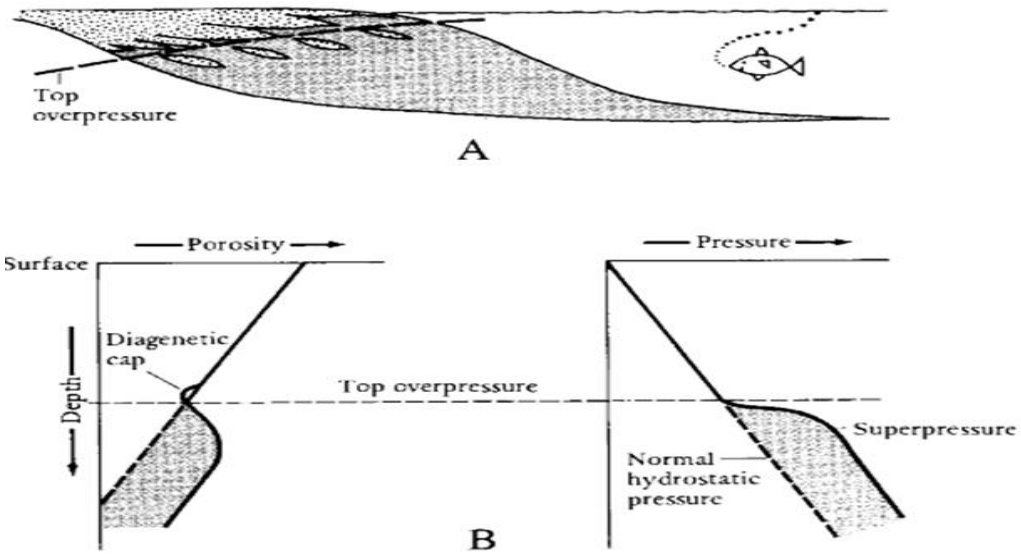

Figure 3A: *(A) cross section through a delta to show that overpressure occurs beneath the break-up zone where there is no longer any sand beds to act as conduits to permit muds to dewater. (B) depth-porosity and depth-pressure curves, indicating how overpressuring may occur due to undercompaction. From (Selley, 1998).*

Fundamentally, seeping fluids in their roots form deep in the subsurface from thermogenic source. As fluid flow is related with hydrocarbon leakage, it is important to identify leakages because it could empty the trap from hydrocarbons. Different leakage mechanisms prevail, when the hydrocarbons are moving from reservoir through a cap rock (Judd and Hovland, 2007).

Fracture flow, Darcy flow and diffusion are the main mechanisms in consolidated sediments. Fracture flow is one group, where fluids are flowing through fractures. It can occur: along fractures; in hydro-fractures, in areas with overpressure; along tectonic fractures, above salt domes (salt has a different density) (Løseth et al, 2009); in natural micro rock fractures (Brown, 2000) or as Løseth et al. (2001) suggested - in fracture pipes. Leakage flow from fractures can be high in terms of rates (Roberts and Nunn, 1995).

One of the mechanisms that help fluids migrate upwards is gravity. When fluids enter a permeable rock they flow through the pore spaces. Using Darcy's law, the rate of flow can be calculated (Judd and Hovland, 2007). The rate of flow (Q) is calculated (Equation 1) using Darcy's law equation:

$$Q = KAh/l$$

Equation 1: *Darcy's law equation to calculate the rate of flow. Coefficient Q: The rate of flow, Coefficient K: permeability of aquifer, Coefficient A: vertical area where fluid flow is possible, H: height, (h/l): hydraulic gradient (must be enough to overcome the frictional resistance and ability to flow through the aquifer). Equation from (Judd and Hovland, 2007).*

Fluid flow in porous sediments depends on Darcy's Law. The ability to flow through the rock depends on its ability to drive fluids, which in return is a result of pore water pressure differences. Darcy's Law is applicable to most types of fluid flows except flows involving blow-outs, small scale flows and large fractures compared to the area of interest (Berndt, 2005).

Fluids may flow through normal pore spaces, open faults, fractures or joints. Conduits are used by fluids after fluid pressure has squeezed through between the mineral grains. Each fluid type has its own physical characteristics that allow them to migrate. For example, methane molecules are larger than water molecules, but smaller than oil molecules. In places where methane molecules can easily go through narrow passages, oil will not pass through. Gas bubbles are bigger and cannot get through the pores, but pore water containing dissolved methane could migrate through the pores (Judd and Hovland, 2007).

When fluids first start moving through a rock or sediment they need to overpass the capillary entry pressure and find a place where resistance is weakest. Migrating fluids then use separate pathways, instead of using the whole area. Impermeable areas, however, will not allow fluids to migrate further, where a thin clay layer for example, will work as effective as thick one (Judd and Hovland, 2007).

There are two types of opinions when talking about fluid flow against faults and fractures. One can say that faults prevent fluid flow, some that they allow fluids to migrate through them (Bethke et al. 1991). Both can be truth, though it depends on the perspective. Clayton and Hay (1994) claim that deep buried faults and fractures act as a seals, not as migration pathways. While Talukder (2012) thinks that faults can act either like seal or conduits.

Fluid flow can be continuous and reactivated. Sometimes it collides with traps or places with lower permeability that prevents flow. Good traps hold flow until the spill point is reached, but bad traps just let fluids go through. Pressure in the subsurface continues to rise as the height of the reservoir increases. When critical overpressure is reached, the fluids are released (Judd and Hovland, 2007). Harrington and Horseman (1999) think that each time when a seal fails it releases a pulse of fluid to shallower sediments, where they can be trapped again. Overpressure that overcomes barriers decreases towards the surface as weaker sediments collide. Overpressure decreases and accumulation will become smaller, that's why in small depth shallow gas accumulation holds less gas than in reservoirs that are deeper (Judd and Hovland, 2007).

A hydrocarbon generates from source rocks, and then they escape from the source rock into permeable layers which is called 'Primary migration'. Movement inside these permeable beds is called 'Secondary migration' (Selley, 1998). Then fluids from the reservoir migrate through the cap rock into the overburden (Judd and Hovland, 2007). This process takes a long time until fluids are finally reaching the seabed (MacDonald et al. 2004). If undisturbed, flowing fluids reach the seabed, yet traps can prevent fluids to flow further, trapping them inside reservoirs (Judd and Hovland, 2007). A trap is one of five essential fundamentals to prevent fluids from further movement (Selley, 1998). Levorsen (1967) defined a trap as (Figure 3.1) *"the place where oil and gas are barred from further movement"*. Some of the traps can leak and fluids continue their way up towards the surface through the cap rock. If there is a continuous flow from a leaking reservoir, the fluid supply will be stable. If there is an intermediate accumulation, the fluid supply will be irregular.

Sometimes good migration pathways can be connected with short-distance faulted pathways and with long distance lateral pathways that end in a single pathway. Nearly all petroleum reservoirs are leaking (Judd and Hovland, 2007).

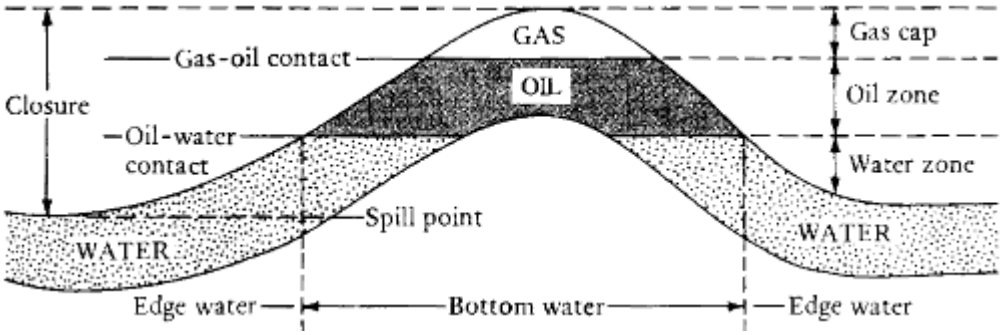

Figure 3.1: *The simplest type of trap - Anticline trap. Modified from (Selley, 1998).*

There exist several examples when sediments and gases interact, resulting in different features. For instance, gas slowly injected under a clay layer results in seabed doming. Or, when gas is injected rapidly under a thin clay layer, it results in a seabed crater. Earthquake events could trigger gas escape as it has been recorded in North Sea. Moreover, it is known that during earthquakes new pockmarks were formed (Judd and Hovland, 2007).

Changes in global sea level are a part of the seabed fluid flow. During times when sea level rises, hydrostatic pressure increases together with shear strength. Hydrostatic pressure is the weight of the water column, so when water depth increases, water is getting heavier. Once hydrostatic pressure drops it causes capillary migration (Judd and Hovland, 2007).

During fluid level increase, pressure is reduced and it will help methane and other gasses to come out of solution, reducing bulk density accordingly. It means, if there will be free gas in bubble-form it will expand and reduce bulk density (Berndt, 2005; Judd and Hovland, 2007) (Figure 3.2.1).

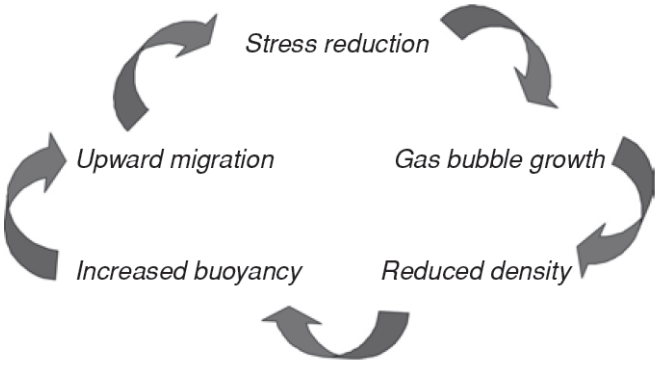

Figure 3.2.1: *Gas migration cycle. Picture adapted from (Judd and Hovland, 2007).*

3.3 Fluid flow systems in the Vestnesa Ridge

The Vestnesa Ridge consists of gas hydrate bearing sediments and evidence shows that there is an active fluid flow. The same structures can be found in the Nyegga region, such as: pockmarks, pipes, and chimney systems (Bünz et al., 2012). There are two study areas in the Vestnesa ridge: A2 (active) and A1 (less active) (Figure 2.1.3). In both areas indications of gas flares and active fluid flow expulsion are visible (Hustoft et al., 2009). However, pockmarks are generally larger at the eastern side of the Vestnesa Ridge (A2) (Figure 3.1.1) than at the end of the Ridge at the western side (A1) (Figure 3.1.2) (Plaza-Faverola et al., 2015; Bünz et al., 2012). Hence, it could be interpreted, that both areas are not equally active.

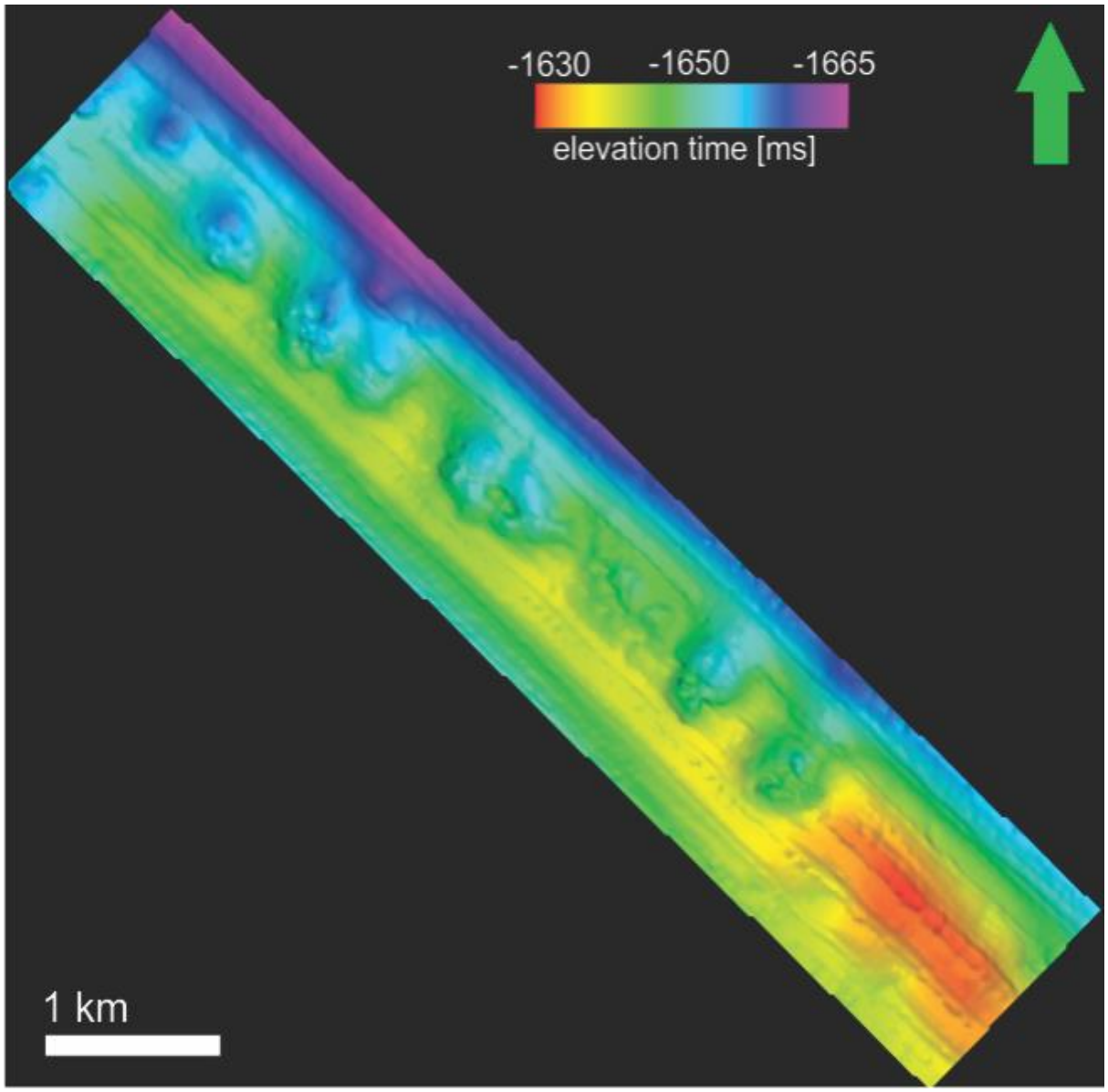

Figure 3.1.1: *Vestnesa rige (A2) active region. Huge depressions aligned at the crest of the ridge are interpreted as pockmarks overlying gas chimneys.*

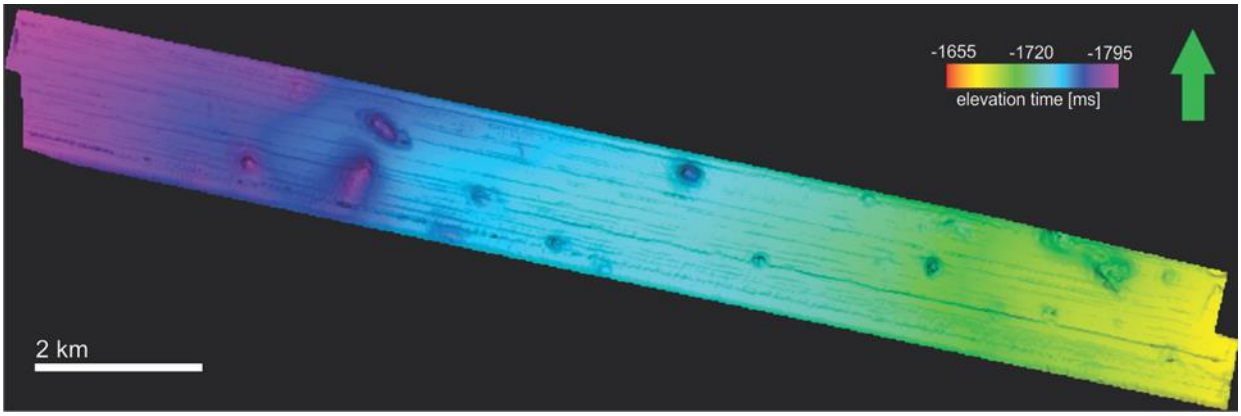

Figure 3.1.2: *Vestnesa ridge (A1) less active region. Depressions scattered in the area are visible as circular, oval dots which are interpreted as pockmarks, where most of them are connected with gas chimneys below.*

The BSR is located at – 160 to - 170 m below seafloor and there is evidence of gas hydrates due to an acoustic blanking zone (Petersen et al., 2010). The BSR is easily seen in seismic (e.g. Figures 5.1.4, 5.1.8, 5.2.4, 5.2.11, 5.2.12, 6.1.2, 6.3.1), because it has a strong reflection and reversed phase, if compared to the seabed reflection (Bünz et al., 2003). In many zones where fluid flow occurs, the BSR reflection is lost, because the flow of fluids pierces through the BSR (Petersen et al., 2010). Features such as pull-up and push-down are identified at the Vestnesa Ridge. In some seismic profiles it can be seen that sediment layers are clearly pushed down, compared to the surrounding strata, in others sediment layers appear clearly pull-up. Push-down often occurs near to the seafloor due to free gas, where velocity is lower than in adjacent areas. Pull-up features occur close to the base of a gas hydrate stability zone due to gas hydrates, where velocity is higher (Hustoft et al., 2009).

3.3.1 Free gas and hydrates in Vestnesa ridge

High amplitude reflections in seismic sections can result from the presence of a high or a very low percentage of free gas, depending on how gas is distributed in sediments (Lee, 2004). Pure gas hydrate has a P-wave velocity (>3000 m/s) (Ecker et al., 1998). Nimblett and Ruppel, (2003) claim that the presence of hydrate in the pore space reduces porosity and permeability of the sediments while free gas significantly reduces velocity and can drop below the acoustic velocity of water (1475 m/s) (Ecker et al., 1998). Further, negative acoustic impedance contrast between gas hydrates and free gas produces a clear boundary of the BSR which suggest that there is free gas beneath and gas hydrates above it. In Vestnesa ridge the BSR can be detected along the whole ridge crest (Bünz et al., 2012). It is predicted that the BHSZ is 155 m below seafloor (mbsf) (Smith et al., 2014). On the other hand, Holbrook et al, (1996) say that the absence of the BSR does not eliminate the presence of gas hydrate. Around 30 - 100 m above the BSR, methane hydrate exists and hydrate capacity

increases towards the BSR (Hustoft et al., 2009). Therefore most hydrates and highest velocities occur right above the BSR. Gas flares in the water column were imaged in 2010, 2012 (Smith et al., 2014) and in 2008 (Hustoft et al., 2009), but not in 2007, which suggests that there is an episodic activity of fluid flow in Vestnesa. Several authors have observed gas flares that reach 750 m (Hustoft et al., 2009) and even 800 m (Bünz et al., 2012).

Acoustic chimneys in Vestnesa seem to have roots within or below highly reflective strata underneath the BSR (Hustoft et al., 2009) and they are fed by a critically pressured free gas column beneath the BSR (Bünz et al., 2012; Smith et al., 2014). The free gas zone is approximately 17 km long and 30 to 100 m thick (Hustoft et al., 2009). It can be documented by the presence of enhanced reflections, push- down and acoustic transparency (Smith et al., 2014), where the reflections are dimmed. Extensional faulting and shear deformation from surrounding transform faults (Plaza-Faverola et al., 2015) can be a main reason in the supply and distribution of methane hydrate and free gas in the Vestnesa Ridge. In addition, hydrate and gas zone can be bigger because of surrounding faults (Hustoft et al., 2009).

3.4 Fluid flow systems in the Nyegga region

As it is in other places offshore, also in the Nyegga region features described as fluid escape pathways are seen in seismic profile as seismic blanking or discontinuous reflections (Plaza-Faverola et al; 2011). Seismic blanking is also known as the vertical dim zone, where the reflections from the stratigraphic layers are visible, but have a lower continuity amplitude compared to adjacent areas. They look like vertical zones, where the parts in between are filled with a chaotic pattern (Løseth et al; 2009). In Løseth et al. (2009) pull-up is described as *"apparent uplift produced by a local, shallower high-velocity region*".

In the Nyegga region offshore Norway, a number of gas chimneys are associated with pockmarks (Figure 3.4). Many chimneys, yet now all of them, connect with the pockmarks at the seabed, but not all of them. Whereas others terminate without reaching the seabed and thus showing no evidence of a pockmark. They pierce through glacigenic debris flows that are thought to have deposited during the last glacial maximum (LGM) (Plaza-Faverola et al., 2010). According to Mazzini et al., (2006) and Plaza-Faverola et al., (2012) there is evidence of micro seepage of methane and shallow gas hydrates in Nyegga.

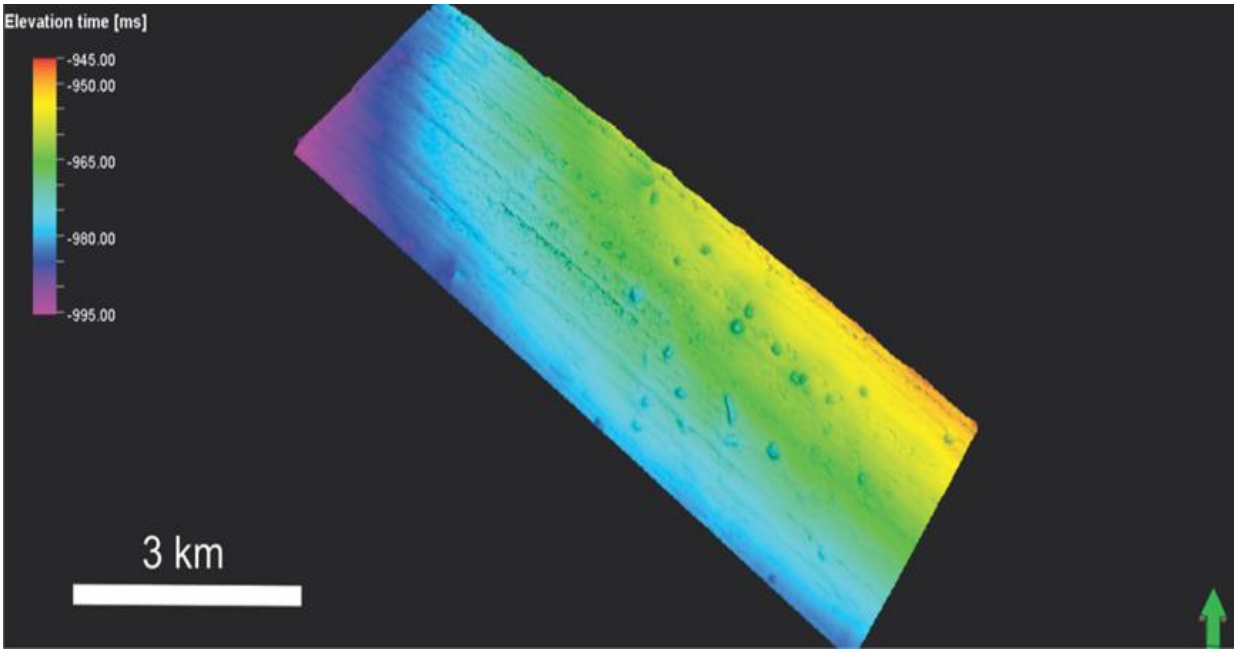

Figure 3.4: *Sea floor of Nyegga area. Seafloor depressions are scattered and covers mostly eastern part of area. Horizontal lines that cut area are interpreted as artifacts.*

Plaza-Faverola et al. (2011) suggested that the deposition of chimneys and fluid flow in this region can be related to glacial-interglacial transitions. With basin modeling Hustoft et al. (2009) and using ^{14}C method, Mazzini et al. (2006) found out that main period of active seepage happened from 16 and 19 kyr (thousands of years). In addition, Plaza-Faverola et al. (2011) suggested, based on the presence of buried pockmarks in the seismic, that there are periodic seepage events that seem to be associated with the last 3 - 4 major glaciation transitions.

In Nyegga there are two types of chimneys: truncated and non-truncated (Plaza-Faverola et al., 2011). Non-truncated chimneys are narrower than truncated chimneys. When pockmarks developed in a particular place, sediments were washed out and truncations indicated the diameter of that area. A difference in diameter of the chimneys can also be related to chimney activity periods, as they weren't active at all times. Plaza-Faverola et al. (2011) claim, that there was a reactivation one or several times. Chimneys can be divided in three different periods: young chimneys, which were formed as single venting systems by rapid loads of sediments; truncated chimneys without any fluid flow at the present day; chimneys with an active fluid flow at present time which have been reactivated several times during last 200 kyr (Plaza-Faverola et al; 2011).

Former periods of fluid expulsion in Nyegga can be related to glacial periodicity in the region (Plaza-Faverola et al., 2011) which is connected with plough mark occurrence (Figure 3.4.1). Each fluid flow activity period is related to the last stages of maximum glaciations in

the region (Plaza-Faverola et al., 2011). INT reflector (Figure 3.4.1) represents the final Saalian ice sheet retreat and is approximately 125 - 130 ka old (Rise et al., 2006; Plaza-Faverola et al., 2011). The age estimate was calculated assuming a sedimentation rate of 1.4 m/ka (Hjelstuen et al., 2005). Yet, the authors also presume a sedimentation rate of 0.5 m/ka, at the deposition time of the INT reflector, leading to an uncertainty of 40 kyr (Hjelstuen et al., 2005). The base of INT, which is part of Naust T unit (e.g., Berg et al., 2005) is rich with buried plough marks. Above INT reflector, silt, sand and gravel is deposited which indicates glacial influence (Berg et al., 2005).

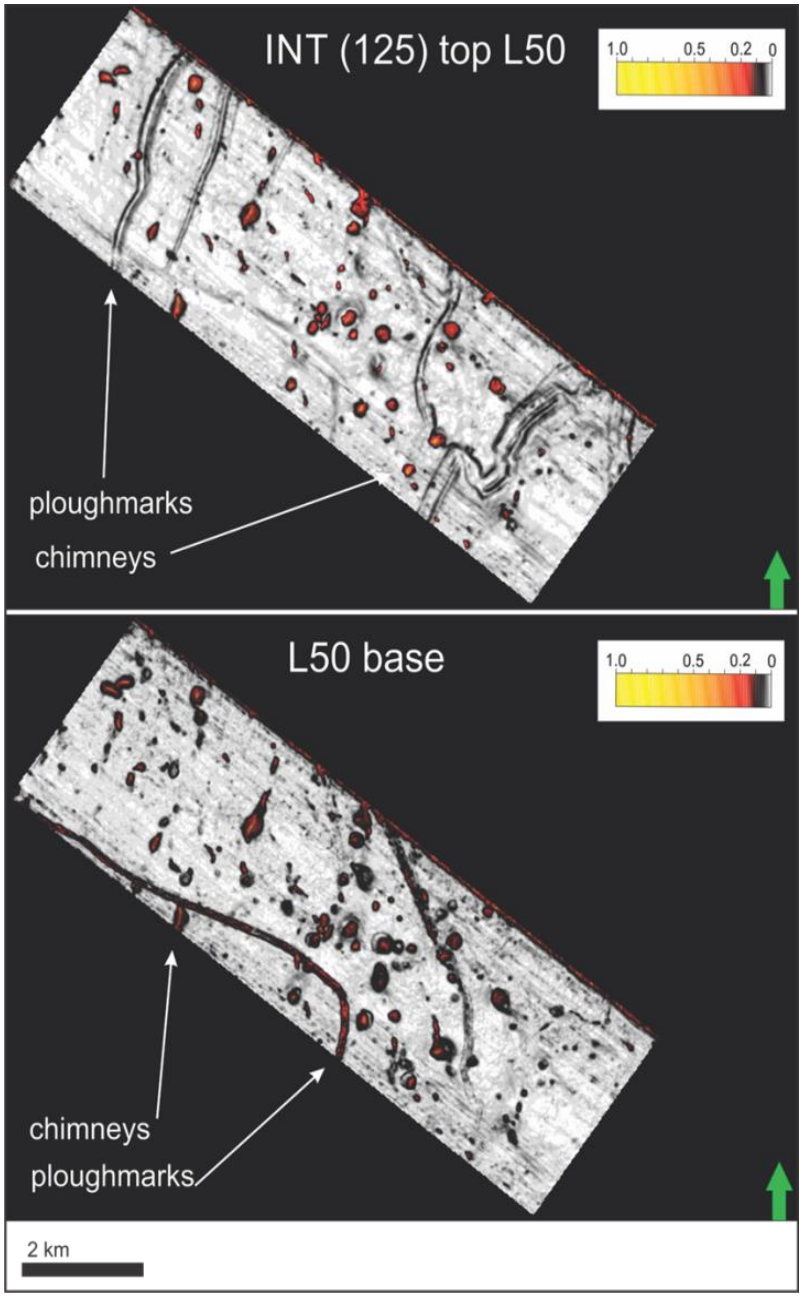

Figure 3.4.1: *Shows top and base of unit L50. In between this unit, plough marks are seen very often and this unit represents the time when fluid flow was active. Ages and overall stratigraphy can be correlated with figure 2.2.6. Figure is made using extract value attribute of variance.*

Factors controlling fluid flow in marine sediments are: tectonic regime and sedimentary environment. Rapid sedimentary loading and emplacement of the Plio-Pleistocene sediments may have caused the generation of excess pore pressure in deeper formations which is a controlling mechanisms for the migration of fluids (lateral and upward) (Plaza-Faverola et al., 2010). In Nyegga hydraulic fracturing is the main process that results in transporting fluids upwards (Berndt et al., 2003). However, Plaza-Faverola et al. (2010) suggest several factors that are responsible for fluid distribution: thickness of glacigenic debris flow deposits, lateral discontinuities in depositional patterns of contourite drifts and different levels of overpressure generation related with active/inactive fluid flow.

Loss of high frequency, acoustic transparency and push-down characterize the reflections beneath the contourite deposits. They can continue 2800 ms (TWT) down, which suggests that major vertical pathways for fluids exists and can migrate from deeper than Naust formation (Plaza-Faverola et al., 2010) (Figure 2.2.6).

Polygonal faults are found in fine grained, hemi-pelagic sediments of Kai, lower Naust Formations and upper Brygge Formation (Figure 2.2.6) (Plaza-Faverola et al., 2012). They are related to active fluid flow since the Miocene (Berndt et al., 2003).

3.4.1 Free gas and hydrates in the Nyegga region

Compressional wave velocity models showed velocity anomalies, which are below the Hamilton reference curve and refer to the free gas in the sediments. Velocity inversions propose that the free gas in the sediments is located in the upper 600 meters below seafloor (mbsf) in Nyegga (Plaza-Faverola et al., 2010). The concentration of the free gas in the sediments can be calculated by using Helgerud's effective- medium model (1999) (e.g, Bünz et al., 2005).

The FGZ (free gas zone) varies in thickness, but mostly it is less than 100 m thick (Bünz et al., 2005). There is an assumption that the FGZ supports the formation of gas hydrates, though free gas migration and the FGZ evolution is not very well understood. Vertical zones with chaotic reflections below the BGHSZ could be pathways for fluids from deeper sources (Plaza-Faverola et al., 2012). During the last 400 ka (the border of GHSZ and base of the Naust S) there was a rapid sediment deposition of Naust sediments and this probably caused enormous excess pore pressure at the apex of the area where fluids accumulated (Rise et al., 2006; Plaza-Faverola et al., 2012).

Fluid structure depends on the origin of gasses: microbial (the product of microbial degradation of organic matter), thermogenic methane (the product of thermal degradation of organic matter) (Rise et al, 1999; Plaza-Faverola et al., 2010).

During sampling in Nyegga gas hydrates were extracted near the surface and therefore great possibility of an active fluid flow persists (Plaza-Faverola et al., 2010). Moreover, evidence of a moderate flux of fluids can form gas hydrate deposits according to Talukder (2012).

The BSR is located at the base of GHSZ and it marks the transition between hydrate bearing sediments 270 - 310 mbsf and free gas accumulation underneath (Bünz and Mienert, 2004). Meaning, the BSR occurs in contouritic and hemipelagic deposits of the Naust formation and not within glacigenic debris flow deposits (Plaza-Faverola et al., 2010).

4 Data and methods

4.1. Data

4.1.1 Vestnesa area

In Vestnesa ridge there are two areas that were interpreted. A2 - which is active (Figure 3.1.1) and (A1) which is less active (Figure 3.1.2). Both locations can be seen in figures 2.1.3, 6.1, 6.2.

- Size of A2 (active) area: inline - 7390 m, x line - 1400 m with total of 10.34 km^2. Resolution of grids was - inline 1182 and x line 227.1.
- Size of A1 (less active) area: inline - 15570 m, x line - 1870 m with total of 29.11 km^2. Resolution of grids was - inline 300 and x line 2500.

In July 2007 University of Tromsø acquired P-Cable 3 D seismic system (Figure 4.1.1). In the survey area 32 profiles with 8 and 12 parallel streamers were used. The seismic source was Two GI (generator-Injector) guns which were fired with a total volume of 240 in^3. Frequency of the seismic data varied from 20 to 250 Hz. The shot point distance was 20 m (Petersen et al., 2010).

4.1.2 Nyegga area

Size of Nyegga area: (inline - 10325 m, x line - 3310 m with total of 34.17 km^2. Resolution of grids was - inline 1800 and x line 568.

Cruise with an R/V Jan Mayen from University of Tromsø in 2008 obtained P-Cable high-resolution 3D seismic data at Nyegga pockmark field (Bünz et al., 2008; Plaza-Faverola et al., 2011). The P-cable seismic acquisition system (Petersen et al., 2010) consisted of an array with 16 streamers, where each was 25 m long with 8 recording channels. Spacing between streamers varied between 8 and 12 m. The seismic source was one GI (generator-Injector) gun fired in true GI mode at 45/105 in^3 at a pressure of approximately 140 bars (Bünz et al., 2008). Frequency of the seismic data was 80 Hz and vertical resolution therefore 5 m (Plaza-Faverola et al., 2011).

In this project Petrel 2012.2 and 2013 were used to interpret data from both main locations.

4.1.3 The P-Cable 3 D system

The P-Cable system (Figure 4.1.1) is a high-resolution 3 D seismic imaging tool. The cable is towed behind a vessel perpendicular to its direction. 24 multi-channel streamers with a length of 25 m are attached to the cross cable. The array of single-channel streamers acquire 24 seismic lines simultaneously and covering approximately 240 m wide swath. Overall, the P-cable seismic system is well known and recognized as a high-quality tool (Petersen et al., 2010).

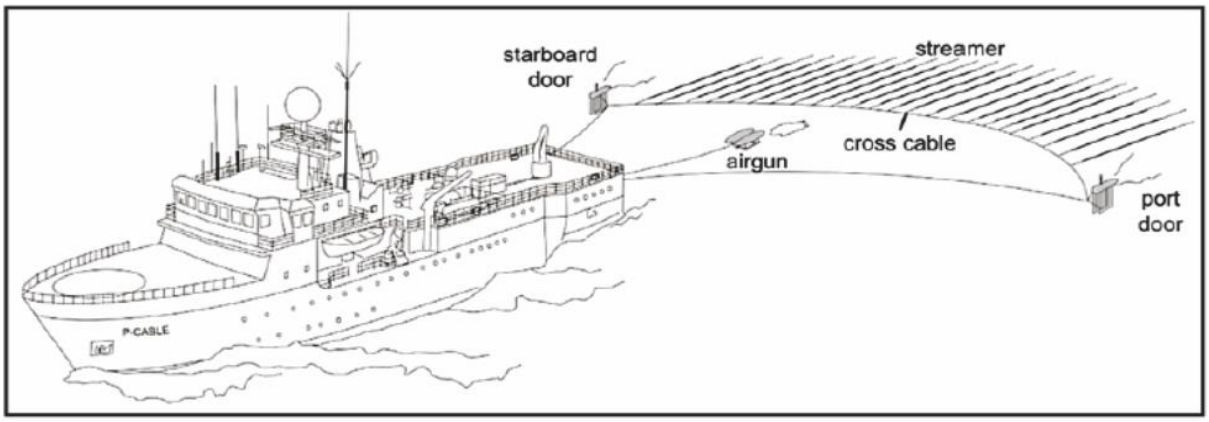

Figure 4.1.1: *Picture of P-Cable 3D seismic system. Modified from (Gay* et al.*, 2007).*

4.1.4 Seismic resolution

Resolution in general is the clarity of the image including how sharp it is. It describes how clearly one can separate objects from each other, no matter if on the screen or on paper.

Seismic resolution is the ability to separate two features on a seismic data (Sheriff, 2006). There are two types of resolution: vertical and horizontal. When seismic waves travel down (vertical resolution) they hit a reflector and waves also spread horizontally. There is an interaction between wave front and reflective boundary (Andreassen, 2009). When a sound wave hits a reflector, it is not only affecting one single point, but also a circular part of the surrounding area. This circular zone is called Fresnel Zone (Figure 4.1) (Brown, 2003).

4.1.5 Attenuation of seismic energy

Seismic energy is lost due to depth. There are several factors that can increase attenuation.

- Spherical divergence: seismic energy is expanding while the wavefront spreads through the crust. Amplitudes are decreasing proportionally because of increasing radius of the wavefront sphere.

- Absorption: For different types of rocks there is a different attenuation of energy. For higher frequencies absorption is faster, than for lower ones.
- Amplitude decrease by reflections, refractions, mode conversations: these three factors cause wavelength to increase and amplitude to decrease, once waves are spreading through the Earth. With increasing depth seismic energy is lost and resolution decreases (Andreassen, 2009).

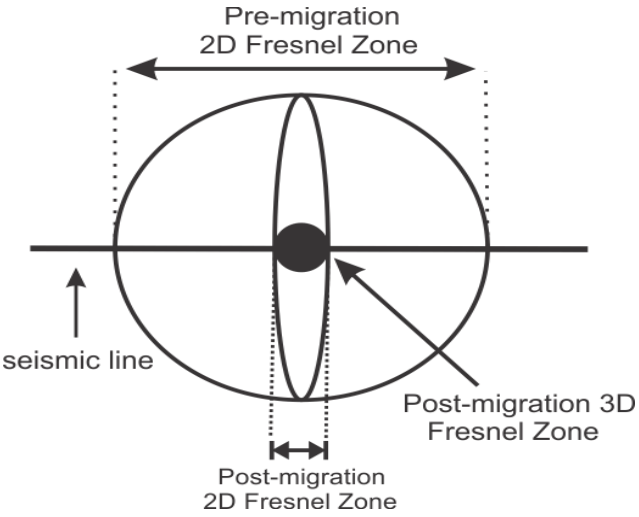

Figure 4.1: *Fresnel Zone for 2D and 3D seismic data before and after migration. Picture is modified after Brown, (2003).*

4.1.6 Artefacts

Bulat (2005) mentions that acquisition footprints can be caused by hydrophone cable deviation from a straight line. Other significant reasons, however, are processing errors and poor acquisition design. Survey footprints are noise that correlates with acquisition geometry (Andreassen et al., 2008).

4.1.7 Graphic design with Corel draw X6 (64-Bit)

Corel Draw X6 is a graphic design software that is very easy to use and can help to make new, or improve old figures.

4.1.8 Seismic interpretation with Petrel

For the visualization and interpretation of the 3D seismic data the software Petrel 2012 and 2013 were used, both made by Schlumberger. The platform was provided by Norges Arktiske Universitet. The software helps to analyze risks and doubts by interpreting horizons, faults, and even wells. It is easy to visualize geophysical and geologic features by using a variety of attribute maps.

4.2 Methodology

First, major stratigraphic reflections were interpreted in each seismic data volume. For Vestnesa (A2) used seismic cube: StackVarea1_211221012_migr and StackVarea2_2007year_migr for (A1). Name of bathymetry: ws_bathyFromSteinarH. For Nyegga used seismic cube: Nyegga_stackMig_and name of bathymetry was: nyeggaSurfKom.xyz.

Bathymetry maps of all study areas, colors and different vertical exaggeration ratio were displayed in order to show best resolution and morphology. For the Vestnesa, vertical exaggeration ratio was set to number 12 and for the Nyegga region to number 15, to better visualize both locations. During horizon interpretation different methods and parameters were used: seeded 2D auto tracking, seeded 3D auto tracking and manual interpretation.

Sea surface is a good reflector because of the high impedance between water and air (Andreassen, 2009), therefore picking up seabed horizon in one of the areas is the first thing to do. I decided to work with the active Vestnesa area (A2) first, because of its complicity (huge amount of chaotic reflections, dimmed zones, faults, irregular seafloor etc.). After the seabed, I interpreted 3 more horizons, which I thought are important to pick, due to their strong reflections. The seabed was located at - 1650 ms (TWT), the following horizons at - 1750 ms, - 1840 ms, - 1885 ms (TWT) respectively. In Vestnesa area less active (A1) seafloor: - 1780 ms (TWT) and 3 horizons: - 1860 ms, - 1945 ms and - 2012 ms (TWT) were interpreted. My choice was random and didn't focus on specific numbers.

In settings - auto tracking, first main task is to choose signal feature. There are few options as peaks, troughs or both, however I chose peaks. Then, in settings - interpretation, there are a lot of parameters that you can choose from. First, when working with horizon (surface), I'm trying different seed confidence percentages which in my case varies from 20 % up to 70 %, it means that confidence level determines how much stack tracker will apply to the seed values, when determining to accept or reject expansion points. Afterwards, changing expansion quality will expand a seed point to its 8 closest neighbors. Finally, the software is making a horizon by your based settings; however, you will hardly ever be content with a result. For that reason it is necessary to also use manual interpretation, which is a time consuming job, because you need to take every 10th, 5th, 2nd or even every inline and then do the same job for every corresponding x line. I figured out that easiest way how to build horizons is the following: First, choose where you want your horizon, it is good idea to use a color button to increase or decrease colors, then it's easy to see high amplitudes and so to pick

horizon that you are interested in. While choosing seed points in seismic interpretation, it is better to mark as many points as possible when following preferable horizon (y axis). Afterwards switch to x axis and look for points, then connect them. Then your horizon will start to make some sense in terms of shape. If the area that you are interpreting contains, faults, fractures or gas chimneys it will be more complicated to make a horizon. For example, in Vestnesa (A2) you can find all these features together, but in Nyegga region, data are not so strongly disturbed.

After picking horizons, surfaces were generated using a gridding algorithm. Under utilities - make/edit surface, I took my brand new horizon placed in 'main input' and 'get limits from selected'. Grid increment putted on X - 5 and Y - 5 which determines increments from selected data and extended boundary with one node. The last task that user can do is changing the color scale and taking off contour lines under settings. At the end of operations I got acceptable horizons, where the observer can see different features in 3D and 2D.

For all areas displaying seafloor, different numbers of vertical exaggeration ratio were used. Smoothing of the data was not used more than one time, since it destroys resolution of different features. To improve resolution for the each areas surface (seabed), I used a low pass filter, which smoothens grid surfaces by removing random noise and spikes. In Vestnesa A1 (less active), I edited a seabed polygon and eliminated points which I wanted to cut out, because few edges of my polygon were too damaged, while I picked horizons and generated surfaces.

In the Vestnesa less active (A1) a total of 4 main surfaces were made: Seafloor, S2, S3 and the BSR (Figure 5.2.5a). As well, several sub surfaces were calculated with the inbuilt software's calculator to get a closer overview of the area. In the Vestnesa active (A2), 4 main surfaces were made: Seafloor, active S1, active S4, the BSR (Figure 5.1.4c) and several sub surfaces were calculated with the inbuilt software's calculator. In addition, seismic attributes (surface, volume) were extracted along these surfaces in order to show different features in 2D and 3D.

To visualize chimney/pipe structures in all areas, **MultiZ interpretation** was used (Figure 6.3.1). This is gained by manually picking points of interest around the structure from the Z line. As this process is complicated and time consuming; only few prominent, considerable size chimneys were made in each area. Additionally, a **Train estimation model** was used for all areas (Figure 6.3). The tricky part of this procedure is to use two volume attributes (Variance and Chaos), because for the software it is easier to calculate an algorithm,

instead of four attributes (e.g. variance, RMS, chaos and reflection intensity), which make it more complicated for the software to understand the parameters.

A Number of seismic attributes were used while focusing on showing differences in chimney/pipe structures which are explained in the next sub-chapter.

4. 2.1 3D Seismic attributes

Seismic attributes are a very important part of seismic interpretation. Over the years types of new different attributes were made. Using different attributes, changing their parameters or mixing them together, the user can get better results of what he wants to show/see in the maps. Sometimes problems can occur when the user is using too many attributes together, because it increases the probability of seeing artifacts (features, which are not real). The interpreter basically asks the computer to find features or depositional patterns that he wants to find. For example, a filter called *'Spectral decomposition'* preserves the signal bandwidth in reservoir and attenuates energy which is above 20 Hz. The result is of this procedure was astonishing - 154 m of net oil sands in reservoir. It is often that a specific attribute can be very sensitive to one geologic feature, where others, can be sensitive to different geologic features (Chopra and Marfurt, 2006).

Seismic attributes that were used for this study:

- **Structural smoothing -** The structural smoothing attribute was used in all areas before interpretation of data. It helps stabilize results, meaning, resolution of seismic data gets smoothened and therefore better. It is recommended to use this attribute prior to using other attributes. It decreases the noise of the seismic data. Using it without Dip guiding (Petrel 2011, Schlumberger) fluid contacts can be accentuated.
- **RMS amplitude map (root-mean-square) -** Calculates the square root of the sum of squared amplitudes (Petrel 2011, Schlumberger). It may show hydrocarbon indications because it points out bright spots (high amplitudes) and geomorphologic features. Handy map to enhance depositional environment.
- **Isochron thickness -** time difference between two horizons and measured in units. Time - milliseconds, Depth - meters (Petrel 2011, Schlumberger). In the Nyegga region, 5 isochron thickness maps were made for stratigraphical correlation between horizons (every map exaggeration ratio: 10). Results were L30, L50, L60, L70 and L100 units (Figure 5.3.11). Terminology from (Plaza-Faverola, 2011).

- **Extract value -** Extracts the input seismic value relative to a single horizon or an existing interpretation (Petrel 2011, Schlumberger). To make, for example the Variance attribute map, the user has to make a volume attribute map first. To make a variance surface attribute map, insert the newly made Variance volume attribute, while choosing an extract value from the surface attributes or from volumes, created with seismic calculator options.
- **Variance -** It is helpful to detect discontinuities in the horizontal continuity of amplitude. This attribute can be useful to detect features such as channels reefs, etc. (Petrel 2011, Schlumberger).
- **Instantaneous frequency -** This attribute shows the seismic attenuation of energy. Useful to detect low and high frequencies, it can identify contact between gas and water (Petrel 2011, Schlumberger). Good for visualizing the BSR boundary.
- **Sweetness -** Square root of the Instantaneous frequency. This attribute is helpful to identify features where energy is changing in the seismic data (Petrel 2011, Schlumberger).
- **Chaos -** Similar to the Variance attribute. Can identify gas migration pathways. It can show faults and discontinuities. Chaos measures '*lack of organization*' in the dip and azimuth estimation method (Petrel 2011, Schlumberger).
- **Neural net -** Generated from seismic attributes and used together with Train estimation model, where the user chooses which attributes to apply together and train.

5 Results

5.1 Vestnesa active (A2)

Using a structural map in the Vestnesa data set (A2) the seabed depth varies from - 1630 ms (milliseconds) (TWT) in the middle of part in SE to - 1670 ms (TWT) in the upper corner in the area in the NW. The water depth increases from SE to N. Total area covers 10.34 km^2. Biggest depressions are mainly aligned from SE to NW and are located on the top of the crest where depth varies from - 1630 ms to - 1655 ms (TWT), while the smallest ones are abundant on a slope (Figure 5.1.1). All 16 seabed depressions in the area are interpreted as pockmarks. The feature shapes are mostly circular, sub circular, semi-circular, irregular and some occur as a merge of two features. By looking at these depressions it seems that they look more complicated than in other two areas in my dataset. Since some of the depressions have a disturbed base and some of them are placed too close to each other, which appear as one big depression, because the edges in between them are eroded. Almost all depressions are aligned to the NW. Their sizes vary from 50 up to 600 m in width (Table 5.1). The spacing between them is irregular. Some of the craters are aligned and especially the biggest ones are located on the ridge crest. Their depth can reach 14 ms (TWT), but they are mostly 10 - 12 ms (TWT) deep (located on the crest) and 6 ms (TWT) for the ones located on the slope. The bowl of the features can be with both sides symmetrical or asymmetrical. The base of the craters can be slightly dipped, sharp v- shaped or one side slightly dipped and the other sharp dipped. Their base often is more rugged than other areas, since it has been eroded by vigorous gas. On the seafloor, acquisition footprints are found, which are likely to be artifacts that cut through the area from SE to NW, as primarily seen on the top of the shallowest place. The Vestnesa (A2) is almost flat, if we look at the numbers where depth changes by 40 ms (TWT) within 7390 meters. The width of the area is only 1400 m and it makes Vestnesa (A2) a quite rugged topography itself. Topography is irregular and it is complicated to measure the true depth of depressions, because they are mostly located in the mid-section of the area, which is higher than the surrounding area. Moreover their both side flanks of the depression continue slightly to deeper water depths. When measuring them, one flank is higher than the other. Average spacing between depressions is 250 - 300 meters.

Table 5.1: *Shows width and depth of 16 pockmarks in the Vestnesa region (A2).*

Pockmark	Width [m]	Depth [ms]	Pockmark	Width [m]	Depth [ms]
1.	600	14	**9.**	520	12
2.	50	2	**10.**	304	6
3.	460	10	**11.**	140	5
4.	500	4	**12.**	370	8
5.	520	10	**13.**	520	7
6.	405	11	**14.**	380	5
7.	411	12	**15.**	230	3
8.	470	12	**16.**	80	1

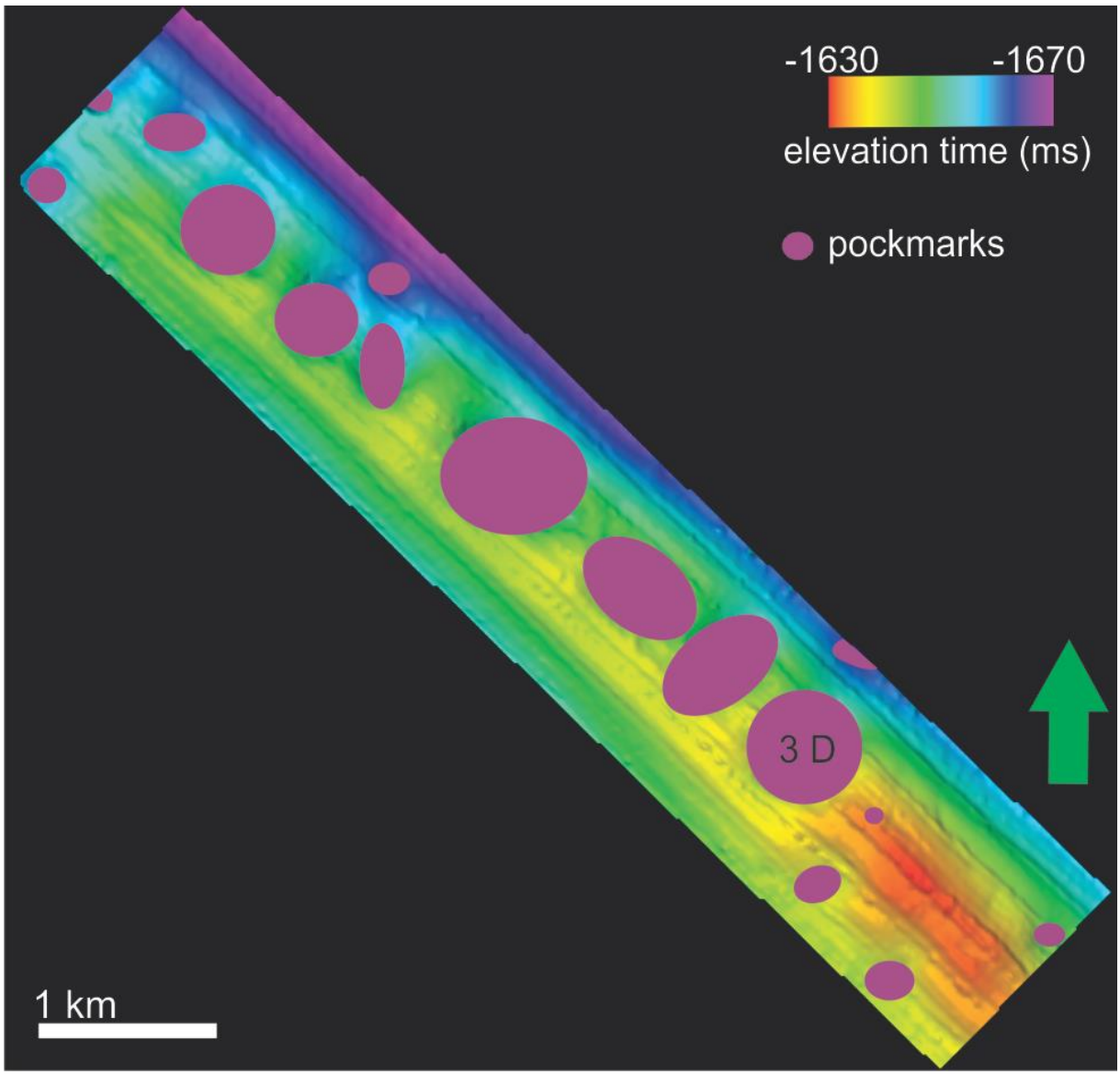

Figure 5.1.1: *Map view of seafloor in Vestnesa (A2). 16 pockmarks are shown in purple color. The pockmark marked with ''3D'' is seen in figure 6.1.1 (C). Vertical exaggeration is 15.*

5.1.1 Gas chimneys underlying pockmarks

Chimneys underlying pockmarks in Vestnesa (A2) terminate in different stratigraphic levels/depths (Figure 5.1.2) (Plaza-Faverola et al., 2010) and their sizes and diameters are different. Only a small portion of the chimneys terminate on the seafloor. Using time slices (Figure 5.1.3), chimneys occur as circular to elliptical features with a jagged outer edge, while showing low amplitude values using the RMS attribute map and values from 0.2 - 0.6 (reddish - orange) using the variance attribute map. There is also a difference in diameter of the chimney conduits (pathways) for fluid flow, characterized as seismic blanking in a seismic section. Chimney and pipe structure widths vary mostly from 30 m (smallest conduits) up to 470 m, but on average, they measure around 200 m in width (Figure 5.1.11). Their diameter also varies from level to level and is not the same. Above the BSR some of the chimneys are wider than below it, which could present changes in the activity period. Chimney shape is more pronounced in the first 110 ms (TWT) below seafloor. Edges are cut strait and chimney shape is almost vertical. Towards the seafloor, reflections get more chaotic and spread more into flanks of the chimneys. It is complicated to say if a chimney as a single feature terminates in a specific layer. Chimneys are made of many pipes and pipe length is not the same. Considering this theory, it can be misleading when determining the actual chimney termination. Figure 5.1.2 shows that most of the chimneys terminate near the seafloor (in 40 - 50 ms (TWT)).

Resolution and a lack of data is the reason why it is complicated to see, where and at what depth chimneys originate, but focusing on chimney structures determinate, that mostly chimneys and pipe structures are between 450 up to 500 ms (TWT) long.

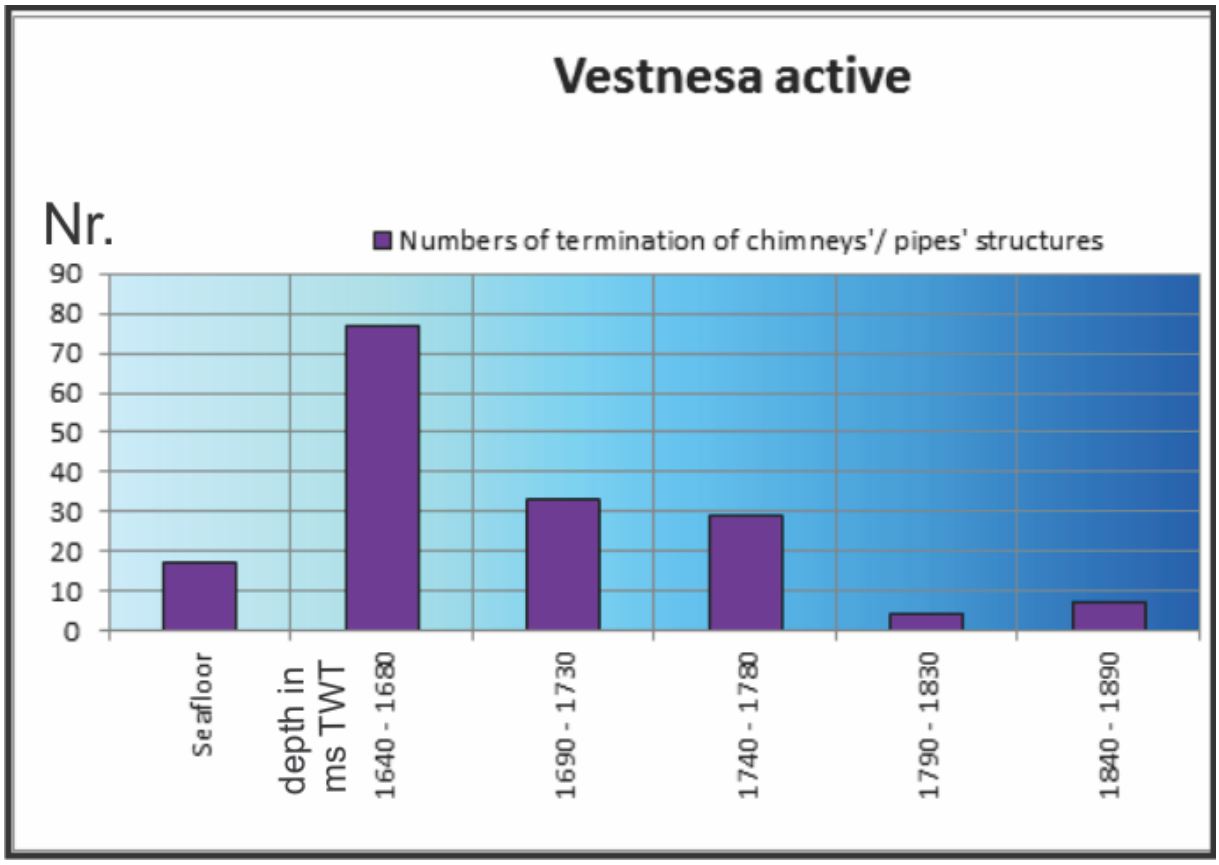

Figure 5.1.2:. *On the left side, the diagram shows number of terminations of chimneys/pipe structures. In the bottom part are depth units, where features terminate.*

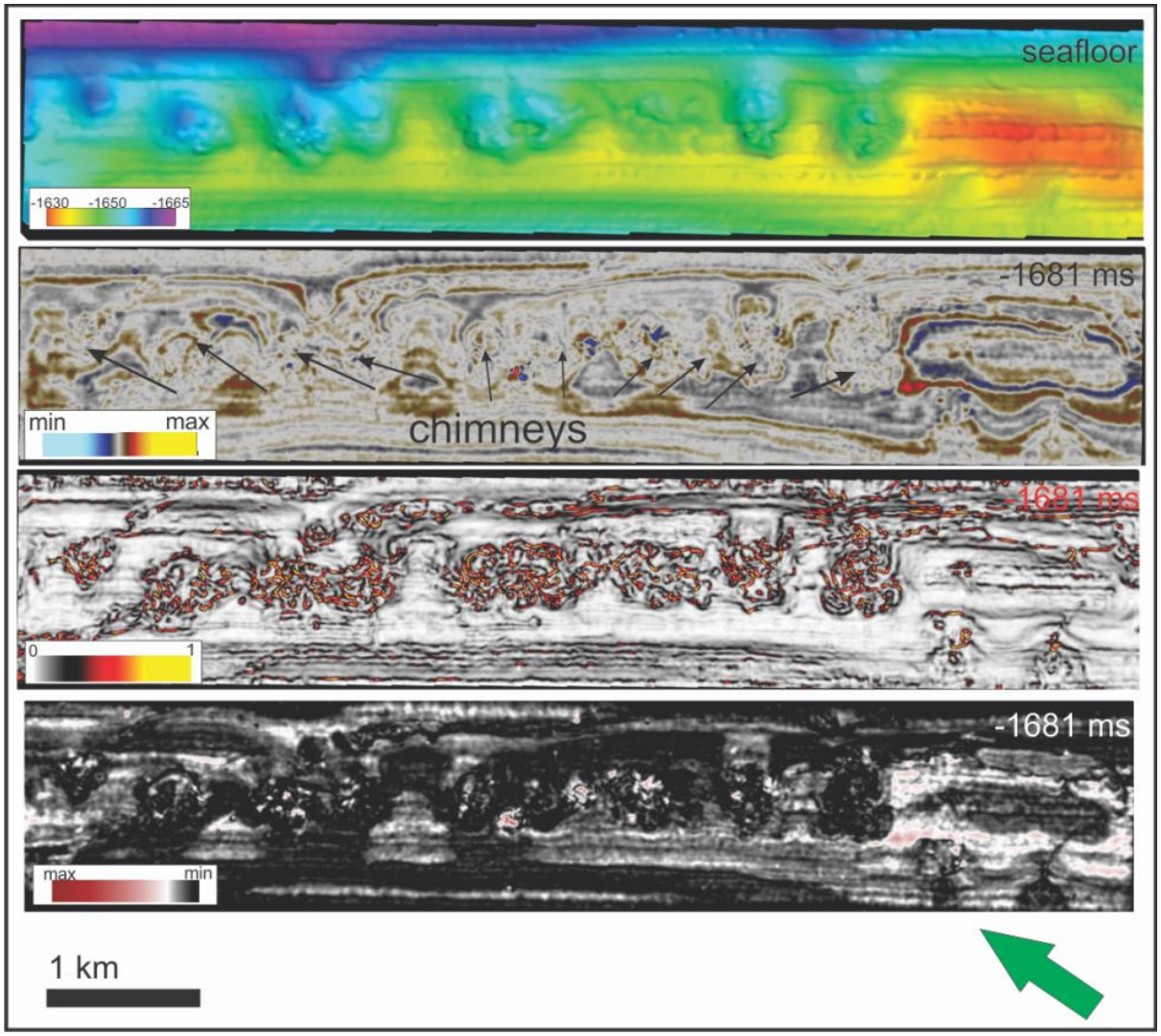

Figure 5.1.3: *Upper part of picture shows seafloor, below it - time slices from - 1681 ms (TWT) using different attributes .Structural map, original amplitude map, variance and rms attribute map.*

Figure 5.1.3 shows Vestnesa ridge A2 from the top, where the different sizes of pockmarks, depressions and craters show that fluid flow has been active recently and still is up to the present. It is easy to determine chimneys in this figure. Using different attribute maps, chimneys show a chaotic structure. Figure 5.1.4A displays the vertical zones of disturbed layers and acoustic transparency which is sometimes connected with pockmarks and pierces through strata. Different pipe structures and gas chimney systems are visible on the seismic data. Chimneys appear as chaotic zones in figure 5.1.4d. Structures (Figure 5.1.8) are similar to those in the Nyegga region and the mid-Norwegian margin (Figure 5.3.4) (Bünz et al., 2003).

5.1.2 The BSR depth and free gas zone thickness

Using the instantaneous frequency volume attribute (Figure 5.1.4) in the Vestnesa active (A2) area, a sudden frequency change below the BSR was found. From ≈ 1900 ms (TWT) down, frequency changes from 150 - 125 down to 0 Hz. Above the BSR frequency is mostly abundant with 125 - 300 Hz. Lowest frequencies are seen right below the BSR and can indicate free gas accumulation.

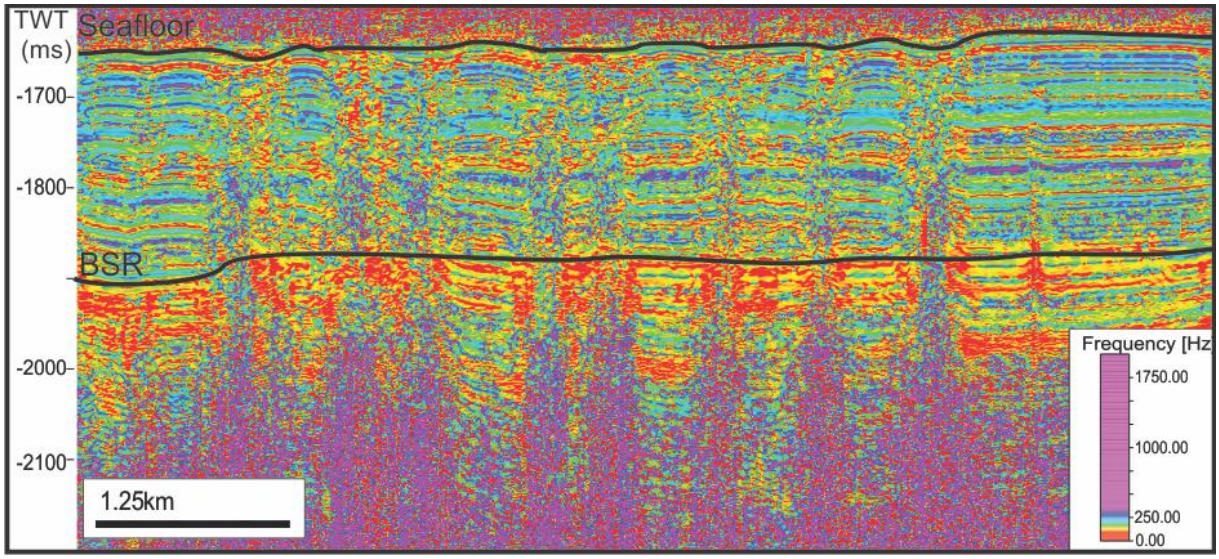

Figure 5.1.4: *Using instantaneous frequency attribute, low and high frequencies were found in Vestnesa (A2). Seafloor and the BSR lines are shown to help see differences. X line 114 was used.*

The BSR (Bottom simulating reflector) is located at 160 - 170 m bsf (below sea floor) which is also the depth for the gas-hydrate stability zone (Vanneste et al., 2005). In parts where fluid flow occurs in gas chimney structures, the BSR is disturbed. Velocity increases with depth. When it reaches the BSR the velocity is approximately 1800 m\s, then it suddenly drops to 1250 m\s because of the appearance of free gas (Petersen et al., 2010). Below the BSR thickness of strong reflections varies from 30 - 35 ms (TWT).

On a seismic data all low velocity layers show the presence of free gas and on other hand, an increase of velocity shows gas hydrate. It is common that acoustic blanking emerges where gas hydrates are present. Petersen et al. (2010), claim that the sub-BSR layer is 35 m thick.

In the Vestnesa ridge velocities increase from 1500 to 1680 m/s, down until it reaches the BSR due to loss of porosity and sediment compaction (Hustoft et al., 2009).

5.1.3 Periods of activity

Truncations in Vestnesa (A2) are complicated to see, because the area is thought to be very active. However, in the SE part of the area, a spot of continuous layers can be seen which makes it easier to see truncations there. However, truncations appear in the rest of the data as well, though it is harder to show them. Active and inactive periods are shown in Figure 5.1.4A.

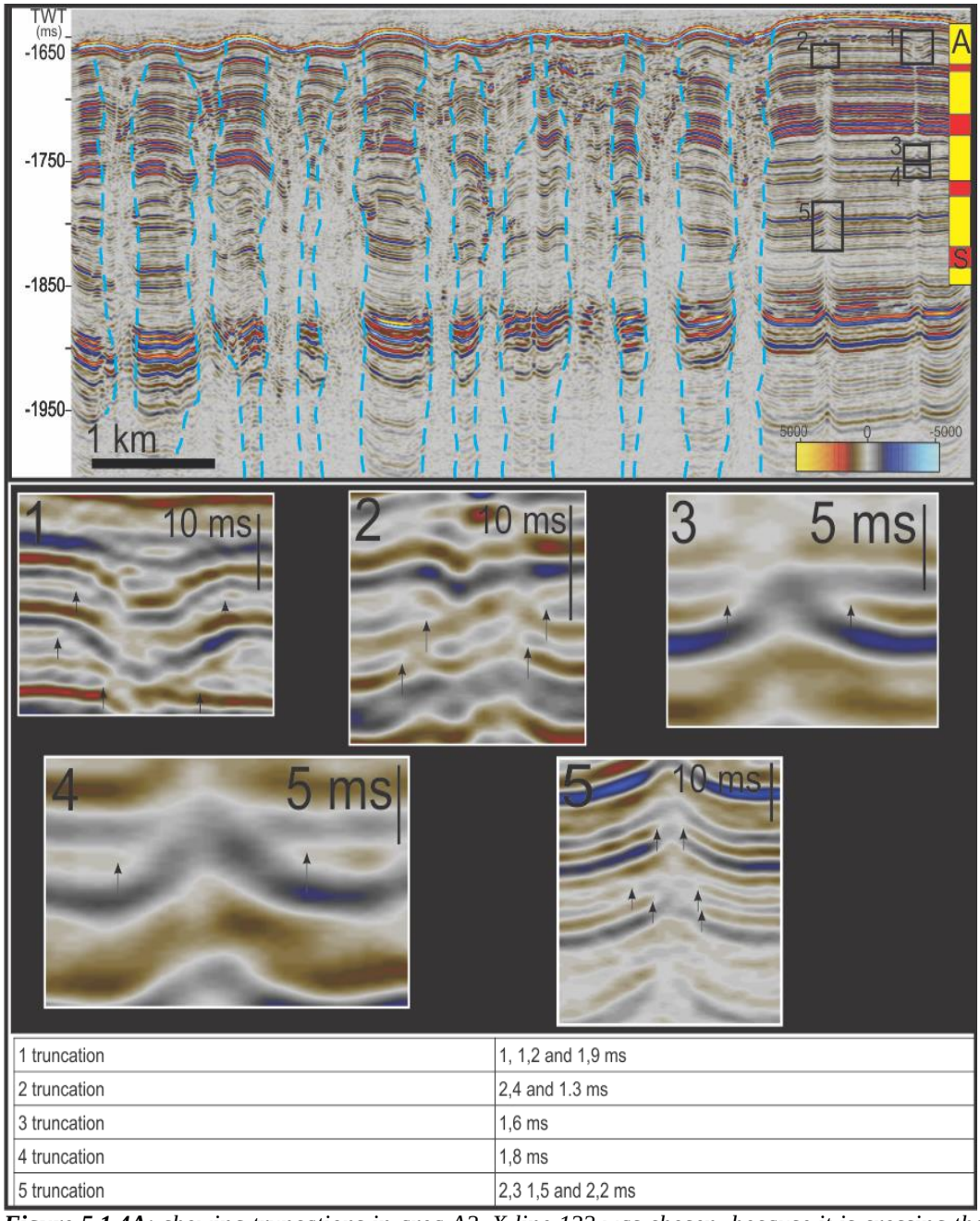

1 truncation	1, 1,2 and 1,9 ms
2 truncation	2,4 and 1.3 ms
3 truncation	1,6 ms
4 truncation	1,8 ms
5 truncation	2,3 1,5 and 2,2 ms

Figure 5.1.4A: *showing truncations in area A2. X line 132 was chosen, because it is crossing the middle of the area, which is the axis of the Vestnesa Ridge. Only in the SE of the area truncations are shown, because there are no pockmarks above truncations on the seafloor. The rest of the area is very active and large amounts of huge chimneys terminate on the seafloor. Chimney structure which is very chaotic holds a lot of pipes in it. Vertical blue, dashed lines mark the chimney outer borders. On the right side the vertical color bar shows the activity in the area. This bar is made considering every stratigraphic layer continuation. Yellow: active venting, red: seeping.*

Based on strata continuation, active and inactive periods in the (A2) area are demonstrated. By following them, it is easy to imagine where periods of active and inactive fluid flow appeared (Figure 5.1.4b). In Figure 5.1.4A on the right side a scale of active and inactive periods is shown.

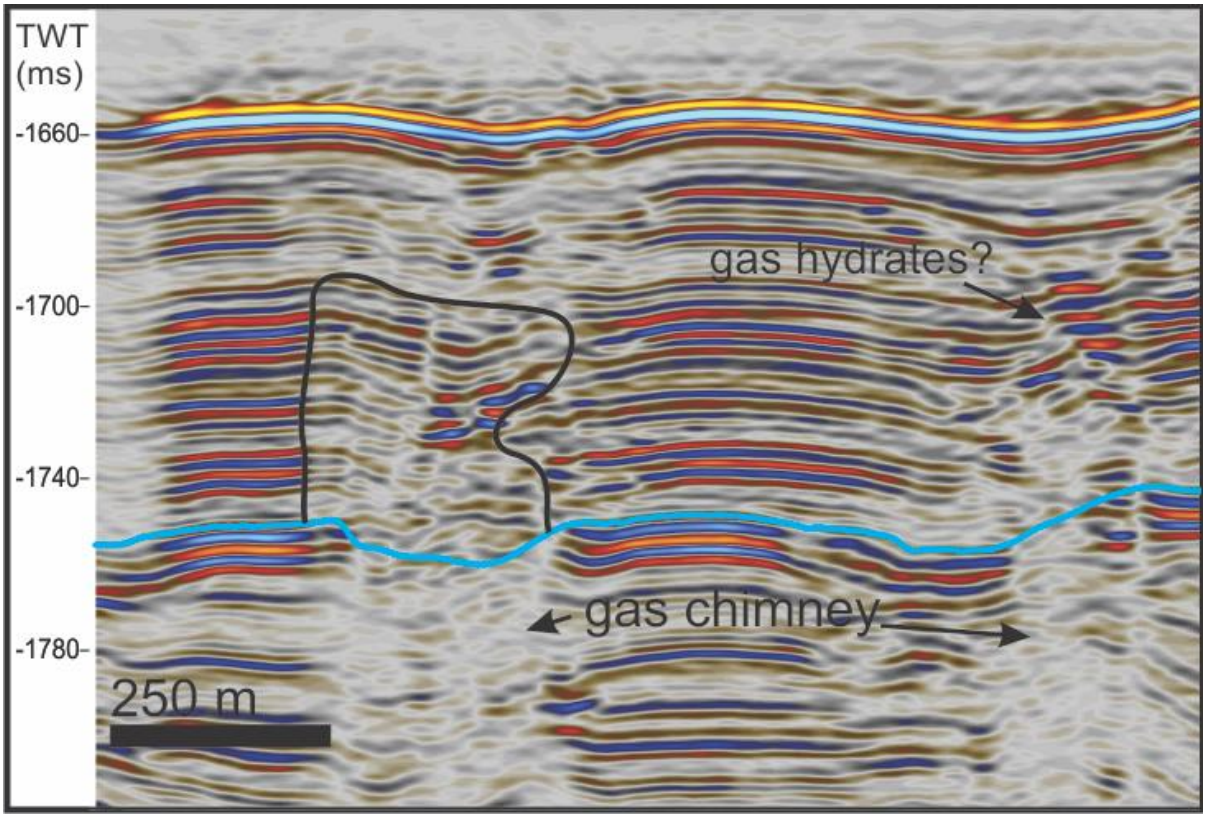

Figure 5.1.4b: *Blue line - S1 layer. Black line around chimney represents less active period. Location is seen in figure 5.1.4d. High amplitudes are thought to be gas hydrates.*

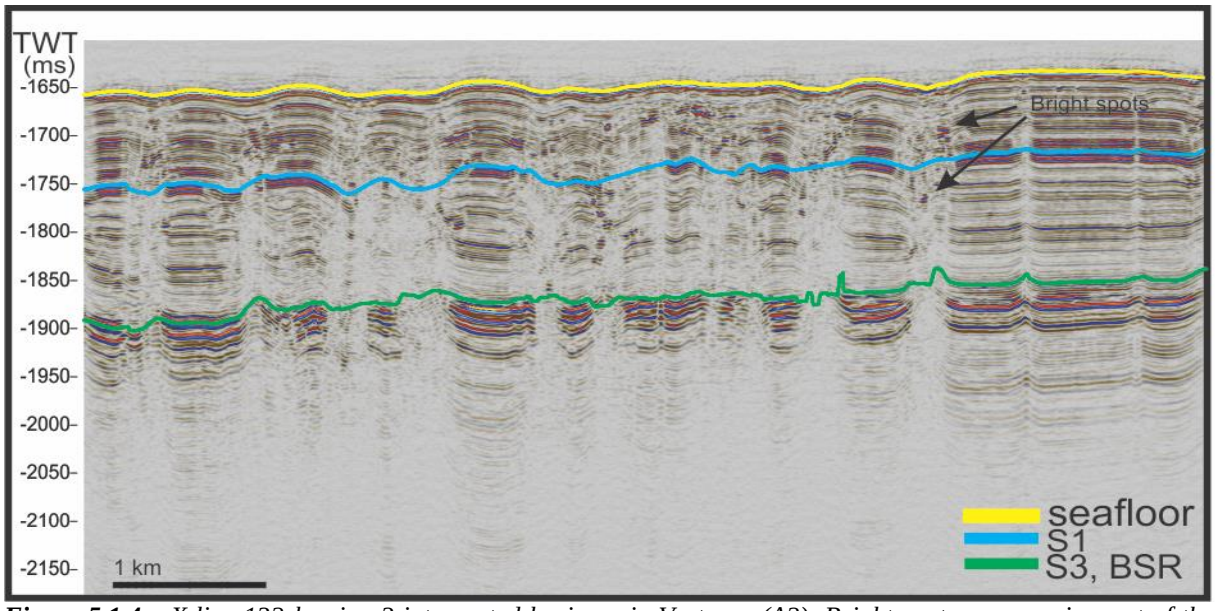

Figure 5.1.4c: *X line 132showing 3 interpreted horizons in Vestnesa (A2). Bright spots are seen in most of the chimneys.*

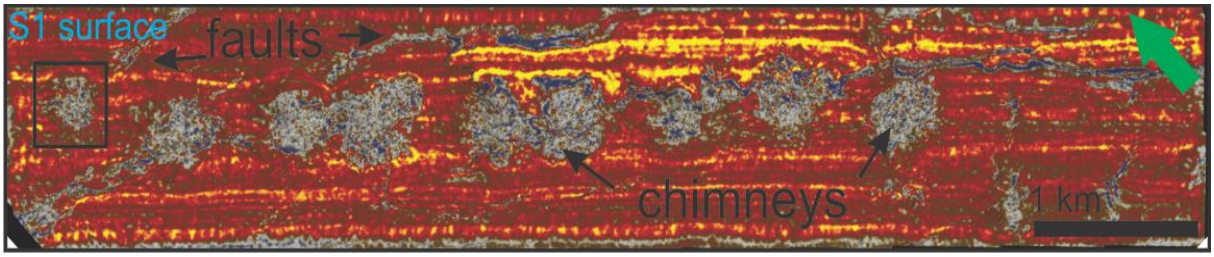

Figure 5.1.4d: *S1 surface generated using variance attribute from extract value. Black rectangle shows area in upper figures 5.1.4b and 5.1.4c. Faults and chimneys are highlighted through arrows.*

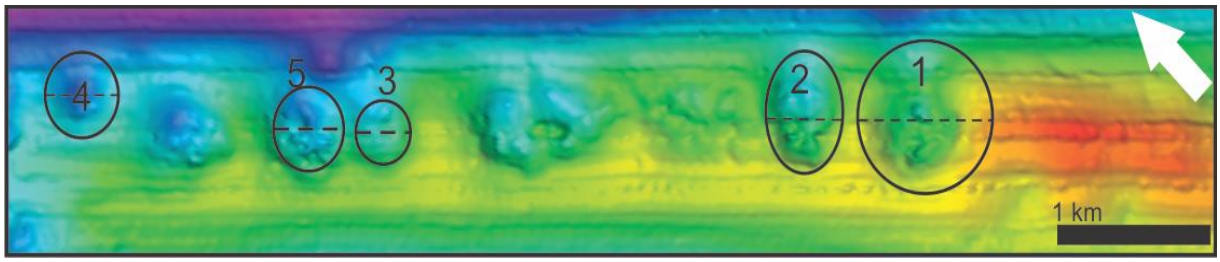

Figure 5.1.5: *Location of 5 chosen chimneys that are connected with the seafloor. This figure can be related to Figure 5.1.6.*

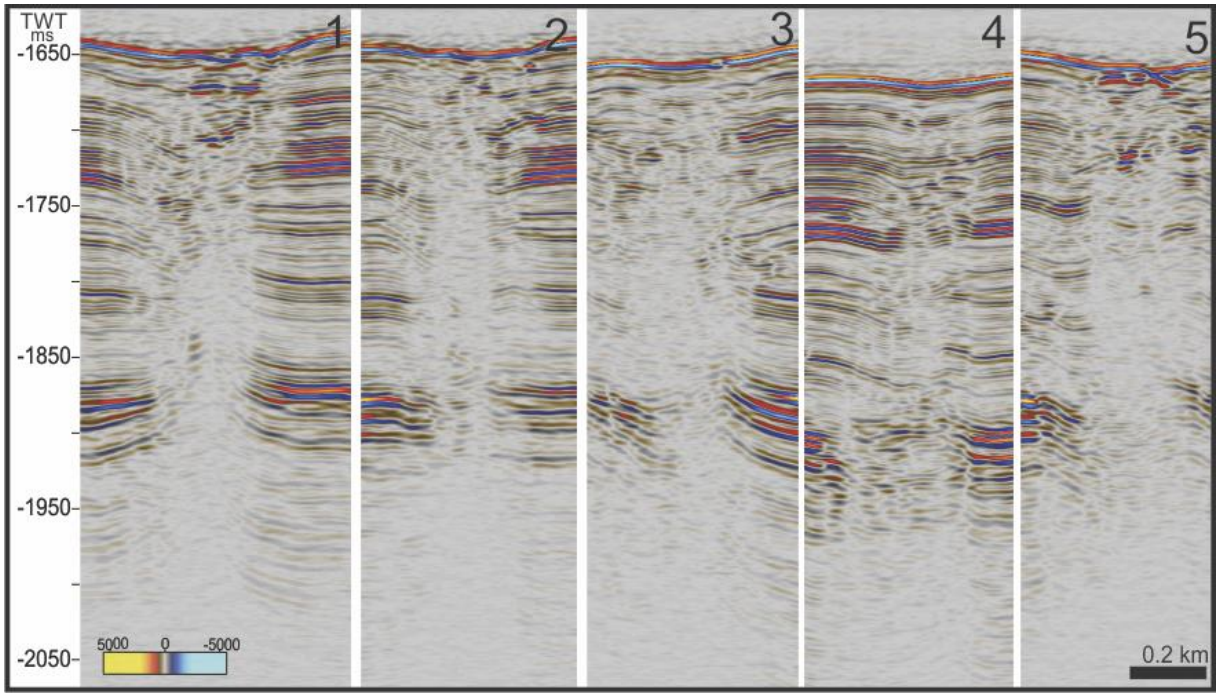

Figure 5.1.6: *Figure shows randomly picked chimneys in Vestnesa in order to show their differences. Different shapes of chimneys and their structure are seen as well their locations in Figure 5.1.5.*

In the Vestnesa active region pull up reflections are up bended through all data, where seepage pipes occur. From bottom up to the BSR biggest chimneys edges are slightly up bended, not as strong as in Nyegga. From the BGHZS, 50 ms (TWT) down, pull-up, push-down and cutted flanks of chimneys are found (Figure 5.1.6). Within GHSZ it is complicated to see, but mostly cut flanks occur together with slight up-bending and down-bending.

5.1.4 Faults

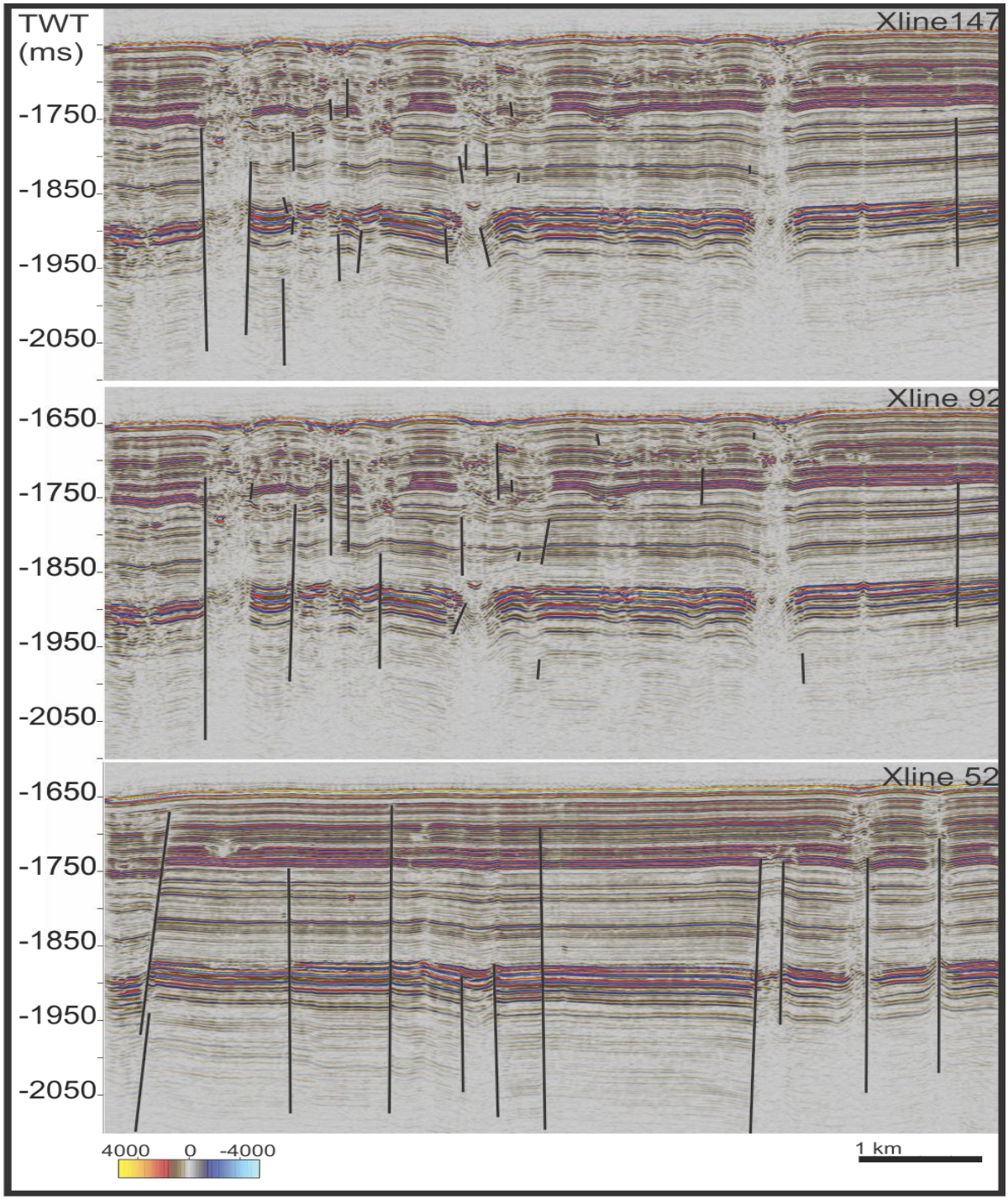

Figure 5.1.6A:*3 x lines are shown to represent faults in Vestnesa active area.*

The area, as seen in Figure 5.1.6A is crowded with faults and fractures, which act as good pathways for fluids which migrate from the deepest parts. Not only one specific point is abundant with faults and fractures, but they are scattered around throughout the whole area. These faults are significant to the area, because they affect fluid flow and are part of the plumbing system.

5.1.5 Chimney differences

Vestnesa area (A2) (Figure 5.1.7) represents different chimney/pipe (Figures 5.1.8, 5.1.9 and 5.1.10) structures: blow out and seepage pipes, which were described by Cartwright et al. (2007). Different structures of chimneys are found, as well as faults and small fractures. High amplitudes and chaotic, transparent chimneys are seen.

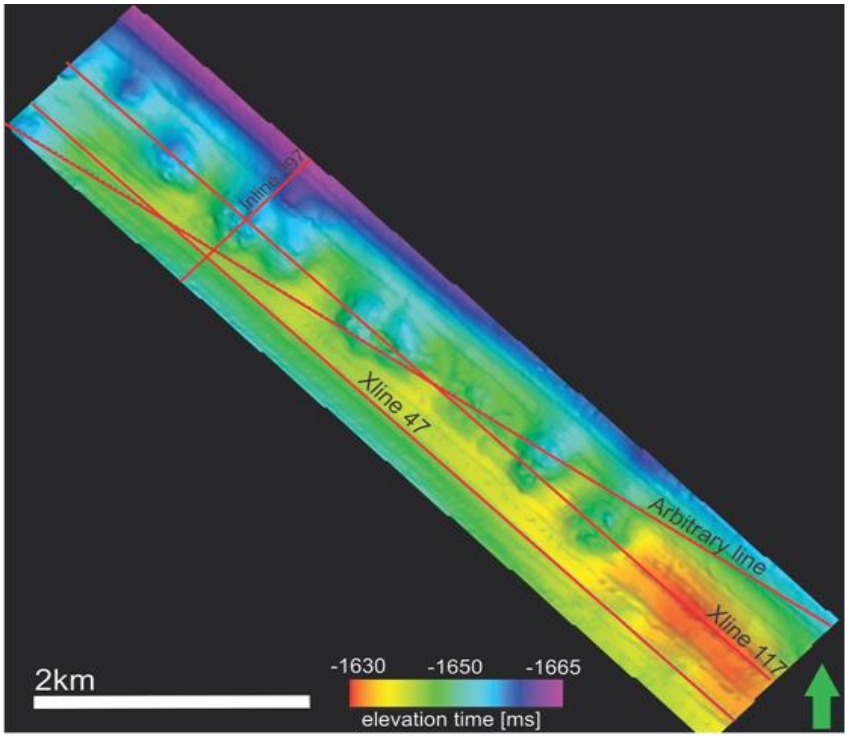

Figure 5.1.7: *Vestnesa ridge A2 (active area seen in figure 2). Depressions seen on the seafloor are described as pockmarks.4 lines cross cut area to show different chimneys/pipe structures.*

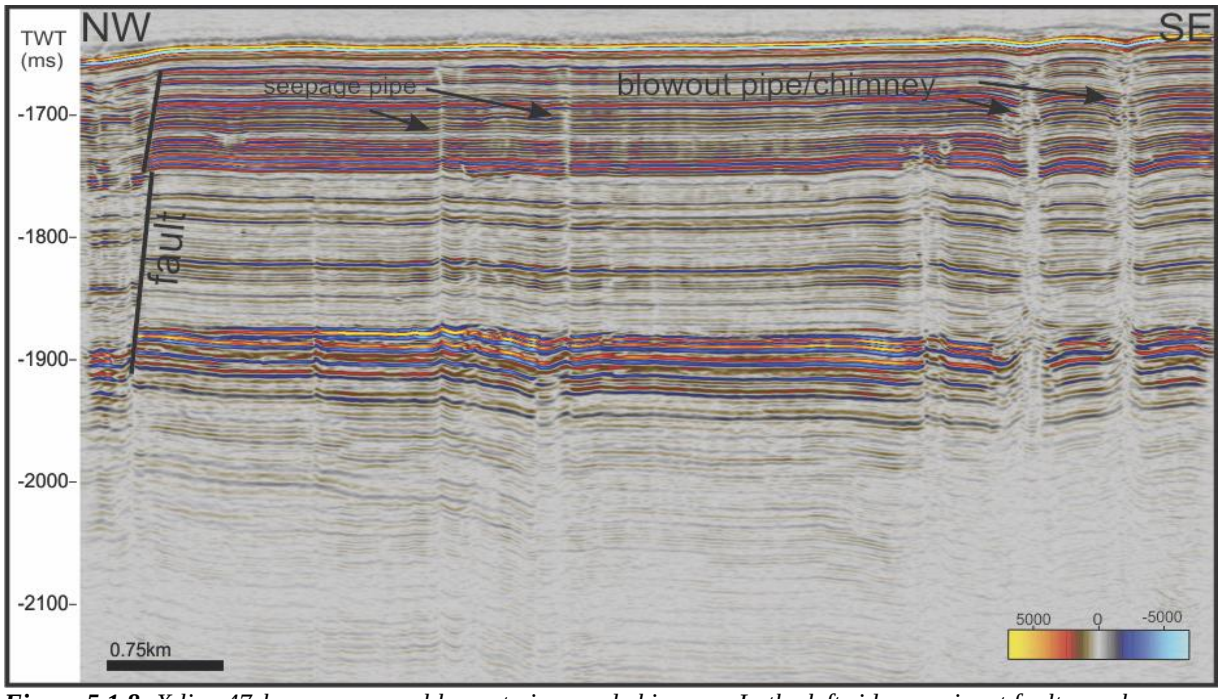

Figure 5.1.8: *X line 47shows seepage, blowout pipes and chimneys. In the left side prominent fault are shown.*

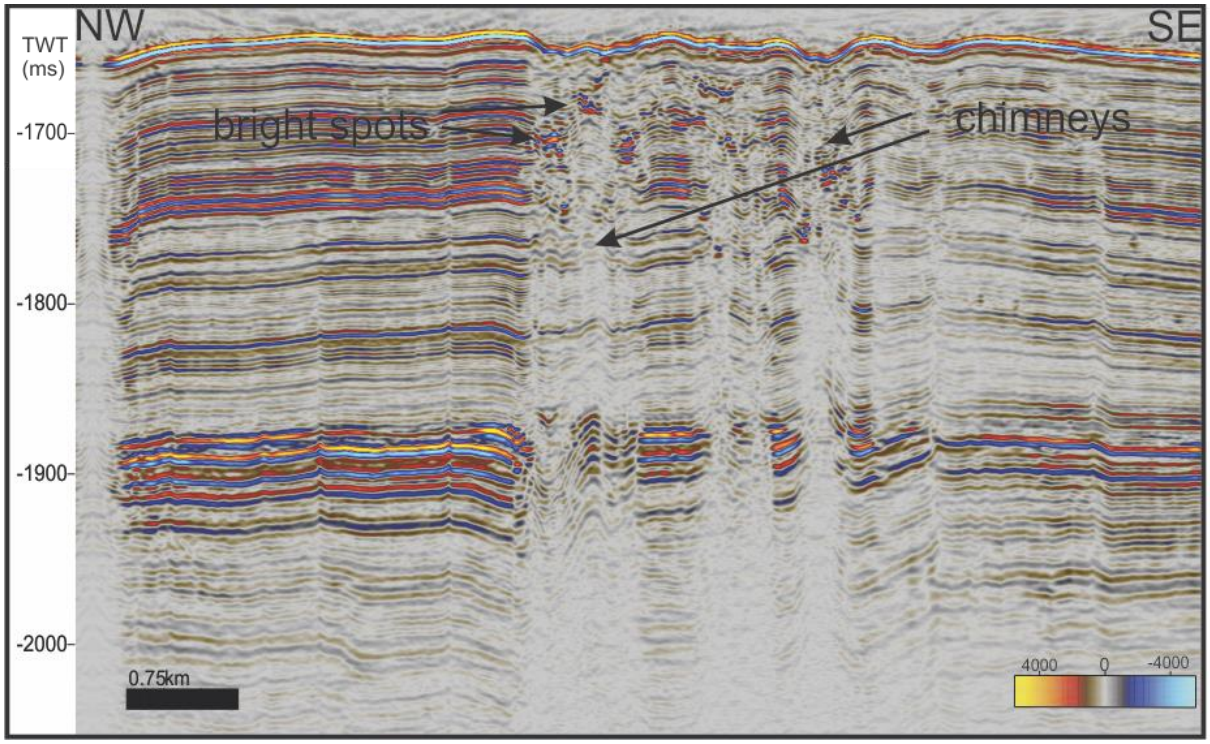

Figure 5.1.9: *Arbitrary line shows chimneys and bright spots.*

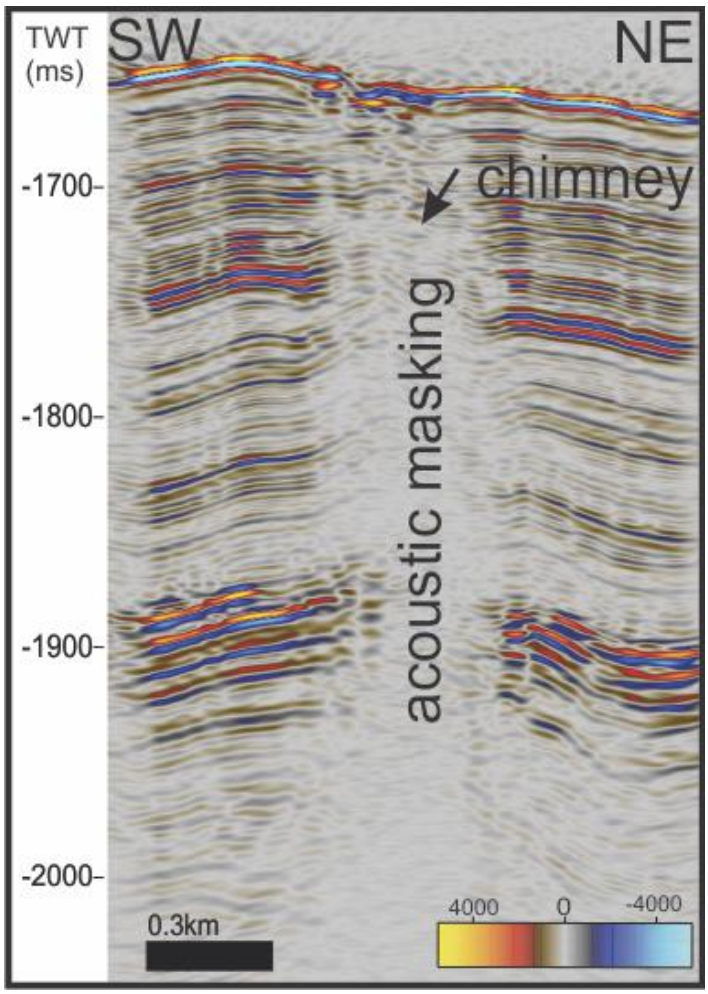

Figure 5.1.10: *Inline 297show acoustic masking and chimney.*

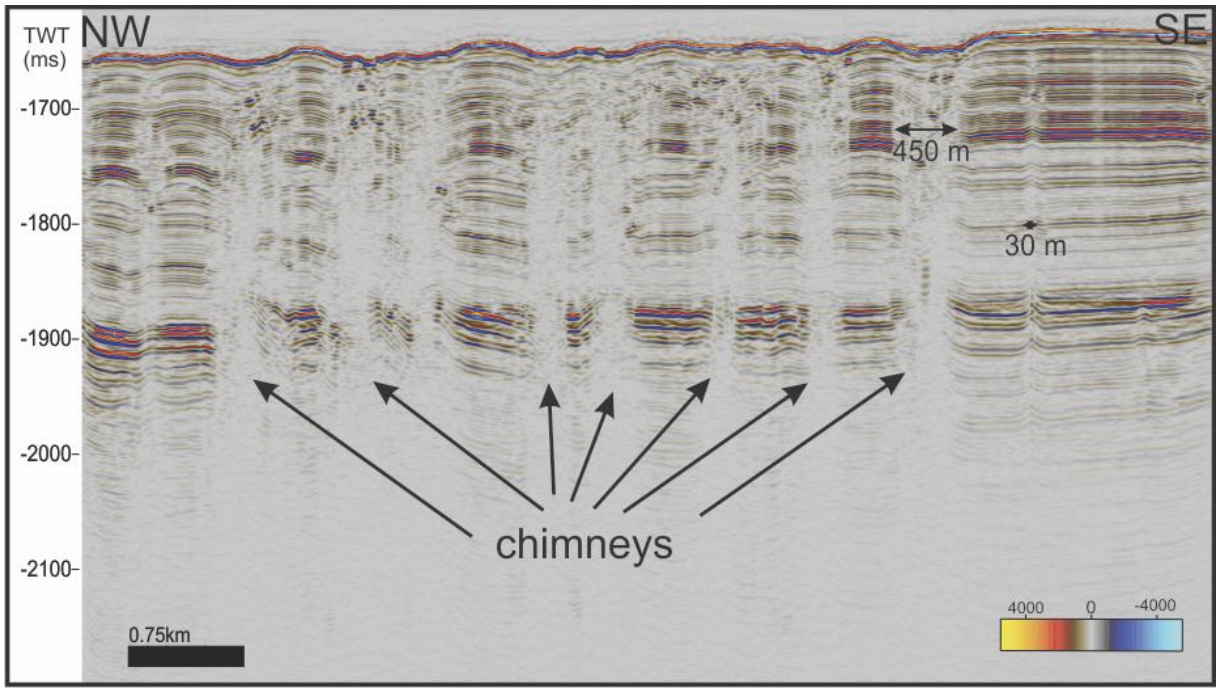

Figure 5.1.11: *Xline 117 showing chimney structures and width difference, between prominent chimneys and pipes.*

5.2 Vestnesa less active (A1)

Using the structural map in the Vestnesa area (A1) (less active) (Figure 5.2.1), the seabed depth varies from - 1655 ms (TWT) in the E, to - 1795 ms (TWT) in the W. The water depth increases towards the W. The whole area covers 29.11 km^2. Seabed depressions, which are located in the given area, are almost separated into two crowds, each almost holding the same number of seabed depressions. In the eastern part of the area the first commune of depressions is found. Further westwards, lies an area with no depressions, which changes to a second crowd of seabed depressions and later again continues without any seabed features. It seems like these depressions are aligned towards the N, NW. Around 25 seabed depressions are found in the Vestnesa (A1) data set. The depression shapes are described as oval, circular, sub circular, semicircular (Figure 5.2.3 and 5.2.8) (Hustoft et al., 2009) and their width varies from 105 up to 700 m (Table 5.2). The spacing between them is irregular. Depressions can reach a depth of 21 ms (TWT) which makes them extremely deep. The shallowest depression is around 2.5 ms (TWT), but average depth ranges from 10 to 17 ms (TWT). Average width lies between 250 - 300 m. The bowl of a depression varies in shapes. It can feature a V or U shape, with both sides symmetrical going deeper and the base being almost flat or asymmetrical, where one side is dipping sharper than the other. In some of the biggest depressions, the area inside is divided by two deeper going depressions, where their sides are quite steep. Yet a depression being big does not necessarily imply that it will also be deep. Some depressions are elongated to the NE and NW. On seafloor an acquisition of footprints is

found which are probably artifacts that cut through the area from E to W. In the whole area the approximate depth difference is 140 m in 15570 m. By using a basic trigonometric formula, the calculated angle of the slope through the area was calculated as only 0.5 degrees. Therefore the area appears to be relatively flat.

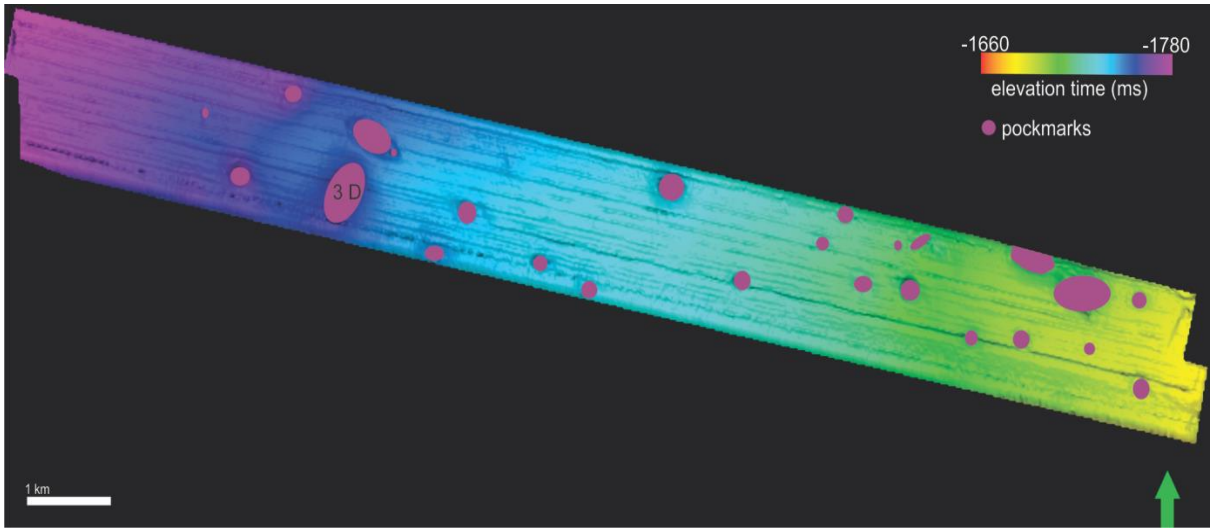

Figure: 5.2.1 *Map view of seafloor in Vestnesa (A1). 25 pockmarks in purple are showed. One of the pockmarks is marked with '3D' and it is shown in figure 6.1.1. (B) Vertical exaggeration is 15.*

Table 5.2: *Shows width and depth of all 25 pockmarks in the area.*

Pockmark	Width, m	Depth, ms	Pockmark	Width, m	Depth, ms
1.	340	13	**13.**	160	3
2.	105	2.5	**14.**	220	11
3.	350	19	**15.**	260	4
4.	700	20 elongated	**16.**	305	16
5.	650	19 elongated	**17.**	125	3.5
6.	170	13	**18.**	480	7 elongated
7.	350	6	**19.**	220	4
8.	170	9	**20.**	230	12
9.	250	5	**21.**	520	14
10.	200	3.5	**22.**	590	21
11.	440	19	**23.**	200	7
12.	260	12	**24.**	120	3.5
			25.	210	5

5.2.1 Gas chimneys underlying pockmarks

Chimneys underlying pockmarks in Vestnesa (A1) terminate in different stratigraphic levels/depths (Figure 5.2.2) and their sizes and diameters are different (Figure 5.2.11). Using time slices, chimneys occur as circular to elliptical features and show low amplitude values using the RMS attribute map and 0 - 0.40 value (black – red), using the variance attribute map (Figure 5.2.3). There is also a difference in diameter of chimney conduits (pathways) for fluid flow, characterized as doming, seismic blanking in seismic section (Figure 5.2.7). Chimney and pipe structure widths vary mostly from 50 m up to 250 m. It is complicated to assume their average, because great amounts of chimneys are wider in their upper part only - for instance in depths of 130 ms, 160 ms and 190 ms (TWT). Their diameter also varies from level to level and it is not the same (5.2.9, 5.2.10 and 5.2.11). Interestingly, only few chimneys increase in width above the BSR.

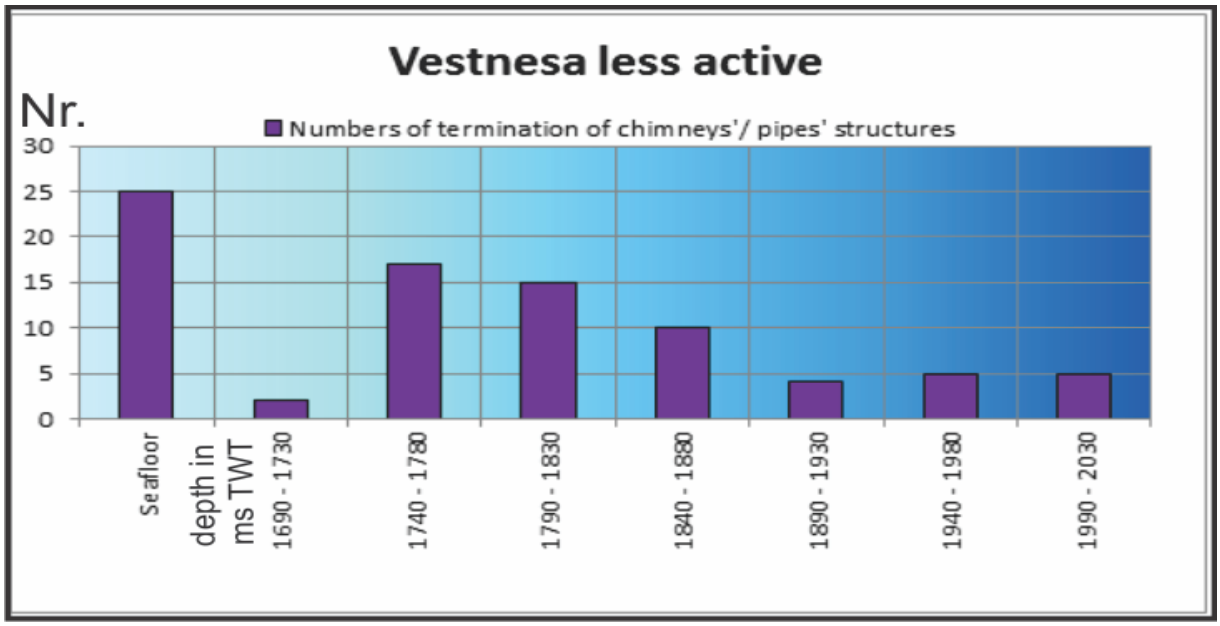

Figure 5.2.2: *On the left side, the diagram shows a number of terminations of chimneys/pipe structures. In the bottom part are depth units where features terminate.*

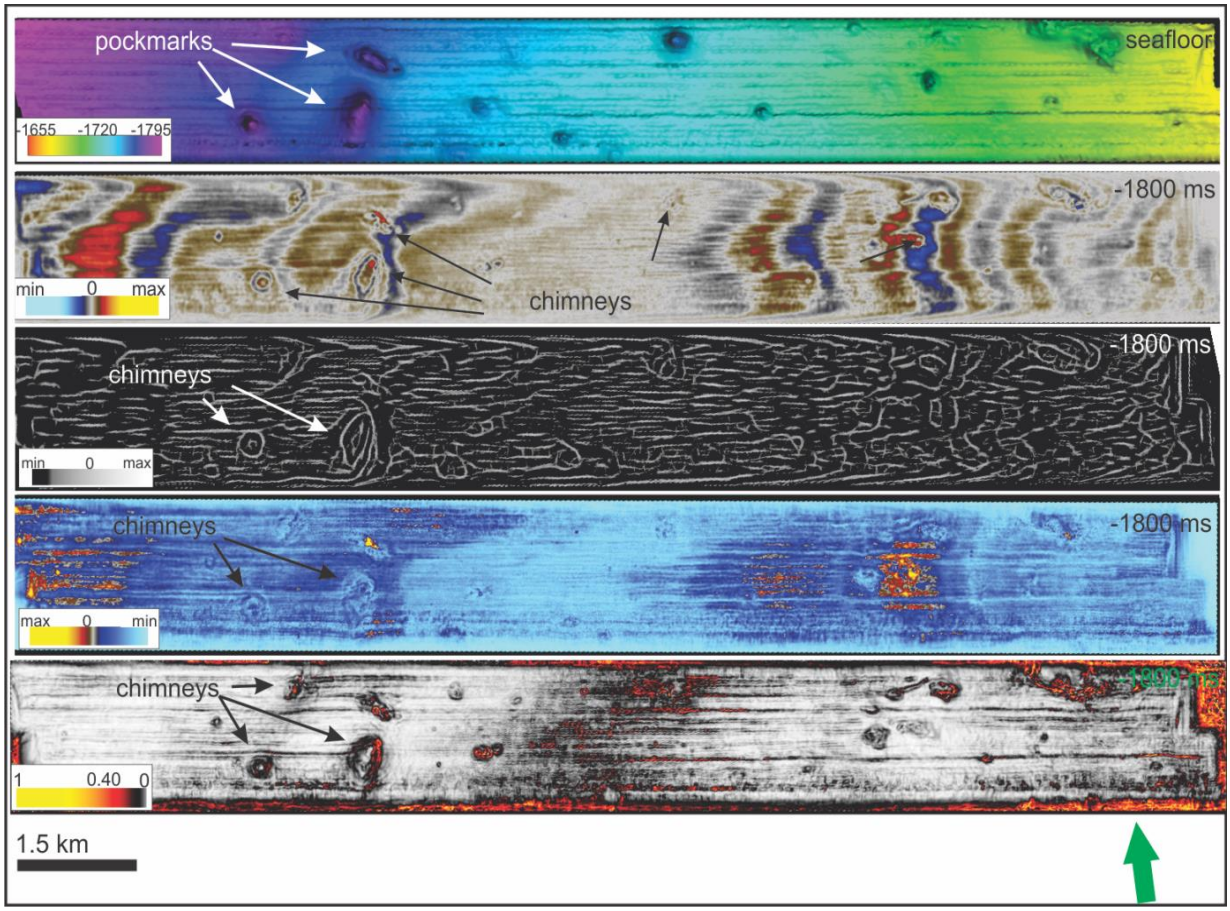

Figure 5.2.3: *Picture shows time slices from - Z line 1800 ms (TWT) using different attributes. From top to bottom: Structural map, original amplitude map, edge, rms amplitude and variance attribute map.*

5.2.2 The BSR depth and free gas zone thickness

The BSR in area (A1) is located 200 - 210 ms (TWT) below seafloor. The free gas zone is 30 - 100 m thick below the BSR according to Hustoft et al. (2009). Using the instantaneous frequency volume attribute (Figure 5.2.4) in Vestnesa less active area (A1) sudden frequency changes below the BSR were found. From ≈2000 ms (TWT) down, frequency changes from 100 - 0 Hz. Above the BSR frequency changes from up to 500 Hz down to 100 Hz. Lowest frequencies are visible right below the BSR and can indicate free gas accumulation which is not more than 100 m thick.

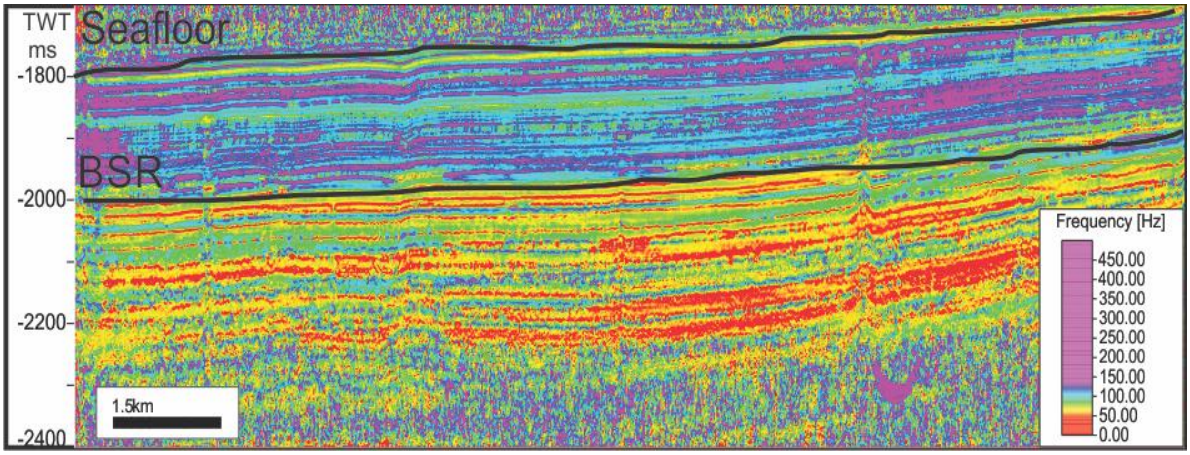

Figure 5.2.4: *Using instantaneous frequency attributes low and high frequencies were found in Vestnesa (A1). Seafloor and the BSR lines are shown to help see differences. X line 150 was used.*

5.2.3 Periods of activity

Chimney flanks at Vestnesa (A1) match the termination of horizontal strata and are characterized as push down reflections within GHSZ. For smaller structures, however, pull-up reflections occur. Pull-up reflections are also seen from the bottom, up to the BSR, in places where pipe structures and chimneys occur. In the BSR, there are both, pull-up and push-down reflections. Within GHSZ reflections are mostly pointed down - push-down, but smaller pipes with width 25 - 34 m are pointed up - pull-up. Between terminations inside the chimney chaotic reflections or seismic blanking is visible. Truncations (Figure 5.2.5), if compared with continuous reflections, terminate in places, where a chimney pierces through sediments or in places where specific stratigraphic events have happened during sediment deposition. Truncations are easily seen at several levels (Figure 5.2.5). Their occurrence is also ‘key’ to interpret active and inactive periods (Figure 5.2.5b). The right side (Figure 5.2.5) is marked with a vertical color bar, where one can distinguish layer continuity and truncations.

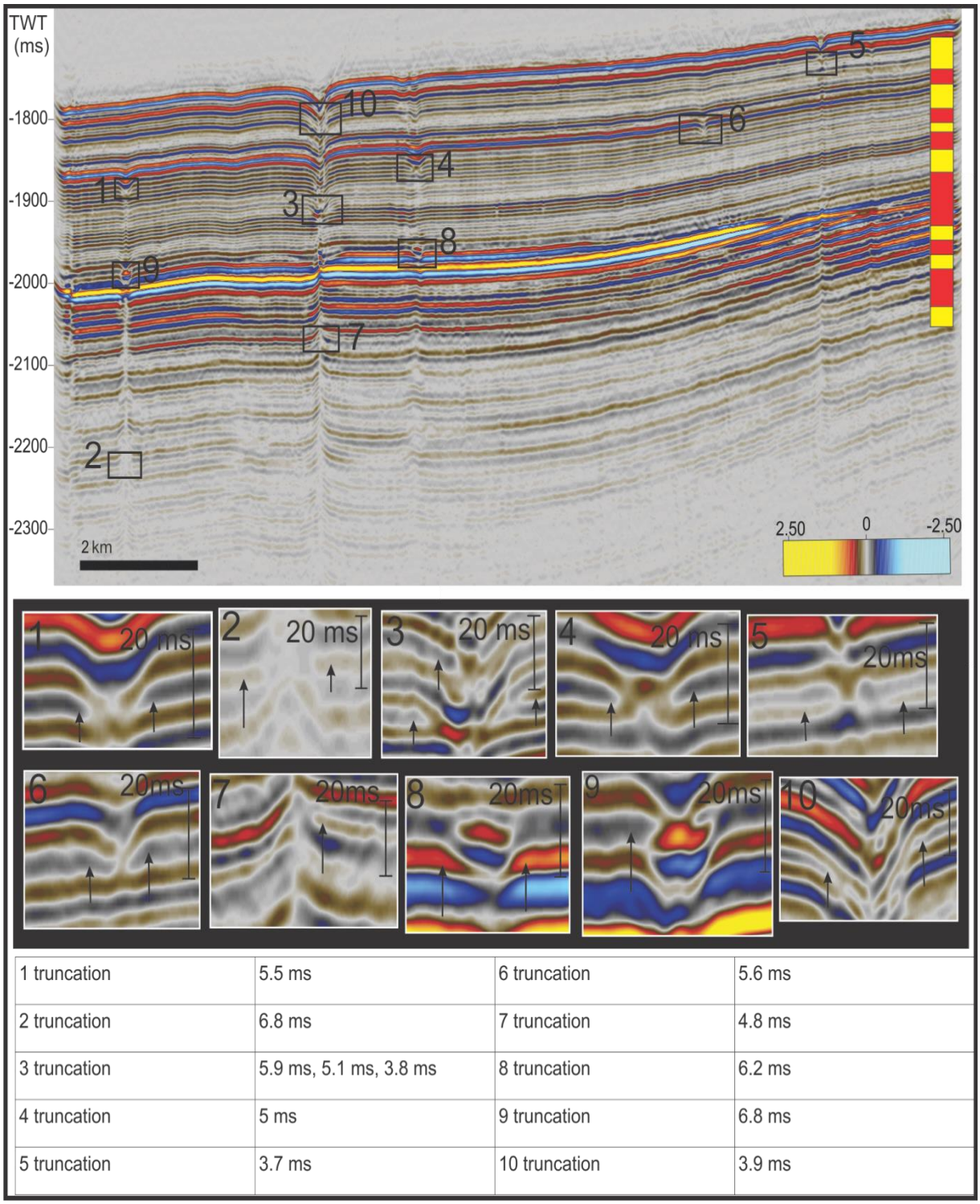

1 truncation	5.5 ms	6 truncation	5.6 ms
2 truncation	6.8 ms	7 truncation	4.8 ms
3 truncation	5.9 ms, 5.1 ms, 3.8 ms	8 truncation	6.2 ms
4 truncation	5 ms	9 truncation	6.8 ms
5 truncation	3.7 ms	10 truncation	3.9 ms

Figure 5.2.5: *Random truncations in area, x line 129 were used. As seen, truncations are scattered around whole data. Lower part of figure shows zoomed in truncations and their thicknesses. In upper right side color bar is indicating active and inactive periods. This bar is made considering every stratigraphic layer continuation. Yellow: active venting, red: seeping.*

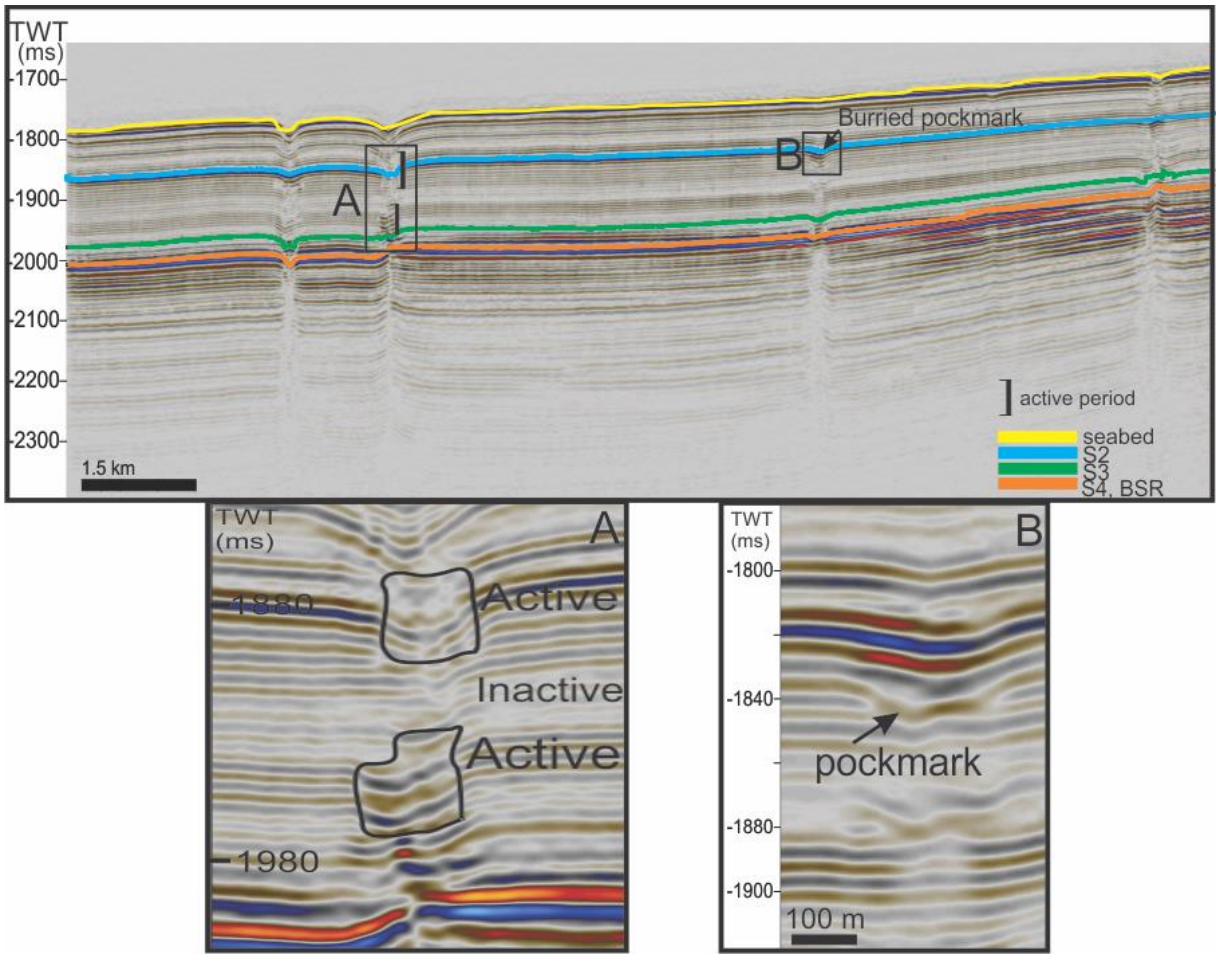

Figure 5.2.5a: *Main period of fluid expulsion. Upper picture shows location of layers S2, S3 and S4. Inline 89 is used to show crosscut of area. Lower picture shows active, inactive period in Vestnesa (A1).*

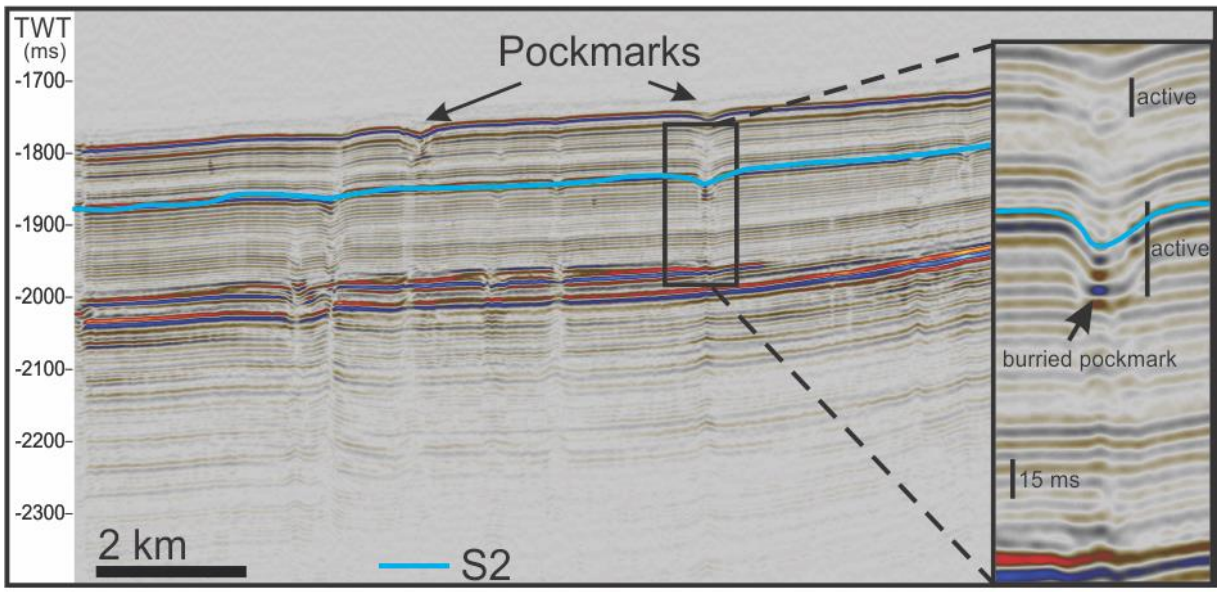

Figure 5.2.5b: *Showing horizon S2, this is interpreted as main period of fluid flow activity in region. Buried pockmark are zoomed in.*

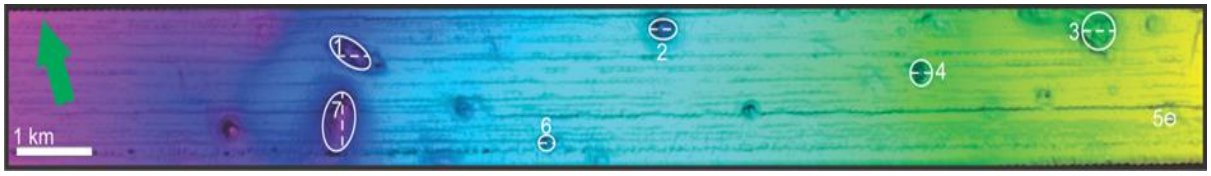

Figure 5.2.6: *Location of 7 chosen chimneys that are connected with seafloor. Figure can be correlated with (Figure 5.2.7).*

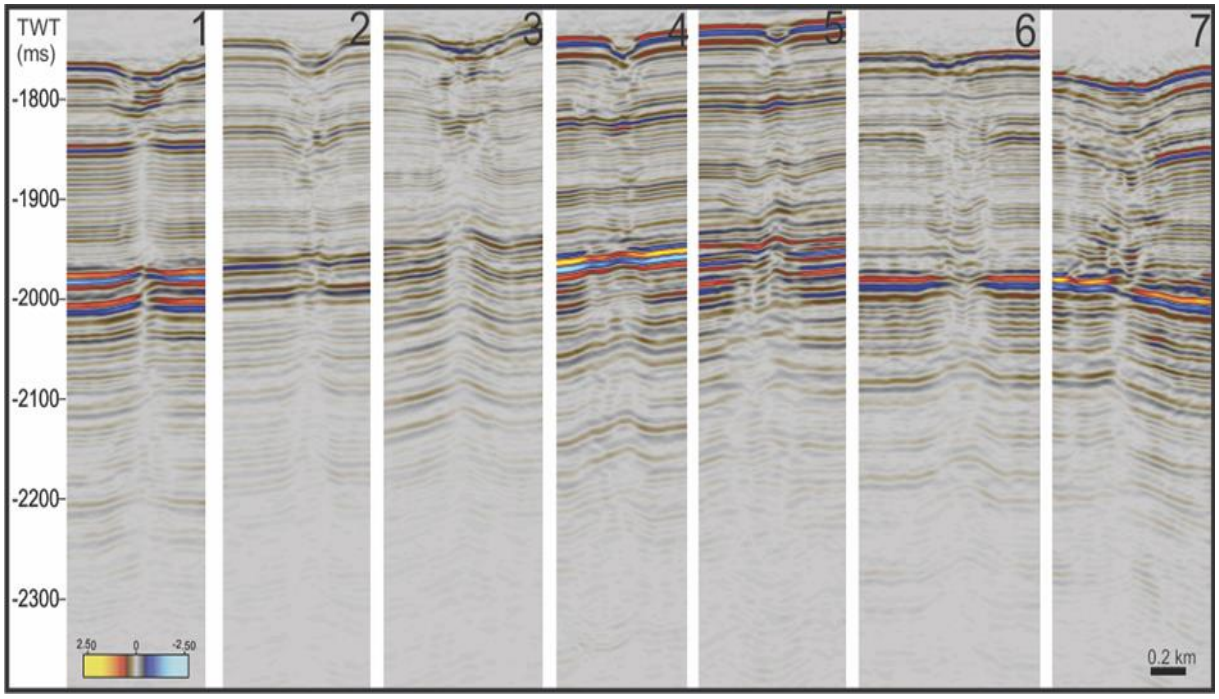

Figure 5.2.7: *7 chimneys internal structures. Location of them is given in figure 5.2.6.*

5.2.4 Faults

Not as faulted as Vestnesa (A2), but still occurrence of faults and fractures represents a complex fluid flow system. Around - 1850 ms (TWT) bsf faults are visible to start to develop (Figure 5.2.7B). They are spread over the whole area, but their covering density is not marked at this point. Some faults at - 2000 ms (TWT) are 500 - 900 m long which is why they are seen in Figure 5.2.7A. Single faults are - 60 m in width and don't represent any defined direction. Larger single faults are located in the NW of the area. Last but not least, no plough marks are observed in the Vestnesa less active region.

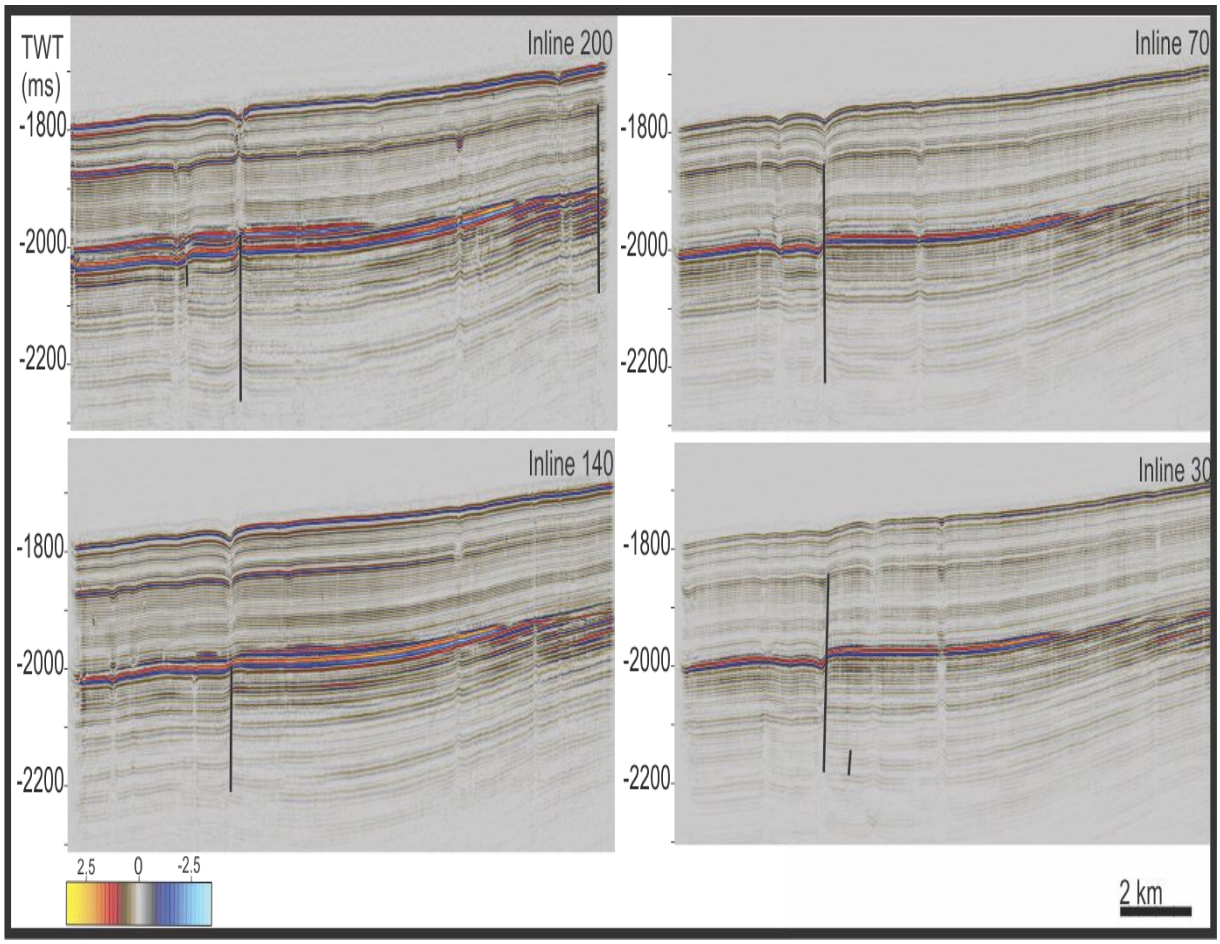

Figure 5.2.7A: *4 different seismic sections showing biggest faults in the region.*

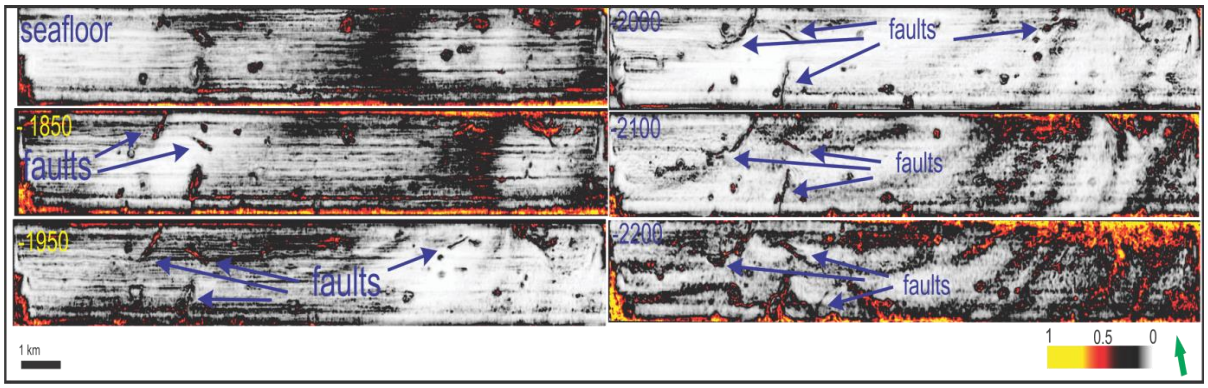

Figure 5.2.7B: *6, 2D pictures showing faults in different depths (seafloor, - 1850, -1950, -2000, -2100 and -2200 ms (TWT) in Vestnesa area (A1).Variance attribute is used to indicate them.*

5.2.5 Chimney differences

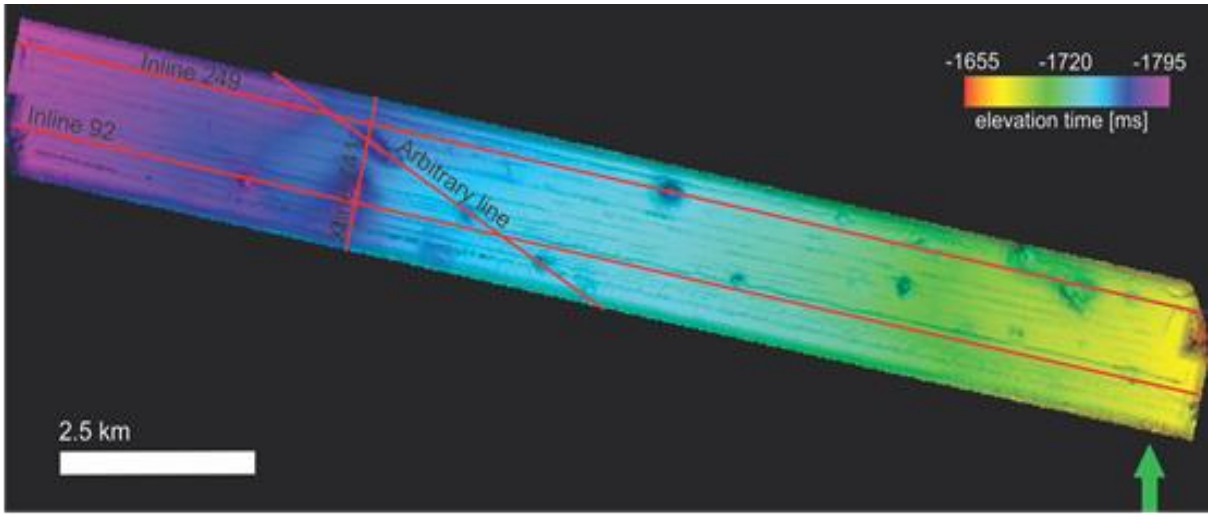

Figure 5.2.8: *Vestnesa ridge A1 (less active area). Depressions are interpreted as pockmarks. 4 red lines crossing area shows most interesting places that can be seen on next figures.*

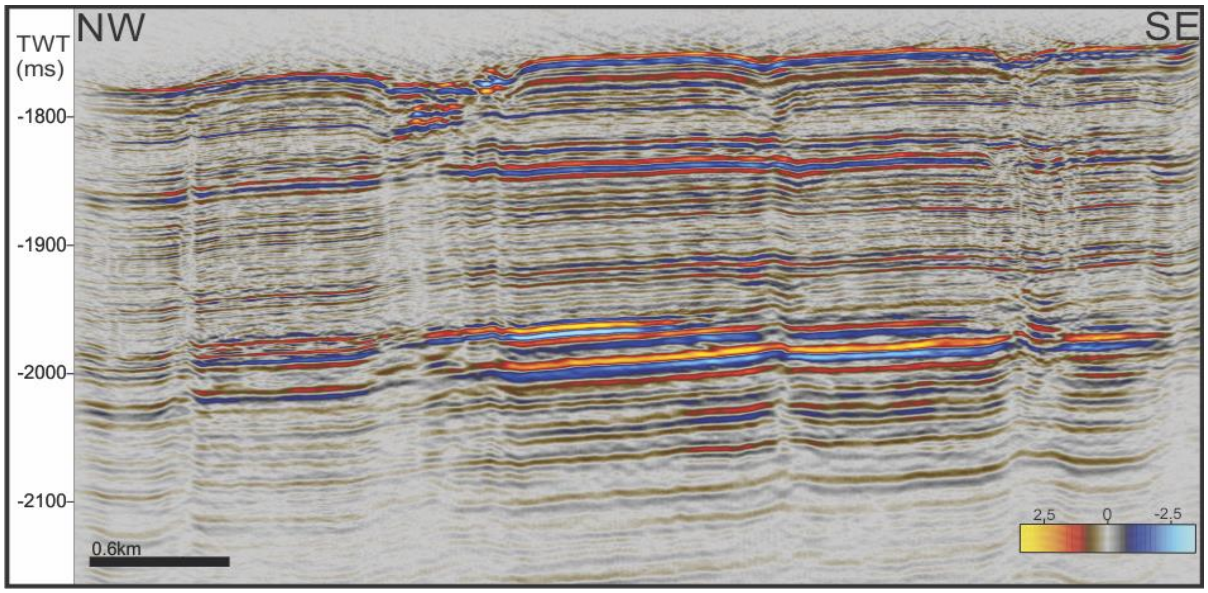

Figure 5.2.9: *Arbitrary line. Big pockmark showing high amplitudes at their shallow base.*

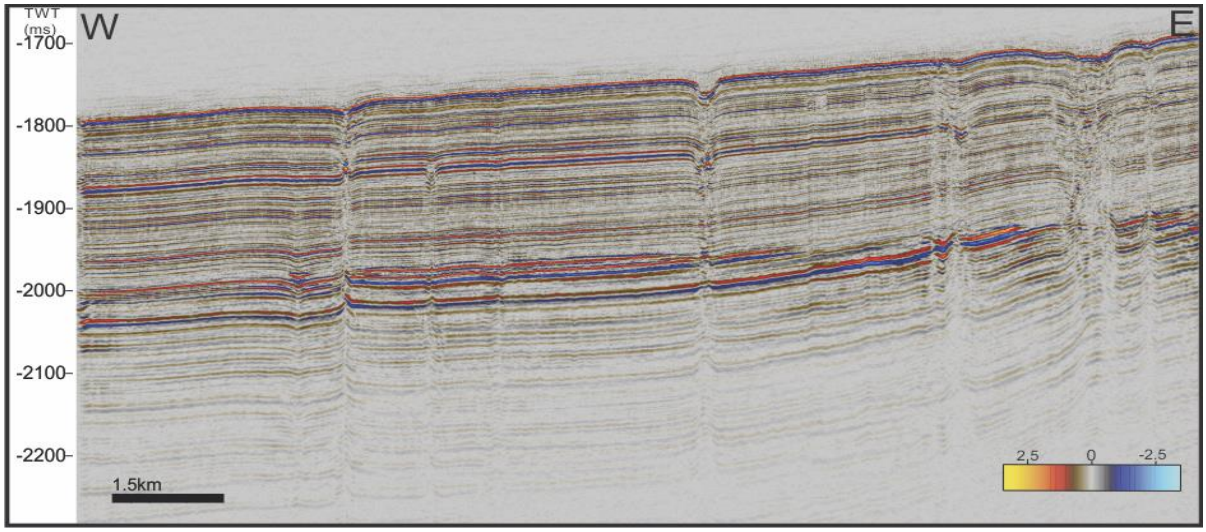

Figure 5.2.10: *Inline249 shows pockmarks and chimneys in the area. Below the BSR, pull up and within GHZS, push down is seen in the flanks of the chimneys.*

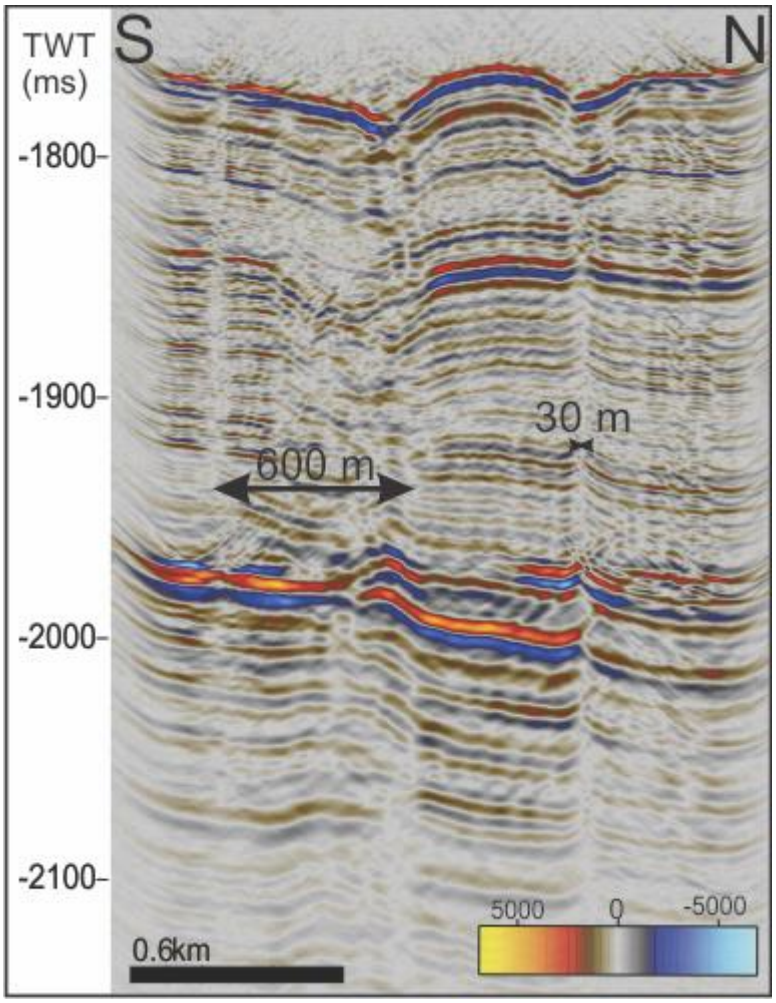

Figure 5.2.11: *Xline 741 showing chimney, pipe structures and their width.*

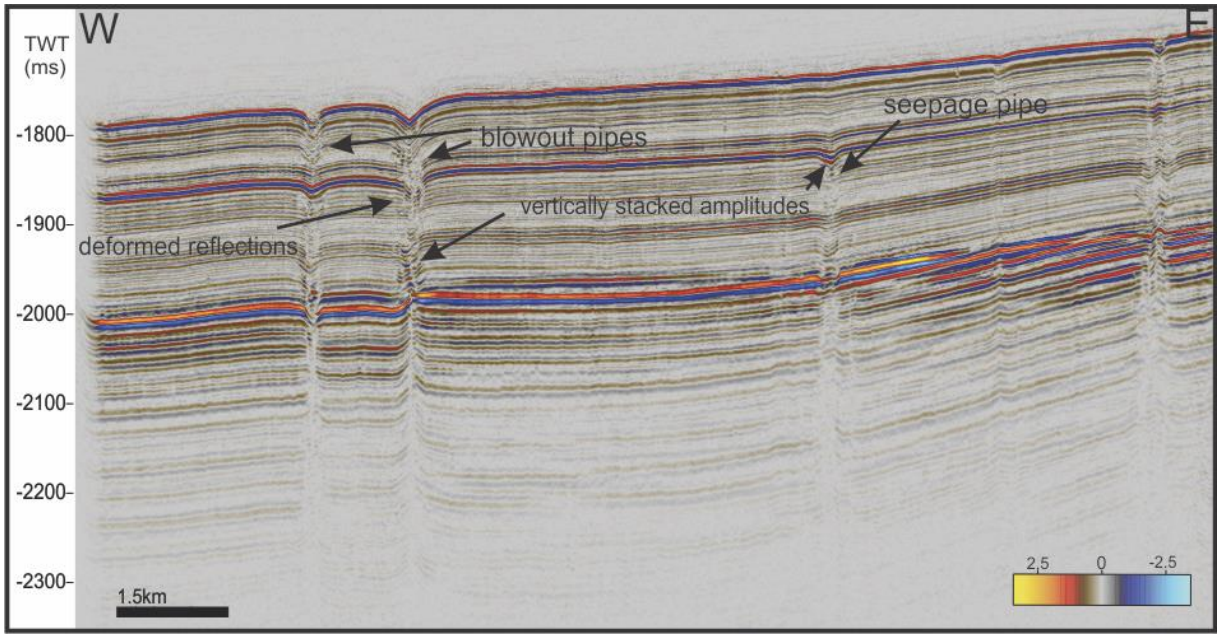

Figure 5.2.12: *Inline 92 showing seepage and blowout pipes. Deformed reflections and stacked amplitudes are visible in chimney structures where push-down occurs.*

5.3 Nyegga

Using a structural map in the Nyegga data set the seabed depth varies from - 995 ms (TWT) in the NW, to - 945 ms (TWT) in the SE. The water depth increases from E to W. The area covers a total of 34.17 km^2 (Figure 5.3.1).

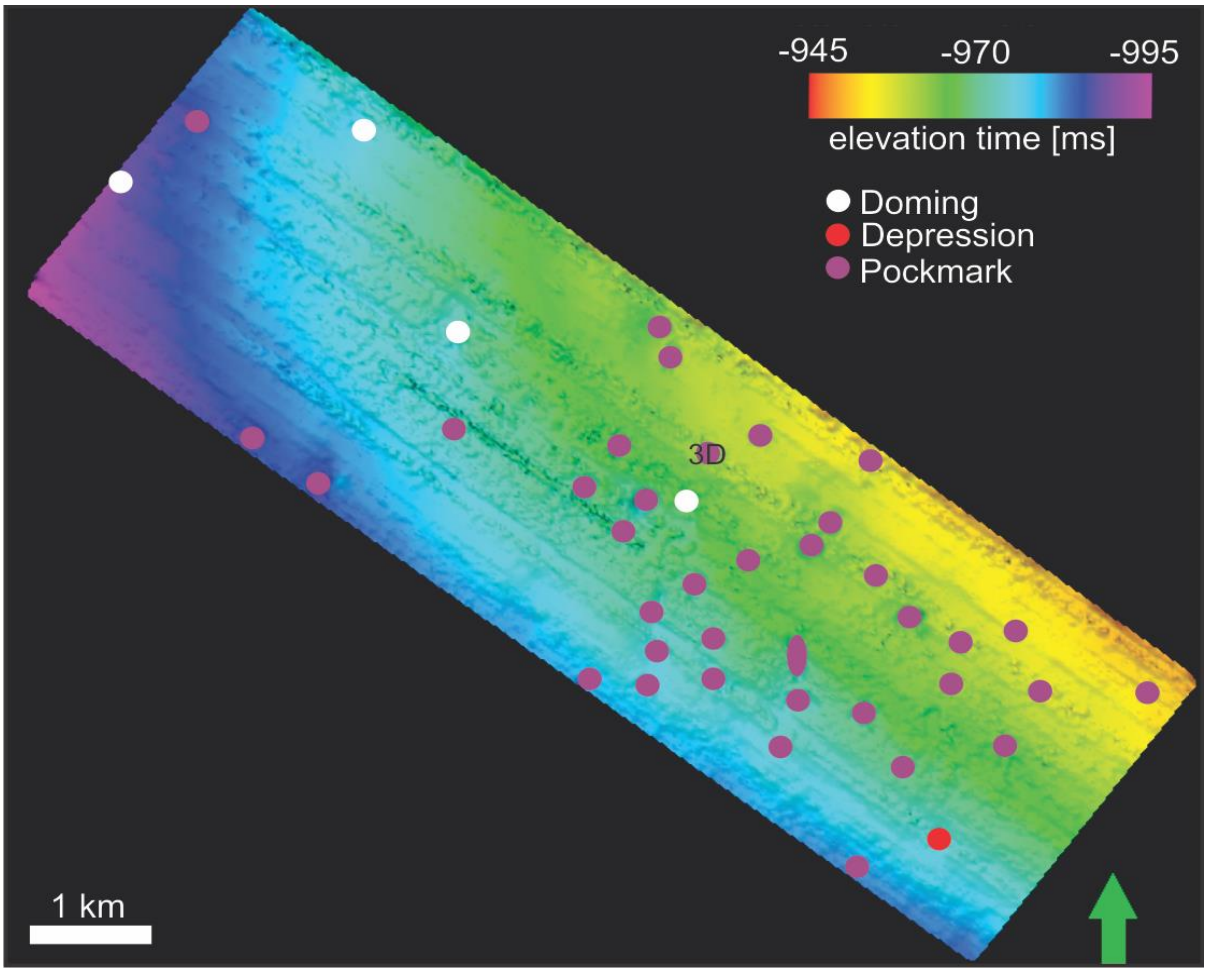

Figure: 5.3.1 *Map view of the seafloor in the Nyegga. 37 pockmarks are showed, 4 domings and 1 depression. Doming is marked as white circle, depression as red circle and pockmarks as purple. One pockmark is marked with '3D' which is shown in figure 6.1.1 (A). Vertical exaggeration is 10. Marked as doming 4 features because under them is a chimney, but instead of crater on the seafloor, they are domed.*

Depressions are scattered all over the area, but in the SE part, most of the seabed depressions are found, where depth varies from - 950 to - 970 ms (TWT) below sea level. In the NW side only a few depressions are visible. The area is abundant with at least 42 seabed features (37 pockmarks, 4 domings and 1 depression). Pockmark shapes are mostly circular to semi-circular (Figure 5.3.3 and 5.3.12) with sizes from 40 up to 450 m wide, and an average width of 140 m (Table 5.3). The spacing between them is irregular. Some of the craters are aligned, but mostly randomly scattered (Figure 5.3.12). They can reach a depth of 12 ms (TWT), but are mostly 6 - 7 ms (TWT) deep. The bowl of the features could be seen as both sides symmetrical or asymmetrical. The bases of the craters vary between slightly dipped,

sharp v-shaped or one side slightly dipped and the other sharp dipped. However, their base is not as disturbed and rugged as in Vestnesa implying that the expulsion of vigorous gas has not disturbed the sediments. Only a few of the pockmarks are elongated towards the N. On the seafloor acquisition footprints are found, which are probably artifacts that cut through the area from SE to NW. It is obvious to say, that the Nyegga given area is almost flat, since from the deepest to the shallowest depth the difference is only 50 ms (TWT) within 10325 meters.

Table 5.3: *Shows width and depth of 37 pockmarks.*

Pockmark	Width [m]	Depth [ms]	Pockmark	Width [m]	Depth [ms]	Pockmark	Width [m]	Depth [ms]
1.	140	6	**14.**	95	3	**27.**	95	3
2.	150	5.5	**15.**	60	2	**28.**	90	2
3.	140	6	**16.**	75	6	**29.**	60	1.5
4.	140	4.5	**17.**	120	3	**30.**	190	3.5
5.	170	6	**18.**	110	3	**31.**	40	1.5
6.	210	9.5	**19.**	110	2.5	**32.**	450	10
7.	145	7	**20.**	170	5	**33.**	200	12
8.	250	9.5	**21.**	180	9	**34.**	110	3.5
9.	130	6	**22.**	135	5.5	**35.**	60	2.5
10.	155	6	**23.**	180	8.5	**36.**	150	5.5
11.	130	5.5	**24.**	85	2	**37.**	60	2.5
12.	65	2	**25.**	145	4			
13.	90	2	**26.**	85	2			

5.3.1 Gas chimneys underlying pockmarks

Chimneys underlying pockmarks in Nyegga terminate in different stratigraphic levels/depths (Figure 5.3.2) and their sizes and diameters differ (Figure 5.3.14). Using time slices, chimneys occur as circular to elliptical features and show low amplitude values using the RMS attribute map and 1 - 0.10 value, (yellow – red) using the variance attribute map (Figure 5.3.5). There is also a difference in diameter of chimney conduits (pathways) for fluid flow, characterized as doming, seismic blanking in seismic section. Chimney and pipe structure widths vary mostly from 40 m up to 280 m, but on average, they are around 100 m in width (Figure 5.3.14). Their diameter also varies from level to level and is not the same. Similar to Vestnesa, sometimes right above the BSR their width is larger than below it. Base of L50 and Top of L50 (Figure 5.3.10A) are horizons where most of the chimneys terminate (Figure 2.2.6). However, numbers of chimneys terminate at the depth of BSR; around 20 to

40 ms (TWT) below the seafloor and at the base of L70. In a few cases, chimneys terminate at one horizon but continue from the horizon as small conduits, which connect to the pockmark. Towards the seafloor chimneys are getting narrower at times. Occasionally chimneys are terminating near the seafloor without any visible pipe, though showing pockmarks on the seafloor. Resolution and a lack of data is the only reason why it is hard to see where, and at what depth chimneys originate, but it is thought chimneys and pipe structures are mostly 350 up to 880 ms (TWT) long with an average of 600 to 700 ms (TWT) in length.

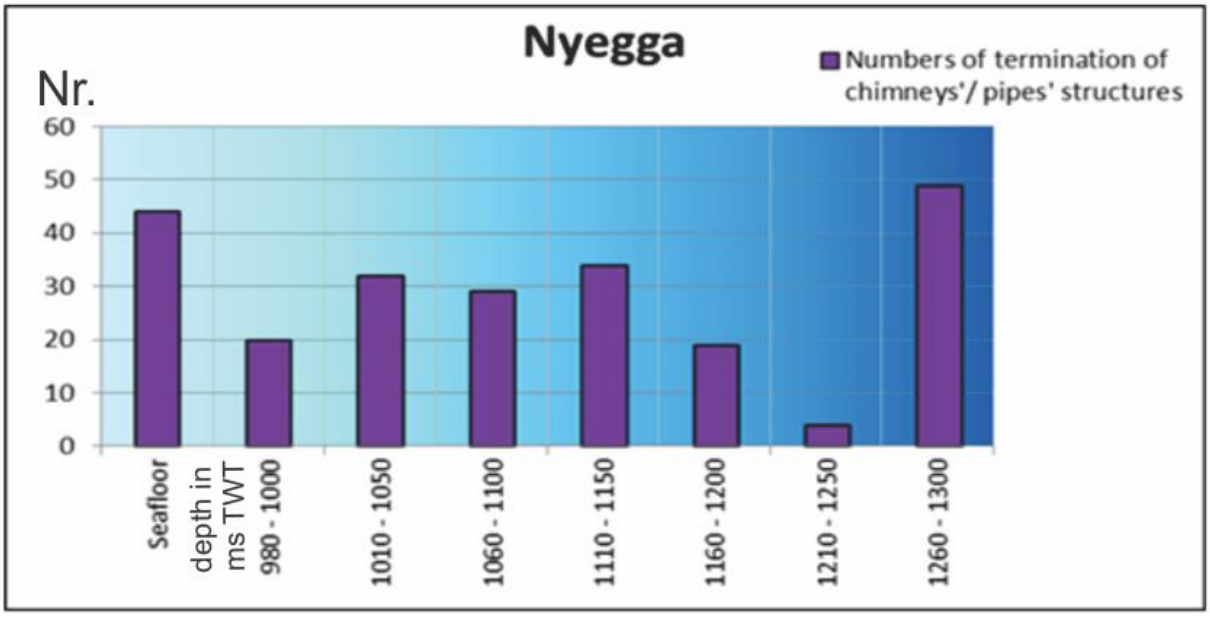

Figure 5.3.2: *In the left side, diagram shows number of terminations of chimneys/pipe structures. In the bottom part are depth units, where features terminate.*

In order to show how different features such as gas chimneys/pipe structures, plough marks and faults look from above in Nyegga, Figure 5.3.5 was created. Three levels were chosen: time slice 1002, which is located near the seafloor; time slice 1097, which is located between top and base of L50 and time slice 1292, which is located at level of the BSR. Pictures from 1 to 3 were made using the variance attribute. The rest of the pictures, 4 - 6 show the same depths, but original seismic amplitude was used instead. It is obvious that by using the variance attribute, structures are easier determined. Yellow color (in 1 - 3) indicates pockmarks, gas chimneys/pipe structures, but (in 4 - 6), it is not easy to determinate them, therefore green circles and arrows are shown.

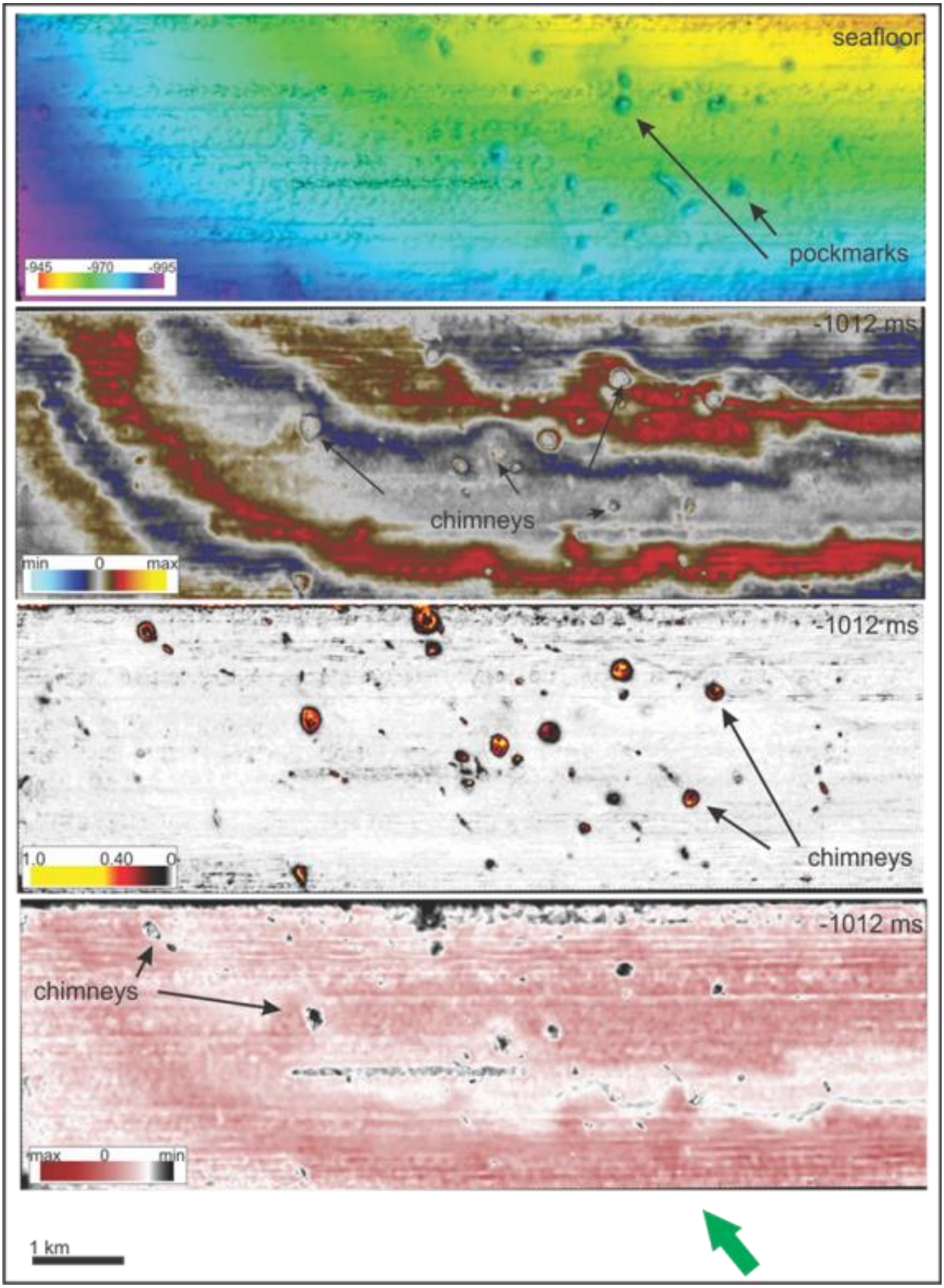

Figure 5.3.3: *Upper part of picture shows seafloor, below it - time slices from - 1012 ms (TWT) using different attributes: Structural map, original amplitude map, variance and rms attribute map.*

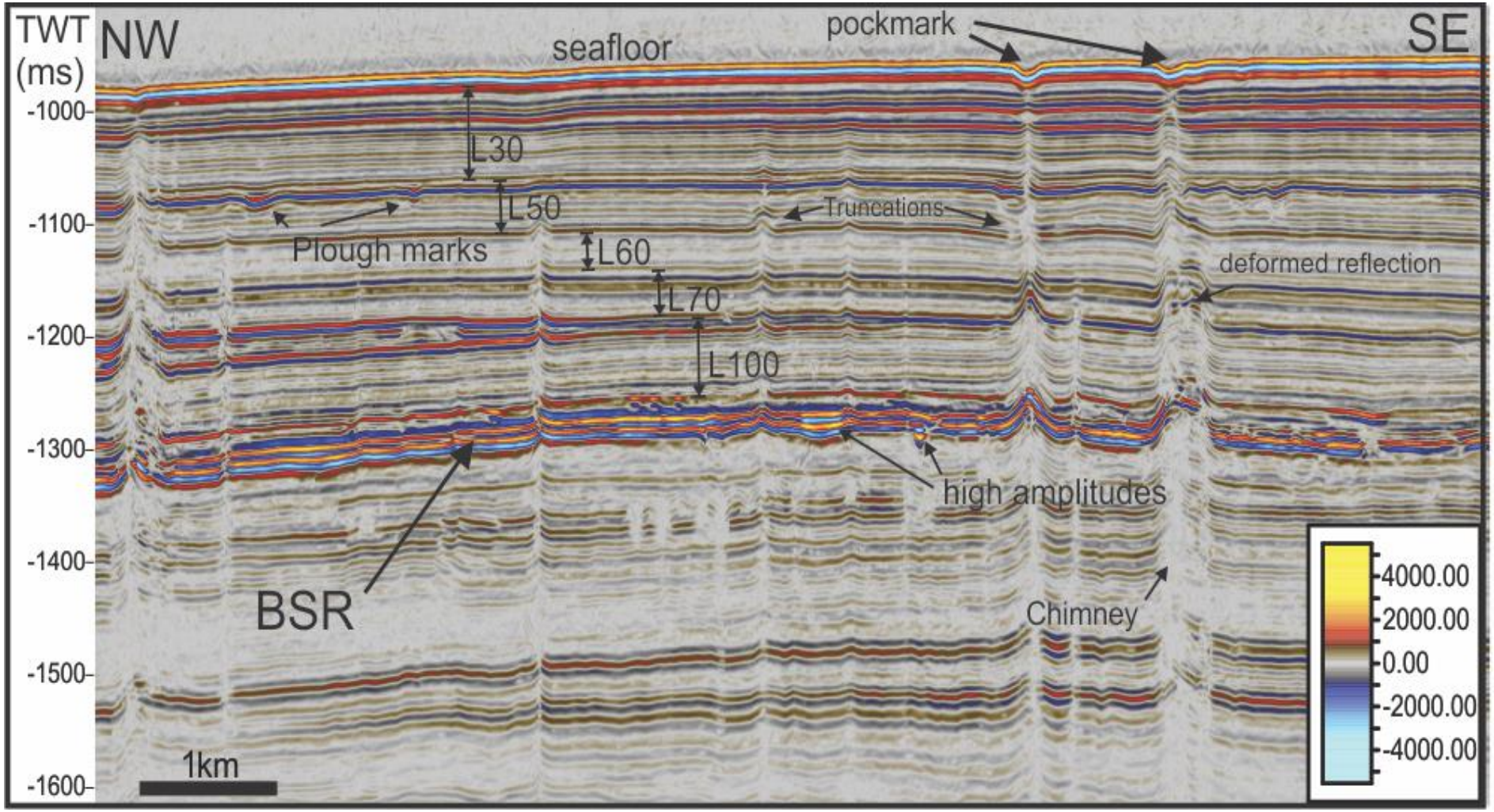

Figure 5.3.4: *Stratigraphic correlation from (Plaza-Faverola* et al.*, 2010b) X line 201 is shown.*

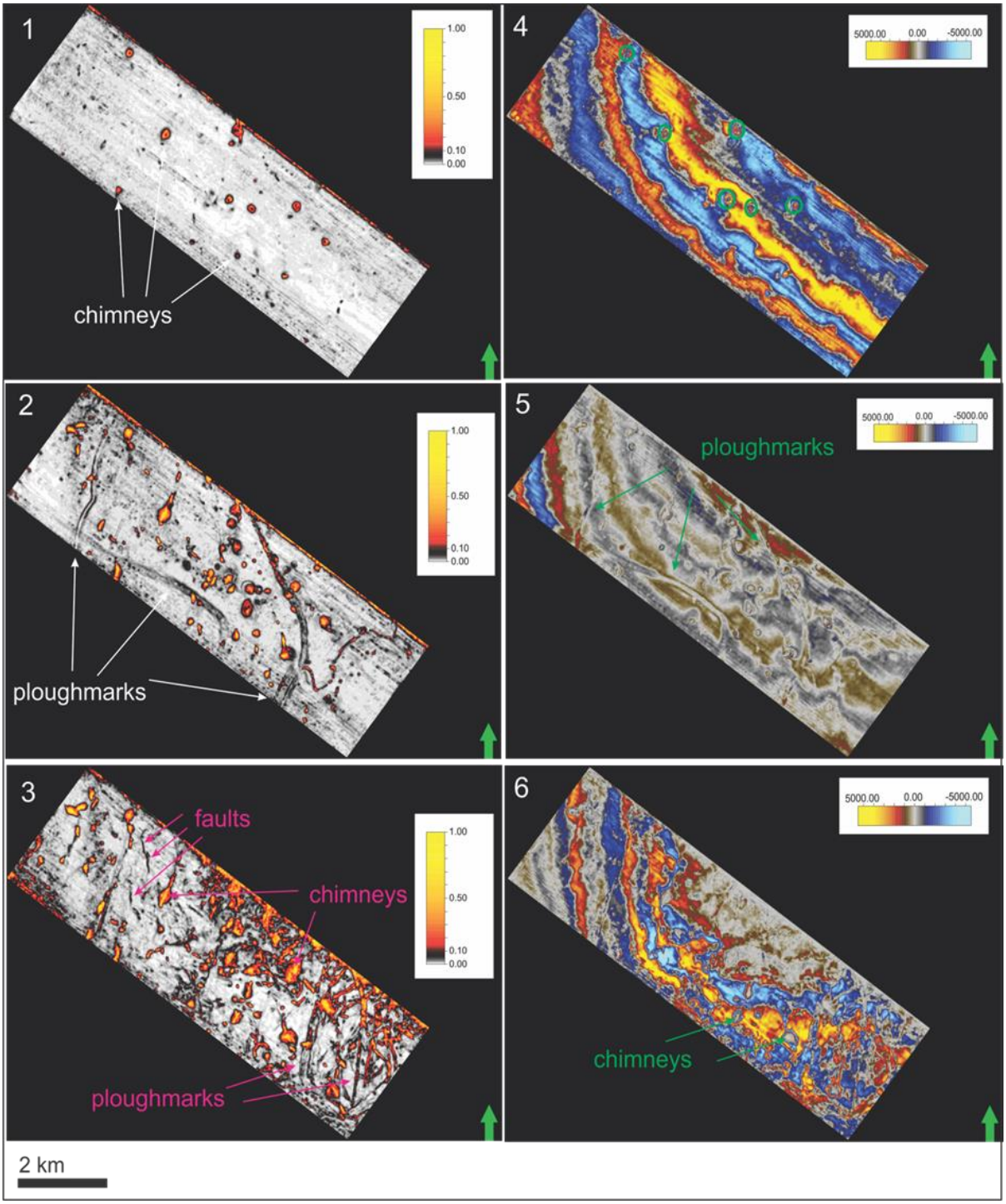

Figure 5.3.5: *1. Time slice 1002 showed using variance attribute 2. Time slice 1097 is located between Top and Base of L50 it is showed using variance attribute. 3. Time slice 1292 (the BSR) using variance attribute. 4. Time slice 1002 showed using original amplitude. 5. Time slice 1097 showed using original amplitude. 6. Time slice 1292 (the BSR) showed using original amplitude.*

5.3.2 The BSR depth and free gas zone thickness

GHSZ thickness in Nyegga varies because GHSZ itself is mainly controlled by several factors: bottom water temperature, sedimentation rate and geothermal gradient etc. (Mienert et al., 2001; Plaza-Faverola et al., 2012). However, existence of the BSR in Nyegga is controlled by the termination of debris flow deposits (Bünz et al., 2003; Plaza-Faverola et al., 2010). The BSR in Nyegga region is located at around - 1320 ms (TWT) from the seafloor, which marks transition of hydrate bearing sediments. The BSR consists of high dense and low permeable material (King et al., 1996) that shows high seismic velocities. Beneath free gas accumulation is found. The BSR occurs only in contouritic and hemipelagic deposits of the Naust formation (Figure 2.2.6) (Plaza-Faverola et al., 2010).

Assuming average velocity through the sediments in Nyegga is 1600 m/s, making calculations (t/1000xvelocity), results in approximately 88 m of free gas (1280 - 1330 ms (TWT)) below the BSR. The FGZ (Free gas zone) has different thicknesses, which is mainly controlled by the BSR border itself, but mostly it is less than 100 m thick in Figure 5.3.15 (Bünz et al., 2005). The debris flow deposits disturb gas hydrate accumulation, but help free gas to accumulate beneath them. Nevertheless, because of the absence of glacial debris deposits, formation of gas hydrates is more effective (Plaza-Faverola et al., 2010).

An interesting example of where free gas can migrate along faults comes from the Blake Ridge. Nevertheless, impedance contrasts caused by the presence of low-velocity free gas is easy to detect, because of the low frequency zone (Taylor et al., 2000). Using the instantaneous frequency and sweetness attribute accordingly, (Figure 5.3.6 and 5.3.7) the BSR was easily detected.

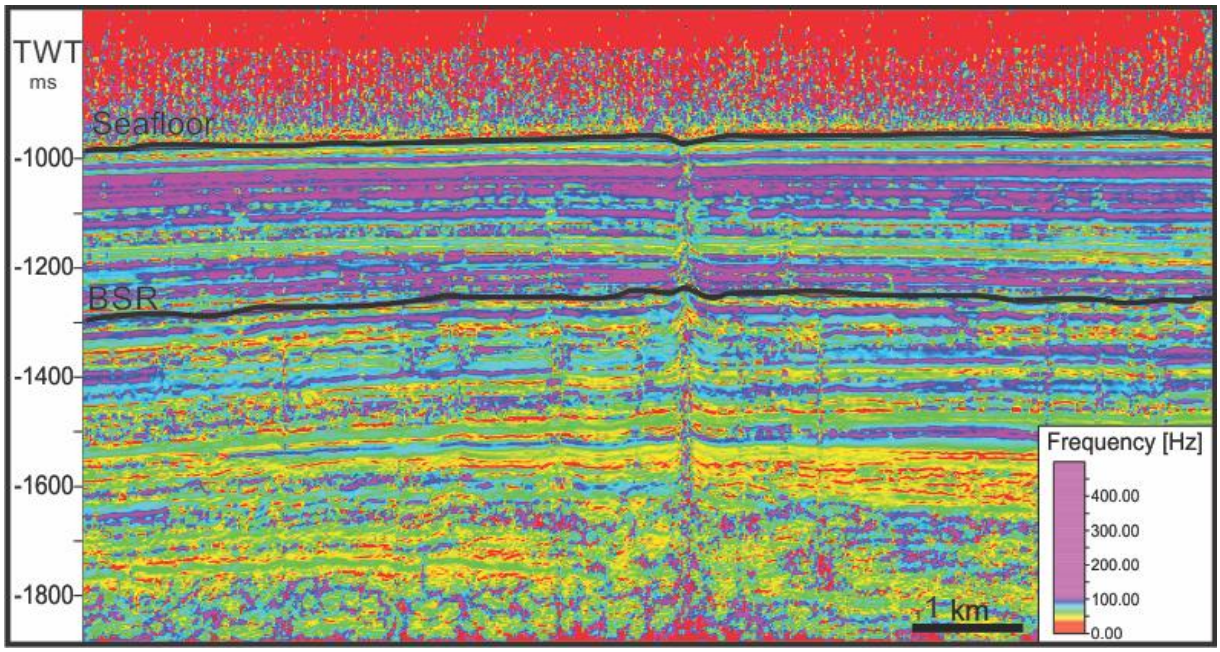

Figure 5.3.6: *Using instantaneous frequency attribute, low and high frequencies were found in Nyegga. Seafloor and the BSR lines are shown to help see differences. X line 293 was used.*

Using instantaneous frequency volume attribute in Nyegga area it is seen that there is slight significant change in frequency below the BSR similar as in Vestnesa. However, below the BSR frequency between 50 - 100 Hz is mostly visible. Using sweetness attribute the BSR was displayed at - 1300 ms (TWT) in red color.

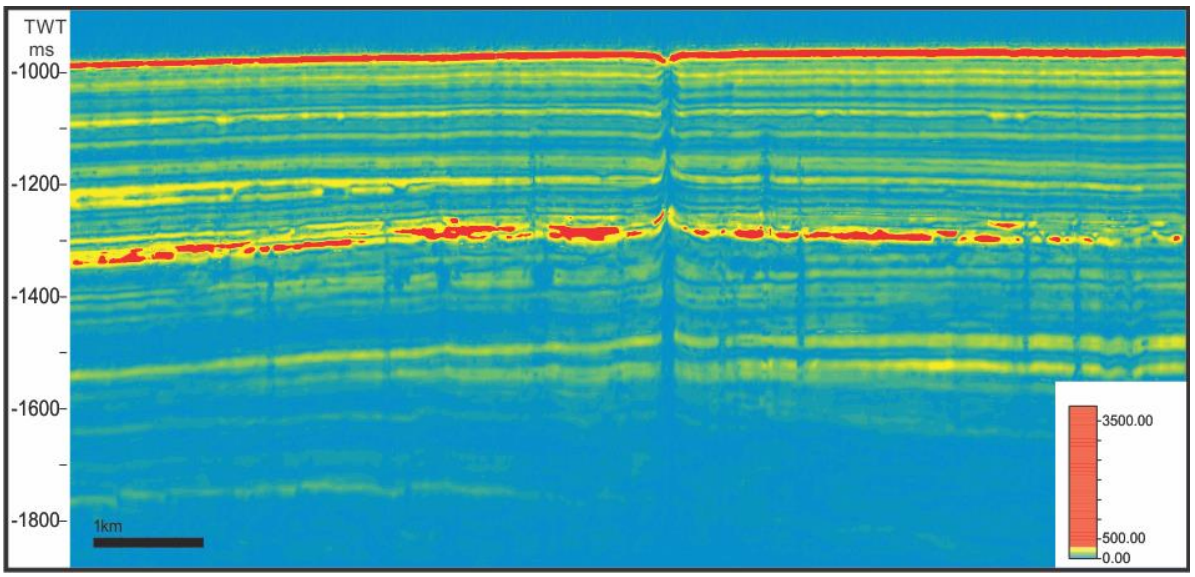

Figure 5.3.7: *Using sweetness attribute, rapid changes in energy were detected, in Nyegga. Seafloor and the BSR are shown in strong red color. X line 293 was used.*

5.3.3 Periods of activity

Chimney flanks at Nyegga terminate where horizontal strata overlies truncation and are characterized as pull-up reflections within GHSZ. In the place between truncations inside the chimney, chaotic reflections or seismic blanking is visible. Truncations (Figure 5.3.8), if

compared with continuous reflections, terminate in places, where the chimney pierces through sediments or in places where specific stratigraphic events have happened during sediment deposition, for instance, plough mark occurrence. Truncations are easily seen at INT reflector (Figure 5.3.10A) and most of them are seen at a depth of 160 ka. Plaza-Faverola et al. (2011) classified chimneys in Nyegga into 8 types and divided chimneys into truncated and non-truncated which are relevant for my study.

Type 1 - Truncated chimney. Above the truncated layer there is no evidence of seismic blanking or doming and therefore they terminate presumably at the depth of the truncation (Figure 5.3.8 nr. 2). Not least important- no pockmarks at the seabed are visible. Type 2 - Truncated chimney. Chimneys that terminate near the seafloor and are connected with pockmarks (Figure 5.3.10 nr. 6). Type 3 - Truncated chimney. Chimneys that are located next to plough marks (complicated to determine the nature of truncation). Type 4 - Truncated chimney. Chimneys that terminate within layer L50 (Figures 5.3.10, 5.3.13 and 2.2.6) (Plaza-Faverola et al., 2010b) and without visible pockmarks on the seabed. Type 5 - Truncated chimney. Terminate at the same depth as truncation, but there are connections with the pockmark on the seabed (Figure 5.3.10 nr. 3 and 4) Type 6 - Non-truncated chimney. There is no evidence of truncation and they are narrower than the chimneys that show truncations. Chimney terminates within layer L50 without visible truncation but on the seafloor there is a pockmark associated with. Type 7 - Non-truncated chimney. Chimney terminates near the seafloor, but without visible pockmark on the seabed (Figure 5.3.10 nr. 7) Type 8 - Non-truncated chimney. Chimney is connected with clearly visible, shaped pockmark (Figure 5.3.10 nr.1, 2, 5, 7 and 8) (Plaza-Faverola et al 2011).

Generally, the truncations are related with pockmark formation and illustrate the diameter of the area that was washed out during the formation of the pockmark. Three possible explanations how truncations were formed exist: 1. Sediment deformation due to pressure that allowed gas escape up to the seafloor. 2. Chimney development through fractures and emplacement of gas hydrates into them (Plaza-Faverola et al., 2011). 3. Precipitation of methane-derived authigenic carbonate within near seafloor sediments respectively (Mazzini et al., 2006; Plaza-Faverola et al., 2011).

The process of chimney truncation and termination occurs as described in the following: A pipe was formed when high pressure in the reservoir formed hydro fracture, which developed in the reservoir and spread up to the seafloor. After a fluid flow activity period, gas movement gradually formed a pipe. Next, the pore pressures in the pipe was

reduced and blow out terminated. At the end, mud and dirt crashed inside the pipe and blocked it (Løseth et al., 2001).

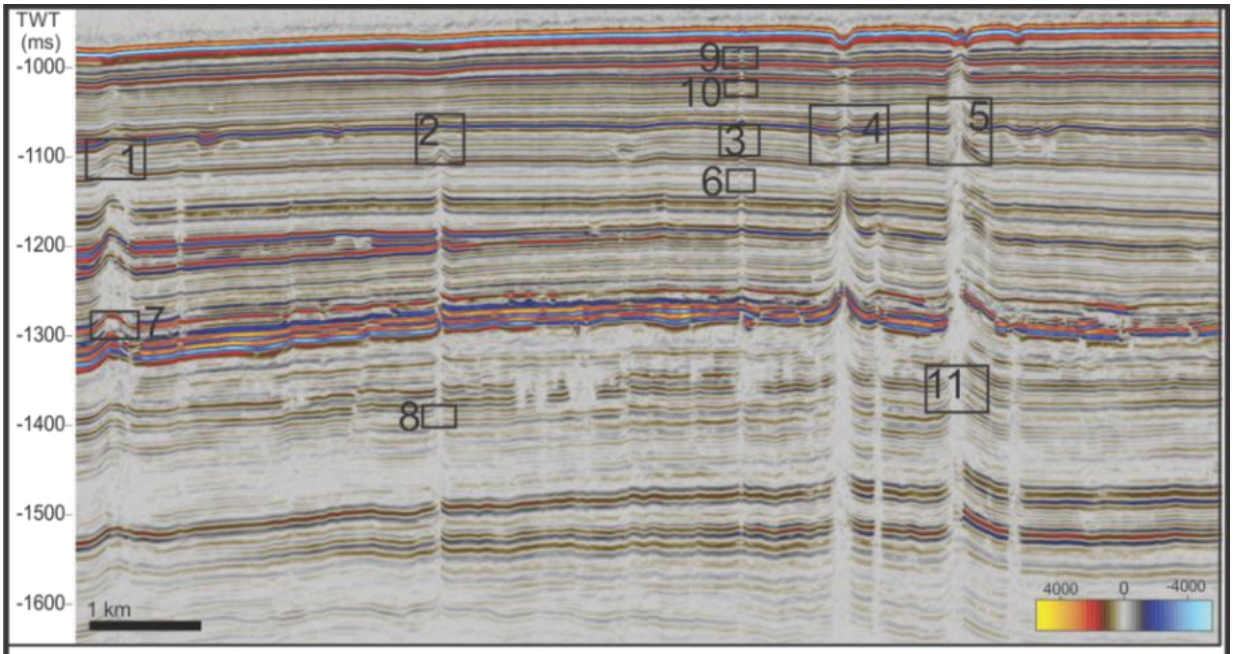

1 truncation	2.6 ms = 4.1 m thick	7 truncation	2.9 ms = 4.6 m thick
2 truncation	2.9 ms = 4.6 m thick	8 truncation	3.1 ms = 4.9 m thick
3 truncation	3 ms = 4.8 m thick	9 truncation	4.2 ms = 6.7 m thick
4 truncation	3.1 ms = 4.9 m thick	10 truncation	3.7 ms = 5.9 m thick
5 truncation	3.6 ms = 5.7 m, 3.1 ms = 4.9 m thick	11 truncation	3.4 ms = 5.4 m thick
6 truncation	2.5 ms = 4 m thick		

Figure 5.3.8: *represent 11 examples of truncations using randomly chosen inline in Nyegga. Lower part of the figure shows zoomed in parts, where truncations are found.*

Places where truncated reflections occur are indications of fluid expulsion at paleo-seafloors and represent the time of fluid flow activity. These reflections may also be the result of a process when sediments are deposited against the flanks of carbonate mounds (Plaza-Faverola et al., 2011).

Chimneys in Nyegga probably developed during one or several periods of activity (as it can be seen from the truncated horizons). They were reactivated one or two times within last 200 kyr (Plaza-Faverola et al., 2011).

Truncations in Nyegga can reach 4.2 ms (TWT) (= 6.7 m) which took approximately 13500 years to develop (considering a sedimentation rate of 0.5 m/kyr (Hjelstuen et al., 2005)), but on average they are 3 ms (TWT) thick. This number can represent the time when chimney was active (thickness of truncation).

In Nyegga, as well as in the Vestnesa ridge area (A1) escape of the fluids continues irregularly after the blow out which formed seabed features such as pockmarks. Even micro seepage of fluids is permissible when a chimney is at the last stage of activity (Mazzini et al., 2006; Plaza-Faverola et al., 2011). However, a chimney can enter dormant periods (self-sealing) which is between two active periods or it can terminate and not be reactivated (Plaza-Faverola et al., 2012).

A leakage of the fluids at the surface can be identified by eye (macro seepage) or may be not visible to the naked eye (micro-seepage). This seepage or expulsion of the fluids largely tells how big the volume of escaping fluids is. Also the presence of the seafloor features such as pockmarks or mud volcanoes can highlight the presence of fluid flow (Brown, 2000; Saunders et al., 1999; Schumacher and Abrams, 1996).

Leakage itself can be continuous or episodic. Continuous leakage can make structures called carbonate mounds (Løseth et al., 2009). In active leakage periods there can be episodic periods that have stopped for a moment, for example, a few hours or thousands of years (Leifer and Boles, 2005) and then reactivate again. During an active period, sometimes seepage can be visible by eye, or it can be a big, dramatic event that erupts (mud volcanoes) and releases gas and mud in the air (mostly methane gas) that can reach 300 m and continues for days (BBC News 29 Oct. 2001; Løseth et al., 2009). A problem with episodic events is that they are difficult to prove by sampling, but easier to detect in the seismic, as they make changes in the sediment structure (Løseth et al., 2009).

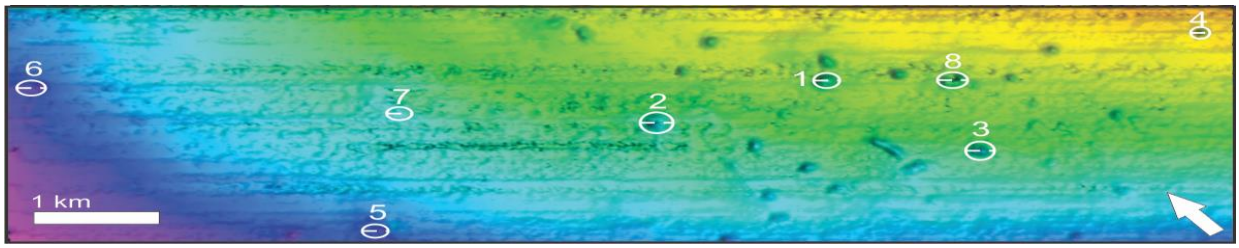

Figure 5.3.9: *Location of 8 chosen chimneys which are connected with seafloor. This figure can be correlated with (Figure 5.3.10).*

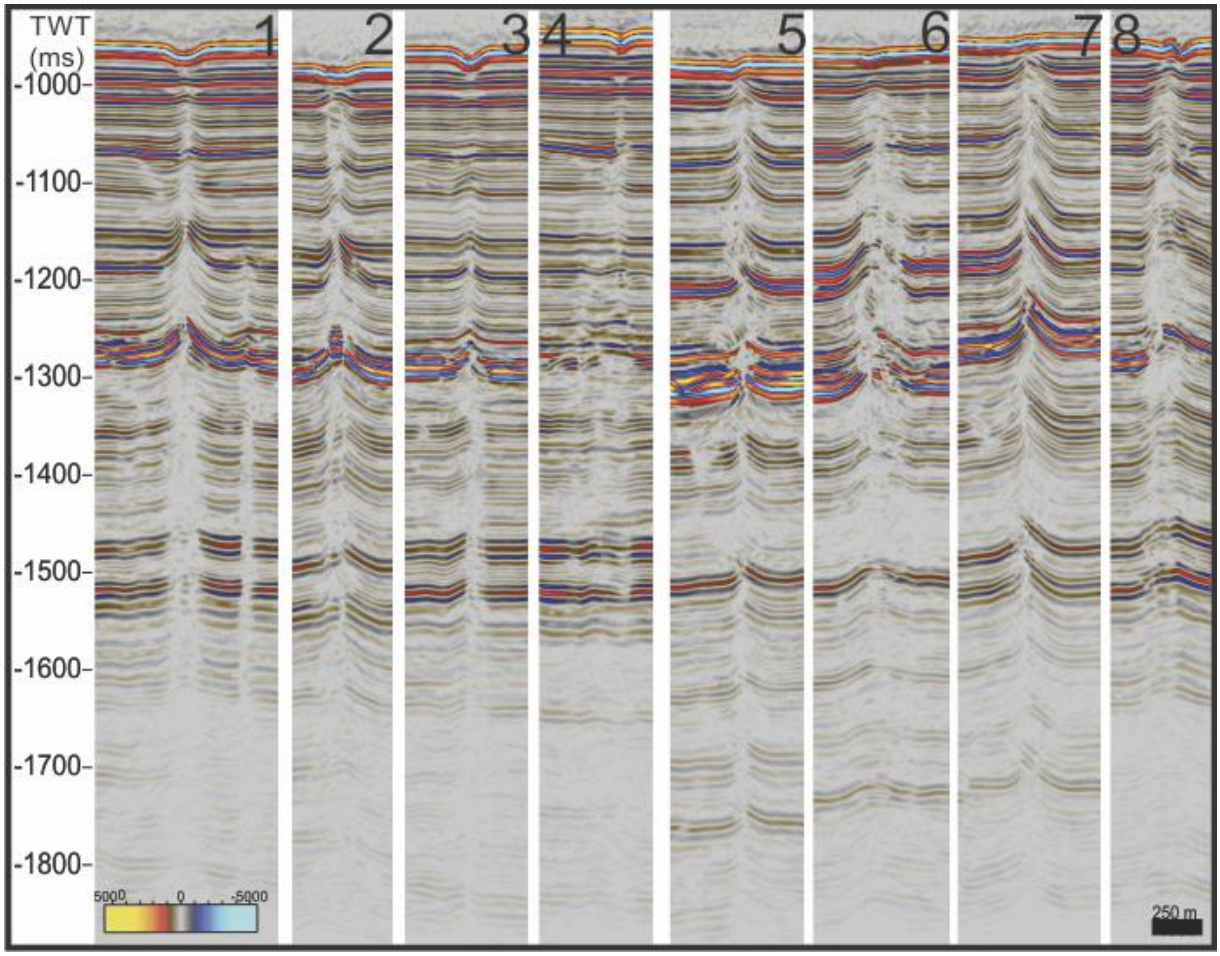

Figure 5.3.10: *Figure shows randomly picked chimneys in Nyegga to show their differences. Various expressions of seafloor craters and pipe structures are seen. Locations of the chimneys are seen in (Figure 5.3.9.).*

Pull up reflections in Nyegga occur within GHZS and can be caused by high velocity material (Plaza-Faverola et al., 2011), but in my observation in Nyegga pull-up reflections occur not only within GHZS, but also at lower parts. These pull-up reflections are found through all data and chimney flanks are steeply up-bended (Figure 5.3.13, 5.3.14 and 5.3.15).

5.3.4 Ice related features and faults

Icebergs can generally be of enormous size. We only see the parts of the icebergs which are exposed above water level, but normally the observer cannot see what lies underneath. The iceberg's lower part is even bigger than what we actually see. Mostly their

base is not flat, but with some kind of keel under them. When icebergs flow to places where the water depth is shallower it can reach the seafloor and therefore start to erode sea floor sediments (Vorren, 2005). When the iceberg continues to move, it forms furrows on the seafloor (Figure 5.3.11) as well as leaving some piles of sediments behind (Judd and Hovland, 2007). By the help of side-scan sonar and other acoustic methods it is easy to reveal plough marks (Vorren, 2005). The depth range of water and the width and depth of plough marks varies from place to place. Let's look at a few examples. For instance, Polyak et al. (2001) observed more than 30 m deep furrows in Chucki borderland. In the Barents Sea, Rafaelsen et al. (2002) found furrows with a width of up to 500 m. In the Norwegian shelf an unknown author found more than 400 plough marks that were up to 250 m wide and 25 m deep (Judd and Hovland, 2007).

In order to understand what type of features exist in Nyegga and especially to detect whether any prominent plough marks are present, a seismic Z line was checked, using volume attribute variance. Every millisecond was checked in order to determine at what specific time, what type of structural features occurred (Figure 5.3.5).

- At - 1054 ms (TWT) in the northern part plough marks appear. Their direction is pointed towards the N, NW and some of them reach more than 380 m in width. Around seven big plough marks are visible and occupy the NW and SE parts grubbing through the whole area while reaching a length of at least 3.5 km. They are strongly visible until - 1093 ms (TWT) (INT reflector, L50) (Figure 5.3.10A). From this point in the SW one plough mark strongly appears similar to curve, while all others slowly disappear. At - 1129 ms (TWT) a large curved plough mark (80 m in width) at SW of Nyegga is completely developed, while there are no signs of other plough marks in the area.
- At - 1151 ms (TWT) the plough mark at SW part has disappeared completely. From - 1151 to - 1171 ms (TWT) no plough marks are visible. From - 1171 ms (TWT) at the N side in the middle of the area a new set of plough marks starts to appear. Their direction is pointed towards N, NW. At - 1199 ms (TWT) these plough marks disappear and a new plough mark in the far west appears directed towards the NW. At - 1206 ms (TWT) it disappears allowing new plough marks to appear in the far NE of the area. However in a few places at the S side of the area, few plough marks appear and last for approximately 10 ms (TWT). At - 1222 ms (TWT) the development of a plough mark starts in the W side of the area and continues from SW to NE and stops in the middle of the area. The disappearing of this plough mark at around - 1244 ms (TWT) marks the significant start of new plough mark development in the area.

They are scattered all around the area and only at - 1319 ms (TWT) start to slowly disappear from the E towards the W. They almost disappear at - 1339 ms (TWT), while a lot of faults are developing all around the area, so do dim amplitude anomalies. Dim amplitudes represent permanent sediment deformation. Plaza-Faverola et al. (2012) suggest that these are real deformation structures and even contain gas today. Plaza-Faverola et al. (2012) also consider that observed dim amplitudes are not related with iceberg scouring. Dim amplitude anomalies are explained as sediment remobilization at the gas sediment contact beneath GHSZ induced by buoyant fluids (gas), or as dissociation of gas hydrates (Plaza-Faverola et al., 2012). Faults have a NW, N direction and their size varies, but they are mostly 20 m in width and at least 600 m in length. They are more pronounced in the NW part of the area. Dim spots are crossing through the whole area and are mainly elongated towards the N, NW, and can reach 230 m in width. They are well developed at - 1357 ms (TWT). Nearly no plough marks are visible after - 1300 ms (TWT). This picture with faults and dim spots continues all the way down and only at - 1720 ms (TWT) well constrained faults are visible in the NW part until they reach - 1870 ms (TWT) and all area is covered with faults. Plough mark activity suddenly disappears below the BSR. During research I counted 7 periods where plough marks are visible using RMS attribute map. Moreover, in the RMS maps mostly high amplitudes 1800 - 1400 (red color) are seen inside plough marks as well as in some chimney structures. In some of these units, plough mark activity is enormous.

Time thickness map was made to see levels were plough marks occur within GHSZ (Figure 5.3.11).

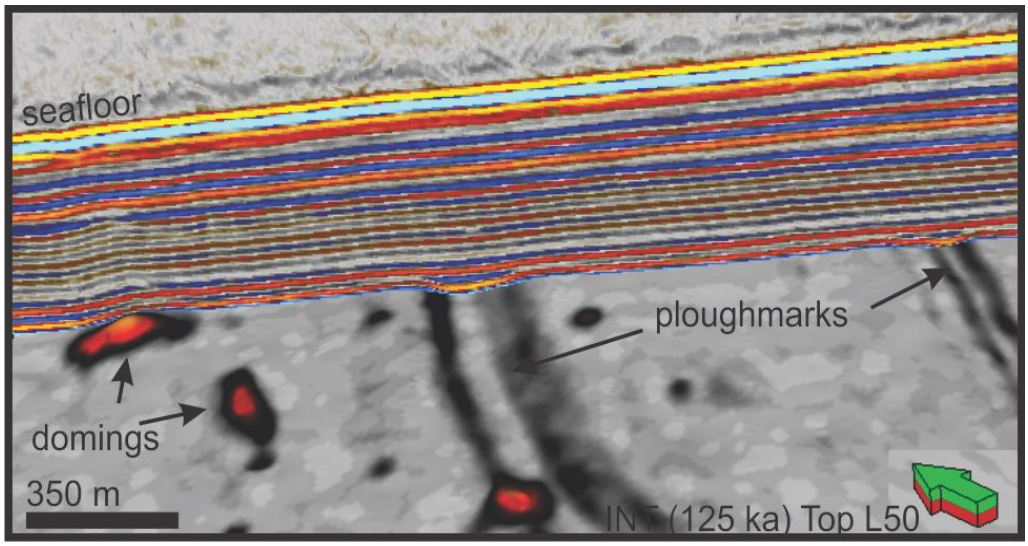

Figure 5.3.10A: *Surface of horizon INT, which is also a top of the L50, is shown, together with seismic section. Extract value from variance attribute was used to visualize domings (orange color) (part where chimney terminates) and plough marks. Impressive widths of plough marks are visible. Attention needs to be paid above doming and plough marks, how deformed are reflections.*

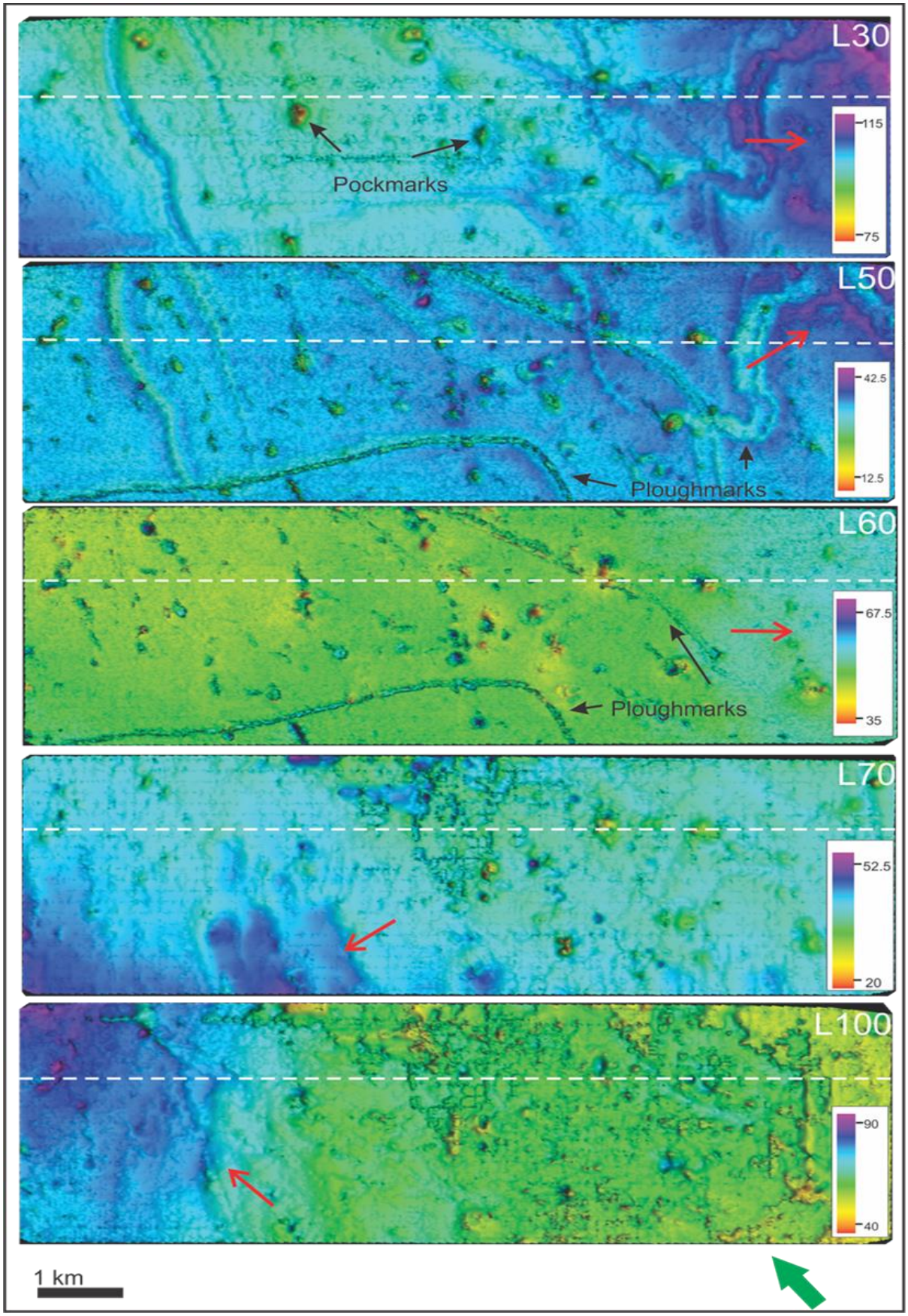

Figure 5.3.11: *Thickness maps for 5 units: L30, L50, L60, L70 and L100. Plough marks and pockmarks are shown. Figures 3.4.1 and 5.3.4 are useful to use with this map. White dotted line is x line 201. Red arrow shows thickness increase.*

5.3.5 Chimney differences

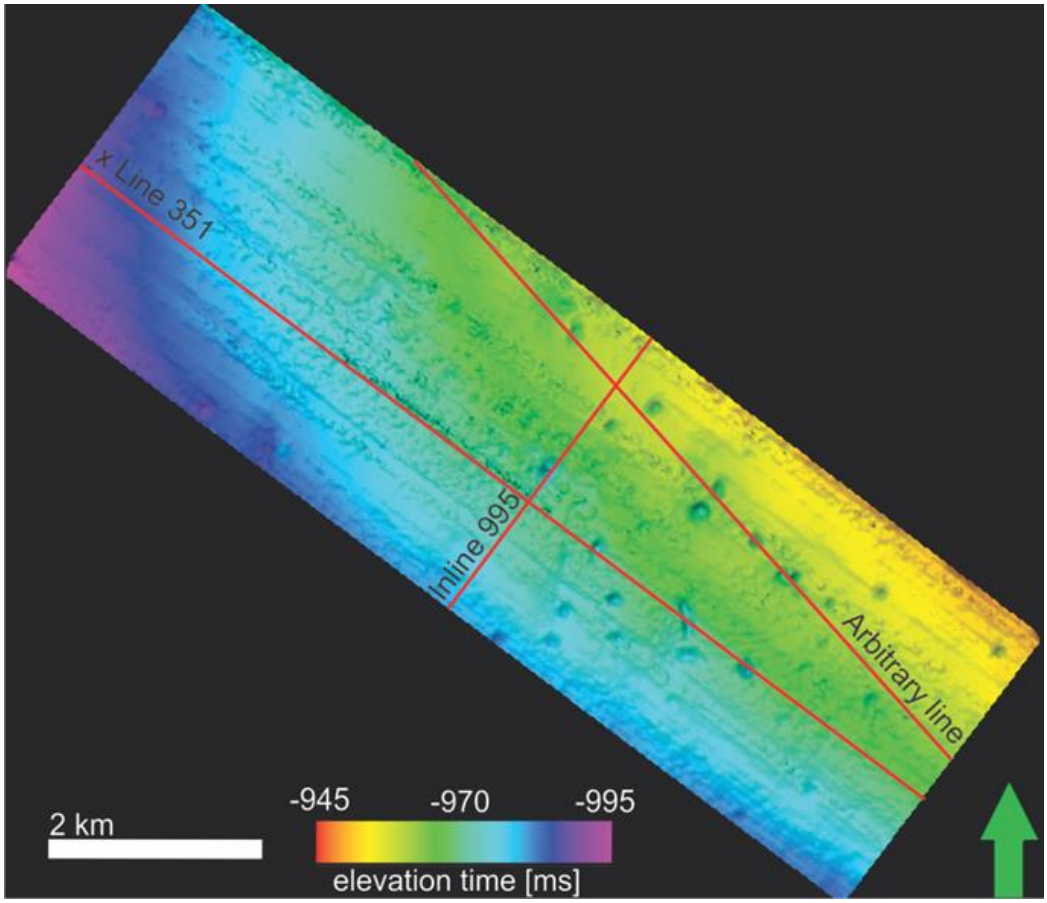

Figure 5.3.12: *Three random seismic lines crossing pockmarks are shown in order to show how different chimneys are compared to other two areas.*

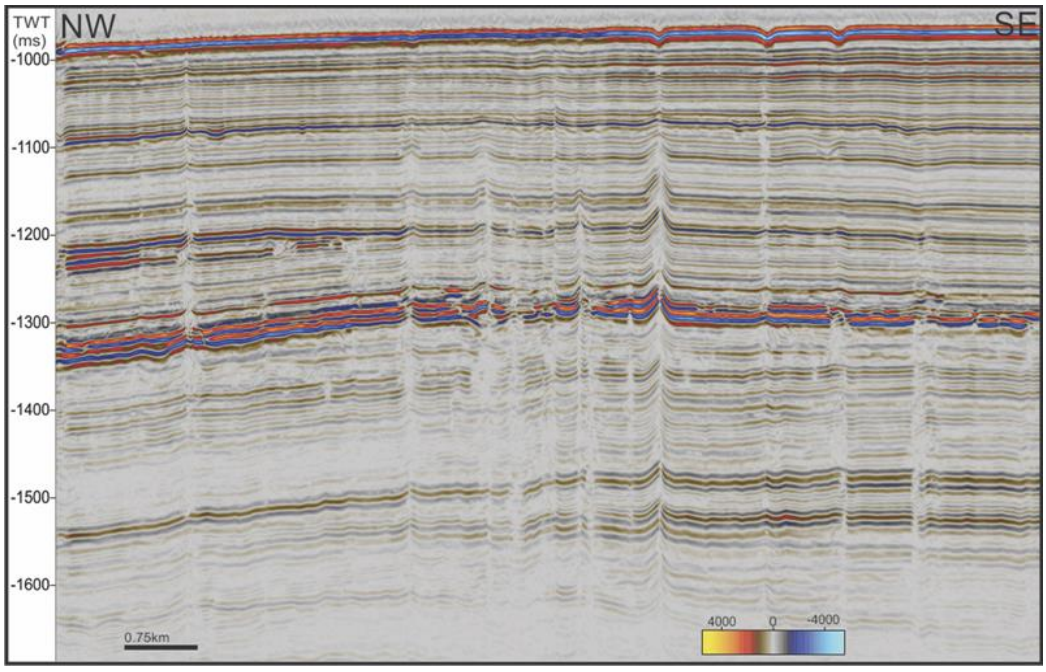

Figure 5.3.13: *X line 351 is shown. Vertically dimmed lines are pipe structures/chimneys with their flanks up-bended.*

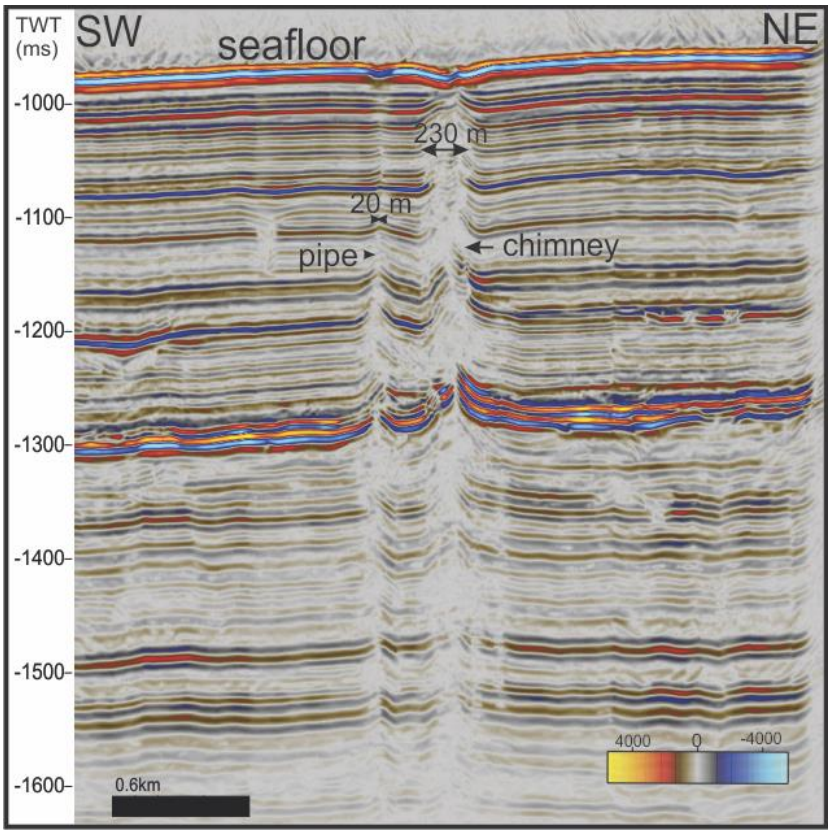

Figure 5.3.14: *Inline 995 shows sizes of pipes and chimneys. Vertically acoustic transparent lines are pipes structures/chimneys.*

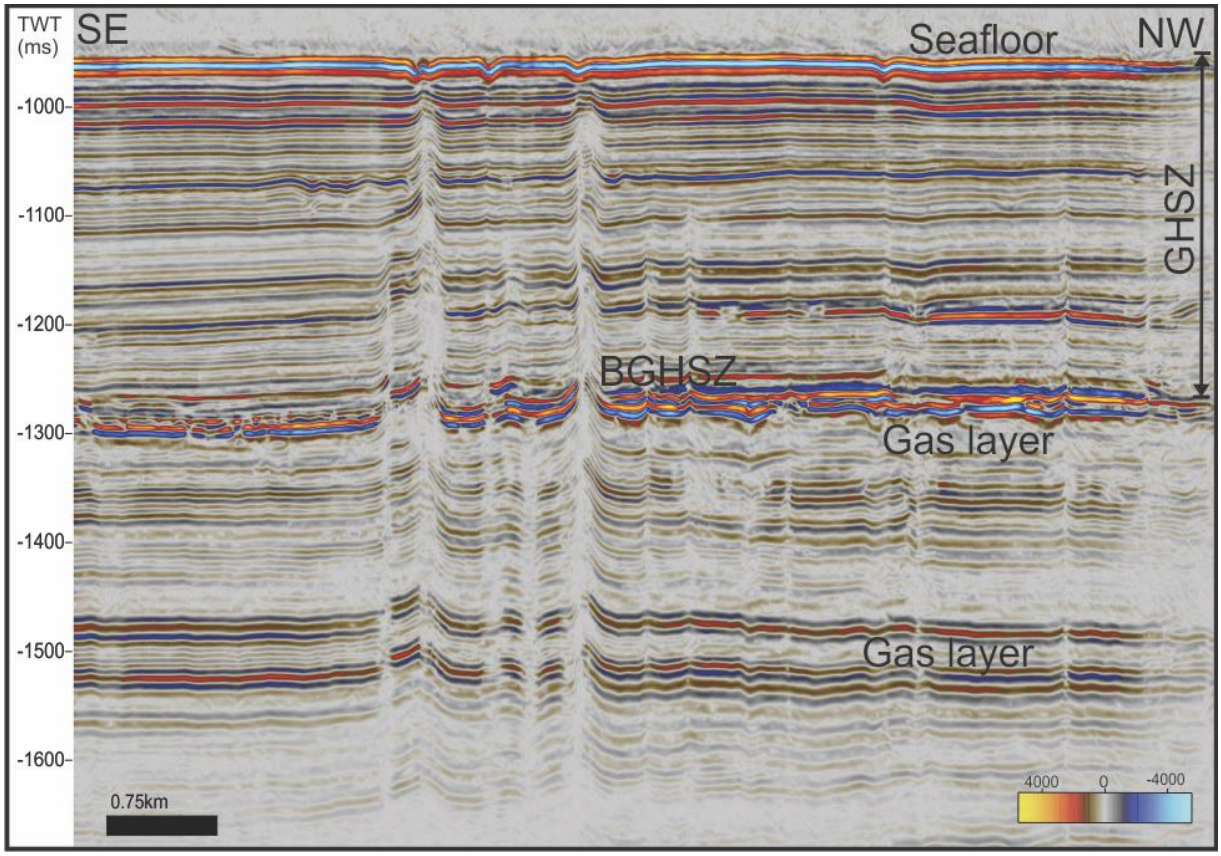

Figure 5.3.15: *The GHSZ and gas layers are shown in this composite line. Vertically dimmed lines are pipes structures/chimneys.*

6 Discussion

6. 1 Periods of activity/ inactivity comparison

6.1.1 Vestnesa (A2)

In the Vestnesa area (A2) (Figure 6.1 (A)), it is hard to see where chimneys terminate. Perhaps, they mostly terminate between horizon S1 and seafloor (Figure 5.1.4.b and 5.1.4.c), because this level divides dimmed amplitudes with chaotic reflections (Figure 5.1.4A). From horizon S3 (represents the BSR) (Figure 5.1.4c) up to horizon S1, pattern with chaotic reflections, dimmed amplitudes, together with horizontal strong reflections are showing vertically tall dimmed chimney structures and bright spots inside them. Above horizon S1 continuous reflections and smaller pathways of fluid flow are visible as alternative of widespread dimmed chimneys (Figure 5.1.11). Small fluid pathways breach through chaotic strata sometimes aligned in perfectly vertical conduits ending in a shallow subsurface. Beyond S1, (Figure 5.1.4b) high amplitudes and bright spots within the chaotic reflection pattern are abundant. At least 4 patches with plenty of sub patches of active fluid flow are interpreted: - 22 to - 35 ms (TWT) bsfl (below seafloor), - 50 to - 90 ms (TWT) bsfl, - 110 to - 120 ms (TWT) bsfl and - 160 to - 180 ms (TWT) bsfl (Figure 6.1.2). Every truncated layer thickness varies from 1 - 2.4 ms (TWT) (Figure 5.1.4A). This number could represent very short, vigorously active fluid expulsion.

Most of the chimneys/pipe structures terminate near the seafloor (in upper 40 - 50 ms (TWT)), from - 1640 to 1680 ms (TWT) down as seen in (Figure 6.1.2). This is followed by great chimney terminations between - 50 to - 90 ms (TWT). Indeed, it is the greatest number, if compared with other stratigraphic horizons. However, it can just be a part of the same chimney or pipe, because their flanks terminate at different depths. This area is believed to be active, not only because of their big chimneys, dimmed amplitudes with chaotic reflections and shape of the pockmarks, but also because of previous work in this area, where some of the chimneys presented acoustic flares while in others gas flares haven’t been seen (e.g Smith et al., 2014; Hustoft et al., 2009). Chimneys that indicated gas flares in the water column are direct evidence of fluid expulsion (Hustoft et al., 2009). Over the years gas flares show an increase in volume and regularity (Smith et al., 2014) which are believed to originate from a dissociation of gas hydrates. In Vestnesa (A2) chimney could be more active than in (A1), because of the large amount of faults and fractures, where fluids migrated upwards (Figures 5.1.4d and 5.1.6A).

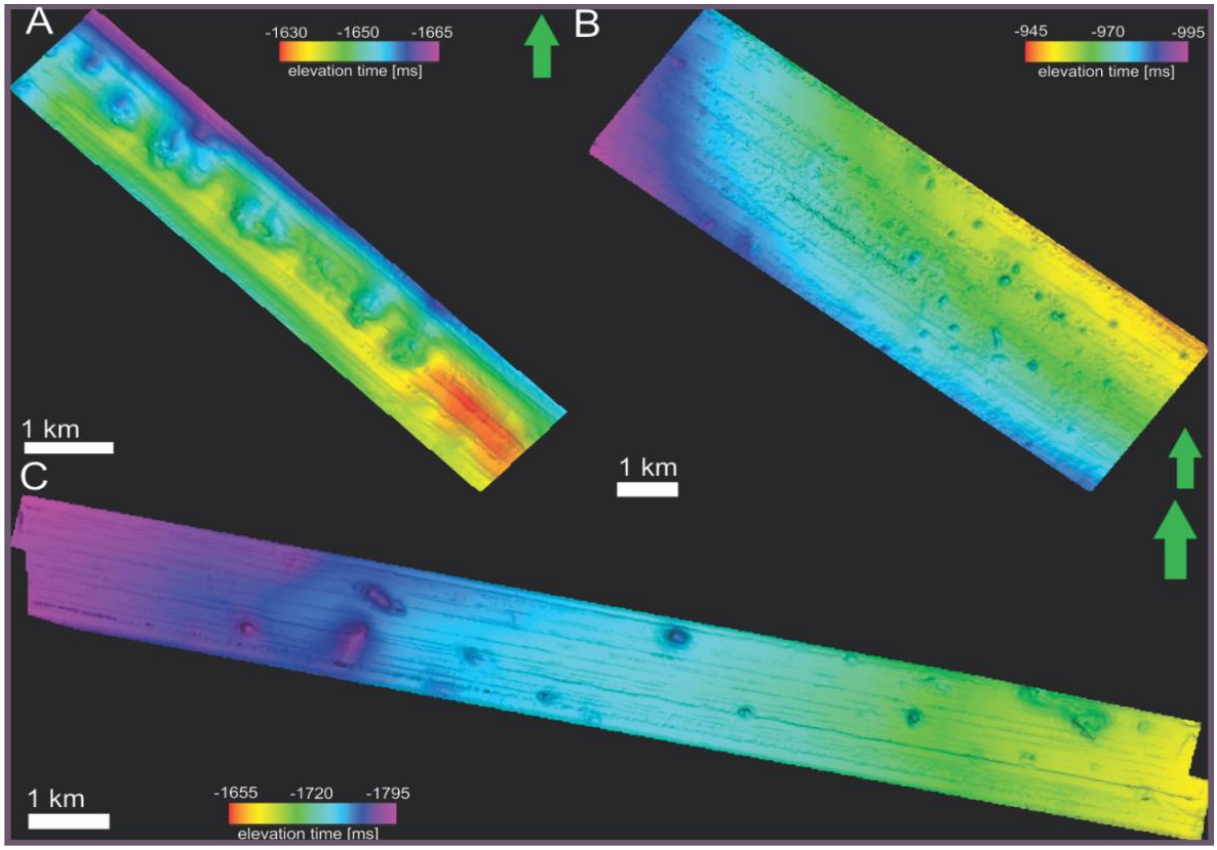

Figure 6.1. Comparison of the seafloors in *all 3 areas. A) Vestnesa active (A2), B) Nyegga C) Vestnesa less active (A1).*

6.1.2 Vestnesa (A1)

In the Vestnesa (A1) (Figure 6.1 B)) area chimneys also terminating at different stratigraphic levels, yet it is thought, that the main period of fluid expulsion is around horizon S2 and S3 (counting horizontal strata's above them) (Figure 5.2.5a and 5.2.5b). These are levels where truncations are seen most. Since there is a large number with truncations in different stratigraphic horizons (Figure 5.2.5), it is proposed that fluid flow activity and reactivation has been more active than in the Nyegga region, but not as active as in Vestnesa (A2). It can be seen in Figure 5.2.5, where color bar on the right side shows active and less active periods. In the Nyegga region, it sometimes is complicated by looking at the seismic section to distinguish buried pockmarks from plough marks made by icebergs. Whereas in the Vestnesa ridge area (A1) and (A2) there has not been any iceberg activity, maybe because of the huge water depth. These buried pockmarks which can be seen as truncations mostly in horizon S2 and S3 can be very relevant (Figure 5.2.5b), because they mark the period when gas seepage was active. In this area chimney flanks showing differences can be explained by gas hydrates and free gas.

6.1.3 Nyegga

Truncations of chimneys are especially seen at INT reflector. Within 200 kyr chimneys have been reactivated more than one time and this assumption is also confirmed by Plaza-Faverola et al. (2011), who says this period can be correlated with the termination of the Saalian glaciation. Based on data, chimney truncations are mostly seen between base of L50 and Top of L50, where also a huge amount of plough marks is found (Figure 3.4.1, 5.3.4 and 5.3.10A). Moreover, most plough marks are seen in this horizon which can be explained by glacial-interglacial transitions, where the Saalian ice sheet brought icebergs to the shelf edge (Berg et al., 2005; Hjelstuen et al., 1999; Plaza-Faverola et al; 2011). It could mean that fluid flow activity was related to plough mark occurrence.

6.1.4 Terminations of chimney/pipe structures

From the chimney/pipe structure termination chart (Figure 6.1.2) it can be seen that different numbers of chimneys terminate in different subsurface depths in all three areas. These numbers are measured by investigating seismic data in every area. It is my interpretation and assumption, where they terminate. The main idea was to show the difference between the areas in terms of chimney/pipe structure terminations. Results were reflected in these charts, but still many problems exist that hindered the determination of the actual number of terminations. One of the problems is seafloor morphological specialty, especially in the Vestnesa area (A1), since this area is irregular in elevation depths, which are the reason why there are huge difference in terminations of actual chimney/pipe structures between the seafloor and a depth of - 1640 to - 1680 ms (TWT). Another problem is to actually divide pipe and chimney termination. Chimneys, to my mind, can contain many smaller and bigger pipes. As, in 3D, a chimney is a spatial feature, that holds hundreds of smaller pipes and its shape is not restricted to one particular shape, it is therefore complicated to say, where a chimney terminates exactly. Flanks of the chimneys can terminate in one place, but the whole chimney in a different one, because it is not shaped perfectly cylindrical. Of course I have mentioned above that chimneys may look like a cigar or a vertical pipe, but in reality they look only somewhat similar to these shapes. These results highlight the complexity of chimney structures and shapes and how different they can actually be.

Truncations show special parts of a chimney where something disturbed sedimentation, probably fluid flow. Hence, they represent the time, when fluid flow was active. When comparing these three areas, it is seen, that in Vestnesa (A2) the average truncations (they were only calculated in places they were seen best, in the SE area respectively, which is less

disturbed and with small pipe structures piercing through sediments) are approximately 1.7 ms (TWT) thick, while thickest reaches 2.4 ms (TWT), and thinnest 1 ms (TWT). In Vestnesa (A1) truncations were taken from the whole area, not from a specific place and resulted in 5.2 ms (TWT) - average, 6.8 ms (TWT) - thickest and 3.7 ms (TWT) thinnest. There is a huge difference between these numbers if compared with Vestnesa (A2), where the average was only 1.7 ms (TWT) thick. However, a reason for that could be because of the sampling site, as truncations, which in my case were only in the SE of the area, where seen clearly. Nyegga

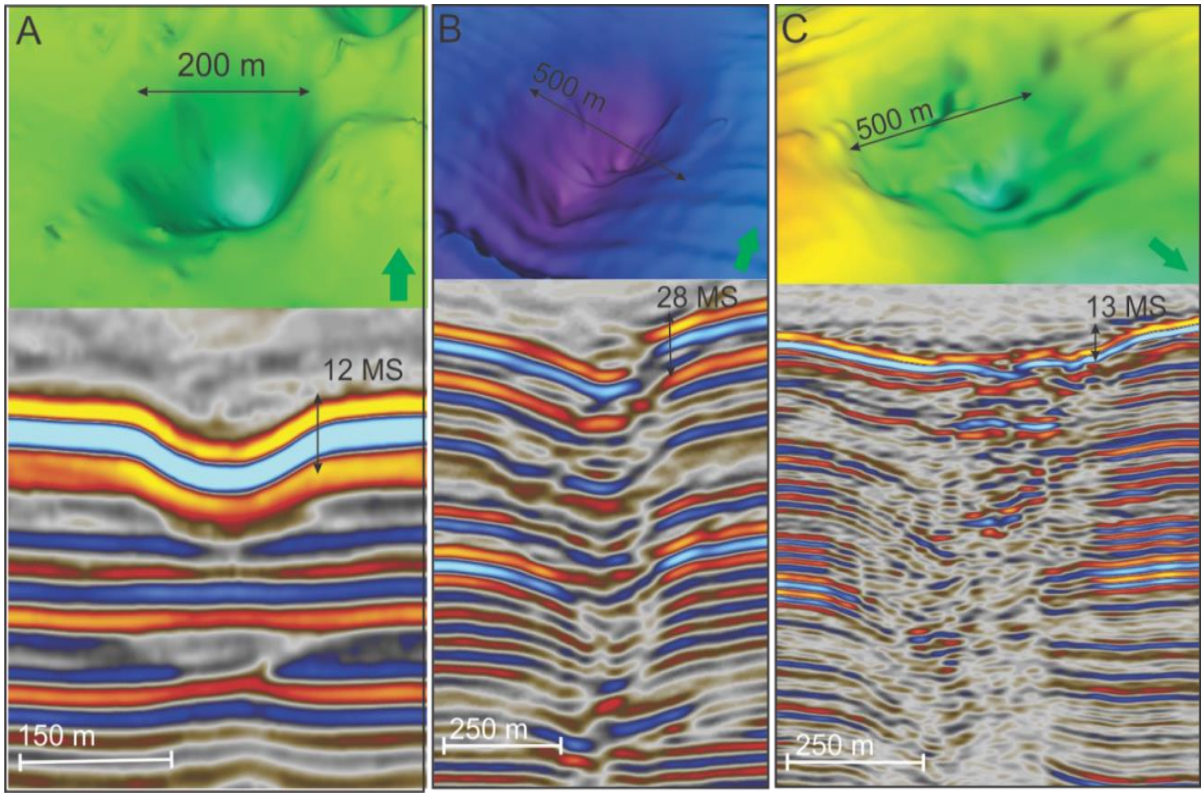

region: 3.1 ms (TWT) average, 4.2 ms (TWT) thickest and 2.5 ms (TWT) thinnest.

Figure 6.1.1: *A) Pockmark in 3 D, located in Nyegga region in figure 5.3.1. Under it – crosscut showing width and depth. B) Pockmark in 3 D, located in Vestnesa (A1) area shown in figure 5.2.1. Under it – crosscut showing width and depth. C) Pockmark in 3 D, located in Vestnesa (A2) area shown in figure 5.1.1. Under it – crosscut showing width and depth.*

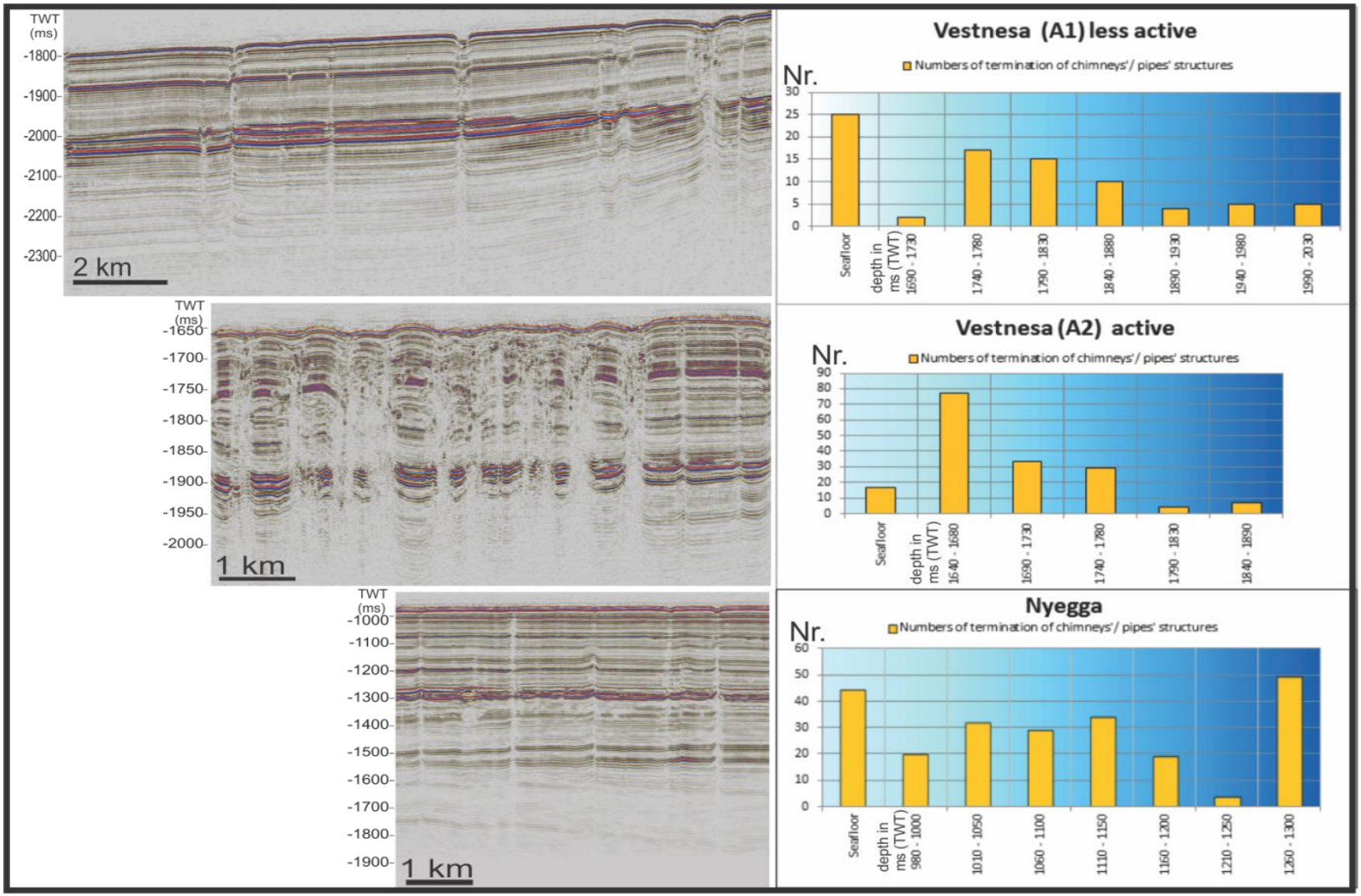

Figure 6.1.2: *Comparison of termination of chimney/pipe structures in all regions in right side. Seismic cross sections of each area in left side.*

6.1.4.1 Vestnesa (A2)

The Vestnesa (A2) active region is the only one of all three regions, with the smallest number of chimney terminations actually reaching the seafloor. This area has a very complicated plumbing system, which is clearly seen because of the chaotic reflections, which is the biggest difference between the three areas. Right below the seafloor, within 40 ms (TWT) the most terminations occur, maybe because the area is actively seeping methane into the water column, since many faults and fractures reside within this area. Many bright spots are seen, mostly showing the presence of methane hydrate, free gas or carbonates. The place where it was easiest to determine where chimneys/pipes actually terminate was in the SE of the area. This part is least disturbed with dimmed amplitudes and chaotic reflections. Moreover, with a lack of these anomalies, almost every continuous layer is seen without any disturbance except for the places where chimneys/pipes are piercing through. This area differs from the other two, because chimneys cover the whole area with a large density of pockmarks. In this area (10.34 km^2) there are only 16 of them. Most of the terminations with increasing depth slightly reduce until they reach the BSR.

6.1.4.2 Vestnesa (A1)

From the chart (Figure 6.1.2), in Vestnesa (A1), less active area, it is seen that most chimneys/pipes terminate at the seafloor. Only a small number of chimneys/pipes terminate right below seafloor, probably because of irregular topography. Almost all other terminations with increasing depth slightly reduce until the BSR is reached, where the border of the chimney termination is located. It is probably because of the presence of the base of the GHSZ, since it is reducing permeability of sediments and therefore strongly affecting fluid flow, as mentioned by several authors (e.g. Nimblett and Ruppel, 2003; Bünz et al., 2012).

6.1.4.3 Nyegga region

Nyegga area is diverse from the other two areas, because of its small and narrow chimney/pipe structures. Compared to the other areas, the biggest number of chimneys terminates at the seafloor, which results in small pockmarks. However, most of the chimneys terminate at the BSR, because of its ability to block fluids from migrating upwards, since it is low permeable (Figure 6.3c) and 6.3.1c)). Based on these assumptions, I suppose that Nyegga is young and not as active as the other areas. A huge number of terminations at the base of GHSZ could be explained by a strong permeability barrier - the BSR or, because of small faults terminating at the base of GHSZ. These polygonal faults have been formed deep below

and connected with other pathways which managed to reach the BSR. Then they stopped vertically, but could still could continue their way laterally, reaching the permeable area, fault or fracture and then migrate upwards. Sometimes small pipes reach the seafloor resulting in pockmarks. It could be explained by a recent activity causing dewatering from the polygonal faults (Figure 5.3.15).

6.2 Architecture of the chimneys

Chimneys are different in their sizes (width and depth), how long/tall they are (which mainly depends on how deep the source of the chimney is located) (Figure 6.3.1) and in what kind of sediments they are located in. In all three areas the upper part of the chimney, which is also a source of driving fluids out from the chimney, is called pockmark. Pockmarks have different sizes, since the sediments they are located in are different, as well as the fluid flux (micro, macro seepage) or venting (strong fluid expulsion) that erodes the sediments (Figures 6.1.1 and 6.2).

Chimneys, to my mind consist of many smaller pipes that help fluids migrate upwards. Cartwright et al., (2007) separated them into blowout and seepage pipes which are more relevant in both datasets - Vestnesa and Nyegga. One of the most important factors which is associated with chimney architecture are sediments, where they are located in and sedimentation rate, which greatly influence fluid migration. Both affect compaction of sediments and differ throughout seismic horizons.

The Vestnesa ridge stratigraphy (Hustoft et al; 2009) consists of YP1, YP2 and YP3 units and they are characterized by contourites, silty turbidities (Bünz, et al 2012) and muddy-silty contourites of Weichselian and Holocene age. It is believed that the rate of deposition was 9.6 cm/ka (thousand years) (Howe et al., 2008). Moreover, YP3 sediments reside GHSZ in Vestnesa. The author also says that the sedimentation was very high, which actually does not match with a rate of 9.6 cm/ka (Hustoft et al., 2009), but more as Howe et al., (2008) mentioned 105 cm/ka (Bünz et al., 2012). When it comes to sedimentation rate, it seems very likely that it represents sediment characteristics, as persistence against tension or compression. In both Vestnesa areas, chimneys are described as zones of disturbed layers and acoustic masking that stands vertical and pierces through the whole data making continuous layers not visible or vague. Based on these results it is believed that these pull up and push down structures show the existence of gas hydrates and free gas.

In the Nyegga region sediments contain debris flow deposits interbedded with thinner hemipelagic and contouric sediment deposits. There are places where several chimneys or pipe structures terminate within horizon, where layer doming occurs. As Judd and Hovland, (2007) claim, it is because sediments and gasses interact when, for instance, gas is slowly injected under clay and it results in layer doming. They can as well be carbonate dome like features, which can be formed during micro seepage at the last stage of each active period (Mazzini et al., 2006; Plaza-Faverola et al., 2011). That is also consistent with previous research, where contouric sediments (consist of fine grained muds) are found there and are impermeable. According to Bryn et al. (2005) the Naust formations consist of contour current controlled deposits. The upper part of the seabed consists of more coarse grained sediments compared with the Vestnesa ridge, resulting in smaller pockmarks at the seafloor. The distribution of pockmarks is controlled by fluids that breach the seal, which is represented by sediments containing gas hydrates. It is widely thought that pockmarks are connected with vertical pipe systems that sources from over pressured reservoirs (Bünz, et al 2003).

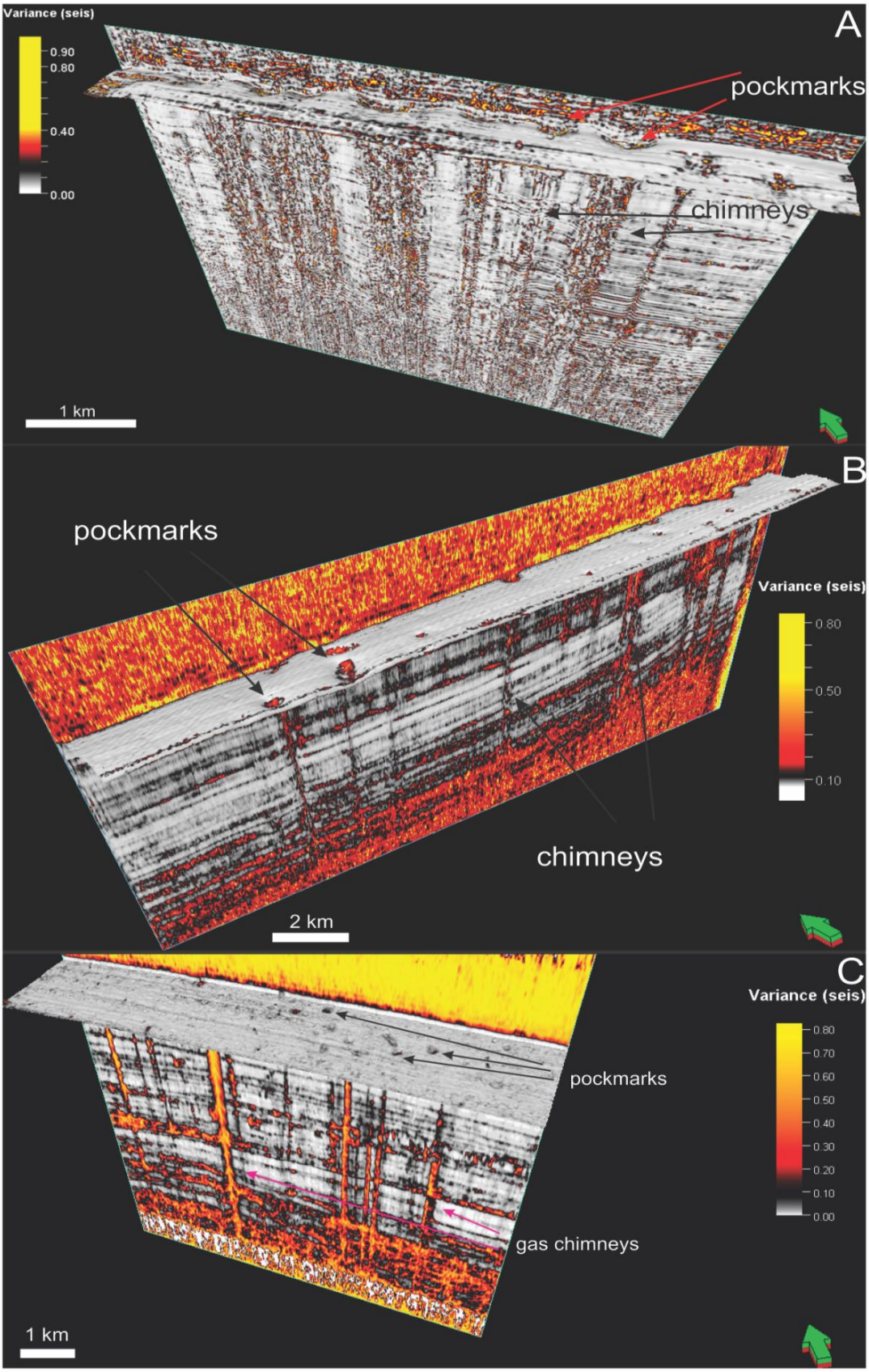

Figure 6.2: *Pockmarks and chimneys in all areas represented by arrows. A) 3D variance of surface attributes 15ms (TWT) below the seafloor in Vestnesa active. Seismic section of x line 108 is shown and vertical exaggeration is 10. B) 3D variance of surface attributes 15ms (TWT) below seafloor in Vestnesa less active. Seismic section of Inline 250 is shown and vertical exaggeration is 10. C) 3D variance of surface attributes 15ms (TWT) below seafloor in Nyegga. Seismic section of x line 250 is shown and vertical exaggeration is 10.*

6.2.1 Vestnesa ridge (A2)

I have separated the words chimney, pipe and pipe structures/conduits. In my opinion chimneys are features that can hold hundreds of pipes, which are smaller structures. Their widths are different and in Vestnesa (A2) mostly don't exceed 350 m. The smallest conduits/pipes in Vestnesa (A2) are only 30 m in width, while a whole chimney can reach 450 m (Figure 5.1.11). On average they are 270 m wide. Chimneys can reach an impressive length, mainly because of the depth of the source. As in every other area, chimneys terminate at different stratigraphic depths, but in the (A2) area chimney structure is extremely chaotic, probably, because of high fluid activity in the present or in the past, making it complicated to determine their termination point. Chimneys in Vestnesa (A2) are very big, wide and acting more vigorous, as something trying to get out of their structure, because of their rugged, edgy shape. It seems as if the fluids inside the chimney were trying to find a way out, crippling chimney structure and shape accordingly (Figures 6.1.1 c), 6.2.a), 6.3.a) and 6.3.1a)). However, in the SE of the area, which represents the highest morphological point where the smallest pipes and conduits are located, it is easier to divide periods of fluid flow activity. Below the BSR thickness of high amplitudes vary from 30 - 35 ms (TWT). The BSR is located at - 1900 ms (TWT). In the whole region pull-up reflections are up-bended throughout all data; where seepage pipes (smallest) occur, it can in fact be a velocity anomaly. Within GHZS the biggest chimney flanks are showing push-down and pull-up and straight cut flanks (Figures 5.1.8, 5.1.9, 5.1.10 and 5.1.11), but pull-up reflections occur mostly on the sides of smaller pipe structures. Within 60 ms (TWT) below the BSR pull-up, push-down and cut flanks of chimneys are found. From the bottom of the data up to 60 ms (TWT) below the BSR chimney flanks are up-bended only.

6.2.2 Vestnesa ridge (A1)

In Vestnesa (A1) chimneys can reach 600 m in width. The smallest ones can be around 30 m (complicated to measure) and referable to pipes (Figure 5.2 11). The average chimney width is 120 to 160 m. Their architecture is more constrained if compared with the (A2) area. Despite a few chimney's enormous width, normally their structures aren't as chaotic. Often in (A1), chimneys are wider above the BSR or within GHSZ. If normally a chimney retains its shape, as it is in Vestnesa (A2), despite their chaotic pattern, here in (A1) it forms as a small pipe breaking through the BSR and continuing upwards with its shape getting wider. Sometimes these really wide parts are truncated (Figure 5.2.7 nr.7). However, their shape can be the direct opposite - after the BSR strongly reducing in width. Chaotic

reflections are often seen in (A1), but not as disordered as in (A2). They probably appear more as dimmed section. Chimneys are less branched with their whole body standing vertical until it terminates or reaches the seafloor. More bright spots are found if compared with Nyegga (Figures 5.2.9, 5.2.10, 5.2.11 and 5.2.12). In Vestnesa (A1) within GHZS mostly chimney flanks are showing push-down, however smallest conduits/pipes are showing that their flanks are up-bended. Below the BSR, around 60 ms (TWT), flanks are showing pull-up, push-down and straight cut strata. Further down below 60 ms (TWT), chimney flanks are only up-bended.

6.2.3 Nyegga region

Chimneys in Nyegga reaching 230 m in width go hand in hand with the smallest pipes of 20 m or less (Figure 5.3.14). Normally in this area chimneys and pipes are relatively small, almost keeping the same width through all the data. In fact, small conduits can reach a significant height, by extending from deep reservoirs into the shallow subsurface nearly reaching the seafloor. High amplitudes are almost absent; nearly no bright spots are detected in the chimney/pipe structures. They hold less chaotic reflections and their architecture makes them perfectly vertical, with their flanks up-bended. Plaza-Faverola et al. (2011) claim that pull-up reflections occur within GHSZ and can be caused by high velocity material, but as it is seen in Figure 5.3.10 not only within GHZS these reflections are up-bended, but through the whole data. Probably below GHSZ pull-up reflections represent an artifact.

6.3 Seepage evolution

There is a great amount of factors that are involved in developing morphological features such as pockmarks. Yet these few features are probably most important: flux of fluid flow and sediment properties.

When the fluid flow is rapid and large amounts of fluids and sediments are transported, pockmarks are formed. If the flow is relatively slow, it forms authigenic carbonates. When there is a moderate flux, gas hydrate deposits are formed (Talukder, 2012). Seepage of methane gas can cause authigenic carbonates precipitation which can be seen near the seabed as high amplitude reflections (Talukder, 2012) as well as the area above the seeping site can be surrounded by bacterial mats (Linke et al., 1994). It is often observed in Vestnesa (A1) (Figure 5.2.7 nr.1, 3), 5.2.9 and (A2) (Figure 5.1.4b, 5.1.4c, 5.1.6 nr. 1 and 5; 5.1.6A, 5.1.9, 5.1.10 and 6.1.1c)) more than elsewhere. Frequently it happens because of slow (Talukder, 2012), but steady fluid flux. Comparing all areas only few differences are seen:

Across the pipe/chimney related structures anticlines can be seen inside (Figure 5.3.14. and 5.3.15). In places where a pipe or chimney terminates there is a continuity of reflections that are crossing them without disturbance. Paleo seafloor pockmark-like craters and buried carbonate dome like features are seen in all areas in different depths which are thought to be formed during micro seepage of fluids at the last stage of each activity period (Mazzini et al., 2006). In Nyegga domes are visible on the seafloor (Figure 5.3.1). The occurance of these features is therefore evidence of fluid flow in the past. According to Plaza-Faverola et al. (2011) these truncations can indicate phases of fluid expulsion activity.

It is largely thought that chimneys consist of structureless material. Løseth et al. (2001) represented a pipe formation model in their study, which could serve as possible explanation for almost all pipe development. When hydro fracture formed, it was filled with gas and a connection between reservoir and seafloor was established. Later a fracture developed into a pipe.

As several pipes consist of stacked high amplitudes with reversed polarity, it is interpreted, that they are geophysical artifacts and don't represent any internal structures in the pipes. Inside the pipe it is more likely that gas was the significant fluid when the pipe formed, because chimneys are almost vertical and this flow eroded and deformed the sides of the pipe (Løseth et al., 2001).

However, pipes can be associated with or without vertically stacked amplitudes (Cartwright et al., 2007). The structure of the pipes is unclear because of its variation. Sometimes they appear as stacked pockmark craters, which can be a gas accumulation, but sometimes as zones of deformed reflections, which formed due to faulting or folding (e.g. Figure 5.1.9, 5.1.6, 5.1.10, 5.2.11). It is likely that fractures found inside pipe structures are high permeable disseminating fluids. Blowout pipes can hold vertically stacked amplitude anomalies and can be associated with paleo pockmarks or present seafloor craters (pockmarks). Therefore episodic fluid flow can be closely related to stacked pockmarks. According to Cartwright et al. (2007) seepage pipes are mainly dependent of the properties of the rock they inhabit, but I also assume the same scenario for blow out pipes.

Gas chimneys can stop, reactivate after some time and continue their flow of gas towards the seafloor. One of the reasons could be overpressure. During burial, normally, pore fluids cannot drain from fine grained sediments since compaction is slower than burial (e.g Judd and Hovland, 2007). Another reason could be faults, which are also affecting pressure in the subsurface. They can be the reason for blocking and letting fluids through them. Hence

faults can be permeable or block fluids from migrating. Permeability of the faults could be one of the controlling factors in a plumbing system (Talukder, 2012), which is closely related to fluid expulsion. When faults are expanding, fluid pressure can overcome lithostatic pressure causing sediments to fail and therefore allowing them to migrate upwards through fractures and/or faults. After some time pore pressure can drop and close fluid pathways until the next overpressure builds (e.g Carson and Westbrook, 1995). Sometimes faults reach depths where permeability decreases, but because of buoyancy and decreased lithostatic pressure, fluids move through overburden (Talukder, 2012). However, flow can be stopped because of the development of carbonates, which seal the fault (Talukder, 2012), first reducing flow and later stopping it by blocking the pipe (Hovland, 2002; e.g Plaza-Faverola et al., 2010).

Theoretically there are no limits for a chimney to spread as long as the right conditions are given, but multiple factors come into play, so it is rather complicated for chimneys to exceed their borders for more than 1 km. Yet, everything is possible.

The plumbing system could be the main reason why chimneys terminate in different depths, as it covers the whole area from the source up to the seafloor. A variety of sediment types, their characteristics, tectonics, faults and pressures compel gas chimneys to concede. In both areas, there are differences in the overall plumbing system which result in active, less active and inactive areas of fluid flow, as well as in inactive and dormant periods.

The GHSZ is closely related with the BSR and gas hydrates (e.g Andreassen, 2009). Depth of the GHSZ varies, because it is controlled by the geothermal gradient, bottom water temperature and sedimentation rate (Mienert et al., 2001; Plaza-Faverola et al., 2012). In Vestnesa, the bottom of the GHZS is located at around - 2000 ms (TWT) (A1). In area (A2), the bottom of the GHSZ is located at - 1900 ms (TWT). In Nyegga: - 1320 ms (TWT) below seafloor, respectively. The base of the gas hydrate stability zone is located where the BSR occur. Free gas is located below the BSR and gas hydrates above.

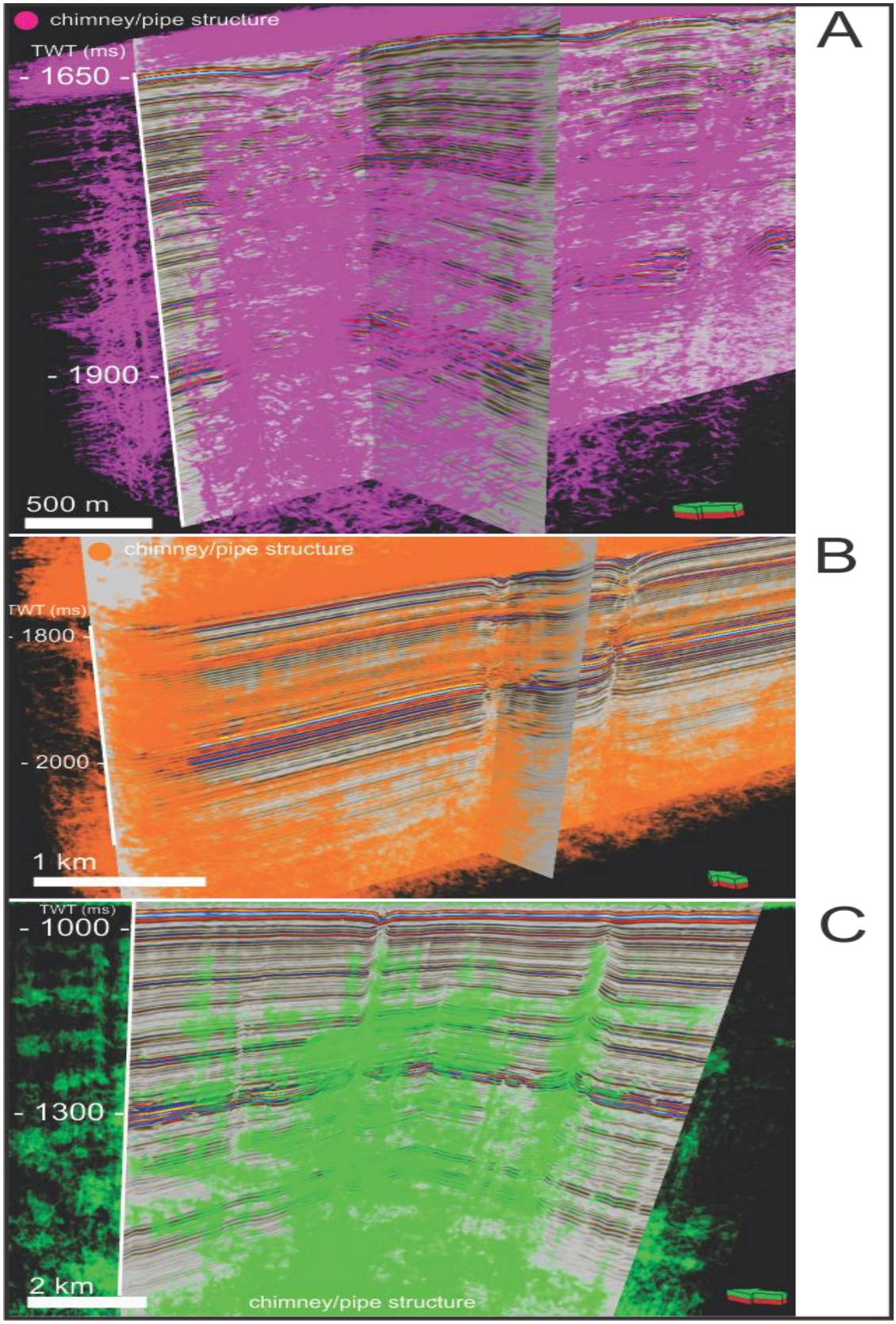

Figure 6.3: *Chimneys made by train estimation model in different colors, in background structural smoothened data for every area was used. A) Vestnesa (2) area showing chimneys in purple color using train estimation model. B) Vestnesa (1) area showing chimneys in orange color using train estimation model. C) Nyegga region showing chimneys in green color using train estimation model.*

6.3.1 Vestnesa ridge

In Vestnesa ridge gas chimneys obviously show high fluid flow activity, not only because of the unique and huge structures, called pockmarks, which are located in the upper parts of the chimneys (on the seafloor), but also due to high reflections near the seabed and the chaotic reflections (inside the chimneys) that cross the data set vertically breaching through sedimentary layers. Heggland, (1998) also agrees that these giant pockmarks are formed by fast migration of pore fluids. Almost at the top of the gas chimneys or in the shallow subsurface, high amplitude anomalies are observed, which also accords with Løseth et al. (2009) and with Plaza-Faverola et al. (2011). This could be a sign of gas hydrates or small carbonate accumulations.

Pore fluids in the subsurface are gas charged and migrating from deeper reservoirs. Based on Hustoft et al. (2009) acoustic chimneys in Vestnesa seem to have their roots within or below highly reflective strata underneath the BSR and Bünz et al. (2012) and Smith et al. (2014) agrees that they are fed by a critically pressured free gas column beneath the BSR. Bacteria mats can be evidence of the active seeping of methane (Linke et al., 1994; Hovland et al., 2005). Also Plaza-Faverola et al. (2011) claim that shallow accumulation of gas hydrate can present evidence for recent, or present fluid migration activity. Moreover, sediments in gas chimneys are heavily disturbed by either previous or ongoing gas migration; again, it also coincided with Judd's and Hovland's (2007) theory. Although, in Vestnesa chimneys are active and have been active, the volume of the gas released from the chimneys might be higher than thought, because vertical gas flares near Fram Strait are affected by strong bottom currents and could therefore show shorter gas flares (Hustoft et al., 2009) thus giving an accurate picture of the amount of gas expelling. Numerous investigations of gas flares from chimneys took place in 2010, 2012 (Smith et al., 2014) and in 2008 (Hustoft et al., 2009), that resulted in the confirmation that not only in Nyegga episodic activity of fluid flow is taking place.

Hustoft et al. (2009) think that the supply of the methane gas in Vestnesa is influenced by the evolution of juvenile oceanic crust and faulting, which could be the main reason for distribution and supply of methane hydrate. The mid-oceanic ridge is relatively close to Vestnesa, therefore hydrothermal circulation is an important aspect for fluids (Bünz et al., 2012). Moreover, the geothermal gradient near the Molly Fracture zone is calculated to be around 115° C/km. However, near the COT (Continent – Ocean Transition) that is located 15 - 20 km to the west from the Vestnesa ridge, the geothermal gradient rapidly decreases to 70°

C/km (Vanneste et al., 2005). Based on the relatively huge geothermal gradient, that is 2 - 3 times higher than in Nyegga, it is though, that the active fluid system can be supplied by thermogenic methane (Hustoft et al., 2009). It is also justified by Bünz et al. (2012) that heat flow values are big if compared with the mid-Norwegian margin.

As Vestnesa ridge consists of low permeable sediments, fluid flow is mainly caused by hydraulic fracturing that could result in steady and active seeping. Semi-circular pockmarks are abundant in Vestnesa Ridge. Higher reflection amplitudes can indicate a high concentration of gas hydrates or authigenic carbonate (Hustoft et al., 2009).

Aside of the faults and fractures a high velocity area is normally found, because of the concentration of hydrates and gas. With the help of developed fractures and faults up to the seafloor, methane gas fluids could form authigenic carbonate precipitation that was mentioned by Mazzini et al. (2006).

Even more, concentration and thicknesses of the gas hydrates can be higher near faults as well as gas hydrates, that can migrate upwards to shallower areas easier, compared with un-faulted regions. However, faults can seal and protect fluids from flowing through, but if a fault is containing clay, it can begin to leak if exposed to overpressure (Løseth et al., 2009). Berndt (2005) mentioned that faulting can appear either through sediment compaction or volcanism controlled processes.

According to Hustoft et al. (2009), pockmarks in Vestnesa (A2) can be correlated with the location of the BSR anticline and suggest that chimneys are defined by a "*topographic trap geometry of the gas hydrate seal*".

To my mind one of the factors making Vestnesa an active region is the presence of a huge amount of faults, which cut the area through the BSR and continue within the GHSZ. The area would probably be less active without these faults (comparing figures 5.1.6 A and 5.2.7 A) and without such a huge geothermal gradient. Of course pressures in the plumbing system can move fluids upwards, and result in seeping features, but the presence of the faults made more effective pathways that released fluids and gas in Vestnesa (A2). Despite the fact that faults can block the flow, (probably for some time, because of impermeable temporary material) later gas continued its flow upwards. Nevertheless, for fluids it is complicated to get through the BGHZ, since it acts as seal and less permeable which is also claimed by Bünz et al. (2012), yet pressure and faults allowed subsequent migration.

However, there are a high number of faults and fractures in the Vestnesa (A2) area. Compared with Vestnesa (A1), which is less active and which is located only 20 km further to the NW it is seen that the area is less faulted and fractured. It needs to be considered, that tectonics has played a main role in Vestnesa (lateral and vertical deformation) that strongly affected the sediments (e.g Talukder, 2012; Saffer and Tobin, 2011; Taylor and Leonard, 1990). Some say that faults prevent fluid flow, others that they allow fluids to migrate through them (Bethke et al. 1991). Both can be true, because it mostly depends on tectonic processes and sediment characteristics, how they will act during tension, stress etc. Clayton and Hay (1994) claim that deep buried faults and fractures act as a seals, not as migration pathways. While according to Talukder, (2012), faults can act either as seals or conduits. However, I tend to agree with Talukder's (2012) opinion. Also Plaza-Faverola et al. (2015) think that extensional faulting and shear deformation from transform faults have played major role in Vestnesa, allowing the distribution and supply of methane hydrate and free gas in the sediments.

Since the Vestnesa (A2) area is scattered with faults this could be the main reason for overpressure and fluid activity. The plumbing system is very complicated. A disequilibrium was probably the main reason for overpressure, since Vestnesa holds silty turbidites and muddy silty contourites. Despite the fact, that Vestnesa (A2) is very faulted and fractured much less of these faults are found in Vestnesa (A1), (only 20 km further). However, because of a lack of chaotic reflections and undisturbed data, faults (Figure 5.2.7A and 5.2.7B) are seen well in (A1).

In both locations in Vestnesa there is no sign of plough marks, since Vestnesa Ridge is located in great depths, where icebergs couldn't reach the seafloor, just as it was the case in Nyegga.

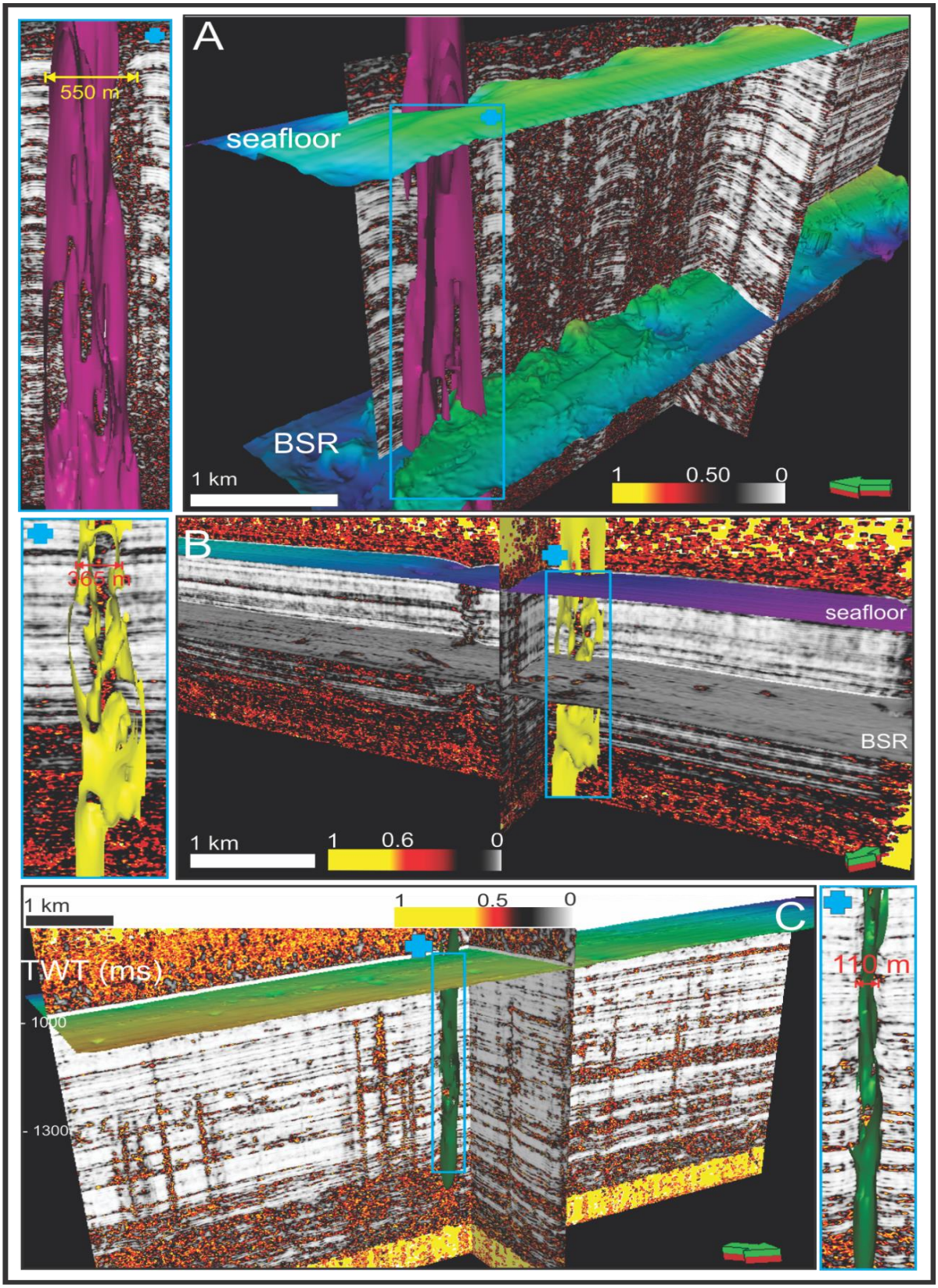

Figure 6.3.1: *Acoustic chimneys showed piercing through the BSR and reaching seafloor. A) Vestnesa (A2) area showing randomly chosen pink colored chimney made with MultiZ interpretation. Rest of the data shown using chaos attributes. B) Vestnesa (A1) is showing a randomly chosen yellow colored chimney made with MultiZ interpretation. Rest of the data shown using chaos attributes. C) Nyegga region showing a randomly chosen green colored chimney made with MultiZ interpretation. Rest of the data shown using chaos attributes.*

6.3.2 Nyegga

It is assumed, that in Nyegga region long term fluid flow could occur (not active in present) from polygonal fault system seen (Figure 2.2.6) at around - 1700 ms (TWT) (located in fine grained, hemi-pelagic sediments) from the top of the Brygge formation. The evidence for this claim could be from Berndt et al. (2003) who say that the North Sea is a great example of long term fluid flow, which can be related with the active flow from the Miocene. Also according to Plaza-Faverola et al. (2012) polygonal faults can be seen in Kai and lower Naust formations. Additionally, Berndt (2005) accepts the assumption that the polygonal faults source could be Tertiary times sediments and says that mostly pipes in the North Sea are rising from the polygonal faults.

Originally, polygonal faults formed as de-watering pathways, allowing pore fluid migration out. In this process sediments shrank and fluids expelled. During later burial sediments compacted and polygonal faults formed. Judd and Hovland (2007) claim that this process could control fluid flow.

Interestingly, there are more stacking pockmark craters in Nyegga than in other areas and as Cartwright et al. (2007) predicate it could be evidence of an episodic fluid (which was active in the recent past). The author also divided pipes in four categories, where seepage and blow out pipes are most common in all areas. Blowout pipes, which are also seen in Nyegga, represent sudden blowout (Berndt, 2005; Løseth et al., 2001) and according to Cartwright et al. (2007), they are formed in a dynamic processes, when maximum fluid expulsion occured at the time of their formation. Blowout pipes are also less common in the Nyegga region, than in the other areas, seepage pipes in this region could represent long term seepage, where pressure is building slightly, but not rapid. These blowout structures are relatively small compared with the Vestnesa ridge. In my opinion seepage pipes in Nyegga are more abundant than blowout pipes and I presume that is because in Nyegga, silty sediments are more abundant than in Vestnesa.

The dissociation of gas hydrates in Nyegga could be one of the reasons for the forming of seepage pipes. Xu and Germanovich (2006) claim that the dissociation of the gas hydrates can be one of the mechanisms that push gasses upwards and can cause seepages. Furthermore, based on this process, it causes fluid migration and expulsion, since developed overpressure resulted in hydro fracturing above the dissociated area which is also mentioned by Talukder (2012). However, Plaza-Faverola et al. (2010) say that the formation of gas hydrates is more

affective in areas where glacial debris is absent. Again, in both datasets there are glacial debris flow deposits, yet gas hydrates are still present. Why?

Free gas tends to migrate upwards and laterally as it is seen in Nyegga, however sometimes sealing faults or strata pinch outs are interrupting this process. The gas will accumulate under seal, but when it reaches structural closure and fills it, fluids will spill and continue their way upwards until they find another seal and this process will repeat the previous steps (Liu et al., 2008).

Gas chimneys occur mostly in fine grained sediments or in marine clays, where fracturing and in-filling of gas hydrates is enabled (Berg et al., 2005). In an early stage when a gas chimney was formed in Nyegga, gas hydrates reduced the amount of gas reaching the paleo seafloor, but later hydrate dissolution supported methane supply up to the seafloor even when the supply of gas was reduced or stopped (Plaza-Faverola et al., 2010). Furthermore, according to Bünz et al. (2012) and Nimblett and Ruppel, (2003) gas hydrates have the ability to reduce the permeability of sediments that later affect fluid flow, because free gas can accumulate beneath hydrate bearing sediments (Figure 5.3.15).

Factors that control fluid flow in marine sediments are the tectonic regime and the sedimentary environment. In Nyegga, above INT reflector silt, sand and gravel is deposited, which indicates glacial influence, claim Berg et al. (2005); as well as plough mark occurrence in data approves that, since plough mark occurrence starts at - 1054 ms (TWT) in the northern part of Nyegga down to - 1339 ms (TWT). Plaza-Faverola et al. (2011) suggested that the deposition of chimneys and fluid flow in this region can be related to glacial-interglacial transitions. Under INT, sediments contain silty, sandy clay which is an effective seal for fluids since these sediments are impermeable (Rise et al., 2006). L50, which is one of the Plaza-Faverola interpreted seismic layers, is located right under INT and shows the part in stratigraphy, where most plough marks occur as well as most chimneys terminate, (especially seepage pipes) (from base of L50 - INT (top of L50)). The base of L50 (Figure 2.2.6, 3.4.1, 5.3.4 and 5.3.10A) is obviously domed, where gas chimneys are piercing through the sediments. It is probably domed by some clay layers that are impermeable (and fluid flow was active in that time), or it could be a velocity artifact. However, when sediments and gasses interact, gas is injected slowly under the clay layer resulting in seabed doming (Judd and Howland, 2007). Besides, doming of the sediments can be the sign of building pressure, that afterwards forms blowout and new pockmarks are forming. However, doming can emerge

when gas hydrates fill the fractures (Plaza-Faverola et al., 2010) and therefore block any further way upwards. In the Nyegga dataset these domings are found (Figure 5.3.8).

Rapid sedimentary loading and emplacement of the Plio-Pleistocene sediments may have caused the generation of excess pore pressure in deeper formations which is controlling mechanisms for the migration of fluids (lateral and upward) (Plaza-faverola et al., 2010). Also polygonal faults located in the Top of the Brygge formation could be a reason that controls Nyegga in long term fluid flow (Berndt et al; 2003). Berndt et al. (2003) agree with Plaza-Faverola et al. (2010) that in Nyegga hydraulic fracturing is the main process that results in transporting fluids upwards, and last but not least important - thickness of glacigenic debris flows, which is responsible for further fluid distribution. That means overpressure is the main reason why fluids are migrating upwards in Nyegga and overpressure generation is related with active and inactive fluid flow and will control permeability of the sediments as well as their further fluid flow (e.g Talukder, 2012). The plumbing system is affected by sediment properties in general, which implies their ability to resist different mechanical deformations. Knowing sedimentation rate in Nyegga is important, to understand sediment characteristics. For example, Hjelstuen et al. (2005) estimated that sedimentation rate was 1.4 m/ka at the INT time, which represents the Saalian ice sheet retreat, but the authors also, presumed that it could be 0.5 m/ka. This big difference in sedimentation rates causes changes in the plumbing system and fluid flow in general. Bottom current activity has affected the sedimentation rate along the mid-Norwegian margin (Bryn et al., 2005) since mid-Miocene time, because in Nyegga, countourite sediments are highly abundant. Probably, due to the plough mark occurrence in Nyegga, there were many active and inactive periods, approving with the assumption by Judd and Hovland, (2007), that fluid expulsion has been triggered by icebergs which have affected sediments during the last deglaciation and afterwards they allowed fluids to migrate easily through the seabed sediments.

Last but not least, the geothermal gradient and bottom water temperatures are not varying greatly across the study area (Bouriak et al., 2000), which makes the BGHSZ to be controlled mainly by pressure. For instance, temperatures at the level of Naust S are between 10 and 40^{o}C, based on a geothermal gradient of 55^{o}C/km (Bouriak et al., 2000).

7 Conclusions

- Fluid flow in Vestnesa is mainly caused by overpressure which leads to hydraulic fracturing of cap rock. Firstly, the great amount of faults and the high geothermal gradient in Vestnesa (A2) help fluids migrate upwards, therefore resulting in active seeping of methane. Secondly, the dissociation of gas hydrates helps fluids actively migrate through gas chimneys into the water column which is seen as gas flares.
- Pull up and push down structures in all regions most likely show the existence of gas hydrates and free gas.
- Reactivation of gas chimneys can be caused by overpressure and permeability of faults. Sediment compaction, meaning tectonics, affects sediments and the distribution of fluids (hydrates and free gas).
- Truncations in all areas represent activity of fluid flow, its reactivation and their thickness allows the calculation of the duration of the active period of fluid flow.
- Chimneys in Vestnesa ridge are bigger, more chaotic in their internal structure and hold more acoustic pipes than those in the Nyegga region, making the plumbing system very complicated.
- Plough mark occurrence in Nyegga is related to glacial influence and it could be related to fluid flow activity.
- Blowout pipes which represent rapid pressure blowout in Nyegga are a minority and seepage pipes are thought to be the main path for fluids, representing long term seepage.
- Chimneys in Nyegga are perfectly vertical and not as wide as in Vestnesa, and their upper part is also not as disturbed.
- The saying: *"The deeper a pockmark – the wider the chimney"*, is not true, because pockmark sizes are effected by host sediments, their characteristics and pressure. The upper part of the seabed in Nyegga, compared with Vestnesa, consists of more coarse grained sediments, resulting in smaller pockmarks.
- Small pockmarks and mounds in Nyegga are the result of polygonal faults located at least at the level of the Top Brygge formation. These faults are connected with gas chimneys/ pipe structures, which transport fluids up to the seabed. Hydro fracturing resulted from overpressure and later controlled the permeability of sediments and helped fluids flow up.
- Blowout pipes are mostly abundant in Vestnesa (A2), which presents very active fluid flow. Thicknesses of truncations are only 1.7 ms (TWT) thick. In Vestnesa (A1) blowout

pipes dominate, but seepage pipes are also present in significant numbers. Average truncation is very thick: 5.2 ms (TWT). Nyegga is the right opposite (A1), with its seepage pipes. Truncations in average are 3.1 ms (TWT) thick.

- I speculate, that in the past fluid flow activity occurred almost at the same time in all areas (not amount of gas expelling). Nowadays their flows are different.
- In Nyegga all sediment layers show the presence of gas hydrates, but below the BSR it could just be an artifact.
- In Vestnesa (A1) within the GHSZ irregularly distributed gas is seen as low velocity layers, but in Vestnesa (A2) within the GHSZ more gas hydrates (high velocity layers) with free gas occur.
- Both in Vestnesa (A1) and in Nyegga buried pockmarks show a high number of chimney reactivations.

Reference List

Abrams, A. (2005) *Significance og hydrocarbon seepage relative to petroleum generation and entrapment*. Mar.Petrol.Geol., 22, pp. 457-477.

Andreassen, K. (2009) *Marine geophysics lecture notes for Geo-3123*. University of Tromsø.

Andreassen, K., Laberg, J.S.,Vorren, T.O. (2008) *Seafloor geomorphology of the SW Barents Sea and its glaci-dynamic implications*. Science direct, Elsevier, geomorphology 97, pp. 157-177

Balkwill, H.R. (1978) *Evolution of Sverdrup Basin, Arctic Canada*. Am. Assoc. Petroleum Geologists Bull. 62, pp. 1004-1028

Barrington, J., and P. F. Kerr (1961) Breccia pipe *near Cameron, Arizona: Geological Society of America Bulletin*, v. 72, pp. 1661-1674

BBC News 29 Oct. 2001

Beaumont, C., Keen, C.E. and Boutilier, R. (1982a) *On the evolution of rifted continental margins: comparison of models and observations for the Nova Scotia Margin*. Geophys. J.R. Astr. Soc. **70**, pp. 667-715

Beaumont, C., Keen, C.E. and Boutilier, R. (1982b*) A comparison of foreland and rift margin sedimentary basins*. Phil. Trans. R.Soc.Lond.A305, pp. 295-317

Behrmann, J. H., 1991. Condition for hydrofracture and the fluid permeability of accretionary wedge. *Earth Planet. Sci. Lett*., **107**, 550-558.

Berg, K., Solheim, A., Bryn, P. (2005) *The Pleistocene to recent geological development of the Ormen Lange area*. Mar. Petrol. Geol. 22, pp. 45-56

Berndt, C. (2005) *Focused fluid flow in passive continental margins.* The royal society, 363, pp. 2855-2871

Berndt, C., Bünz, S. and Mienert, J. (2003) *Polygonal fault systems on the mid-Norwegian margin: a long term source for fluid flow*. In: Subsurface sediment mobilization (ed. P. van Rensbergen, R.R. Hillis, A.J. Maltman and C.K. Morley). Special Publication 216, pp. 283-290. London: Geological Society of London.

Bethke, C. M., Reed, J. D., and Oltz, D. F. (1991) Long-range petroleum migration in the Illinois Basin. *American Association of Petroleum Geologists (Bulletin)*, **75**, pp. 925–45

Birkelund, T. and Perch-Nielsen, K. (1976) *Late Paleozoic-Mesozoic evolution of central East Greenland*, in: Geology of Greenland (Eds. Escher, A. and Watt, W.S.), Geol. Surv. Greenland, Copenhagen, pp. 304-339

Blinova, B. N., Ivanov, M. K., and Bohrmann, G., 2003.Hydrocarbon gases in deposits from mud volcanoes in the Sorokin Trough, north-eastern Black Sea. *Geo-Marine Letters*, **23**, 250–7.

Bøen, F.,Eggen, S., and Vollset,J. (1984) *Structures and basins of the margin from 62-69oN and their development*. In Spencer, A.M., et al. (Eds.), Petroleum Geology of the North European Margin: London (Graham and Trotman), pp. 3-28

Bott, M.H.P. (1979) *Subsidence mechanism at passive continental margins*, in: Geological and Geophysical investigations of continental margins, (Eds Watkins, J.S.,Montadert, L. and Wood-Dickerson, P.), Am. Assoc. Petrol. Geol. Mem. 29, pp. 3-9

Bott, M.H.P. (1981) *Crustal doming and the mechanism of continental rifting*. Tectonophysics 73, pp. 1-8

Bouriak, S., M. Vanneste, and A. Saoutkine (2000), Inferred gas hydrates and clay diapirs near the Storegga Slide on the southern edge of the Vøring Plateau, offshore Norway, Mar. Geol., 163 (1-4), 125-148.

Branney, M.J., 1995, Downsag and extension at calderas: Bulletin of Volcanology, v. 57, p. 303-318

Bredehoeft, J.D. and Hanshaw, B. B. 1968. On the maintenance of anomalous fluid pressures. 1. Thick sedimentary sequences. Geol. Soc. Am. Bull. 79, 1097-1106.

Brekke, H., 2000, The tectonic evolution of the Norwegian Sea continental margin with emphasis on the Vøring and Møre basins: Geological Society, London, Special Publications, v. 136, pp. 327-378.

Brown, A., 2000. Evaluation of possible gas micro seepage mechanisms. *AAPG Bulletin 84* (**11**), pp. 1775-1789.

Brown, AR. 2003. Interpretation of Three Dimensional Seismic Data, 6th edition, *AAPG. Mem.* **42**, 541., Tulsa, OK.

Brown, K.M., 1994. Fluids in deforming sediments. In: Geological Deformation Of Sediments (A. Maltman, ed.), pp. 205-237. Chapman & Hall, London.

Bryn, P., Berg, K., Stoker, M.S.,Haflidason, H., Solheim, A., 2005. Contourites and their relevance for mass wasting along the Mid-Norwegian Margin. Mar. Petrol. Geol. 22, 85-96

Bryner, L., 1961, Breccia columns associated with epigenetic ore deposits: Economic Geology, v. 56, p. 488-508

Bugge, T., Befring, S., Belderson, R. H., et al., 1987. A giant three-stage submarine slide off Norway. Geo-Marine

Bugge, T., Lien, R.L. and Rokoengen, K. 1979, Store ras pa continental – skraningen utenfor Midt-Norge, Continental Shelf Institute Trondheim Contribution No. P-155/12/79

Bugge, T.,Prestvik, T. and Rokoengen, K. (1978) Lower Tertiary volcanic rocks off Kristiansund-Mid Norway, Continental Shelf Institute Trondheim Contribution No. P-155/11/78

Bukovics, C. and Ziegler, A.P. (1984) Tectonic development of the Mid-Norway continental margin; Marine and Petroleum geology, 1995, Vol2, February, 2-22

Bulat, J.,2005. Some considerations on the interpretation of seabed images based on commercial 3D seismic in the Faroe-Shetland Channel. Basin research 17, 21-42

Bünz, S., Mienert, J., 2004. Acoustic imaging of gas hydrate and free gas at the Storegga Slide. Journal of geophysical Research – Solid Earth 109, B4

Bünz, S., Mienert, J., Berndt, C., 2003. Geological controls on the Storegga gas hydrate system of the mid-Norwegian continental margin. Earth and Planetary Science Letters 209 (3-4), 291-307

Bünz, S., Mienert, J., Bryn, P., Berg, K., 2005. Fluid flow impact on slope failure from 3D seismic data: a case study in the Storegga Slide. Basin Research 17 (1), 109-122.

Bünz, S., Petersen, C.J., Hustoft, S., Mienert, J., 2008. Environmentally-sensitive gas hydrates on the W-Svalbard margin at the gateway to the Arctic ocean. In: Proceedings of the 6th International Conference on Gas Hydrates, Vancouver, British Colombia, Canada, pp. 6

Bünz, S.,Polyanov, S., Vadakkepuliyambatta, S., Consolaro, C., Mienert, J., 2012. Active gas venting through hydrate-bearing sediments on the Vestnesa Ridge, offshore W-Svalbard. Marine Geology 332 – 334 (2012) 189 – 197

Carson, B. And Westbrook, G.K., 1995. Modern fluid flow in the Cascadia accretionary wedge: a synthesis. In: *Proc. ODP, Sci. Results* (B.Carson, G.K. Westbrook, R.J. Musgrave and E. Suess, eds), **146**, 413-421.

Cartwright, J. A. and Dewhurst, D. N., 1998. Layer-bound compaction faults in fine grained sediments. *Geological Society of America (Bulletin)*, **110**, 1242–57.

Cartwright, J. A., 1996. Polygonal fault systems: a new type of fault structure revealed by 3D seismic data from the North Sea basin. In Weimer, P. and Davis, T. L. (eds.),

Applications of 3-D Seismic Data to Exploration. American Association of Petroleum Geologists, Studies in Geology No. 42 and SEG Geophysical Developments Series No. 5, pp. 225–30.

Cartwright, J. A., James, D. and Bolton, A. 2003 The genesis of polygonal fault systems: a review. In: Subsurface sediment mobilization (ed. P. van Rensbergen, R.R. Hillis, A.J. Maltman and C.K. Morley). Special Publication 216, pp. 223-243. London: Geological Society of London.

Cartwright, J., Huuse, M., Aplin, A., (2007) Seal bypass systems. AAPG Bulletin, V. 91, NO. 8, pp. 1141-1166

Cathles, L.M., Su, Zheng, Chen, D. 2010. The physics of gas chimney and pockmark formation, with implications for assessment of seafloor hazards and gas sequestration. *Elsevier Marine and Petroleum Geology*, **27**, 82-91

Chopra, S., Marfurt, K., 2006. Seismic Attributes – a promising aid for geologic prediction. CSEG RECORDER, 111-121.

Clayton, C. J. and Hay, S. J., 1994. Gas migration mechanisms from accumulation to surface. Bulletin of the Geological Society of Denmark, 41, 12–23.

Cragg, B. A., Parkes, R. J., Fry, J. C., et al., 1996. Bacterial populations and processes in sediments containing gas hydrates (ODP Leg 146: Cascadia Margin). *Earth &Planetary Science Letters*, **139**, 497–507.

Dalland, A.,Worsley, D., Ofstad, K., 1988. A lithostrategraphic scheme for the Mesozoic and Cenozoic succession offshore mid- and northern Norway. Oljedirektoratet, Januar, NPD-Bulletin No 4, pp. 3-65

Dewhurst, D. N., Cartwright, J. A., and Lonergan, L., 1999. The development of polygonal fault systems by syneresis of colloidal sediments. *Marine & Petroleum Geology*, **16**, 793–810.

Dimitrov, L. I., 2002. Mud volcanoes – the most important pathway for degassing deeply buried sediments. *Earth-Science Reviews*, **59**, 49–76.

Dugan, B. and Flemings P. B., 2000. The New Jersey margin: compaction and fluid flow. Journal of Geochemical Exploration, 69–70, 477–81.

Ecker, C., Dvorkin, J., Nur, A., 1998. Sediments with gas hydrates: internal structure from seismic AVO. *Geophysics* **63**, 1659-1669.

Edgerton, H. E., Seibold, E., Vollbrecht, K., and Werner, F.,1966. Morphologische Untersuchungen am Mittelgrund (Eckernf¨order Bucht, westliche Ostsee).*Meyniana*, **16**, 37–50. (In German)

Egorov, A. V., Crane, K., Rozhkov, A. N., and Vogt, P. R., 1999. Gas hydrates that outcrop on the sea floor: stability models. *Geo-Marine Letters*, **19**, 68–75.

Eidvin, T., Jansen, E., Rundberg, Y., Brekke, H., Grogan, P., 2000. The upper Cainozoic of the Norwegian continental shelf correlated with the deep sea record of the Norwegian Sea and the North Atlantic. Mar. Petrol. Geol. 17, 579-600

Eiken, O. and Hinz, K., 1993, Contourites in the Fram Strait: Sedimentary Geology, v. 82, pp. 15-32.

Eldholm, O. and Talwani, M. (1977) Sediment distribution and structural framework of the Barents Sea, Geol. Soc. America Bull. 88, 1015-1029

Eldholm, O., Sundvor, E., Myhre, A. M., and Faleide, J.I., 1984. Cenozoic evolution of the continental margin off Norway and western Svalbard. North European Margin Symp. Proc. Norw. Pet. Soc.: London (Graham and Trotman), 3-18

Eldholm, O., Thiede, J. and Taylor, E., 1989. Evolution of the Vøring Volcanic Margin.Proceedings of the Ocean Drilling Program, Scientific Results, 104.pp. 5-25

Engen, Ø., Faleide, J.I., Dyreng, T.K., 2008. Opening of the Fram Strait gateway: a review of plate tectonics constraints. Tectonophysics 450 (1-4), 51-69

Faleide, I.J., Gudlaugsson, S.T. and Jacquart, G., 1984. Evolution of the western Barents Sea. *Marine and Petroleum Geology*, **1**, 123-150.

Faleide, J.I., Solheim, A., Fiedler, A., Hjelstuen, B.O., Andersen, E.S., and Vanneste, K., 1996, Late Cenozoic evolution of the western Barents Sea Svalbard continental margin: Global and Planetary Change, v. 12, pp. 53-74.

Faleide, J.I., Tsikalas, F., Breivik, A. J., Mjelde, R., Ritzmann, O., Engen, Ø., Wilson, J., Eldholm, O., 2008. Structure and evolution of the continental margin off Norway and the Barents Sea, pp. 82-91, Episodes, Vol. 31 No. 1

Gabrielsen, R.H., Færseth, R.B.,Jensen, L.,N.,Kalheim, J.,E.,Riis, F. 1990. Structural elements of the Norwegian continental shelf, Part I: The Barents Sea Region, Oljedirektoratet, NPD-Bulletin NO 6, pp 3-33

Gay, A., Lopez, M., Berndt, C., Seranne, M., 2007. Geological controls on focused fluid flow associated with seafloor seeps in the Lower Congo Basin. Marine Geology 244 (1e4), 68e92.

Gay, A., Lopez, M., Cochonat, P. and Sermondadaz, G. 2004 Polygonal faults-furrows system related to early stages of compaction – upper Miocene to Recent sediments of the Lower Congo Basin. Basin Res. 16, 101-116. (doi:10.1111/j.1365-2117.2003.00224.x.)

Gebhardt, A.C., Geissler, W.H.,Matthiessen, J.,Jokat, W., 2014. Changes in current patterns in the Fram Strait at the Pliocene/Pleistocene boundary. Quaternary science reviews, volume 92, 15 may 2014, Pages 179-189

Gibbons, H. ECS project, 2010. http://continentalshelf.gov/missions/10arctic/logs/aug11/aug11.html

Gloppen, T.G. and Westre, S. (1982) Large potential off northern Norway, Oil and Gas Jour. 80 (23), 114-127

Graue, K., 2000. Mud volcanoes in deepwater Nigeria. *Marine and Petroleum Geology*, **17**, 959–74.

Grogan, P., Østvedt-Ghazi, A.M., Larssen, G. B., Fotland, B., Nyberg, K., Dahlgren, S., and Eidvin, T., 1999, Structural elements and petroleum geology of the Norwegian sector of the northern Barents Sea, in Fleet, A.J. and Boldy, S.A.R., eds., Petroleum geology of Northwest Europe; proceedings of the 5th conference: Geological Society London, pp. 247-259.

Guliev, I. S., 1992. *A Review of Mud Volcanism*. Baku,Geology Institute of Azerbaijan, Azerbaijan Academy of Sciences.

Haller,J. (1971) Geology of the East Greenland Caledonites, in: Regional Geology Series (Ed. De Sitter, L.V.), Wiley Interscience Publ., London.

Hammerschmidt, E.G. 1934 august. Formation of Gas Hudrates in Natural Gas Transmission Lines, pp 851-855, Industrial & Engineering Chemistry, Volume 26, Issue 8

Hanisch, J. (1984) The Cretaceous opening of the NE Atlantic and the west Spitsbergen orogeny – a plate tectonic model, in: Proceedings of the North European Margin Symposium, Trondheim 1983, (Eds Spencer, A.M. et al.) Graham and Trotman, London

Hansen, J.P.V., J.A. Cartwright, M. Huuse, and O.R. Clausen, 2005, 3 D seismic expression of fluid migration and mud remobilization on the Gjallar Ridge, offshore mid-Norway: Basin Research, v. 17, p. 123-140

Harland, W.B. (1965) The tectonic evolution of the Arctic-North Atlantic region, Royal Soc. London Philos. Trans. 258, 59-75

Harrington, J. F. and Horseman, S. T., 1999. Gas transport properties of clays and mudrocks. In Aplin, A. C., Fleet, A. J., and Macquaker, J. H. S. (eds.), Muds and Mudstones:

Physical and Fluid Flow Properties. Geological Society of London, Special Publication 158, 107–24.

Heggland, R. (1998) Gas seepage as an indicator of deeper prospective reservoirs. A study based on exploration 3D seismic data. Marine petroleum geology 15, 1-9

Hellinger, J.S., Sclater, J.G. (1983) Some comments on two-layer extensional models for the evolution of sedimentary basins, J. Geophys. Res. B, 88 (10), 8251-8269

Hinz, K., Døstmann, H.J. and Hanisch, J. (1982) Structural framework of the Norwegian Sea, Offshore Northern Seas Conference, proc., Stavanger, 1982 ONS-82/E/4, 1-22

Hjelstuen, B.O., Eldholm, O., and Faleide, J.I., 2007, Recurrent Pleistocene mega-failures on the SW Barents Sea margin: Earth and Planetary Sciience Letters, v. 258, pp. 605-618.

Hjelstuen, B.O., Eldholm, O., Skogseid, J., 1999. Cenozoic evolution of the northern Vøring margin. Geol. Soc. Am. Bulletin 111, 1792-1807

Hjelstuen, B.O., Sejrup, H.P., Haflidason, H., Nygard, A., Ceramicola, S., Bryn, P., 2005. Late Cenozoic glacial history and evolution of the Storegga Slide area and adjacent slide flank regions, Norwegian continental margin. *Mar. Petrol. Geol.* **22**, 57-69

Holbrook, S.W., Hoskins, H., Wood, W.T., Stephen, R.A., Lizzarralde, D., Party, L.S., 1996. Methane gas-hydrate and free gas on the Blake Ridge from vertical seismic profiling. Science 273, 1840-1843.

Hovland, M. and Judd, A. G., 1988. *Seabed Pockmarks and Seepages: Impact on Geology, Biology and the Marine Environment*. London, Graham and Trotman Ltd.

Hovland, M., 1981. Characteristics of pockmarks in theNorwegian Trench. *Marine Geology*, **39**, 103–17.

Hovland, M., 1983. Elongated depressions associated with pockmarks in the western slope of the Norwegian Trench. *Marine Geology*, **51**, 35–46.

Hovland, M., 2002. On the self-sealing nature of marine seeps. *Cont. Shelf Res*., **22**, 2387-2394.

Hovland, M., Svensen, H., Forsberg, C.F., Johansen, H., Fichler, C., Fossa, J.H., Jonnson, R., Rueslatten, H., 2005. Complex pockmarks with carbonate-ridges off mid-Norway: products of sediment degassing. Marine Geology 218 (1-4), 191-206.

Howe, J.A., Shimmield, T.M., Harland, R., 2008. Late Quaternary contourites and glaciomarine sedimentation in the Fram Strait. Sedimentology 55 (1), 179-200

Hustoft, S., Bünz, S., Mienert, J., Chand, S., 2009. Gas hydrate reservoir and active methane-venting province in sediments on <20 Ma young oceanic crust in the Fram Strait, offshore NW-Svalbard. Earth and Planetary Science Letters 284 (1-2), 12-24

Jakobsson, M., Backman, J., Rudels, B., Nycander, J., Frank, M., Mayer, L.A., Jokat, W., Sangiorgi, F., O'Regan, M., Brinkhuis, H., King, J.W., Moran, K., (2007) The early Miocene onset of a ventilated circulation regime in the Arctic Ocean. Nature, 447,pp. 986-990

Jebsen, C. and Faleide, 1998, Tertiary rifting and magmatism at the western Barents Sea margin (Vestbakken volcanic province): III international conference on Arctic margins, ICAM III; abstracts; plenary lectures, talks and posters, pp. 92.

Jokat, W., Geissler, W.H., Voss, M. (2008) Basement structure of the north-western Yermak Plateau. Geophysical research letters, 35, p. L05309

Judd, A.G. and Hovland, M. (2007) Seabed fluid flow. The impact on geology, biology and the marine environment, Cambridge University Press, New York, pp 442.

King, E.L., Sejrup, J.P., Haflidason, H., Elverhoi, A., Aarseth, I., 1996. Quaternary seismic stratigraphy of the North Sea Fan: glacially-fed gravity flow aprons, hemipelagic sediments, and large submarine slides. Marine Geology 130 (3-4), 293-315.

King, L. H. and MacLean, B., 1970. Pockmarks on theScotian Shelf. *Geological Society of America (Bulletin)*, **81**, 3141–8.

Kvenvolden, K.A., 1993. Gas hydrates-geological perspective and global change. Rev. Geophys. 31, 173-187.

Lee, M. W. (2004), Elastic velocities of partially gas-saturated unconsolidated sediments, Mar. Pet. Geol., 21(6), 641–650, doi:10.1016/j.marpetgeo.2003.12.004.

Leifer, I., Boles, J., 2005. Measurment of marine hydrocarbon seep flow through fractured rock and unconsolidated sediment. Marine and petroleum geology 22, 551-568 Letters, 7, 191–8.

Levorsen, A.I. 1967. Geology of petroleum. 2ed. Freeman, San Francisco.

Linke, P., Suess, E., Torres, M., Martens,V.,Rugh, W.D., Ziebis, W., Kulm, L.D. In situ measurement of fluid flow from cold seeps at active continental margins, Elsevier, 721-739, 1994.

Liu, X., Zhong, G., Yin, J.,He, Y., Li, X. 2008. GIS-based modeling of secondary hydrocarbon migration pathways and its application in the northern Songliao Basin, northeast China. *Elsevier, Computers & Geosciences*, **34**, 1115-1126.

Long, D., 1992. Devensian Late-glacial gas escape in thecentral North Sea. *Continental Shelf Research*, **12**, 1097–110.

Løseth, H., Gading, M., Wensaas, L., 2009. Hudrocarbon leakage interpreted on seismic data. Marine and petroleum geology 26 (2009) 1304-1319

Løseth, H., L. Wensaas, B. Arnsen, and M.Hovland, 2003, Gas and fluid injection triggering shallow mud mobilization in the Hordaland group, North Sea, in P. van Rensbergen, R. Hilis, A. Maltman, and C. Morley, eds., Subsurface sediment mobilization: Geological society (London) Special publication 216, p. 139-157

Løseth, H., Wensaas, L., Arntsen, B., Hanken, N., Basire, C., Graue, K., 2001. 1000 M long gas blow-out pipes: 63rd European Association of geoscientists and engineers conference and exhibition, EAGE, Extended abstracts, Amsterdam p.524

MacDonald, I. R., Bohrmann, G., Escobar, E., et al., 2004. Asphalt volcanism and chemosynthetic life in the Campeche Knolls, Gulf of Mexico. Science, 304, 999–1002.

Magalhaes, V.H., Pinheiro, L.M., Ivanov, M.K., Kozlova, E., Blinova, V., Kolganova, J., Vasconcelos, C., McKenzie, J.A., Bernasconi, S.M., Kopf, A.J., Diaz-del-Rio, V., Gonzalez, F.J., Somoza, L., 2012. Formation processes of methane-derived authigenic carbonates from the Gulf of Cadiz. In: Sedimentary geology., Elsevier, 243-244 (2012) 155-168.

Mascle, A. and Moore, J.C., 1990. ODP Leg 110: tectonic and hydrologic synthesis. In: *Proc. ODP, Sci. Results* (J.C. Moore, A.Mascle, E.Taylor, M.B. Underwood and W.R. Winker, eds), **110**, 409-422.

Mazzini, A., Svensen, H., Hovland, M., Planke, S. 2006. Comparison and implications from strikingly different authigenic carbonates in a Nyegga complex pockmark, G11, Norwegian Sea. Elsevier Marine Geology, 231, 89-102

Mazzini, A., Svensen, H., Planke, S., Guliyev, I.,Akhmanov, G.G., Fallik, T. and Banks, D., 2009. When mud volcanoes sleep: insight from seep geochemestry at the Dashgil mud volcano, Azerbaijan. *Mar. Petrol. Geol*., **26**, 1704-1715.

McKenzie, D. (1978) Some remarks on the development of sedimentary basins, Earth Planet. Sci. Lett. 40, 25-32

Mienert, J., Posewang, J., Lukas, D., 2001. Changes in the hydrate stability zone on the Norwegian Margin and their consequences for methane and carbon releases into the oceanosphere. In: Schäfer, P., Ritzrau, W., Schlüter, M., Thiede, J. (Eds.), The Northern North Atlantic: a Changing Environment. Springer Press, pp. 259-280.

Morgan W.J. (1972) Deep mantle convenction plumes and plate motions. Am. Ass. Petrol. Geol. Bull. 56, 203-13

Morgan, K., Backman, J., Brinkhuis, H., Clemens, S.C, Cronin, T., Dickens, G.R., Eynaud, F., Gattacceca, J., Jakobsson, M., Jordan, R.W., Kaminski, M., King, J.W., Koc, N., Krylov, A., Martinez, N.,Matthiessen, J., Mclnroy, D., Moore, T.C., Onodera, J., O'Regan, M., Palike, H., Rea, B., Rio, D., Sakamato, T., Smith, D.C., Stein, R., St John, K., Suto, I., Suzuki, N., Takahashi, K., Watanabe, M., Yamamoto, M., Farrell, J., Frank, M., Kubik, P., Jokat, W., Kristoffersen, Y. (2006) The Cenozoic palaeoenvironment of the Arctic Ocean. Nature, 441, pp. 601-605

Nalivkin, D.V. (1973) Geology of the U.S.S.R. Oliver and Boyd, Edinburgh

Neugebauer, H.J. (1978) Crustal doming and the mechanisms of rifting, part I: Rift formation, Tectonophysics 45, 159-186

Neugebauer, H.J., Woitt, W.D. and Wallner, H., 1983, Uplift, volcanism, tectonics: evidence for mantle diapirs, in: Plateau Uplift – the Rhenisch Shield. A case of history (Ed. Fuchs, K.), Springer, Berlin, 1983

Neuzil, C.E., 1986. Ground water flow in low permeability environments. *Water Resour. Res.*, **22**, 1163-1195

Nimblett, J., Ruppel, C., 2003. Permeability evolution during the formation of gas hydrates in marine sediments. Journal of Geophysical Research, Solid Earth 108

Nygård, A., Sejrup, H.P., Haflidason, H., Bryn, P., 2005. The glacial North Sea Fan, southern Norwegian Margin: architecture and evolution from the upper continental slope to the deep-sea basin. Mar. Petrol. Geol. 22, 71-84

Osborne, M.J. and Swarbrick, R.E., 1997. Mechanisms for generating overpressure in sedimentary basins: a reevaluation. *AAPG Bull.*, **81**, 1023-1041.

Petersen, C.J., Bünz, S., Hustoft, S., Mienert, J., Klaeschen, D., 2010. High-resolution P-Cable 3D seismic imaging of gas chimney structures in gas hydrated sediments of an Arctic sediment drift. Mar. Petrol. Geol. 1-14. Doi:10.1016/j.marpetgeo.2010.06.006

Petrel 2012, 2013; Petrel geophysics, Schlumberger, pp. 1-469,

Plaza-Faverola, A., Bunz, S., Johnson, J.,E., Chand, S., Knies, J., Mienert, J., Franek, P., 2015. Role of tectonic stress in seepage evolution along the gas hydrate-charged Vestnesa Rige, Fram Strait. AGU Publications, Geophysical Research Letters.p. 1- 10.

Plaza-Faverola, A., Bünz, S., Mienert, J., 2010. Fluid distributions inferred from P-wave velocity and reflection seismic amplitude anomalies beneath the Nyegga pockmark field of the mid-Norwegian margin. In: Marine and petroleum geology 27 (2010) 46-60 pp

Plaza-Faverola, A., Bünz, S., Mienert, J., 2011. Repeated fluid expulsion through sub-seabed chimneys offshore Norway in response to glacial cycles. Earth and Planetary science letters 305 (2011) 297-308

Plaza-Faverola, A., Bünz, S.,Mienert, J., 2012. The free gas zone beneath gas hydrate bearing sediments and its link to fluid flow: 3-D seismic imaging offshore mid-Norway. Marine Geology, Elsevier, Volumes 291-294, 211-226.

Plaza-Faverola, A., Westbrook, G.K., Ker, S., Exley, R., Gailler, A., Minshull, T.A., Broto, K., 2010b. Evidence from three-dimensional seismic tomography for a substantial accumulation of gas hydrate in a fluid-escape chimney in the Nyegga pockmark field, offshore Norway. J. *Geophys. Res*. 115. doi:10.1029/2009JB007078 (B08104).

Polyak, L., Edwards, M.H., Coakley, B.J, Jakobsson, M., 2001. Ice shelves in the Pleistocene Arctic Ocean inferred from glaciogenic deep-sea bedforms. Nature 410, 453-457.

Rafaelsen, B., K. Andreassen, L.W. Kuilman, E. Lebesbye, K. Hogstad and M. Mitbø. 2002. Geomorphology of buried glacigenic horizons in the Barents Sea from three-dimensional seismic data. In Dowdeswell, J.A. and C.O Cofaigh, eds. Glacier-influenced sedimentation on high-latitude continental margins. London, Geological Society, 259-276. (Special Publication 203).

Rebesco, 2005, sedimentary environments, encyclopedia of geology, pages 513-527

Rise, L., Ottesen, D., Berg, K., Lundin, E., 2005. Large-scale development of the mid-Norwegian margin during the last 3 million years. Mar. Petrol. Geol. 22, 33-44

Rise, L., Ottesen, D., Longva, O., Solheim, A., Andersen, E.S., Ayers, S., 2006. The Sklinnadjupet slide and its relation to the Elsterian glaciation on the mid-Norwegian margin. Mar. Petrol. Geol. 23, 569-583

Rise, L., Sættem, J., Fanavoll, S., Thorsnes, T., Ottesen, D., Bøe, R., 1999. Sea-bed pockmarks related to fluid migration from Mesozoic bedrock strata in the Skagerrak offshore Norway. Mar. Petrol. Geol. 16, 619-631.

Ritzmann, O., Jokat, W., Czuba, W., Guterach, A., Mjelde, R., Nishimura, Y., 2004. A deep seismic transect from Hovgård Ridge to northwestern Svalbard across the continental-ocean transition: a sheared margin study. Geophysical Journal International 157 (2), 683-702

Roberts, S., Nunn, J.A., 1995. Episodic fluid expulsion from geopressured sediments. *Marine and Petroleum geology,* **12**, 195-204

Rønnevik, H.C., Bescow, B. and Jacobsen, H.P. (1982) Structural and stratigraphic evolution of the Barents Sea, Can. Soc. Petroleum Geologists, Mem. 8, 431-440

Rove, O.N., 1947, Fluid flow and the genesis of breccia pipes: Economic Geology, v. 42, p. 161-193

Ryseth, A., Augustson, J.H., Charnock, M., Haugerud, O., Knutsen, S.-M., Midbøe, P.S., Opsal, J.G. and Sundsbø, G., 2003, Cenozoic stratigraphy and evolution of the Sørvestsnaget Basin, southwestern Barents Sea: Norwegian Journal of Geology, v. 83, pp. 107-130.

Saffer, D. and Tobin, H.J., 2011. Hydrogeology and mechanics of subduction zone forearcs: fluid flow and pore pressure. *Annu. Rev. Earth Planet. Sci*., **39**, 157-186.

Saunders, D.F., Burson, K.R., Thompson, C.K., 1999. Model for hydrocarbon micro-seepage and related near-surface alterations. AAPG Bulletin 83, 170-185

Schumacher, D., Abrams, M.A., 1996. Hydrocarbon migration and its Near-surface Expression. AAPG Memoir 66

Selley, R.C., 1998. Elements of petroleum geology, second edition, pp.470

Sheriff, RE. 2006. Encyclopedic Dictionary of Exploration Geophysics, 5th. Ed. Tulsa: Society of Exploration Geophysics.

Skogseid, J., 1983. A marine geophysical study of profiles between the Vøring Plateau margin and the Jan Mayen Ridge. (Cand. Scient. Thesis), University of Oslo, Norway.

Smith, A.J., Mienert, J., Bunz, S., Greinert, J. 2014. Thermogenic methane injection via bubble transport into the upper Arctic Ocean from the hydrate-charged Vestnesa Ridge, Svalbard.. *AGU Publications*. 1945-1959.

Sohnge, P., 1963, Genetic problems of pipe deposits: Geological Society of South Africa Transactions, v. 66, p. 19-22

Stanton, R. J., 1966, The solution brecciation process: Geological Society of America Bulletin, v. 77, p. 843-848

Steel, R.J., 1976, Devonian basins of Western Norway: sedimentary response to tectonism and varying tectonic context, Tectonophysics 36, 207-224

Svensen, H., Planke, S., Malthe-Sørenssen, A., Jamtveit, B., Myklebust, R., Rasmussen, T., and Rey, S., 2004, Release of methane from a volcanic basin as a mechanism for initial Eocene global warming: Nature, v. 429, pp. 542-545.

Talukder, A. R., 2012. Review of submarine cold seep plumbing systems: leakage to seepage and venting. Terra Nova, Blackwell publishing Ltd, pp. 255-272

Talwani, M. and Eldholm, O. (1977) Evolution of the Norwegian-Greenland Sea, Geol. Soc. America Bull. 88, 969-999

Taylor, E. and Leonard, J., 1990. Sediment consolidation and permeability at the Barbados forearc. In: Proc. *ODP Sci. Results* (J.C. Moore and A. Mascle, eds), **110**, 289-308.

Taylor, S.W., Lollar, B.S., Wassenaar, L.I., 2000. Bacteriogenic ethane in near-surface aquifers: implications for leaking hydrocarbon well bores. Environmental Science and Technology 34 (22), 4727-4732.

Traynor, J. J. and Sladen, C., 1997. Seepage in Vietnam – onshore and offshore examples. *Marine and Petroleum Geology*, **14**, 345–62.

Turcotte, D.L. (1981) Rifts-Tensional Failure of the Lithosphere, in: papers presented to the Conference on Processes of Planetary Rifting. Christian Brother's retreat house. Napa Valley, California (1981) Lunar and Planet. Inst. Contrib. 451, 5-8

Vanneste, M., Guidard, S., Mienert, J., 2005. Bottom-simulating reflections and geothermal gradients across the western Svalbard margin to the Molloy Transform Fault. Terra Nova 17 (6), 510-516

Vogt, P.R., 1986. Geophysical and geochemical signatures and plate tectonics. In: Hurdle, B.G. (Ed.), The Nordic Seas. Springer, New York, pp. 413-664

Vogt, P.R., Crane, K., Sundvor, E., Max, M.D., P. Firman, S. L., 1994. Methane-generated (?) pockmarks on young, thickly sediment oceanic crust in the Arctic: Vestnesa Ridge, Fram Strait. Geology **22**, 255-258

Vorren, T.O.2005. Subaquatic landsystems: continental margin In: Evans, D. and Gooster, L. eds Glacial landsystems. New York: Amold, pp. 289-312

Voss, M. and Jokat, W., 2007, Continental-ocean transition and voluminous magmatic underplating derived from P-wave velocity modeling of the East Greenland continental margin: Geophysical Journal International, v. 170, pp. 580-604.

Weibull, W., Mienert, J., Bünz, S., Hustoft, S. (2010). Fluid migration directions inferred from gradient of time surfaces of the sub seabed. *Marine and petroleum geology. Elsevier*, **27,** 1898-1909.

Wensaas, L., Løseth, H., Arntsen, B., Hermannrud, C., Hanken, H.M. (2000) Seismic leakage anomalies – links to well data and field exposures. In: Extended Abstract Book from NPF, Hydrocarbon Seal Quantification. Stavanger, Norway

Westbrook, G.K., Minshull, T.A., Nouze, H., Exley, R., Gailler, A.,Jose, T., Ker, S., Plaza, A. (2008) High-resolution 3D seismic investigations of hydrate-bearing fluid-escape chimneys in the Nyegga region of the Vøring plateau, Norway. In: Proceedings of the 6th International Conference on Gas Hydrates (ICGH 2008). 6-10 July, Vancouver, British Colombia, Canada, 12 pp.

Xu, W. And Germanovich, L.N., 2006. Excess pore pressure resulting from methane hydrate dissociation in marine sediments: a theoretical approach. *J. Geophys. Res.,* **111**, B01104

Ziegler, P.A. (1978) North-Western Europe: tectonics and basin development, in: Key-notes of the MEGS-II (Amsterdam, 1978) (Ed. Van Loon, A.J.), Geol. Mijnbouw, 57, 589-626

Ziegler, P.A. (1981) Evolution of sedimentary basins in North-West Europe, in: Petroleum geology of the continental shelf of North-West Europe (Eds. Illing, L.V. and Hobson, G.D.), Inst. Petrol., London, 3-39

Ziegler, P.A. (1982) Geological atlas of western and central Europe, Elsevier, Amsterdam.

Ziegler, P.A. (1983) Comments to: Crustal thinning and subsidence in the North Sea, Nature 304, 561